LEABHARLANN CHOLÁISTE NA TRÍONÓIDE, BAILE ÁTHA CLIATH | TRINITY COLLEGE LIBRARY DUBLIN
Ollscoil Átha Cliath | The University of Dublin

Terms and Conditions of Use of Digitised Theses from Trinity College Library Dublin

Copyright statement

All material supplied by Trinity College Library is protected by copyright (under the Copyright and Related Rights Act, 2000 as amended) and other relevant Intellectual Property Rights. By accessing and using a Digitised Thesis from Trinity College Library you acknowledge that all Intellectual Property Rights in any Works supplied are the sole and exclusive property of the copyright and/or other IPR holder. Specific copyright holders may not be explicitly identified. Use of materials from other sources within a thesis should not be construed as a claim over them.

A non-exclusive, non-transferable licence is hereby granted to those using or reproducing, in whole or in part, the material for valid purposes, providing the copyright owners are acknowledged using the normal conventions. Where specific permission to use material is required, this is identified and such permission must be sought from the copyright holder or agency cited.

Liability statement

By using a Digitised Thesis, I accept that Trinity College Dublin bears no legal responsibility for the accuracy, legality or comprehensiveness of materials contained within the thesis, and that Trinity College Dublin accepts no liability for indirect, consequential, or incidental, damages or losses arising from use of the thesis for whatever reason. Information located in a thesis may be subject to specific use constraints, details of which may not be explicitly described. It is the responsibility of potential and actual users to be aware of such constraints and to abide by them. By making use of material from a digitised thesis, you accept these copyright and disclaimer provisions. Where it is brought to the attention of Trinity College Library that there may be a breach of copyright or other restraint, it is the policy to withdraw or take down access to a thesis while the issue is being resolved.

Access Agreement

By using a Digitised Thesis from Trinity College Library you are bound by the following Terms & Conditions. Please read them carefully.

I have read and I understand the following statement: All material supplied via a Digitised Thesis from Trinity College Library is protected by copyright and other intellectual property rights, and duplication or sale of all or part of any of a thesis is not permitted, except that material may be duplicated by you for your research use or for educational purposes in electronic or print form providing the copyright owners are acknowledged using the normal conventions. You must obtain permission for any other use. Electronic or print copies may not be offered, whether for sale or otherwise to anyone. This copy has been supplied on the understanding that it is copyright material and that no quotation from the thesis may be published without proper acknowledgement.

The identification and functional characterization of substrates of the *C. elegans* caspase CED-3

Rebecca C. Taylor

Thesis submitted to Trinity College Dublin
for the degree of Doctor of Philosophy

Thesis supervisor: Prof. Seamus J. Martin

Molecular Cell Biology Laboratory,
Department of Genetics,
University of Dublin,
Trinity College,
Dublin 2

January 2007

TRINITY COLLEGE
05 JUL 2007
LIBRARY DUBLIN
THESIS
8108

DECLARATION

I certify that this thesis, submitted to Trinity College Dublin for the degree of Doctor of Philosophy, has not been submitted as an exercise for a degree at this or any other university. I certify that the work presented here is entirely my own, except where otherwise acknowledged. This thesis may be made available for consultation within the university library and may be copied or lent to other libraries upon request.

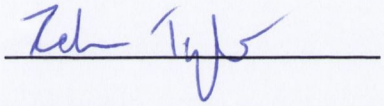

Rebecca Taylor
August 2006

ACKNOWLEDGEMENTS

I would first of all like to thank Dr. Colin Adrain and Dr. Emma Creagh, for the use of some of their data in this thesis, and Dr. Gabriela Brumatti, for her invaluable help with the immunodetection of cell surface calreticulin. I am also grateful to Prof. Hengartner and Prof. Derry and members of their laboratories, who collaborated with us in the generation and analysis of transgenic *C. elegans* lines, and who have been extremely helpful in discussing results with us.

I would also like to thank my supervisor, Prof. Seamus Martin, for all the help and advice he has provided throughout the course of this project. I have learned more in these past years under your supervision than I could have imagined possible. Many thanks are due as well to the other members of the lab, past and present, for all their help and support, and for making the lab such a great place to work. In particular, Dr. Colin Adrain and Dr. Patrick Duriez have been consistently generous with their help; Petrina Delivani has been great to work with on all the *C. elegans*-related projects; and Alexander Luthi has patiently fixed everything that I've managed to break during my time in the lab.

My friends deserve another big thank you, for sticking with me despite my constant disappearances into the depths of the lab. In particular, Cat Kiernan, George Yeats, Nav Sethi, and Elena Corchero have all made major contributions at various times to the cause of this thesis. And even more, I owe so much to Jon, for giving me a place to live while writing up, making me endless cups of tea, and generally being wonderful.

Most of all, I would like to thank my family for all their support. Joanna, Richard, Michael, Holly, Stephen and Sophie have all done their bit to cheer me up and keep me going. And my biggest thanks are of course due to Mum and Dad. I couldn't have done any of this without the love and support you have always given me, every step of the way.

Finally, I am grateful to Science Foundation Ireland, who funded this work.

TABLE OF CONTENTS

Page

SUMMARY

ABBREVIATIONS

PUBLICATIONS

CHAPTER I: INTRODUCTION

1.1 APOPTOSIS AND NECROSIS 2

1.2 ROLES OF APOPTOSIS 3
- 1.2.1 Control of cell number 3
- 1.2.2 Maintenance of genome integrity 3
- 1.2.3 Elimination of infected cells 4
- 1.2.4 Organ sculpting and deletion 4
- 1.2.5 Cell differentiation 4
- 1.2.6 Regulation of the immune system 5

1.3 APOPTOSIS IN DISEASE 5
- 1.3.1 Apoptosis in cancer 5
- 1.3.2 Immune disorders 5
- 1.3.3 Neurological disorders 6
- 1.3.4 Cardiovascular disease 6

1.4 GENETIC ANALYSES IN *C. elegans* 7
- 1.4.1 Identifying genes involved in programmed cell death 7
- 1.4.2 Establishing an order 9

1.5 HUMAN HOMOLOGUES OF THE *C. elegans* PCD GENES 9
- 1.5.1 CED-3 is homologous to human ICE 9
- 1.5.2 The caspase family 10
- 1.5.3 Caspase activity and activation 11

1.5.4 Caspase substrate specificity 13
1.5.5 CED-4 is an activator of Ced-3 and homologous to human Apaf-1 14
1.5.6 *ced-9* is homologous to human Bcl-2 16
1.5.7 Anti-apoptotic Bcl-2 family members 17
1.5.8 Pro-apoptotic multi-domain Bcl-2 family members and mitochondrial permeabilization 18
1.5.9 The BH3-only Bcl-2 family members 19
1.5.10 EGL-1 is a BH3-only Bcl-2 family member 22

1.6 PATHWAYS TO APOPTOSIS IN MAMMALIAN CELLS 24
1.6.1 The intrinsic pathway 24
1.6.2 The extrinsic pathway 24

1.7 PATHWAYS TO DEATH IN *C. elegans* 25
1.7.1 Developmental PCD 25
1.7.2 Germline PCD 26
1.7.3 Necrotic cell death 27

1.8 DOWNSTREAM OF CASPASE ACTIVATION 28
1.8.1 Caspase substrates 28
1.8.2 Downstream events in apoptosis 29
1.8.3 Phagocytosis 30
1.8.4 Caspase substrates in *C. elegans* 34

1.9 THESIS AIMS
1.9.1 Overall aims 35
1.9.2 Chapter III: Generation and characterization of recombinant CED-3 36
1.9.3 Chapter IV: Proteomic identification of CED-3 substrates 36
1.9.4 Chapter V: Functional analysis of CED-3 substrates 36

CHAPTER II: MATERIALS AND METHODS

2.1 REAGENTS 39

2.1.1 Chemicals and general reagents 39
2.1.2 Enzymes 39
2.1.3 Antibodies 39

2.2 PURIFICATION AND MANIPULATION OF NUCLEIC ACIDS 40
2.2.1 Bacterial strains 40
2.2.2 Preparation of competent bacteria 40
2.2.3 Transformation of competent bacteria 40
2.2.4 Plasmid purification 41
2.2.5 Agarose gel electrophoresis 42
2.2.6 DNA quantitation 42
2.2.7 Genecleaning procedure 42
2.2.8 Restriction digests 43
2.2.9 DNA ligation reactions 43
2.2.10 PCR 43
2.2.11 Site-directed mutagenesis 44

2.3 PROTEIN PRODUCTION 44
2.3.1 Induction of fusion proteins in bacteria 44
2.3.2 Purification of fusion proteins expressed in bacteria 45
2.3.3 Preparation of purified inclusion bodies 46
2.3.4 Refolding of insoluble proteins from inclusion bodies 46
2.3.5 Preparation of protein from HEK293T cells 47
2.3.6 *In vitro* protein synthesis in *E. coli* HY lysates 47
2.3.7 *In vitro* protein synthesis in rabbit reticulocyte lysates 48

2.4 PROTEIN ANALYSIS 48
2.4.1 Fluorimetric analysis of enzymatic activity 48
2.4.2 SDS-PAGE electrophoresis 48
2.4.3 Coomassie Blue staining 49
2.4.4 Immunoblotting 49
2.4.5 Fluorography 49
2.4.6 2-dimensional SDS-PAGE 50

2.4.7 MS-compatible silver staining 50
2.4.8 Trypsin digestion for MALDI-TOF mass spectrometry 51
2.4.9 MALDI-TOF mass spectrometry 51

2.5 HUMAN CELL CULTURE-BASED METHODS 52
2.5.1 Cell culture conditions 52
2.5.2 Transient transfection 52
2.5.3 Induction of apoptosis 53
2.5.4 FACS analysis 54
2.5.5 Light and UV microscopy 54
2.5.6 Immunostaining for analysis by FACS 54
2.5.7 Immunostaining for analysis by microscopy 55
2.5.8 Cell lysate preparation 55
2.5.9 Preparation of Jurkat cell-free extract 55
2.5.10 Assembly of cell-free reactions 56

2.6 NEMATODE CULTURE-BASED METHODS 56
2.6.1 *C. elegans* culture conditions 56
2.6.2 *C. elegans* extract preparation 57
2.6.3 Assembly of reactions in *C. elegans* CFE 57
2.6.4 Isolation of embryos from *C. elegans* 58
2.6.5 *C. elegans* embryonic extract preparation 58
2.6.6 Treatment of temperature-sensitive mutant strains 58
2.6.7 Confocal microscopy 58
2.6.8 Hoechst staining of embryos 59
2.6.9 MitoTracker staining of embryos 59

CHAPTER III: PURIFICATION AND CHARACTERIZATION OF RECOMBINANT CED-3

3.1 CHAPTER INTRODUCTION 61

3.2 CHAPTER SUMMARY 62

3.3 RESULTS 64

3.3.1 Induction of CED-3 as a His^6-tagged fusion protein in *E. coli* 64
3.3.2 Refolding CED-3 from bacterial inclusion bodies 65
3.3.3 *In vitro* transcription and translation in bacterial lysates 66
3.3.4 Expression of CED-3 in a human cell line 67
3.3.5 Low temperature induction of recombinant CED-3 68
3.3.6 Generating CED-3-specific polyclonal antibodies 69
3.3.7 Expression and purification of GST-CED-$3^{221-503}$ 70
3.3.8 Determining the active site concentration of GST-CED-$3^{221-503}$ 71
3.3.9 Comparing the activity of GST-CED-$3^{221-503}$ and caspase-3 against peptide substrates 72
3.3.10 Testing the activity of GST-CED-$3^{221-503}$ against protein substrates 72

3.4 DISCUSSION 74
3.4.1 Summary 74
3.4.2 Purification of CED-3 74
3.4.3 CED-3 is relatively promiscuous 75
3.4.4 CED-3 can also act as an initiator caspase 78
3.4.5 CED-3 does not cleave the substrates of inflammatory caspases 79
3.4.6 Caspases in *Drosophila melanogaster* 80
3.4.7 Predicting CED-3 substrates 80
3.4.8 Further work with recombinant GST-CED-$3^{221-503}$ 82

CHAPTER IV: IDENTIFICATION OF CED-3 SUBSTRATES BY PROTEOMIC ANALYSIS

4.1 CHAPTER INTRODUCTION 85

4.2 CHAPTER SUMMARY 86

4.3 RESULTS 87
4.3.1 Preparation of soluble protein extracts from 87

C. elegans
4.3.2 Characterizing CED-3 activity in *C. elegans* extract 87
4.3.3 Treatment of *C. elegans* extracts with GST-CED-$3^{221-503}$ and analysis by 1D SDS-PAGE 88
4.3.4 Treatment of *C. elegans* extracts with GST-CED-$3^{221-503}$ and analysis by 2D SDS-PAGE 89
4.3.5 Identification of CED-3 substrates by mass spectrometry 89
4.3.6 ced-9^{ts} mutant embryos as a source of endogenous active CED-3 91
4.3.7 Production of embryonic extracts for 2DE analysis 93
4.3.8 Confirmation of substrate cleavages by Western blotting 94
4.3.9 Cleavage of CRT-1, TBB-2 and FTT-2 by CED-3 *in vitro* 95
4.3.10 Identification of CED-3 cleavage sites in CRT-1, TBB-2 and FTT-2 96
4.3.11 Comparison of CED-3 cleavage sites in five substrate proteins 97

4.4 DISCUSSION 99
4.4.1 Summary 99
4.4.2 2D SDS-PAGE as a means of protease substrate identification 99
4.4.3 Comparing substrates cleaved in different organisms 100
4.4.4 Artificial vs endogenous systems 102
4.4.5 Cytoskeletal substrates 104
4.4.6 ATP synthesis 105
4.4.7 Metabolic proteins 106
4.4.8 Chaperone proteins 106
4.4.9 Proteases 107
4.4.10 Signalling proteins 108
4.4.11 DNA and protein synthesis 108
4.4.12 Cleavage site specificity of CED-3 109
4.4.13 Advantages and disadvantages of biochemistry and genetics in the identification of substrates for proteases 109

CHAPTER V: FUNCTIONAL CHARACTERIZATION OF CED-3 SUBSTRATES

5.1 CHAPTER INTRODUCTION 112

5.2 CHAPTER SUMMARY 112

5.3 RESULTS 114

5.3.1 Over-expression of CED-3 substrates in *C. elegans* 114

5.3.2 Human homologues of CRT-1, TBB-2 and FTT-2 are cleaved during apoptosis 114

5.3.3 FTT-2 does not modulate apoptosis in human cells 116

5.3.4 Calreticulin does not modulate apoptosis in human cells 117

5.3.5 Knock-down of alpha-tubulin causes apoptosis 117

5.3.6 Microtubule morphology is altered during apoptosis but reduction in alpha-tubulin levels does not affect nuclear fragmentation or apoptotic body formation 118

5.3.7 Calreticulin is cleaved in cells undergoing apoptosis 119

5.3.8 Calreticulin is detected on the surface of cells treated with a range of apoptotic stimuli 120

5.3.9 z-VAD-fmk prevents the exposure of calreticulin on the surface of cells treated with actinomycin D 121

5.3.10 Over-expression of Bcl-2 inhibits cell surface exposure of calreticulin in cells treated with actinomycin D 121

5.3.11 Over-expression of calreticulin leads to increased calreticulin surface exposure on treatment with actinomycin D 121

5.3.12 Over-expression of calreticulin leads to a substantial increase in calreticulin surface exposure on treatment with brefeldin A 123

5.3.13 Caspase-mediated cleavage of calreticulin may lead to its cell surface exposure and role as a ligand for phagocytes 124

5.4 DISCUSSION 125

5.4.1 Summary 125

5.4.2 Selection of substrates for analysis 126

5.4.3 FTT-2 and the 14-3-3 protein family 126
5.4.4 Alpha- and beta-tubulin 127
5.4.5 Calreticulin 130
5.4.6 Transgenic *C. elegans* lines 134

CHAPTER VI: CONCLUDING DISCUSSION

6.1 SUMMARY 137

6.2 CONCLUSIONS OF CHAPTER III 139

6.3 CONCLUSIONS OF CHAPTER IV 140

6.4 CONCLUSIONS OF CHAPTER V 142

APPENDICES

REFERENCES

FIGURES

CHAPTER I

Figure 1.1 Apoptosis in human cells
Figure 1.2 Genetic pathway of programmed cell death in *C. elegans*
Figure 1.3 The core death machinery in *C. elegans*
Figure 1.4 The human caspase family
Figure 1.5 Caspase activation
Figure 1.6 Apoptosome structures in *C. elegans* and humans
Figure 1.7 The human Bcl-2 protein family
Figure 1.8 Apoptosome-mediated caspase activation
Figure 1.9 Death receptor-mediated caspase activation
Figure 1.10 The *C. elegans* cell death pathway
Figure 1.11 Caspase substrate cleavage
Figure 1.12 Phagocytosis in *C. elegans*

CHAPTER III

Figure 3.1 His^{6}-tagged CED-3 constructs generated for bacterial expression and purification of CED-3
Figure 3.2 Expression from CED-3 constructs in *E. coli*
Figure 3.3 Refolding $CED\text{-}3^{221\text{-}503}$ using a range of buffer conditions
Figure 3.4 Expression of CED-3 using an ITT system
Figure 3.5 Expression of CED-3 in HEK 293T cells
Figure 3.6 Expression of $CED\text{-}3^{FL}$ at 25°C
Figure 3.7 Expression of $CED\text{-}3^{221\text{-}503}$ at 25°C
Figure 3.8 Generation of a polyclonal antibody against $CED\text{-}3^{221\text{-}503}$
Figure 3.9 Induction of $GST\text{-}CED\text{-}3^{221\text{-}503}$
Figure 3.10 Western blotting analysis of $GST\text{-}CED\text{-}3^{221\text{-}503}$
Figure 3.11 Active site titration of $GST\text{-}CED\text{-}3^{221\text{-}503}$
Figure 3.12 Comparing the activity of $GST\text{-}CED\text{-}3^{221\text{-}503}$ and human caspase-3 against a range of peptide substrates
Figure 3.13 Activity of $GST\text{-}CED\text{-}3^{221\text{-}503}$ against CED-3 and CED-9

CHAPTER IV

Figure 4.1 Preparation of *C. elegans* soluble protein extract

Figure 4.2 Incubation of CED-3 with *C. elegans* soluble protein extract
Figure 4.3 1DE analysis of *C. elegans* extract treated with GST-CED-$3^{221-503}$
Figure 4.4 Identification of substrates using SDS-PAGE and mass spectrometry
Figure 4.5 2DE analysis of *C. elegans* extract treated with GST-CED-$3^{221-503}$
Figure 4.6 Percentage of the proteome cleaved by caspases in humans, *C. elegans*, and *D. melanogaster*
Figure 4.7 GST-CED-$3^{221-503}$ substrates on 2DE gels
Figure 4.8 Peptide spectra of GST-CED-$3^{221-503}$ substrates
Figure 4.9 The phenotype of *ced-9*^{ts} mutant embryos
Figure 4.10 Protein extracts prepared from *C. elegans* embryos on 2DE gels
Figure 4.11 Western blotting analysis of actin and β-tubulin cleavage by CED-3 in extracts
Figure 4.12 Confirmation of FTT-2, TBB-2 and CRT-1 cleavage by CED-3 *in vitro*
Figure 4.13 *C. elegans* proteins not identified as substrates are not cleaved by CED-3 *in vitro*
Figure 4.14 Identification and mutation of CED-3 cleavage sites in FTT-2, TBB-2 and CRT-1
Figure 4.15 Comparison between CED-3 cleavage sites

CHAPTER V

Figure 5.1 *C. elegans* expression constructs encoding wild-type and cleavage-resistant TBB-2, FTT-2 and CRT-1
Figure 5.2 Both alpha-tubulin and beta-tubulin are substrates for human caspases
Figure 5.3 14-3-3 beta, epsilon and tau are substrates for human caspases
Figure 5.4 Calreticulin is a substrate for human caspases
Figure 5.5 FTT-2 does not affect apoptosis in human cells
Figure 5.6 Calreticulin does not affect apoptosis in human cells
Figure 5.7 Knock-down of human tubulin induces apoptosis but does not affect death induced by apoptotic stimuli
Figure 5.8 Knock-down of human tubulin does not affect apoptotic body formation or nuclear fragmentation in apoptotic cells
Figure 5.9 Domain structure and alignment of human and *C. elegans* calreticulin
Figure 5.10 Calreticulin is cleaved in cell undergoing apoptosis

Figure 5.11 Calreticulin is exposed on the surface of apoptotic cells
Figure 5.12 z-VAD-fmk blocks the exposure of calreticulin on the surface of cells treated with apoptotic stimuli
Figure 5.13 Bcl-2 blocks the exposure of calreticulin on the surface of cells treated with apoptotic stimuli
Figure 5.14 Over-expression of calreticulin in HeLa cells leads to a small increase in calreticulin exposure in response to actinomycin D
Figure 5.15 Over-expression of calreticulin in HeLa cells leads to substantially increased calreticulin exposure in response to brefeldin A
Figure 5.16 Apoptotic cell recognition through caspase-mediated cleavage of calreticulin

TABLES

CHAPTER IV

Table 4.1 Mass spectrometry identifications of CED-3 substrates

APPENDICES

Table A.1 Potential CED-3 substrate identifications
Table A.2 Constructs generated by the author for use in this study
Table A.3 Primers used by the author for generation of constructs used in this study
Table A.4 Point mutations generated by the author for use in this study
Table A.5 Primers used by the author for site-directed mutagenesis
Table A.6 Constucts obtained for use in this study

SUMMARY

The founding member of the caspase family of proteases is the *C. elegans* caspase, CED-3. CED-3 is the only caspase required for programmed cell deaths in the worm, but we know very little about how this protease coordinates the complex and reproducible downstream events of cell death. In this study, we aimed to gain a better understanding of how CED-3 controls the execution of programmed cell death by identifying its cellular substrates through proteomic analysis. It was anticipated that a better understanding of the role of CED-3 in worm programmed cell death (PCD) would also generate insights into the coordination of PCD by the mammalian counterparts of this enzyme.

The first phase of the project involved the generation of sufficient recombinant CED-3 for use in the proteomic screen. Initial attempts to express the enzyme in bacteria were hampered by the insolubility of CED-3 in bacterial cells. Refolding of denatured CED-3, use of an *in vitro* transcription/ translation system, and expression in human cells all failed to yield sufficient quantities of enzyme. We were however able to achieve good yields of soluble CED-3 in bacteria, using low induction temperatures and a GST protein tag to yield large amounts of active soluble GST-CED-$3^{221-503}$. GST-CED-$3^{221-503}$ was able to cleave relevant *C. elegans* protein substrates, and shared with human caspase-3 a preference for a DEVD peptide substrate sequence, although CED-3 exhibited greater substrate site promiscuity than its human counterpart, caspase-3.

Soluble protein extracts of *C. elegans* were used as a substrate pool for proteomic screening. GST-CED-$3^{221-503}$ was added to these extracts and samples were analysed by one-dimensional SDS-PAGE. No proteome changes were observed under these conditions, demonstrating that CED-3 is a highly specific protease. We then used a two-dimensional SDS-PAGE screening method and observed a set of reproducible protein changes upon addition of GST-CED-$3^{221-503}$. Using mass spectrometry, we were able to identify 22 of these altered proteins. The proteins identified encompass a range of cellular functions, and provide us with a blueprint for the coordination of the cell death process by CED-3. Three of the CED-3 substrates were cloned (FTT-2, TBB-2 and CRT-1) and we demonstrated

that they were genuine CED-3 substrates *in vitro*. The CED-3 cleavage sites in these substrates were also identified by site-directed mutagenesis.

To explore the functional effects of CED-3-mediated substrate cleavages, we cloned wild-type and cleavage-resistant FTT-2, TBB-2 and CRT-1 ORFs into *C. elegans* expression vectors. These constructs were then used to generate transgenic *C. elegans* strains. However, none of the transgenic nematodes showed a reproducible cell death phenotype. We also studied the human homologues of FTT-2, TBB-2 and CRT-1, and found that they are conserved substrates for human caspases. Over-expression of wild-type and cleavage-resistant FTT-2 and CRT-1, and human calreticulin, in HeLa cells, had no obvious effect on cell death. Knock-down of human alpha-tubulin by RNAi induced some spontaneous apoptosis, but did not affect death induced by other apoptotic stimuli.

A report suggesting that calreticulin acts as a phagocytic ligand on apoptotic cells led us to examine the possibility that caspase-mediated cleavage of calreticulin provokes its translocation to the cell surface during apoptosis (Gardai *et al.*, 2005). We found that calreticulin is indeed cleaved in cells undergoing apoptosis, and that the detection of calreticulin on the cell surface is a general feature of apoptosis induced by a range of stimuli. We also found that calreticulin translocation can be blocked by over-expression of the anti-apoptotic molecule Bcl-2, and by treatment with the poly-caspase inhibitor z-VAD-fmk. This suggests a model in which the proteolysis of calreticulin by activated caspases is necessary for the translocation of an N-terminal fragment of this molecule to the cell surface, where it triggers ingestion of dying cells through binding to CD91 on phagocytes.

ABBREVIATIONS

1DE	1-dimensional electrophoresis
2DE	2-dimensional electrophoresis
Ac	Acetylated
Act D	Actinomycin D
AFC	7-amino-4-trifluoromethyl coumarin
ALPS	Acute lymphoproliferative syndrome
APAF	Apoptotic protease activating factor
APC	Antigen presenting cell
ASP	Aspartic protease
ATP	Adenosine triphosphate
BCL	B-cell lymphoma
BH	Bcl-2 homology region
BSA	Bovine serum albumin
bZIP	Basic region leucine-zipper
CAD	Caspase-activated DNase
CARD	Caspase activation and recruitment domain
CASPASE	Cysteinyl aspartate-specific protease
CEB	Cell extract buffer
CeCFE	*C. elegans* cell-free extract
CED	Cell death defective
CES	Cell death specification
CFE	Cell-free extract
CFTR	Cystic fibrosis-associated transmembrane receptor
CHAPS	3-[(3-Cholamidopropyl)dimethylammonio]-1-propanesulfonate
CHX	Cyclohexamide
CTL	Cytotoxic lymphocyte
CRT	Calreticulin
Cyt c	Cytochrome c
dATP	Deoxyadenosine triphosphate
Dauno	Daunorubicin
DCI	3,4-Dichloroisocoumarin
DD	Death domain
ddH_2O	Double distilled H_2O
DED	Death effector domain
DEVD	Aspartic acid-glutamic acid-valine-aspartic acid
DISC	Death-inducing signalling complex
DMEM	Dulbecco's modified eagle medium
DMSO	Dimethyl sulphoxide
DNA	Deoxyribonucleic acid
DR	Death receptor
DTT	Dithiothreitol
EDTA	Ethylenediaminetetraacetic acid
EGL	Egg-laying defective
ER	Endoplasmic reticulum
FACS	Fluorescence-activated cell sorter
FADD	Fa-associated protein with death domain
FasL	Fas ligand
FCS	Fetal calf serum
FITC	Fluorescein isothiocyanate
FL	Full length

FMK	Fluoreomethylketone
FTT	Fourteen three three protein
FZO	Fuzzy onions-related protein
GNEF	Guanine nucleotide exchange factor
GFP	Green fluorescent protein
GHCl	Guanidine hydrochloride
GOF	Gain of function
GSH	L-glutathione reduced
GSSG	L-glutathione oxidised
GST	Glutathione-S-transferase
GTP	Guanine triphosphate
GDP	Guanine diphosphate
HBS	Hepes-buffered saline
HEK	Human embryonic kidney
HEPES	N-(2-hydroxyethyl) piperazine-N'-(2-ethanesulphonic acid)
HY	High-yield lysates
IAA	Iodoacetic acid
ICAD	Inhibitor of caspase-activated DNase
ICD	Inhibitor of cell death
ICE	Interleukin-1β-converting enzyme
Ig	Immunoglobulin
IEF	Isoelectric point focusing
IETD	Isoleucine-glutamic acid-threonine-aspartic acid
IL-1β	Interleukin-1β
IPG	Immobilised pH gradient strip
IPTG	Isopropylthio-β-D-galactoside
ITT	*In vitro* transcription and translation
kDa	kilodaltons
L-arg	L-arginine
LEHD	Leucine-glutamic acid-histidine-aspartic acid
LOF	Loss of function
MALDI-TOF	Matrix-assisted laser desorption and ionisation time-of-flight MS
MAP	Microtubule-associated protein
MES	2-morpholin-4-ylethanesulphonic acid
MFN	Mitofusin
MS	Mass spectrometry
MWCO	Molecular weight cut-off
MLC	Myosin light chain
M/Z	Mass:charge ratio
N/C	Non-cleavable
NCBI	National centre for biotechnology information
NGF	Nerve growth factor
NGM	Nematode growth medium
NK	Natural killer cell
NTA	Nitrilotriacetic acid
NP40	Nonidet P40
Oligo	Oligonucleotide
ORF	Open reading frame
PAR	Abnormal embryonic partitioning
PCD	Programmed cell death
PAGE	Polyacrylamide gel electrophoresis
PARP	Poly(ADP-ribose) polymerase

PBS	Phosphate-buffered saline
PCD	Programmed cell death
PCR	Polymerase chain reaction
PEG	Polyethylene glycol
PIPES	Piperazine-N-N'-bis(2-ethanesulphonic acid)
PMSF	Phenylmethylsulphonylfluoride
PRB	Protease reaction buffer
PS	Phosphatidylserine
RAIDD	RIP-associated Ich-1/CED homologous protein with a DD
RNA	Ribonucleic acid
RNAi	RNA interference
RPMI	Roswell Park Memorial Institute
SDS	Sodium dodecyl sulphate
siRNA	Small interfering RNA
TAE	Tris acetate EDTA
TBA	Tubulin alpha
TBB	Tubulin beta
TE	Tris EDTA
TFA	Trifluoroacetic acid
TNF	Tumour necrosis factor
TNFR	Tumour necrosis factor receptor
TPCK	*N*-tosyl-l-phenylalanine chloromethyl ketone
TRADD	TNFR-1-associated death domain protein
TRAIL	Tumour necrosis factor-related apoptosis-inducing ligand
TRAIL-R	Tumour necrosis factor-related apoptosis-inducing ligand receptor
UV	Ultraviolet irradiation
VH	Volt-hours
VP-16	Etoposide
WT	Wild-type
WEHD	Tryptophan-glutamic acid-histidine-aspartic acid
YVAD	Tyrosine-valine-alanine-aspartic acid
z-VAD-fmk	Benzylocarbonyl-Val-Ala-Asp-(OMe) fluoromethylketone

PUBLICATIONS

Taylor, R. C., Brumatti, G., Ito, S., Derry, W. B., Hengartner, M. O., and Martin, S. J. (2006). Establishing a blueprint for CED-3-dependent killing through identification of multiple substrates for this protease. In revision.

Delivani, P., Taylor, R. C., Adrain, C., Duriez, P., and Martin, S. J. (2006). Role for CED-9 and Egl-1 as regulators of mitochondrial fission and fusion dynamics. *Mol. Cell* **21**, 761-773.

Taylor, R. C., Adrain, C., and Martin, S. J. (2005). Proteases, proteasomes and apoptosis: breaking Ub is hard to do. *Cell Death Differ.* **12**, 1213-1217.

CHAPTER I

Introduction

1.1 APOPTOSIS AND NECROSIS

The phenomenon of physiological cell death was first observed and recorded by anatomists and embryologists of the mid nineteenth century (Lockshin and Zakeri, 2001). However, the term apoptosis was coined only in the 1970s to describe a controlled form of cell death occurring in physiological as well as pathological circumstances (Kerr *et al.*, 1972). Apoptotic cell death is characterized by a defined series of cellular changes. These include cell shrinkage and nuclear condensation, followed by inter-nucleosomal DNA fragmentation and plasma membrane blebbing (Figure 1.1). The cell's organelles are then dismantled and cell constituents packaged into small, membrane-bound "apoptotic bodies". The dead cell is finally consumed by phagocytes as a result of the exposure of "eat-me" signals on the cell's surface.

This phenotype differs markedly from that of cells undergoing unregulated pathogenic cell death, termed necrosis. Cells dying through necrosis display rapid swelling followed by cell rupture, causing the release of cellular contents into the vicinity and activation of an inflammatory response. This is in sharp contrast to apoptotic cells in which maintenance of plasma membrane integrity and rapid recruitment of phagocytes prevents any spilling of cell contents and thus avoids activating cells of the immune system. In addition, evidence suggests that the consumption of apoptotic cells by macrophages actively suppresses the release of pro-inflammatory mediators (Meagher *et al.*, 1992), and their uptake by dendritic cells prevents co-stimulation of T-cells (Sauter *et al.,* 2000). In this way, the functional end-points of these two forms of cell death are fundamentally different. Apoptosis is an immunologically "safe", physiological form of cell disposal, while necrosis alerts the immune system to a potentially dangerous pathological state.

The reproducible appearance of apoptotic cells, and the non-damaging nature of apoptosis and apoptotic cell clearance, implied that it is a conserved and regulated process. Kerr *et al.* suggested that apoptosis is in fact a widespread phenomenon accounting for most cell death occurring in the body (Kerr *et al.*, 1972). It is now known that programmed cell death is present in all multicellular organisms studied, and occurs on a large scale during mammalian embryogenesis, juvenile development, and adult tissue homeostasis. Deregulated apoptosis has also been

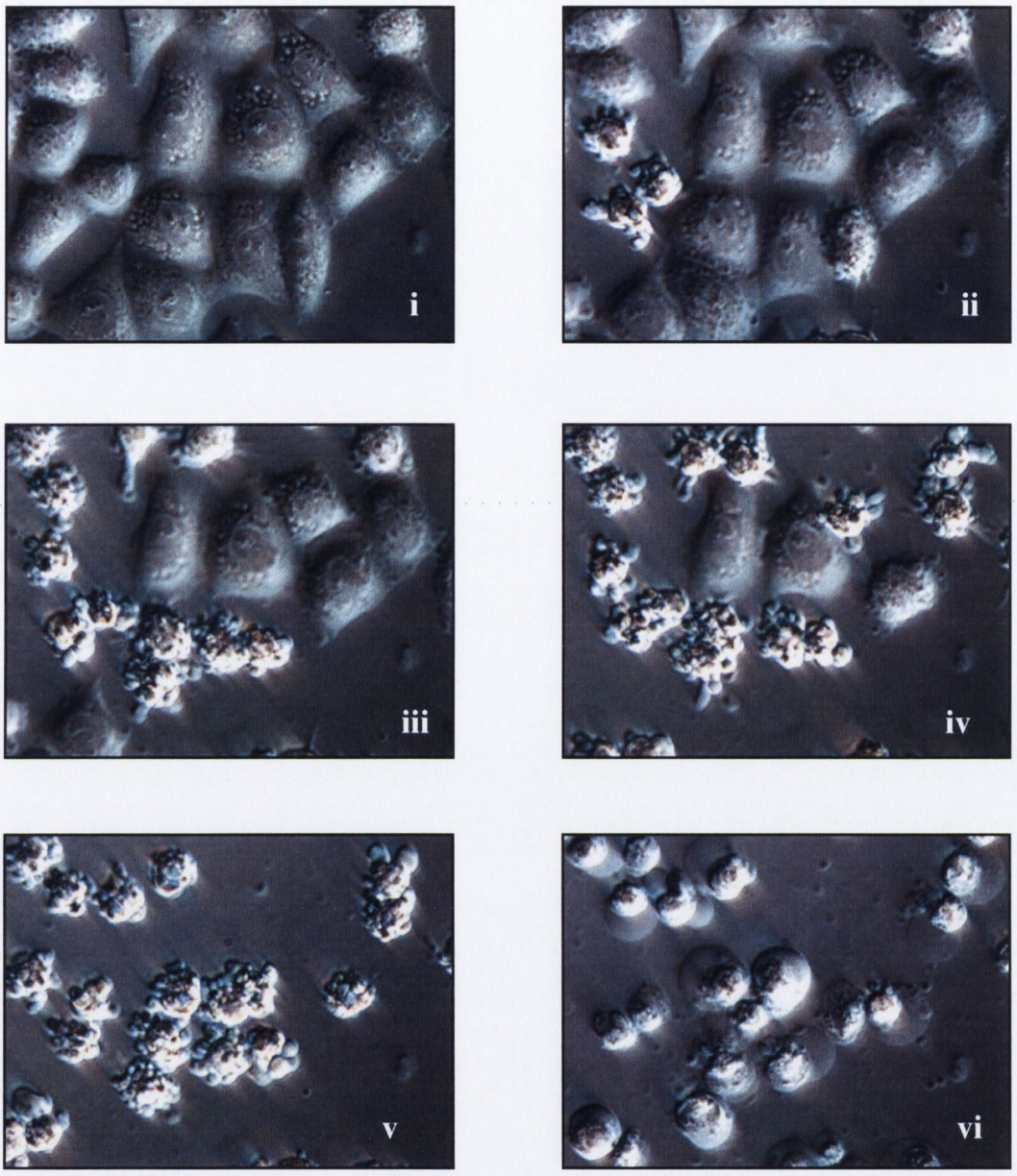

Figure 1.1

Apoptosis in human cells

HeLa cells were induced to undergo apoptosis by exposure to 10 mM daunorubicin. Phase contrast images were taken 110 (i), 205 (ii), 235 (iii), 260 (iv), 310 (v), and 560 (vi) minutes after addition of daunorubicin to the culture. Cells show a characteristic apoptotic morphology. At early timepoints cells detach from the substratum and become rounded. Cell shrinkage and plasma membrane blebbing are then evident. At later timepoints the cells fragment into apoptotic bodies. Finally, secondary necrosis occurs; cells cease to bleb and lose plasma membrane integrity, spilling their contents into the surroundings (vi).

observed in several pathological states. The following paragraphs will outline some of these roles of apoptosis, and the importance of its correct regulation.

1.2 ROLES OF APOPTOSIS

1.2.1 Control of cell number

The body maintains a population of cells that are continually dividing. This allows cells to be replaced if they have aged or become damaged. However, for this replacement to occur while a constant cell number is maintained, older cells must be eliminated in a manner that avoids damage to their neighbours. This is achieved through apoptosis (Jacobson *et al.*, 1997). The ability to remove damaged cells allows the body to eliminate a source of danger and malfunction, and allows organs to work efficiently through a process of constant regeneration. This tissue homeostasis is particularly apparent in organs where cells have a high turnover rate, such as the skin and intestinal surface epitheliums (Hall *et al.*, 1994). In addition, during development of many organs, cells are over-produced and surplus cells subsequently undergo apoptosis, allowing a fine-tuning of cell number. A good example is the developing nervous system. Generation of excess neurons and oligodendrocytes is followed by death of up to half of these cells, creating a precise match between neuron and target cell numbers. This process is controlled by the availability of a trophic factor, NGF (nerve growth factor), which these cells depend upon for survival (Barde, 1989; Yuan and Yankner, 2000).

1.2.2 Maintenance of genome integrity

Cells that have undergone genetic damage are able to activate mechanisms that lead to either cell cycle arrest and DNA repair, or apoptosis (Levine, 1997). p53, a tumour suppressor with roles in both these processes, can induce death after DNA damage (Clarke *et al.*, 1993; Lowe *et al.*, 1993). Apoptosis is triggered by transcriptional up-regulation of pro-apoptotic proteins such as Noxa and Puma, or directly via the mitochondria (Nakano and Vousden, 2001; Oda *et al.*, 2000; Chipuk *et al.*, 2005). This prevents the development of genetic heterogeneity and progression towards cancer. This mechanism also prevents the birth of defective offspring following genetic damage; irradiation of pregnant mice leads to a reduction in birth numbers, as irradiated embryos die, but there is little increase in

birth defects. Ablation of the p53 gene, however, leads to the birth of the irradiated embryos and a large increase in abnormalities (Norimura *et al.*, 1996).

1.2.3 Elimination of infected cells

Apoptosis can also be used as a mechanism for destroying cells harbouring infectious agents, and thus preventing the spread of infection (Meinl *et al.*, 1998). This apoptosis can be triggered externally by cells of the immune system, or cell-autonomously, on detection of the foreign agent. In response, many viruses have evolved anti-apoptotic mechanisms to prolong survival of infected cells. These include the expression of anti-apoptotic molecules such as p35, and the ability to modulate host gene expression to deregulate apoptotic control (Meinl *et al.*, 1998).

1.2.4 Organ sculpting and deletion

The sculpting of vertebrate organs is a process in which apoptosis plays an important role (Jacobson *et al.*, 1997). For example, the formation of vertebrate digits is dependent upon the elimination of interstitial cells, and the hollowing-out of luminal organs such as the preamniotic cavity of early mouse embryos relies on the programmed death of cells within a solid structure (Coucouvanis and Martin, 1995). Other organs formed from the invagination or fusion of epithelial sheets, such as the mammalian palate and the vertebrate neural tube, also involve extensive cell death (Glucksmann, 1951). In addition, some organs formed during development must be entirely deleted. This can occur as a part of sexual differentiation, such as the Wolffian duct required only in males and eliminated in females; to eliminate structures needed only early in development, including sub-plate neurons required only briefly in the development of the cerebral cortex; or to remove vestigial organs, such as the pro-nephral tubes used as kidneys in fish and amphibians, but not required in mammals (Jacobson *et al.*, 1997).

1.2.5 Cell differentiation

Some cells must go through either a partial or full cell death process to achieve their final differentiated phenotype. Mammalian erythrocytes and lens epithelial cells, for example, lose their nucleus and other organelles in a process similar to apoptosis, although the cells themselves remain alive. Keratinocytes, on the other hand, undergo full cell death in order to fulfil their function as a dead cell layer, and

this differentiation can be inhibited by the expression of the anti-apoptotic molecule Bcl-2 (Nataraj *et al.*, 1994).

1.2.6 Regulation of the immune system

The immune system undergoes extensive regulation by apoptosis both during development, and during homeostasis in the adult. In the developing immune system, lymphocytes with either inactive receptors or those exhibiting recognition of self-antigens are induced to die by apoptosis. This process eliminates around 95% of cells entering the thymus (Nagata, 1997). During the adult lifespan, infection triggers the rapid production of immune cells. Surplus cells remaining after clearance of the infection are again eliminated by the induction of apoptosis (Savill *et al.*, 1989; Haslett, 1992).

1.3 APOPTOSIS IN DISEASE

1.3.1 Apoptosis in cancer

Increases in cell division and decreases in cell death rates are hallmarks of tumourigenesis. As discussed, apoptosis is an important agent in the removal of genetically damaged cells, and is therefore a potent anti-cancer mechanism. With the apoptotic machinery disabled or disregulated, cells carrying other neoplastic transformations are better able to survive, and therefore have a strong selective advantage (Martin and Green, 1995b). The important apoptotic agent p53 is frequently mutated in cancer, preventing it from inducing apoptosis in cells with further mutations. In addition, the anti-apoptotic protein Bcl-2 was identified due to its up-regulation in B-cell lymphomas (Bakhsi *et al.*, 1985). A chromosomal translocation between chromosomes 14 and 18 results in heightened levels of Bcl-2 that prevent apoptosis by disturbing the equilibrium between pro- and anti-apoptotic molecules in the cell. As oncogenic factors such as c-Myc have pro-apoptotic as well as pro-proliferative effects, increasing anti-apoptotic factors within cells in which oncogenic factors such as c-Myc have been up-regulated can produce a strongly co-operative effect in tumour progression (Vaux *et al.*, 1988).

1.3.2 Immune disorders

As apoptosis is so important in the development and maintenance of the immune system, defects in its regulation can cause major immunological disorders. Failure to eliminate T cell populations expanded during infection, caused by mutations in

FasR and FasL, components of the apoptotic signalling machinery, result in Autoimmune Lymphoproliferative Syndrome (ALPS) (Cohen and Eisenberg, 1991). In this disease, surplus T cells accumulate in lymphoid organs. Defects in apoptosis during developmental lymphocyte selection can lead to the recognition of self-antigens and autoimmuity (Watanabe-Fukunaga *et al.*, 1992). In addition, tumour cells may develop the ability to protect themselves from the immune system by exploiting apoptotic pathways. For example, some secrete apoptotic mediators such as FasL, protecting them from immune cells through the induction of cell death (Hahne *et al.*, 1996). The HIV virus also targets cells of the immune system, blocking apoptosis of infected cells (Geleziunas *et al.*, 2001; Wolf *et al.*, 2001) and forcing the cell to induce apoptosis in neighbouring immune cells (Zauli *et al.*, 1999).

1.3.3 Neurological disorders

Toxic insults to adult neurons can cause the inappropriate cell death that characterizes several neurological disorders. For example, cells exhibiting features of apoptosis can be found in Alzheimer's disease, probably caused by amyloid-β protein deposition (Yuan and Yankner, 2000). Amyloid-β can be neurotoxic both *in vitro* and *in vivo*, although the mechanism is unclear, and its massive accumulation in Alzheimer's disease is believed to be caused by mutations in the presenilin genes. Huntingdon's disease, another adult-onset neurodegenerative condition, is characterized by loss of neuronal sub-populations due to the accumulation of toxic polyglutamine-expansion proteins (Yuan and Yankner, 2000). Again, the mechanisms by which these proteins may induce apoptosis is unclear. Another disease associated with neuronal apoptosis is amyotrophic lateral sclerosis (ALS), a progressive motor disease in which the death of motor neurons in the brain and spinal cord lead to paralysis (Yuan and Yankner, 2000). Mutations in the superoxide dismutase (SOD-1) gene appear to induce cell death in this case, possibly again by forming aggregates.

1.3.4 Cardiovascular disease

Cardiovascular disease may lead to apoptosis, in the neurons of the brain. In this case, apoptosis is the result of ischemia following heart malfunction or stroke that restricts blood flow to the brain. In the most severely affected zones, necrosis occurs, but in cells receiving less severe ischemia the apoptotic pathway can be

triggered and a later wave of apoptotic cell death may follow. The application of caspase inhibitors may be able to significantly attenuate this delayed wave of programmed cell death (Yuan and Yankner, 2000).

Apoptosis therefore plays important roles in many processes, both physiological and pathological. The realisation of the widespread relevance of apoptosis triggered a strong interest in its regulation and control that continues today. However, key insights into the regulation of physiological programmed cell death were first arrived at not through further studies on mammalian cells, but by genetic analyses in a quite different organism – the microscopic soil nematode *Caenorhabditis elegans*.

1.4 GENETIC ANALYSES IN *C. elegans*

1.4.1 Identifying genes involved in programmed cell death

C. elegans was first selected as an organism suitable for genetic analysis by Sydney Brenner, who saw in its simple transparent body plan and invariant cell lineage a means of exploring the contribution of genetics to development. During the course of early studies tracking cell lineages in the developing worm larva and embryo, John Sulston and Bob Horvitz observed that, of the 1060 cells created in the *C. elegans* hermaphrodite, 131 die shortly after their formation to leave only 959 cells in the adult (Sulston and Horvitz, 1977; Sulston *et al.*, 1983). The pattern of these cell deaths proved to be invariant, with the same cells dying in each developing individual. 113 of the cell deaths occurred during embryonic development, and the remainder during the development of the larva. The morphology of the dying cells was also reproducible, involving a brief increase in nuclear refractility followed by a decrease in refractility, and the crumpling and disappearance of the cell within one hour. These observations suggested that cell death could be thought of as a specific cell fate, and therefore under genetic control. The Horvitz laboratory set out to identify genes involved in cell death – cell death defective, or ced genes - through a process of genetic screening.

The first genes found to cause cell death defects when mutated, *nuc-1*, *ced-1* and *ced-2*, proved to be involved in the processes of DNA fragmentation (*nuc-1*) and the engulfment of dead cells (*ced-1* and *ced-2*) (Sulston, 1976; Hedgecock *et al.*, 1983). The *ced-1* mutant went on to become an invaluable tool in identifying

further ced mutants. In *ced-1* worms, corpses failed to be engulfed, and differences in numbers of dead cells could be more easily recognised. Following mutagenesis of *ced-1* worms, a mutant was identified in which no cell corpses were present. This mutant was termed *ced-3*, and reduction or elimination of the *ced-3* gene product allowed virtually all of the 131 cells that typically die to survive (Ellis and Horvitz, 1986). Cells surviving inappropriately in *ced-3* mutants were in some cases able to adopt other cell functions, suggesting complete rescue from the death phenotype (Avery and Horvitz, 1987). *ced-3* became the founder member of a pathway of genes controlling the cell death process, upstream of the cell corpse engulfment process controlled by *ced-1* and *ced-2*.

The next mutant found to act in cell death regulation was isolated in a screen designed to identify not mutants defective in cell death, but those with defects in egg laying. A mutation in the egg-laying abnormal gene 1 (*egl-1*) was discovered that resulted in the inappropriate death of the hermaphrodite-specific neurons that drive egg laying (Trent *et al.*, 1983). When combined with a mutation in *ced-3*, these cell deaths were blocked and egg-laying behaviour restored, suggesting that *egl-1* acted in the same cell death pathway, upstream of *ced-3*. Further screens then aimed to identify other suppressors of the *egl-1* phenotype, and in this way the mutant *ced-4* was identified. *ced-4*, like *ced-3*, proved critical for the occurrence of almost all programmed cell deaths (Ellis and Horvitz, 1986).

The fourth core regulator of nematode programmed cell death (PCD), *ced-9*, was isolated in a screen for mutations causing survival of the NSM sister cell that normally dies during development (Hengartner *et al.*, 1992). Of the mutants creating this phenotype, some caused cell-specific survival, and others caused widespread inappropriate survival. Several *ced-3* and *ced-4* mutants were identified in this second class, along with one *ced-9* mutant. This lesion in the *ced-9* gene appeared to be a gain-of-function (gof) mutation, due to its dominant nature, rarity, and the fact that a *ced-9* deletion did not behave in the same way. Identification of loss-of-function (lof) *ced-9* alleles showed that homozygous *ced-9* lof hermaphrodites exhibited sterility and maternal effect lethality. In addition, first-generation homozygotes showed many ectopic cell deaths, including death of the ventral motor cord neurons and HSNs. These phenotypes strongly suggested that *ced-9* acted in a protective capacity within the PCD pathway.

1.4.2 Establishing an order

Further analyses of these four cell death regulators established an ordered pathway in which the genes seemed to act (Figure 1.2). *ced-3* and *ced-4* were both found to be required cell-autonomously to control PCD (Yuan and Horvitz, 1990) and had initially indistinguishable phenotypes. However, overexpression studies showed that ectopic expression of *ced-3* alone was able to induce cell death even in a *ced-4* mutant background, while expression of *ced-4* was dependent upon wild-type *ced-3* to kill cells (Shaham and Horvitz, 1996). *ced-3* therefore seemed to have a downstream role, with *ced-4* acting upstream, possibly acting as a *ced-3* activator. Mutations of either *ced-3* or *ced-4* abolished the defects observed in *ced-9* lof animals, suggesting that *ced-9* acts upstream of both of these regulators, in an inhibitory fashion (Hengartner *et al.*, 1992).

The initial mutations in the *egl-1* gene later proved to be gof lesions, and the subsequent identification of lof *egl-1* alleles showed that in these animals, developmental PCD was virtually abolished (Conradt and Horvitz, 1998). Killing induced by over-expression of *egl-1* was dependent upon the presence of both *ced-3* and *ced-4*, placing *egl-1* upstream of these two regulators. However, *egl-1*-induced killing could be suppressed by *ced-9* gof mutations, and *egl-1* lof mutants did not suppress a *ced-9* lof phenotype, suggesting that *egl-1* also acted upstream of or in parallel to *ced-9* (Conradt and Horvitz, 1998). Additional experiments confirmed that *egl-1* action was dependent upon functional *ced-9*.

These epistasis experiments therefore defined a genetic order for the PCD pathway involving *ced-3*, *ced-4*, *ced-9* and *egl-1*, and provided a framework for studying cell death regulation (Figure 1.2). The relevance of these studies for mammalian systems became startlingly apparent as the genes involved were cloned and found in each case to have human homologues also involved in PCD. The discovery of this conservation of function provided a basis for the explosion of research into apoptosis that continues today.

1.5. HUMAN HOMOLOGUES OF THE *C. elegans* PCD GENES

1.5.1 CED-3 is homologous to human ICE

Upon cloning the *ced-3* cell death gene, sequence similarity was found between *ced-3* and the gene encoding a recently purified human enzyme, the cysteine

protease interleukin-1β-converting enzyme (ICE) (Yuan and Horvitz, 1993; Miura *et al.*, 1993). This enzyme is responsible for the proteolytic maturation of the cytokine pro-interleukin-1β to its active, truncated form during inflammation (Ceretti *et al.*, 1992; Thornberry *et al.*, 1992). Homology between the two molecules was highest in a region containing an entirely conserved pentapeptide sequence, QACRG, which is essential for ICE activity, and six *ced-3* mutants displayed lesions in residues conserved between CED-3 and ICE (Thornberry *et al.*, 1992; Yuan and Horvitz, 1993) (Figure 1.3). This suggested that proteolytic activity might be important during cell death. Moreover, on finding this homology, over-expression experiments in mammalian cells established that ICE was also able to induce an apoptotic phenotype (Miura *et al.*, 1993). This immediately suggested that ICE might be essential for apoptosis in human cells, as CED-3 is in nematode cells. The discovery was groundbreaking, as for the first time a link was made between controlled proteolysis and the execution of programmed cell death.

1.5.2 The caspase family

CED-3 and ICE proved to be the founder members of a family of enzymes, named caspases, defined by their cysteine-dependent proteolytic mechanism and their absolute dependence on a cleavage site aspartic acid residue (Creagh and Martin, 2001; Lamkanfi *et al.*, 2002; Nicholson, 1999). Further members of the family were rapidly identified. Although it had initially been suspected that ICE might be the human functional equivalent of CED-3, it became clear that the physiological role of ICE was restricted to cytokine maturation, and that at least one other enzyme was responsible for the proteolytic events occurring during apoptosis. Although all the caspases appeared able to induce cell death upon over-expression, caspase-3 was the first enzyme definitively shown through inhibitor studies to be required for substrate cleavages and apoptosis in human cells (Nicholson *et al.*, 1995).

There are now known to be 12 members of the human caspase family (Figure 1.4). These can be functionally divided into those involved, like ICE, in inflammation (caspase-1 (ICE), -4, -5 and –12), and those involved in apoptosis (caspase-2, -3, -6, -7, -8, -9, -10). Despite their functional differences, members of the caspase family are highly conserved in their catalytic mechanism.

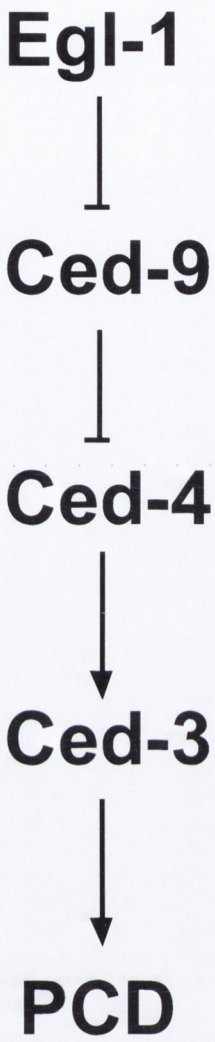

Figure 1.2

Genetic pathway of programmed cell death in *C. elegans*

The regulatory pathway controlling programmed cell death in *C. elegans* as established by genetic screens and epistasis studies. *egl-1* is the most upstream element; it inhibits the activity of *ced-9*, which in turn inhibits *ced-4*. *ced-4*, once released from inhibition, activates the downstream gene *ced-3*, leading to programmed cell death.

Core regulators of apoptosis in *C. elegans*

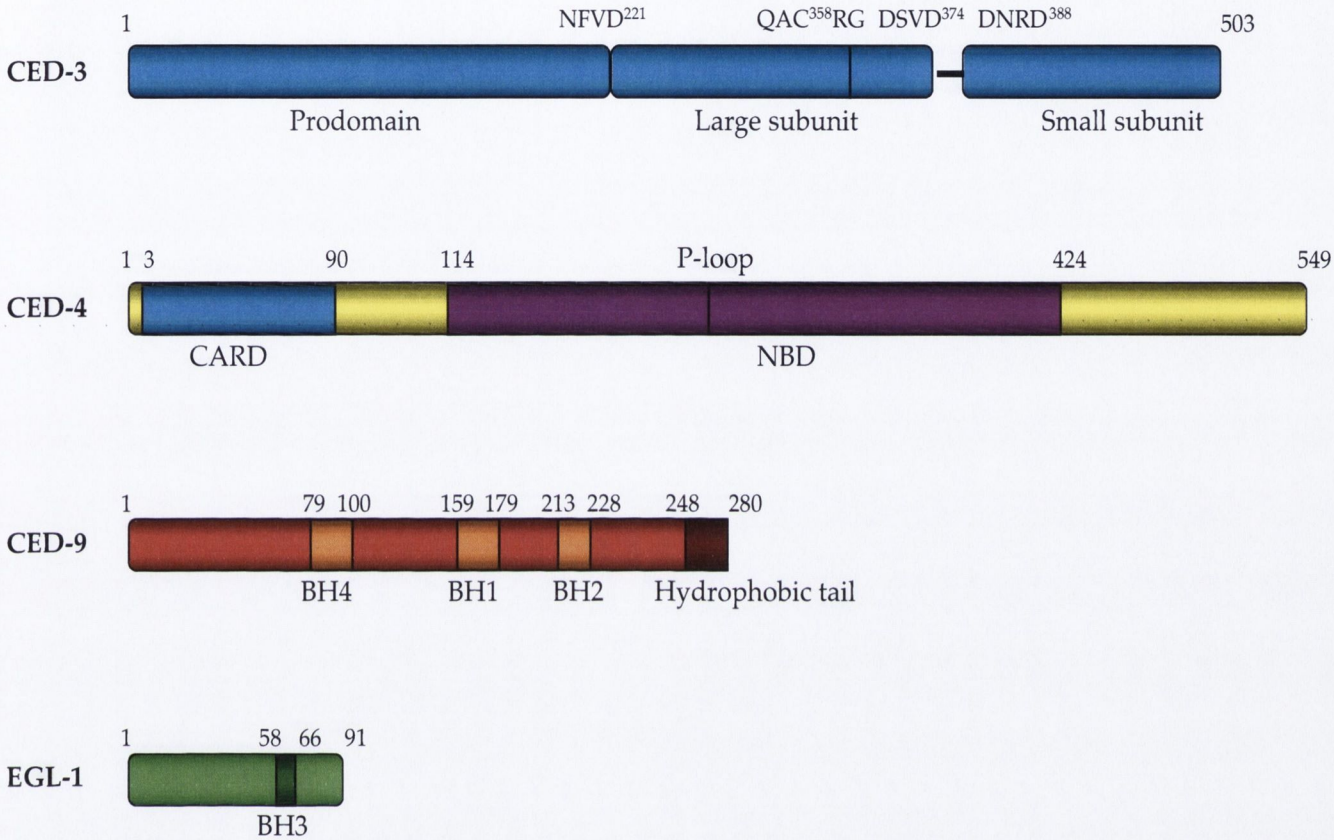

Figure 1.3

The core death machinery in *C. elegans*

The principle regulators of programmed cell death in *C. elegans*. The caspase CED-3 and the adapter protein CED-4 are essential downstream elements of PCD in the nematode. Tetramers of CED-4 bind to CED-3 and cause its auto-activation through induced proximity. The three subunits of CED-3 are shown with internal processing sites and the active site pentapeptide indicated. The caspase-binding CARD domain of CED-4, and its nucleotide-binding domain, are labelled. The ability of CED-4 to activate CED-3 is inhibited by the Bcl-2 family member CED-9. The EGL-1 BH3-only protein binds to CED-9 and displaces CED-4, allowing it to activate CED-3. The BH domains in these proteins are indicated.

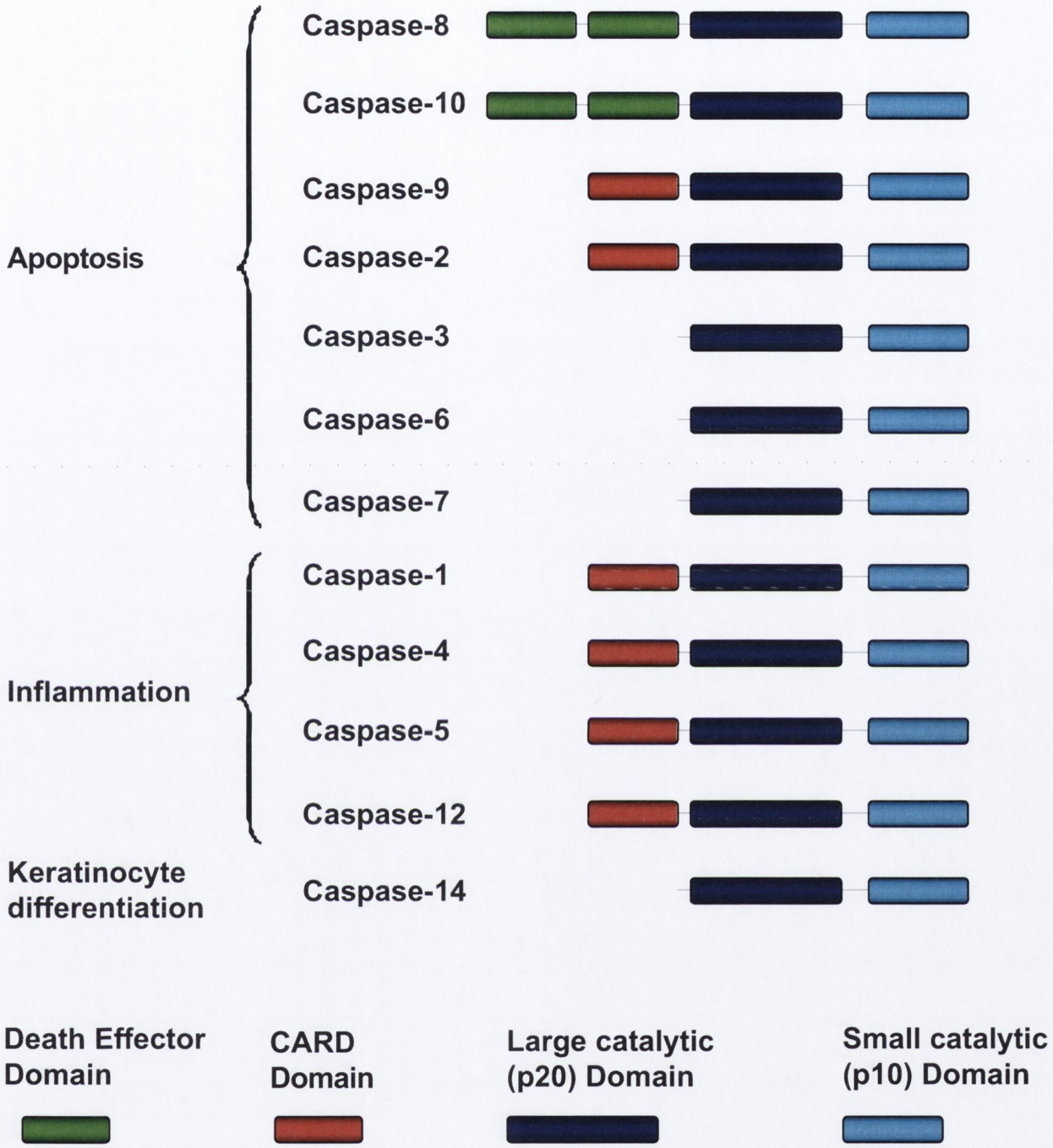

Figure 1.4

The human caspase family

Schematic representation of human caspases. There are 12 known caspases in man. Of these, caspases 1, 4, 5 and 12 have been implicated in inflammatory processes, although it should be noted that full-length caspase-12 is present in only a small minority of individuals. Caspases 2, 3, 6, 7, 8, 9, and 10 are involved in apoptosis. The function of caspase 14 is unclear, but it may play a role in keratinocyte differentiation.

1.5.3 Caspase activity and activation

All caspases are endopeptidases that contain a conserved active site pentapeptide (Stennicke and Salvesen, 1999a). Catalysis is dependent upon an active site cysteine residue that allows the breakage of a peptide bond in the substrate polypeptide by nucleophilic attack (Figure 1.5). Cleavage sites in the substrate protein are defined by a tetrapeptide cleavage motif, with an absolute requirement for an Asp residue at the P1 position. The caspase active site forms a groove extending along the surface of the molecule, and is made up of residues from both catalytic domains. The larger of the two domains contains the active site cysteine and histidine residues, while the sequences required for substrate specificity are derived from both the large and the small subunits (Shi, 2002). Caspases are synthesized as inactive zymogens, and activation of the enzyme depends upon proteolysis between the two catalytic subunits (Nicholson, 1999). Through hydrophobic interactions, these domains form a catalytically active heterodimer that is then believed to further dimerize, forming a heterotetramer. The inter-chain proteolysis may be accompanied by removal of the N-terminal pro-domain. Inter-chain maturation sites contain caspase-consensus tetrapeptide motifs with Asp at the P1 position, consistent with the ability of caspases to activate both themselves and other caspases (Figure 1.5).

The activation of caspase zymogens in mammalian cells can occur by three mechanisms (Nicholson, 1999). In the first, enforced clustering of the caspase molecules leads to autoproteolysis and activation (Salvesen and Dixit, 1999). Alternatively, caspases can be processed and activated by other members of the caspase family, creating proteolytic activation cascades (Figure 1.5) (Slee *et al.*, 1999a; Slee *et al.*, 1999b). Thirdly, caspases can be activated by other proteases, notably the serine protease granzyme B, found in the cytolytic granules of T cells and also able to cleave substrates at tetrapeptide Asp-containing sites (Martin *et al.*, 1996). Caspases can be divided into initiators and executioners depending on which of the first two mechanisms represents their dominant mode of activation.

Initiator caspases are able to initiate caspase activation cascades, and are characterized by a long (> 90 amino acid) N-terminal pro-domain. This pro-domain typically contains one of two protein-protein interaction domains, the CARD (caspase activation and recruitment domain) or the DED (death effector

domain). These domains mediate interactions between the caspase pro-domain and an adapter molecule. Clustering of the adapter molecules through oligomerization or binding to clustered receptor molecules leads to the enforced proximity of caspase molecules. Low levels of constitutive activity in the zymogen are then sufficient to process and activate adjacent caspase molecules (Salvesen and Dixit, 1999). These active caspase proteins are then free to activate both further initiator caspase molecules, and executioner caspases. Initiator caspases are represented among both cell death –associated and inflammation-associated caspases (caspases-2, -8, -9, and -10; and caspase-1, -4, -5, -12, respectively). Initiator caspases can be associated with specific activation pathways, and are therefore functionally distinguishable. In accordance with this, mice lacking intiator caspases such as caspase-9 or -8 show profound, and different, phenotypes (Zheng *et al.*, 1999).

Executioner caspases are defined by a short (<90 amino acid) N-terminal pro-domain. They are activated through proteolysis by active initiator caspases, in proteolytic activation cascades (Slee *et al.*, 1999a; Slee *et al.*, 1999b). It is the executioner caspases that are subsequently responsible for cleaving the majority of downstream substrate proteins. Although several executioner caspases are activated during apoptosis in mammals (caspase-3, -6, and -7) these proteases play separate and non-redundant roles in substrate proteolysis (Slee *et al.*, 2001). They have distinct substrate specificities, probably allowing the cleavage of a broader range of downstream targets. Caspase-3 and –7 appear to have similar tetrapeptide cleavage site preferences, suggesting that their differences in substrate specificity may be due to requirements for extended sequences or particular three-dimensional contexts (Thornberry *et al.*, 1997; Slee *et al.*, 2001). Immunodepleting caspase-3 in cell extracts prevents cleavage of most substrates, suggesting that it is the dominant executioner. However, although mice deficient in either caspase-3 or -7 are viable, albeit with some neuronal defects, those lacking both died as newborns and had significant heart defects (Lakhani *et al.*, 2006). This suggests that there must exist some redundancy between these enzymes.

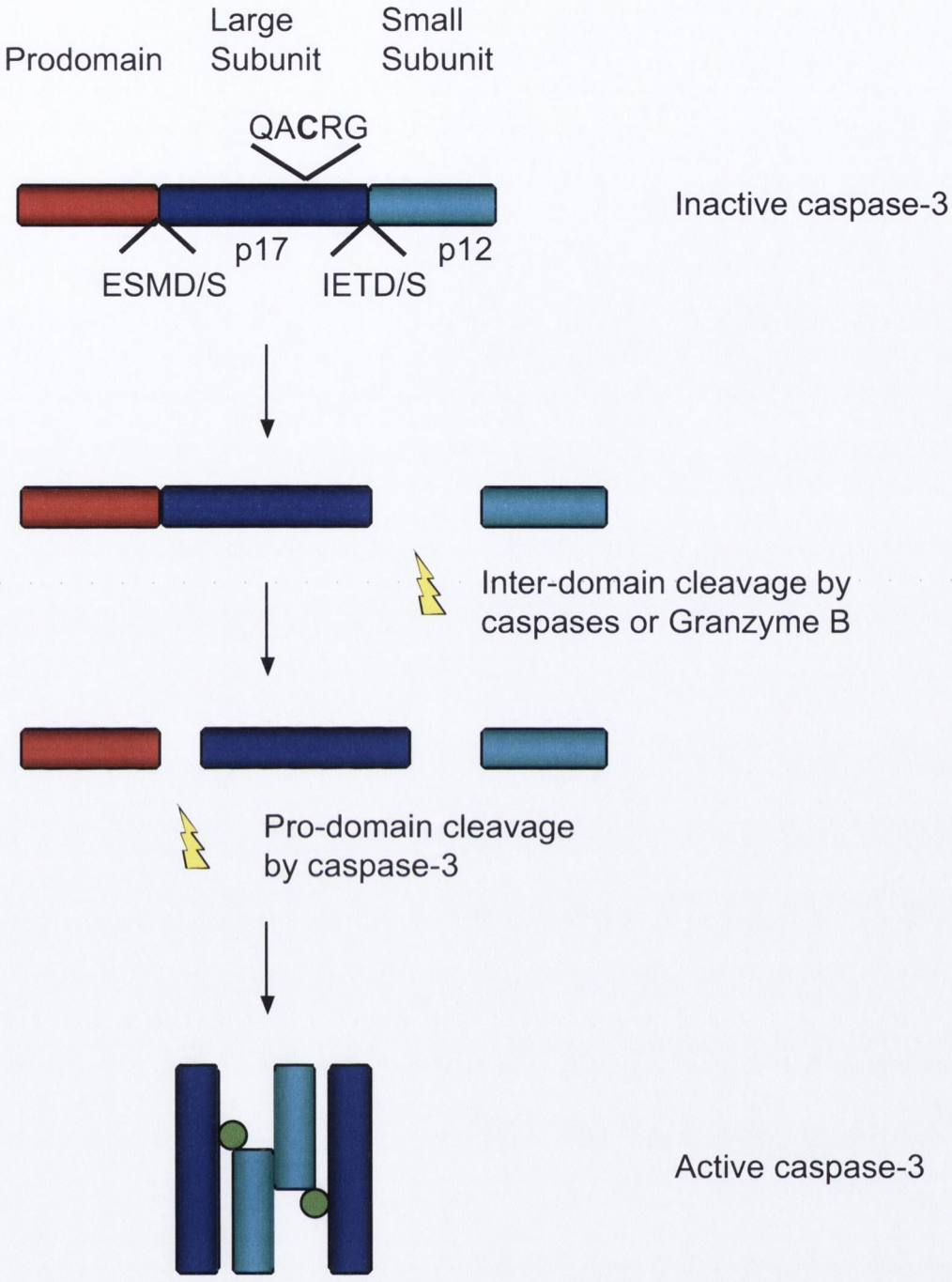

Figure 1.5
Caspase activation
Schematic representation of the activation of human caspase-3. Caspases are activated by the separation of the large and small subunits. This can be mediated by caspases, either auto-activation in the case of initiator caspases ,or through cleavage by an upstream caspase or the serine protease granzyme B in the case of executioners. This can be followed by the removal of the pro-domain. The active caspase forms heterotetramers containing two active sites. The active site pentapeptide with its essential cystein residue, and the inter-domain maturation sites of caspase-3, are indicated.

Studies of CED-3 have established that it too is dependent on its active site cysteine residue to promote cell killing (Miura *et al.*, 1993; Xue *et al.*, 1996; Hugunin *et al.*, 1996), and the use of peptide aldehydes as inhibitors has demonstrated its requirement for an Asp residue at the P1 position in the substrate cleavage site. It has been shown to cleave several substrates of human caspases *in vitro* (Hugunin *et al.*, 1996; Xue *et al.*, 1996). CED-3 also appears to be able to auto-activate *in vitro*, liberating two catalytic subunits and a serine-rich N-terminal pro-domain, in a manner dependent upon its active site cysteine residue (Hugunin *et al.*, 1996). Mutations affecting the inter-subunit cleavage sites identified by microsequencing analysis abrogate its cell killing activity (Xue *et al.*, 1996; Shaham *et al.*, 1999). This suggests that CED-3 has similar activity and activation mechanisms to human caspases. However, it is less easy to classify CED-3 as either an initiator or an executioner caspase. Despite the identification of three other potential caspase sequences in the *C. elegans* genome, and the ability of at least one of these potential transcripts to exhibit caspase activity *in vitro* (Shaham, 1998), there has been no demonstrated requirement for any caspase other than CED-3 during *C. elegans* apoptosis *in vivo*. This leaves CED-3 to act in both an initiator and an executioner capacity in the worm. Its long pro-domain resembles that of an initiator caspase, while the sequence of its catalytic domains show greatest similarity to the human executioner caspase-3, consistent with the dual role of CED-3 in the nematode.

1.5.4 Caspase substrate specificity

The different substrate site specificities of caspases provide another means of sub-dividing the family. Although all caspases by definition require an Asp residue at the P1 position of the cleavage site, individual members have more or less stringent requirements for the other three residues comprising the substrate cleavage site. The use of combinatorial peptide substrate libraries have defined optimal tetrapeptide cleavage motifs for each caspase, which provides a basis for dividing the caspases into three groups based largely on their preferred P4 residue (Thornberry *et al.*, 1997). The first family, encompassing the inflammation-associated caspases-1, -4 and -5, have a preference for bulky hydrophobic residues at P4, their consensus cleavage motif being WEHD. This is consistent with their role in inflammatory processes, as few known apoptotic caspase substrates have sites that fit this consensus, while IL-1β and caspase-1 do contain

similar sites. The second family, made up of the executioner proteases caspase-3 and -7, caspase-2, and CED-3, have a preference for an Asp at P4. This is consistent with the cleavage sites identified in many apoptotic caspase substrates, and also cements a functional relationship between CED-3 and human effector caspases. The third family, comprising the initiator caspases-8, -9 and -10, and the executioner caspase-6, prefer an I/V/L P4 residue. This specificity is generally similar to the activation sites within these caspases, allowing effective auto-activation.

The crystal structures of several caspase active sites have shed light on the three-dimensional context for these specificities (Fesik, 2000; Shi, 2002). The substrate-binding groove is composed of four loops, L1-L4, of which L1 and L3 are relatively conserved, and L2 and L4 are divergent. These loops form binding pockets for the four cleavage-site residues, subsites S1-S4, largely situated between the base (L3) and the sides (L1 and L4) of the groove. S2 and S4 are mainly made up from the L3 and L4 loops, and are relatively variable compared to the other two subsites. On inter-domain cleavage the active site adopts an open conformation. In particular, the L2' loop of one subunit switches to an open conformation where it is able to form a bundle with and stabilize the L2 and L4 loops of the other subunit. In this active conformation the P1 Asp residue fits into a highly restrictive S1 pocket in the active site tethered by three residues, derived from loops L1, L2 and L3 that are conserved in all caspases. The S2 and S3 binding positions are distinct in various caspases, but are tolerant of broad substitutions. The S4 site, however, varies widely between the different subgroups. The caspase-1 site, for example, is a shallow surface groove capable of accommodating a large hydrophobic amino acid (Walker *et al.,* 1994; Wilson *et al.*, 1994). In contrast, the site of caspase-3 is very narrow and polar, resulting in a decided preference for Asp (Rotonda *et al.*, 1996; Mittl *et al.*, 1997).

1.5.5 CED-4 is an activator of CED-3 and homologous to human Apaf-1

Cloning of the second gene essential for nematode programmed cell death, *ced-4*, showed that it encoded a novel 546 amino acid protein (Yuan and Horvitz, 1992) (Figure 1.3). *In vitro* interaction studies with the CED-4 and CED-3 proteins showed that they were able to interact directly, through their N-terminal sequences, leading to CED-3 auto-processing (Irmler *et al.*, 1997; Chinnaiyan *et*

al., 1997a; Chinnaiyan *et al.*, 1997b; Chaudary *et al.*, 1998). Co-transfection of *ced-3* and *ced-4* in insect and human cells greatly enhanced cell killing compared to that induced by *ced-3* alone, and this was accompanied by accelerated processing of CED-3 (Seshagiri and Miller, 1997; Wu *et al.*, 1997). These experiments, along with the genetic data, suggested that CED-4 might be able to directly activate CED-3.

A human homologue of CED-4 remained elusive until it was purified in an elegant chromatographic analysis of factors required for the initiation of apoptosis in human cell-free extracts. It had already been demonstrated that apoptosis could be modelled in extracts made from human cells that had been induced to die (Martin *et al.*, 1995). Wang and his colleagues now found that caspase activation could be initiated in unprimed extracts on addition of dATP, but in a manner dependent upon several factors present in the extracts, termed Apafs (apoptotic protease activating factors) (Liu *et al.*, 1996). The first of these factors to be identified was cytochrome c (Apaf-2). A requirement for mitochondria in the initiation of apoptosis in *Xenopus* egg extracts had previously been indicated (Newmeyer *et al.*, 1994), and it now seemed that cytochrome c might be the mitochondrial factor involved. Cells treated with the drug staurosporine did indeed release cytochrome c from the mitochondria early during cell death (Liu *et al.*, 1996). Then, the purification of Apaf-1 revealed that it was a homologue of the novel worm protein CED-4, containing a CED-4 homologous region as well as a WD40 repeat region and a CARD domain (Zou *et al.*, 1997). Apaf-1 proved able to bind to cytochrome c, and to the prodomain of caspase-9 (also required for extract activation and identified as Apaf-3) in a cytochrome c- and dATP-dependent fashion, leading to its activation and the activation of downstream caspases (Li *et al.*, 1997). Apaf-1 is able to oligomerize through its CED-4 homologous and linker domains, but this dimerization is inhibited by the WD40 repeat region, and a truncated Apaf-1 lacking its WD40 repeats is constitutively active (Adrain *et al.*, 1999; Srinivasula *et al.*, 1998; Hu *et al.*, 1999). Cytochrome c binding to Apaf-1 is able to relieve the inhibition mediated by the WD40 repeat region, leading to Apaf-1 oligomerization, induced proximity of bound caspase-9 molecules, and caspase-9 auto-activation (Zou *et al.*, 1999; Jiang and Wang, 2000) (Figure 1.6). The resulting complex was termed the apoptosome, and

allows apoptosis initiation to be tightly regulated by the control of cytochrome c release from the mitochondria where it is safely sequestered in healthy cells.

Structural studies have now given us a better understanding of apoptosome formation (Figure 1.6). It appears to show seven-fold symmetry, and is roughly wheel-shaped with a diameter of ~280 A and a thickness of ~70 A (Acehan *et al.*, 2002; Yu *et al.*, 2005). Seven oligomerized Apaf-1 molecules form Y-shaped spokes, with WD40 repeats forming the branches of the Y, CARD domains forming a central ring, and the CED-4-like nucleotide binding domains associating laterally around them to form the hub. A cytochrome c molecule binds to each pair of β-propellers, between the lobes of the Y. The structure suggests that the binding of cytochrome c might displace the "hub" regions from the WD40 repeats, allowing them to oligomerize. Caspase-9 molecules are positioned at the CARD ring and central hub, allowing the efficient activation of downstream caspases. Images intriguingly suggest that two apoptosomes may interact laterally through pro-caspase-9 molecules to create apoptosome dimers.

No structural analyses have yet been made of the interaction between CED-4 and CED-3. However, experiments have shown that induced oligomerization is sufficient to induce activation of CED-3 (Yang *et al.*, 1998). In addition, mutations eliminating the ability of CED-4 to oligomerize abolished its enhancement of CED-3 auto-processing and death-inducing activity (Yang *et al.*, 1998). This evidence suggests that a similar process of CED-3:CED-4 binding, oligomerization, and proximity-induced caspase activation is at work in the nematode model. Further evidence has come from the study of interactions between CED-4 and CED-9.

1.5.6 *ced-9* is homologous to human Bcl-2

An inhibitory role of *ced-9* on *ced-3* and *ced-4* activity had been predicted by the mutational analysis of the ced genes. Cloning of *ced-9* revealed that it encoded a 280 amino acid protein homologous to the mammalian proto-oncogene Bcl-2 (Hengartner and Horvitz, 1994) (Figure 1.3). Moreover, expression of human Bcl-2 in worm cells could protect from programmed cell death, and could substitute for *ced-9* in a *ced-9* mutant (Vaux *et al.*, 1992; Hengartner and Horvitz, 1994). This discovery was extremely exciting, as up-regulation of Bcl-2 expression had already been linked to the development of B cell lymphomas through a suppressive effect

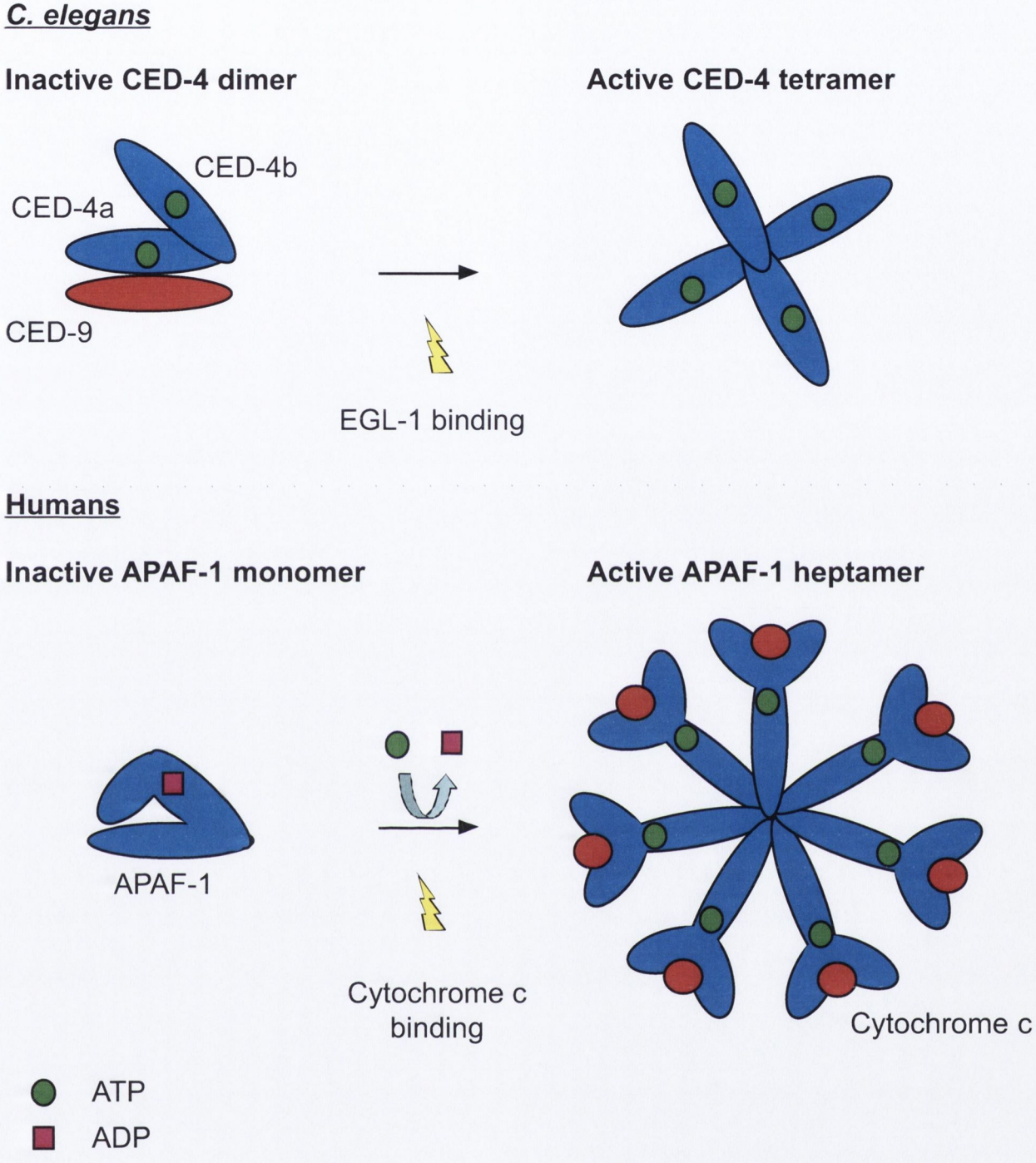

Figure 1.6

Apoptosome structures in *C. elegans* and humans

Formation of caspase-activating complexes in *C. elegans* and humans. CED-4 dimers are maintained in an inactive conformation by CED-9 binding, involving extensive interactions between CED-4a and CED-9, leaving the CARD domain of CED-4b disordered. Binding of CED-9 by Egl-1 allows CED-4 tetramerization and CED-3 binding. Human APAF-1 is usually inactive through auto-inhibition by the WD40 repeat region. Cytochrome c binding to this region allows APAF-1 molecules to form active heptamers that are able to bind to caspase-9. Note that in human APAF-1, ADP is exchanged for ATP during activation, while no nucleotide exchange appears to occur in CED-4 molecules.

on cell death (Bakhsi *et al.,* 1985; Hockenberry *et al.*, 1990). This suggested that Bcl-2 might also be a crucial regulator of apoptosis, and underlined the relevance of the worm model as a framework for understanding apoptosis in human cells.

However, study of the mechanisms underlying the death-suppressive effects of the two molecules has revealed important differences. Immunoprecipitation analyses established that CED-9 could interact directly with CED-4 and indirectly with CED-3, through CED-4 (Chinnaiyan *et al.*, 1997; Wu *et al.*, 1997; Chaudary *et al.*, 1998). CED-9 was able to inhibit CED-4 oligomerization but not it's binding to CED-3. This suggested that a trimeric complex could be formed between CED-3, CED-4 and CED-9, resulting in the inhibition of CED-4 oligomerization and CED-3 auto-activation. Substantiating this hypothesis, co-transfection of the three genes abolished the CED-4-mediated enhancement of CED-3 activity and auto-processing, without affecting basal levels of CED-3 activity (Seshagiri and Miller, 1997; Wu *et al.*, 1997). Structural evidence now suggests that before the induction of apoptosis, an asymmetric dimer of CED-4 binds to each molecule of CED-9 (Yan *et al.*, 2004; Yan *et al.*, 2005). CED-9 binds to only one CED-4 molecule in the dimer, CED-4a, the CED-4b molecule binding to the other side of CED-4a with a disordered CARD domain. The extensive interaction interface involves the N-terminal regions of both molecules. This arrangement does not affect the CED-9 transmembrane region, which localizes the complex to the mitochondrial membrane, as shown by *in vivo* immunofluorescence studies (Chen *et al*, 2000). Release of CED-9 promotes tetramerization of CED-4, suggesting that the *C. elegans* apoptosome may involve CED-4 tetramers bound to CED-3 molecules. Indeed, a mutant molecule of CED-4 unable to further dimerize into tetramers was unable to activate CED-3 *in vitro* (Yan *et al.*, 2005). *In vivo*, this mutant *ced-4* incompletely rescued a *ced-4* null mutant phenotype, and another monomeric *ced-4* mutant induced almost no cell deaths.

1.5.7 Anti-apoptotic Bcl-2 family members

Human Bcl-2 is now known to represent a family of molecules with either pro- or anti-apoptotic activity, that can be defined and sub-divided by their possession of BH domains 1-4 (Figure 1.7). No convincing evidence for direct interaction between Bcl-2 family members and Apaf-1 (or any other adapter molecule) has been demonstrated in human cells. Instead, the Bcl-2 family regulate the release

from mitochondria of the cytochrome c that is required for Apaf-1 oligomerization and caspase activation. Class I Bcl-2-like molecules are anti-apoptotic, and this sub-family includes Bcl-2 itself, Bcl-xL, A1 and Mcl-1. They contain BH domains 1 - 4 and a transmembrane domain that localizes them to the mitochondrial membrane. From there, they are able to prevent the release of cytochrome c from the mitochondria (Kluck *et al.*,1997; Yang *et al.*, 1997). The mechanism by which they do this, and the roles of different members of the family, are controversial.

1.5.8 Pro-apoptotic multi-domain Bcl-2 family members and mitochondrial permeabilization

Class II Bcl-2 family members, including Bax and Bak, contain BH domains 1 - 3 and are pro-apoptotic (Figure 1.7). They are necessary for the induction of apoptosis by several stimuli known to engage the apoptosome pathway (Lindenstein *et al.*, 2000; Wei *et al.*, 2001). Upon exposure to these stimuli, Bax is believed to undergo a conformational change exposing its amino terminus, and translocates to the mitochondria, where it inserts into the mitochondrial outer membrane. A mitochondrial membrane channel is formed from oligomerized molecules of Bax and/ or Bak, which allows the exit of cytochrome c from the mitochondrial inter-membrane space and thus triggers apoptosome formation. The formation of these channels is inhibited by anti-apoptotic Bcl-2 family members, and it is the equilibrium between these two classes that determines whether a cell lives or dies.

How mitochondrial membrane permeabilization might occur has been a matter of some debate. Experiments with isolated mitochondria and progressively simplified artificial systems have helped to define the requirements for mitochondrial outer membrane permeabilization. In artificial liposomes of defined content, activation of Bax by an activator protein, Bid, in a membrane containing the lipid cardiolipin, is sufficient to achieve permeabilization (Kuwana *et al.*, 2002). Bax oligomerization alone, induced by detergents *in vitro*, seems to allow the formation of membrane-spanning pores that have been visualized by atomic force microscopy (Epand *et al.*, 2002) ruling out the need for involvement of other proteins in the structure of the pore. The cardiolipin requirement is surprising, and suggests a possible formation of lipidic rather than proteinaceous pores; but other studies have observed large (>100 kDa) Bax aggregates in cells induced to undergo apoptosis ,

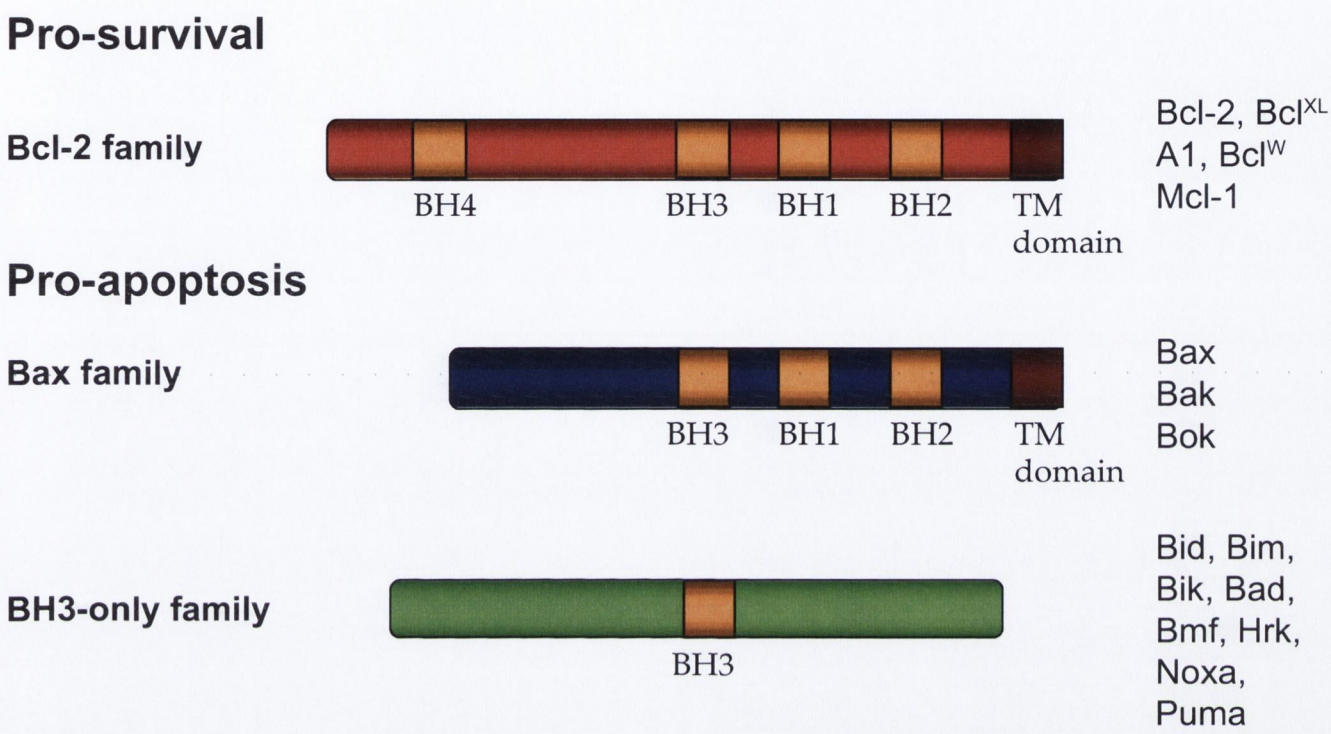

Figure 1.7

The human Bcl-2 protein family

Schematic representation of human Bcl-2 family proteins. These can be divided into three sub-families based on their complement of BH domains. The Bcl-2 family of anti-apoptotic BH proteins contain BH domains 1-4. The multidomain pro-apoptotic Bcl-2 family proteins contain BH domains 1-3. The BH3-only proteins have little overall homology other than a single BH3 domain.

suggesting that protein oligomerization is indeed required *in vivo* (Saito *et al.*, 2000). Molecules can be selectively released through the liposome pores from (Kuwana *et al.*, 2002) - selective release of cytochrome c from mitochondria would be essential to ensure maintenance of mitochondrial viability and the continued production of dATP/ATP that is required for apoptosome formation (Liu *et al.*, 1996). However, the ability of these artificial pores to release relatively large dextran molecules raises doubts as to the degree of selectivity and the relevance of these artificial pores.

1.5.9 The BH3-only Bcl-2 family members

Members of the third class of Bcl-2 family members, the BH3-only proteins, have only a BH3 domain in common, and are pro-apoptotic (Figure 1.7). They act as upstream detectors or transmitters of apoptotic stimuli. Each member appears to respond to a limited set of stimuli, causing them to translocate to the mitochondria and interact with class I and II Bcl-2 family members, shifting their equilibrium towards apoptosis (Green, 2006).

The great diversity of stimuli inducing apoptosis in mammalian cells may have necessitated the emergence of a wide variety of BH3-only molecules, each responding to specific signals and located in the optimum cellular location to receive them. These signals activate the BH3-only molecules, either by converting them to an active conformation, releasing them from tethering, or inducing their transcription. For example, the BH3-only molecule Bid is inactive and innocuous in the cytosol until cleaved by caspases or the serine protease granzyme B, yielding a p15 C-terminal truncation product. This translocates to the mitochondria where it exerts its pro-apoptotic effect and provides positive feedback to the apoptotic pathway (Li *et al.*, 1998; Luo *et al.*, 1998; Barry *et al.*,2000; Sutton *et al.*,2000). Phosphorylation may inhibit this cleavage (Desagher *et al.*, 2001). Interestingly, Bid also now appears able to play a novel pro-survival role in the response to DNA damage (Kamer *et al.*, 2005; Zinkel *et al.*, 2005). Phosphorylation of Bid (either already present in the nucleus of healthy cells, or translocating rapidly on DNA damage) by the ATM PI3-like kinase after sensing DNA double-strand breaks leads to cell cycle arrest at S-phase, independent of the BH3 domain. Even a very low, non-apoptotic dose of agents causing double-strand breakage leads to Bid phosphorylation; but Bid is also involved in the

induction of apoptosis on DNA damage. This suggests that Bid may help to determine whether an apoptotic response or a cell cycle arrest is the result of DNA damage. It certainly plays a crucial role in the prevention of transformation, particularly in the immune system; mice lacking Bid develop a myoproliferative disorder that becomes a form of fatal chronic myelomonocytic leukaemia (Zinkel *et al.*, 2003).

The BH3-only proteins Puma and Noxa are also involved in the induction of apoptosis after DNA damage. These molecules are transcriptionally up-regulated by p53, an important component of the cell's DNA damage response pathway, and seem to represent an important aspect of the death-inducing action of p53 (Nakano and Vousden, 2001; Han *et al.*, 2001; Oda *et al.*, 2000). In mice lacking Puma or Noxa, there is a decrease in levels of DNA damage-induced apoptosis in fibroblasts, and Puma knockouts fail to respond to a variety of p53-mediated death signals, including cytokine deprivation and exposure to glucocorticoids, staurosporine, or phorbol ester (Jeffers *et al.*, 2003; Villunger *et al.*, 2003).

The BH3-only protein Bad is believed to be regulated by phosphorylation mediated by the kinase Akt in response to survival factors, which causes its retention in the cytoplasm through binding to 14-3-3 proteins (Zha *et al.*, 1996; Datta *et al.*, 1997; del Peso *et al.*, 1997). It is also believed to localize within a mitochondrial complex with glucokinase, which may allow it to integrate information on the glycolytic state of the cell with the death machinery (Danial *et al.*, 2003). Bim, on the other hand, plays a role in immune cell selection (Bouillet *et al.*, 1999; Bouillet *et al.*, 2000).

On arrival at the mitochondria, activated BH3-only molecules must activate the Bax-Bak channel to allow release of cytochrome c. How this is achieved has been the focus of intense recent research. It was initially thought that anti-apoptotic Bcl-2 family members directly inhibited Bax and Bak oligomerization and were neutralized by the binding of BH3-only molecules, allowing Bax and Bak to form mitochondrial pores. The reality seems to be more complex. The affinity of different BH3-only proteins for different anti-apoptotic Bcl-2 family members varies (Chen *et al.*, 2005). Bim and Puma are able to bind all tested, whereas Noxa can only bind Mcl-1 and A1, and Bad is restricted to binding Bcl-2 and Bcl-xL. This suggests that while some BH3-only molecules could promote apoptosis alone by

neutralizing all anti-apoptotic Bcl-2-like proteins, others are required in combination in order to fully neutralize the cell's complement of anti-apoptotic molecules. This would explain their different potencies in cell killing assays and the different severities of their knockout phenotypes. However, others believe that BH3-only proteins are required to activate pro-apoptotic Bax and Bak and induce oligomerization, in order to cause cytochrome c release (Letai *et al.*, 2002; Kuwana *et al.*, 2005). Indeed, in *in vitro* systems, Bax oligomerization and liposome permeabilization can be induced by treatment with truncated (t) Bid or Bim. In this model, "direct activator" BH3-only proteins tBid and Bim function to bind directly to and activate Bax and Bak, while the other "displacer" BH3-only molecules bind anti-apoptotic Bcl-2 family members to displace "direct activator" BH3 molecules sequestered there. Again, different BH3 molecules of the "displacer" variety have different specificities for different Bcl-2 family members. In cellular tests of this model, "direct activator" molecules kill more efficiently if "displacer" molecules are present, and "displacer" molecules must act in concert with the induction of "direct activator" molecules to result in apoptosis.

A logical extension to this model is that idea that cells might be "primed" by a stimulus that activates "direct activator" molecules, but then requires derepression of anti-apoptotic members to induce apoptosis – or vice versa (Certo *et al.*, 2006). In this way, a single "displacer" molecule might be sufficient to induce apoptosis of cells already stressed. Apoptosis of cells treated with UV is potentiated by prior treatment with "displacer" BH3-only molecules (Kuwana *et al.*, 2005). And although studies show that only Bid and Bim so far display "direct activator" activity, other molecules may be able to act in this way. A possible example is the tumour suppressor p53 (Chipuk *et al.*, 2003; Chipuk *et al.*, 2004; Chipuk *et al.*, 2005). Recent reports suggest that p53 might have a transcription-independent role in the induction of cell death. After its activation and stabilization, p53 translocates to the nucleus where it activates the transcription of target genes such as Puma and Noxa. However, some p53 also accumulates in the cytosol where it seems able to directly activate Bax leading to direct release of cytochrome c. p53 can also be found in a complex with anti-apoptotic Bcl-xL on treatment with UV irradiation, suggesting that it might be sequestered like "direct activator" BH3-only proteins. Puma is also present in this complex and seems to be able to displace a fraction of bound p53 from Bcl-xL, leading to Bax activation

and apoptosis. This suggests that p53 is able to act as a "direct activator" protein in these circumstances, in parallel inducing transcription of "displacer" molecules, and therefore causing a robust apoptotic response to DNA damage. This proposed pathway emphasizes that the "direct activator" role could possibly be played by proteins other than BH3 family members (Green, 2006).

The existence of many members of the BH3-only sub-family therefore enables the cell to respond to a wide range of apoptotic stimuli, and to induce responses to these stimuli that differ in severity. They also allow cross-talk and co-ordination between different stimuli received by the cell, and therefore allow the cell to respond in a complex and sophisticated manner to its environment.

1.5.10 EGL-1 is a BH3-only Bcl-2 family member

The publication in 1998 of the sequence of the *egl-1* gene product revealed that it contained a BH3 domain, and it can therefore be categorized as a BH3-only molecule (Conradt and Horvitz, 1998) (Figure 1.3). This demonstrated that the BH3-only class of Bcl-2 family members is an evolutionarily ancient pro-apoptotic mechanism – older than their multi-domain pro-apoptotic cousins, which have no homologues in the worm. *egl-1* was found to act downstream of (or in parallel to) two genes involved in the specification of cell fates, *ces-1* and *ces-2* (Ellis and Horvitz, 1991). *ces-2* encodes a protein with a bZIP DNA-binding domain found in transcription factors, and is able to suppress transcription of the Snail-family zinc finger protein CES-1, suggesting that *egl-1* may be transcriptionally regulated to control cell death induction (Metzstein *et al.*, 1996; Metzstein and Horvitz, 1999).

Interaction studies demonstrated that EGL-1 is able to bind to CED-9 in a BH3 domain-dependent manner, suggesting that it might directly regulate CED-9 function. Co-expression of EGL-1 with CED-3, CED-4, and CED-9 in human cells showed that EGL-1 abolishes the CED-9-mediated inhibition of CED-4 through disrupting the interaction between the two molecules in a BH3-dependent manner (del Peso *et al.*, 1998; del Peso *et al.*, 2000). In *C. elegans* embryos, expression of EGL-1 causes CED-4 to relocalize from the mitochondrial membrane to the peri-nuclear region, suggesting a disruption of the interaction between CED-9 and CED-4 (Chen *et al.*, 2000). Gain of function *ced-9* mutants are able to resist EGL-

1-induced disruption of the CED-4:CED-9 complex both in human cells and in the worm (del Peso *et al.*, 2000; Chen *et al.*, 2000).

Structural studies have now revealed the nature of the interactions between EGL-1 and the CED-9:CED-4 complex (Yan *et al.*, 2004). The C-terminal half of EGL-1 is required for binding to a region of CED-9 within residues 68-237, forming a compact globular structure. An amphipathic EGL-1 helix packs against CED-9 helices over a hydrophobic surface cleft. Its interaction interface on CED-9 is different to that of CED-4, but EGL-1 binds with a higher affinity. Its binding induces substantial conformational changes in CED-9, causing steric clashes between CED-9 and CED-4a, suggesting a mechanism by which EGL-1 binding can displace CED-4 from CED-9 (Yan *et al.*, 2005). Titration of EGL-1 into a CED-9:CED-4 complex does indeed cause efficient dissociation of CED-4 at a dissociation constant of 98± 18 nM.

These conformational changes induced by EGL-1-binding are quite different to those observed in human Bcl-xL on binding a Bak BH3 peptide (Sattler *et al.*, 1997). However, the mechanism by which BH3-binding induces apoptosis is clearly different in the two systems. EGL-1 acts to displace CED-9 from a direct inhibitory complex with CED-4, while human pro-apoptotic Bcl-2 family members interact with anti-apoptotic members to control the release of cytochrome c from the mitochondria. The different conformational changes induced must therefore reflect these differences in mode of action.

A second BH3-only protein in *C. elegans* has now been identified, CED-13. The presence of only two BH3-only proteins in *C. elegans* cells, compared to the many that function in human cells, suggests that this family has diversified through evolution as cells have become responsive to many more stimuli in "higher" species. In somatic cells of *C. elegans*, there is no need to respond to a panoply of environmental cues; cells die predictably during development, so only need to respond to a very limited set of signals. As human cells have evolved and apoptosis has become important in so many physiological and pathological processes, the cells ability to respond co-ordinately to multiple cues has had to increase, and may have become more important to prevent adventitious activation of apoptosis. Thus an extra layer of regulation has evolved based around the

mitochondria, and this has necessitated the expansion both in number and function of the Bcl-2 family.

1.6 PATHWAYS TO APOPTOSIS IN MAMMALIAN CELLS

1.6.1 The intrinsic pathway

Together, the mammalian proteins outlined above represent an intrinsic pathway to the induction of apoptosis, that senses and responds to cues originating within the cell (Figure 1.8). A diverse variety of damage and stimuli can be sensed by the multiple BH3-only Bcl-2 family members, such as Bid or Bad, that are positioned appropriately in the cell to receive specific types of signal. Alternatively, signals can be sensed by a different molecule such as p53 that transcriptionally up-regulates BH3-only proteins, such as Puma and Noxa. These molecules then act at the mitochondria where, through a combination of Bax/Bak activation and anti-apoptotic Bcl-2 family member de-repression, a mitochondrial pore can be formed and cytochrome c is released. This mitochondrial membrane permeabilization is the point of no return in the intrinsic cell death pathway. Even on inhibition of the downstream caspases, once the mitochondria have been permeabilized the cell will die, albeit in a caspase-independent and necrotic fashion (Kroemer and Martin, 2005). Although the time between receipt of a stimulus and permeabilization of the cell's mitochondria is variable, once it is initiated it is tightly synchronised within the cell, all mitochondria discharging all their cytochrome c over a short space of time (Goldstein *et al.*, 2000). The subsequent stages of apoptosis then occur relatively swiftly. Release of cytochrome c stimulates apoptosome formation by allowing the oligomerization of Apaf-1 and bound caspase-9. The proximity-induced auto-activation of caspase-9 then allows it to cleave and activate molecules of caspase-3, which in turn activates other effector caspases and further molecules of caspase-9. The executioner caspases are then able to cleave their target substrate proteins in the execution phase of apoptosis.

1.6.2 The extrinsic pathway

A second pathway leading to apoptosis in human cells responds to signals received from outside the cell (Figure 1.9). Death receptors on the cells surface, comprising a subset of the TNF/NGF receptor family and including Fas.APO-1/CD95, TNFR1, DR3/TRAMP, DR4/TRAIL-R1, DR5/TRAIL-R2, and DR6

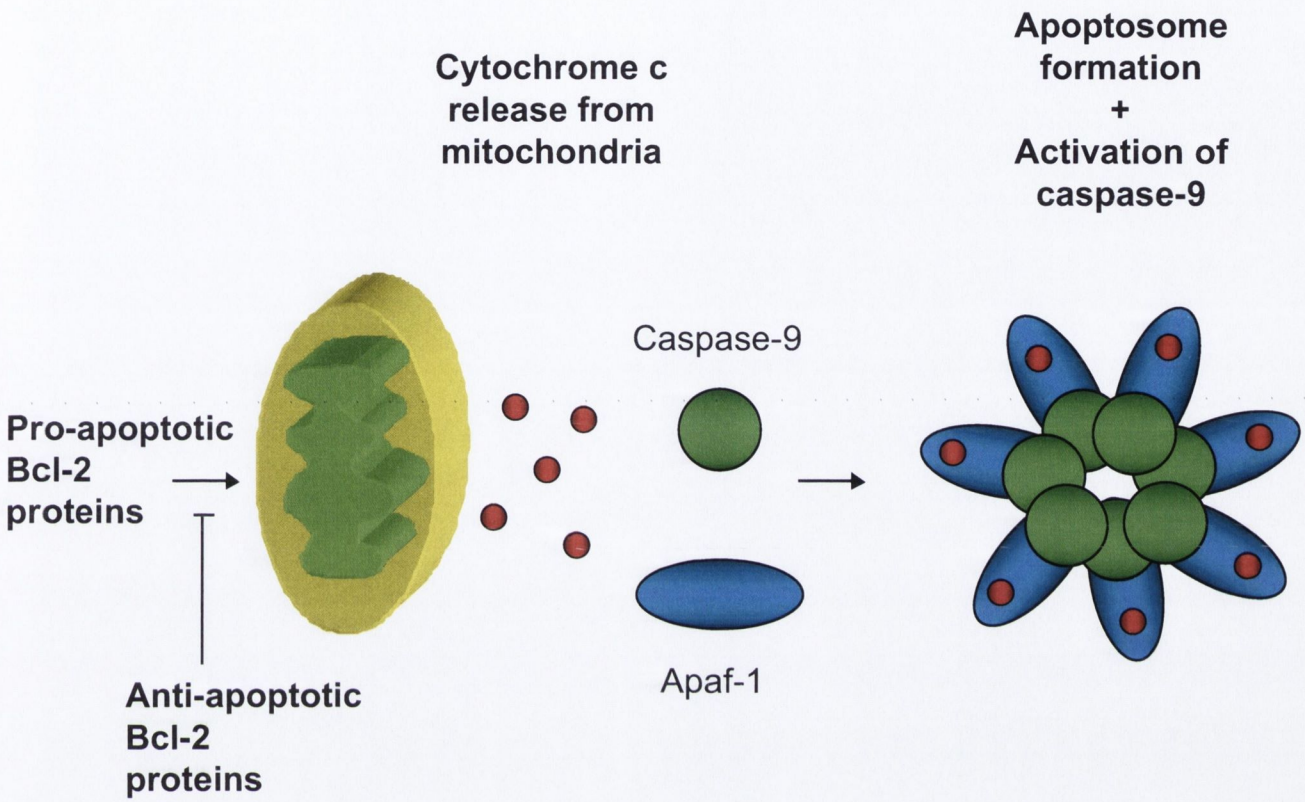

Figure 1.8

Apoptosome-mediated caspase activation

Activation of caspase-9 by the apoptosome. Mitochondrial cytochrome c release triggers apoptosome formation. Apaf-1 is bound by cytochrome c and forms heptamers. It then binds to caspase-9 through its CARD domain, and this induced oligomerization of caspase-9 causes its auto-activation. Caspase-9 then cleaves and activates downstream executioner caspases.

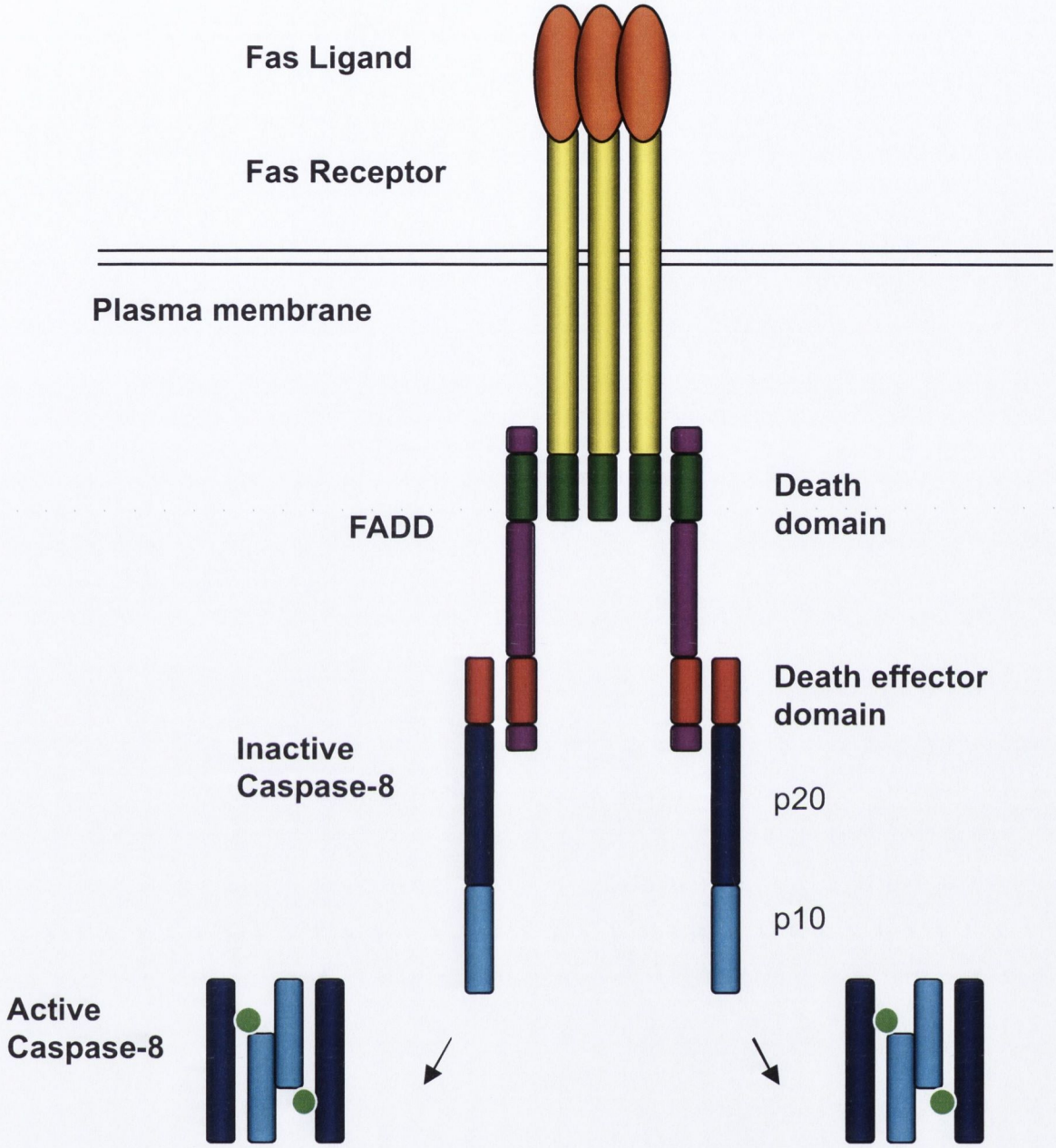

Figure 1.9
Death receptor-mediated caspase activation
Activation of caspase-8 by Fas receptor activation. Fas ligand induces the oligomerization of the Fas receptor. The adapter molecule FADD is recruited and, in turn, recruits caspase-8 resulting in proximity-induced autoprocessing and activation of the caspase. Caspase-8 goes on to cleave Bid, activating the intrinsic pathway, and downstream executioner caspases.

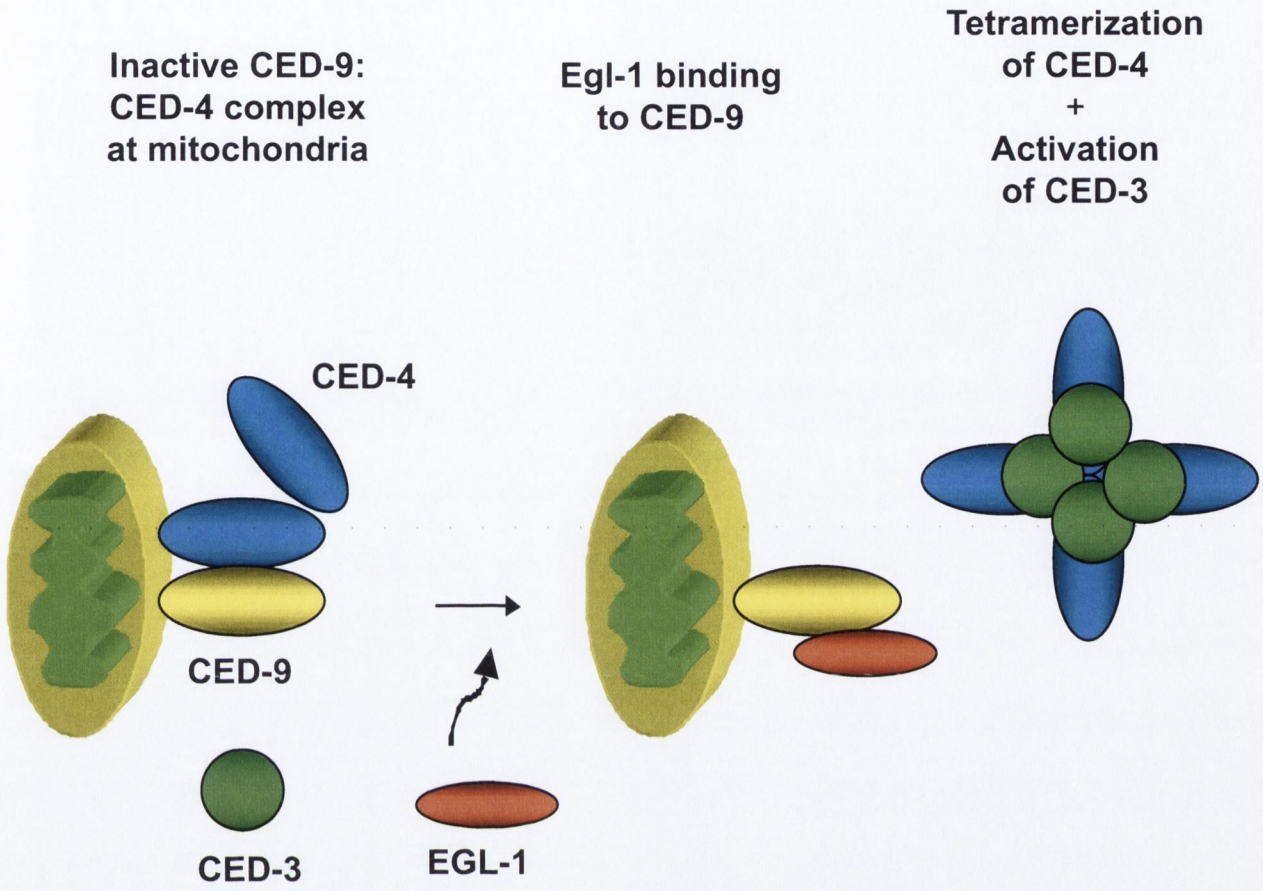

Figure 1.10

The *C. elegans* cell death pathway

The programmed cell death pathway in *C. elegans*. Dimers of CED-4 are bound to CED-9 at the mitochondria. The EGL-1 BH3-only protein disrupts the interaction between CED-9 and CED-4, allowing CED-4 dimers to tetramerize and activate CED-3. CED-3 goes on to cleave substrate proteins necessary for the execution of programmed cell death. Note that there are no structural analyses of CED-3:CED-4 interactions.

(Ashkenazi and Dixit, 1998) respond to ligands such as Fas that are secreted by other cells. Ligation of death receptors induces their aggregation, which brings into close proximity their intracellular death domains (DDs). These death domains are able to recruit adapter molecules such as FADD and TRADD, which contain death effector domains (DEDs) in their N-termini. These death effector domains in turn bind to DEDs in the pro-domain of caspase-8 or -10, forming what is called a death-inducing signalling complex (DISC) (Boldin *et al.*, 1996; Muzio *et al.*, 1996). This binding through an adapter to the clustered receptor molecules leads to proximity-induced caspase auto-activation, and a downstream apoptotic cascade (Medema *et al.*, 1997).

There are several similarities between the extrinsic and intrinsic pathways. Both use a sensor system to detect signals telling the cell that apoptosis is appropriate. In the intrinsic pathway these are the BH3-only or other intrinsic proteins such as p53 that activate BH3-only family members; in the extrinsic system, these are the death receptors. The signal transducers then recruit an adapter molecule. In the intrinsic system this is indirect, through the induction of cytochrome c release that leads to Apaf-1 activation, while in the extrinsic system adapters are recruited directly to the activated receptors. Initiator caspases are then recruited to the clustered adaptor molecules, which enables them to undergo auto-activation. Each pathway then goes on to activate the same effector caspases.

The two pathways are not entirely separate, however. The BH3-only protein Bid can be cleaved and activated by caspase-8, recruited and activated through the death receptors (Li *et al.*, 1998; Luo *et al.*, 1998). It is then able to activate Bax oligomerization and cause cytochrome c release, in this way activating the intrinsic pathway. It therefore acts to amplify the apoptotic signal, ensuring that apoptosis is completed quickly and fully. In some cells, such as neurons and cardiomyocytes, it is possible that this caspase-mediated positive feedback is essential for the completion of programmed cell death (Adrain and Martin, 2006).

1.7 PATHWAYS TO APOPTOSIS IN *C. elegans*

1.7.1 Developmental PCD

The nematode developmental cell death pathway, outlined already, has distinct parallels with the mammalian intrinsic cell death pathway (Figure 1.10). The

homologies between the key proteins and mechanisms involved in both worm and mammalian cell death show that the pathways have been substantially conserved through evolution. The upstream transcriptional regulators CES-1 and CES-2 induce the expression of the BH3-only protein EGL-1, in a manner similar to the transcriptional upregulation of human BH3-only proteins such as Noxa and Puma. EGL-1 is then able to alleviate the repression of CED-9 on dimeric CED-4 through direct binding to CED-9, inducing conformational changes that displace CED-4. Somewhat similarly, a displacement mechanism may also be used by human BH3-only proteins binding to Bcl-2 family members, releasing sequestered "activator" BH3-only molecules. CED-4 is then able to undergo oligomerization, like human Apaf-1, although forming tetramers rather than heptamers (Adrain *et al.*, 2006b). This oligomerization then mediates the clustering of CED-3 molecules, causing their auto-activation, like caspase-9 in the human model.

However, there are also conspicuous differences between the pathways. The biggest of these lies in the mechanisms of CED-4 and Apaf-1 repression and activation. In *C. elegans*, CED-9 directly represses CED-4, and binding of EGL-1 to CED-9 is sufficient to directly allow CED-4 activation. On the other hand, in the human system, anti-apoptotic Bcl-2 family members instead act to guard the integrity of the mitochondrial outer membrane. Their de-repression and the additional activation of Bax/Bak allows the release of cytochrome c from the mitochondria, which activates Apaf-1 oligomerization. In the human system there is therefore an extra level of control exerted over apoptosis activation, at the mitochondria. In addition, both pathways activate an initiator caspase, but in *C. elegans*, this caspase then goes on to cleave downstream target proteins itself while in mammals, the initiator caspase proceeds to cleave downstream effector caspases and initiate a proteolytic activation cascade.

1.7.2 Germline PCD

The somatic cells of *C. elegans* undergo only defined developmental PCDs and are unable to induce cell death in response to environmental cues. The same is not true of all cells in the organism, however. Cells of the *C. elegans* hermaphrodite germline undergo apoptosis physiologically on exiting the pachytene stage of meiosis (Gumienny *et al.*, 1999). These deaths are not invariant, and as well as a degree of physiological death, cells can undergo

programmed death in response to environmental cues. Levels of cell death increase dramatically in response to ionising radiation, for example, suggesting the existence of a DNA damage pathway (Gumienny *et al.*, 1999). These surprising findings indicate that there may be more similarities between apoptotic signalling mechanisms in humans and *C. elegans* than were previously thought, and that the worm might be a good system in which to study DNA damage-induced apoptosis.

Both physiological and DNA damage-induced germline PCD are dependent upon *ced-3* and *ced-4*, and are inhibited by *ced-9*, confirming that these deaths operate through the core cell death mechanism. Damage-induced germline PCD is dependent upon *egl-1* but physiological PCD is not, suggesting that a different induction mechanism must operate here (Schumaker *et al.*, 2004). Transcription of the second BH3-only gene, *ced-13*, is up-regulated upon DNA damage, suggesting that this molecule might play a role in the process, although mutant phenotypes have not yet confirmed this (Schumaker *et al.*, 2004). In DNA damage-induced germline apoptosis an upstream signalling pathway has been intensively studied and several components identified. A damage response complex composed of the DNA damage sensor and repair proteins HUS-1, RAD-5 and MRT-2 appears to be crucial (Gartner *et al.*, 2000; Ahmed and Hodgkin, 2000; Ahmed *et al.*, 2001; Hofmann *et al.*, 2002). Interestingly, downstream of these proteins is a homologue of mammalian p53, CEP-1 (Derry *et al.*, 2001; Schumaker *et al.*, 2001). The homology between p53 and CEP-1 is largely confined to the DNA-binding domain and transcriptional transactivation domain. It appears to operate solely in inducing cell death without a cell cycle arrest function, suggesting that apoptosis induction may be the ancestral activity of p53. CEP-1 does not play a role in the death of somatic cells, but is involved specifically in DNA-damage-induced germline apoptosis. *C. elegans* has therefore become a good model for studying the mechanisms underlying apoptosis induced by DNA damage.

1.7.3 Necrotic cell death

Recent work has also elucidated a sequence of events leading to a necrotic form of cell death in *C. elegans* neurons. This type of death results in the vacuolation, swelling and subsequent lysis of cells, and is therefore very similar to human necrosis (Hall *et al.*, 1997). Study of the pathway holds promise as a model for events causing a similar form of death in human neurodegenerative diseases.

Necrotic cell death can be induced by the expression of constitutively active degenerin channels such as MEC-4 and DEG-1 in touch-receptor neurons (Driscoll and Chalfie, 1991; Hong and Driscoll, 1994). These channels allow an influx of calcium to the cell and cause a subsequent calcium-induced release of calcium from the ER, dependent upon the presence of the calcium-binding ER chaperone calreticulin (Xu *et al.*, 2001; Bianchi *et al.*, 2004). This sudden increase in cellular calcium activates specific aspartyl and calpain proteases that go on to cause cell death, presumably through uncontrolled proteolysis (Syntichaki *et al.*, 2002). An acidic intracellular environment is required for efficient activation of the proteases, and this is dependent upon intact lysosomes and the vacuolar H^+-ATPase (Syntichaki *et al.*, 2005). The identification of this conserved mechanism for this necrotic cell death may be useful in the development of treatments for human neurodegenerative disease; and although it is a non-apoptotic form of death, it underlines the ability and importance of proteases in killing cells.

1.8 DOWNSTREAM OF CASPASE ACTIVATION

1.8.1 Caspase substrates

Upstream events in apoptosis are tightly regulated to ensure that the apoptotic machinery is only activated when appropriate, as mitochondrial permeabilization and caspase activation quickly render the process irreversible. Activation of caspases is the ultimate mechanism of all apoptosis-inducing pathways, and it is this family of enzymes that catalyze directly or indirectly all the subsequent changes that characterize apoptosis. However, although we now know much about the upstream regulation of apoptosis, the downstream demolition phase is still something of a black box, despite its obvious importance in the death process. Although non-specific proteolysis does cause cell death, the physiological importance of specific downstream apoptotic events makes it clear that this mechanism cannot be acting during apoptosis. In order to create such a stereotypical series of cellular events, it makes sense that caspases must cleave specific proteins to create the required phenotype. The packaging of the cell and its phagocytosis, without the release of inflammatory material, for example, is crucially important to the health of the body and must be tightly regulated. It should therefore be possible to pinpoint key substrate cleavages responsible for conserved events in apoptosis.

However, although there are a bewildering number of caspase substrates identified, very few of these cleavage events are known to be of any significance (Fischer and Schulze-Osthoff, 2003). On the basis of these few significant substrates, cleavage events can be divided into three broad categories (Figure 1.11). In the first of these categories, proteolysis of a substrate may lead to amplification of caspase activation. For example, the cleavage of Bid allows it to bind and activate Bax, feeding into the mitochondrial apoptosome pathway (Li *et al.*, 1998; Luo *et al.*, 1998). The second category of substrate cleavages activate a protein, either conferring a new function or enhancing its usual activity. Cleavage of PAK-2, for example, has been suggested to separate its N-terminal regulatory domain from its C-terminal catalytic domain, leading to constitutive activation and therefore contributing to cytoskeletal changes (Rudel *et al.*, 1997).

The third group of cleavage events comprise those resulting in protein inactivation. These inactivation events can be further subdivided into four categories. Firstly, inactivation of an inhibitory protein can lead to the subsequent activation of the protein that is normally inhibited. A classic example is the cleavage of the ICAD inhibitor, allowing CAD (caspase-activated DNase) to catalyse DNA fragmentation (Sakahira *et al.*, 1998). Secondly, loss of function of a protein can lead in itself to cellular changes - cleavage of a cytoskeletal protein, for example, could cause loss of cytoskeletal structure, cell rounding and detachment. Inactivation of cellular repair factors, thirdly, prevents futile attempts to repair the damage done by caspases. And finally, the cleavage and loss of function of proteins essential for viability contributes to the irreversibility of the apoptotic process once initiated.

However, many substrate cleavage events do not seem to play any important role in the progress of apoptosis. These proteins can perhaps best be thought of as "innocent bystanders" caught in the crossfire of proteolysis, that merely through chance possess an exposed caspase cleavage sequence. These random cleavage events make it harder to identify those cleavages that actually are important to mediate the events of the demolition phase of apoptosis.

1.8.2 Downstream events in apoptosis

Despite these problems, some of the characteristic downstream events in apoptosis have been linked to the cleavage of a specific protein substrate. DNA

laddering, for example, was one of the first biochemical features of apoptosis to be described. During apoptosis, inter-nucleosomal cleavage of chromatin results in the production of a series of chromatin fragments that can be resolved into a ladder-like pattern on agarose gels. This DNA cleavage is caused by the activation of a specific DNase, CAD, as mentioned above. The activation of CAD is mediated by the caspase-3-mediated cleavage of the CAD inhibitor, ICAD (Enari *et al.*, 1998). In addition, cleavage of the DNA repair protein PARP prevents the cell attempting to repair this damage in an energy-depleting manner (Los *et al.*, 2002). The entire nucleus is then dismantled, an event coordinated by the cleavage of nuclear matrix and laminal substrates. Caspase-6-mediated proteolysis of lamins contributes to this breakdown of the nuclear lamina (Rao *et al.*, 1996). During apoptosis, other cell organelles are also dismantled for packaging into apoptotic bodies – for example, the breakdown of the Golgi apparatus, which may be caused by the proteolysis of golgin-160 and GRASP65 (Mancini *et al.*, 2000; Lane *et al.*, 2002).

Membrane dynamics are another classical feature of apoptosis. The cell's plasma membrane undergoes a ruffling movement that becomes increasingly pronounced, until the cell fragments into small pieces called apoptotic bodies. Actin cytoskeleton dynamics are crucial to these processes, and cleavage of several substrates have been limplicated. The proteolysis of gelsolin may cause its constitutive activation, enabling it to depolymerize F-actin (Kothakota *et al.*, 1997). In addition, the cleavage of ROCK 1, a kinase, also causes its constitutive activation, leading to myosin light chain phosphorylation and actin contraction (Sebbagh *et al.*, 2001; Coleman *et al.*, 2001). The cleavage and constitutive activation of another kinase, PAK-2, appears to be involved in apoptotic body formation (Rudel and Bokoch, 1997).

1.8.3 Phagocytosis

The ultimate consequence of these apoptotic changes is to package the cell up into components that can be consumed by phagocytes. However, how caspases induce phagocytosis itself is not well understood. Although, in general, much less is known about downstream events in *C. elegans* programmed cell death than in human apoptosis, studies into phagocytosis in *C. elegans* have advanced more rapidly than those in human systems, suggesting pathways and molecules that

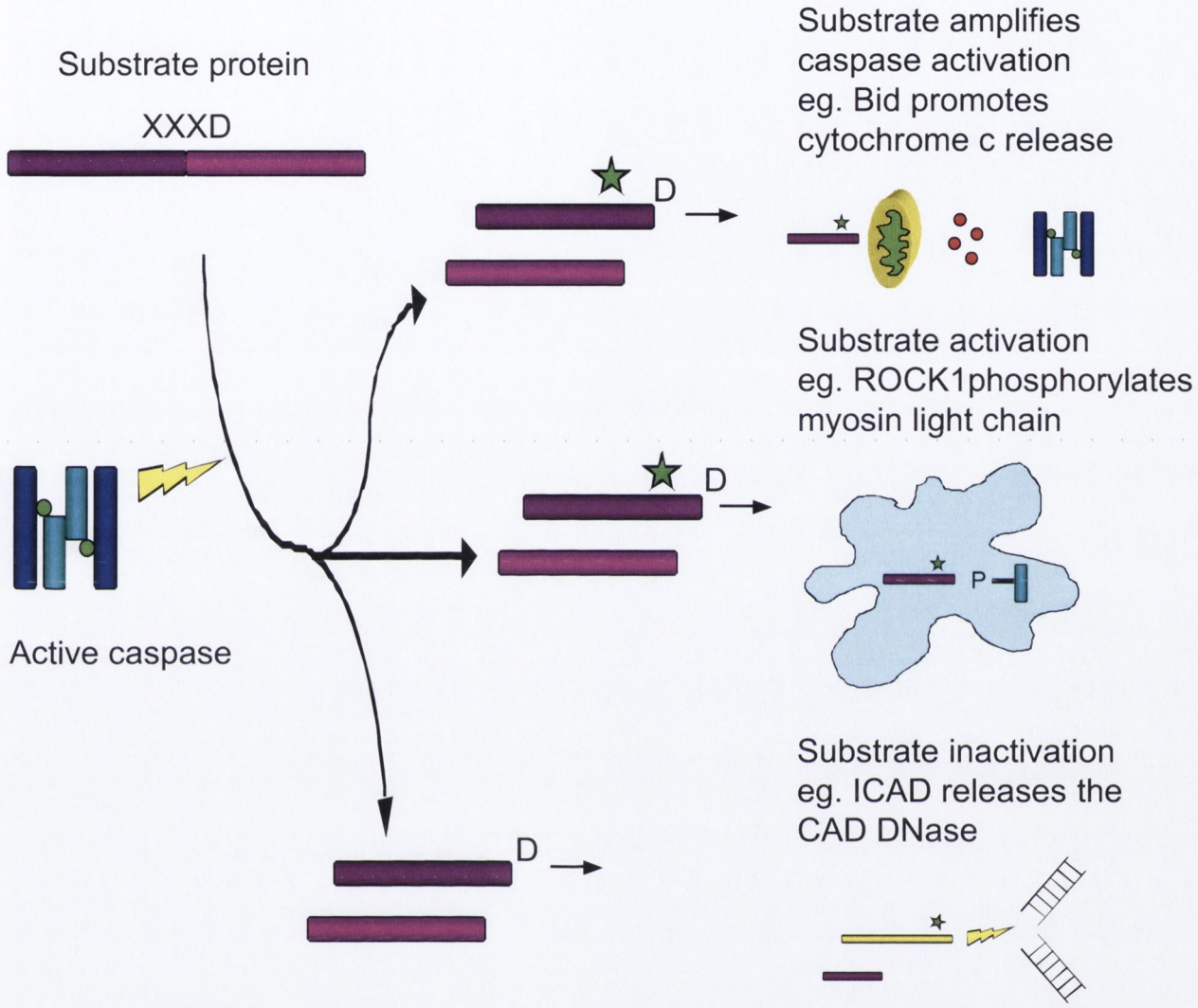

Figure 1.11
Caspase substrate cleavage
Schematic of effects of caspase cleavage on substrate proteins. Caspases cleave substrates at tetrapeptide motifs containing an aspartic acid residue at the P1 position. This proteolysis can have three effects: proteins can go on to amplify the caspase activation cascade, in a positive-feedback loop; proteins can become constitutively active; or proteins can become inactivated.

may co-ordinate phagocytosis (Mangahas and Zhou, 2005). Several genes involved in the *C. elegans* engulfment pathway have been identified through genetic analyses. *ced-1*, *ced-2*, *ced-5*, *ced-6*, *ced-7*, *ced-10*, and *ced-12*, were identified in screens for cell death defective mutants (Hedgecock *et al.*, 1983; Ellis *et al.*, 1991b; Zhou *et al.*, 2001). *ced-12* was also independently identified in several other screens (Nishiwaki, 1999; Chung *et al.*, 2000; Wu *et al.*, 2001). Following loss of function mutations in all these genes, neighbouring cells fail to complete engulfment of dying cells at the appropriate time, although the majority of cell corpses are phagocytosed later in development. However, some double engulfment gene mutants exhibit a more severe phenotype and fail entirely to engulf dead cells, which persist to adulthood. This suggests that the two genes may act in different engulfment pathways that cooperate in the induction of phagocytosis. Using this type of analysis, the engulfment genes could be grouped into two sets, suggesting the existence of two independent phagocytic pathways (Ellis *et al.*, 1991b; Zhou *et al.*, 2001; Wu *et al.*, 2001; Gumienny *et al.*, 2001). One group consists of *ced-1*, *-6* and *-7*, while the other is made up of *ced-2*, *-5*, *-10* and *-12*. Both these pathways appear to act in parallel in all programmed cell deaths that occur during *C. elegans* development and in the germline. More surprisingly, they also both appear to be required for the engulfment of cells dying by necrosis, suggesting that the same or similar phagocytic ligands, for example those detected by CED-1, must be exposed in both types of death (Chung *et al.*, 2000). Engulfment of necrotic cells is, however, somewhat slower in kinetics.

The *ced-2/ -5/ -10/ -12* pathway is the more substantially elucidated of the two (Figure 1.12). This pathway is also involved in cell migration and seems to regulate the formation of membrane extensions. *ced-5* and *ced-2* act upstream to and control the activity of *ced-10*, the *C. elegans* Rac homologue and a member of the Rho/Rac/Cdc42 family of small GTPases that regulate cytoskeletal dynamics (Reddien and Horvitz, 2000). *ced-5* and *ced-2* encode homologues of human DOCK180 and CrkII, respectively, both proteins that regulate membrane extensions in human cells, and physically interact (Wu and Horvitz, 1998; Reddien and Horvitz, 2000). CED-12, a homologue of three human proteins, ELMO1, ELMO2, and BAB14712, also interacts with CED-5, forming a tripartite complex (Zhou *et al.*, 2001; Wu *et al.*, 2001; Gumienny *et al.*, 2001). CED-2 may recruit CED-5/CED-12 to the plasma membrane, where CED-5/CED-12 may act as a

bipartite GNEF for CED-10. CED-10 then appears to regulate the actin cytoskeleton to coordinate corpse uptake (Kinchen *et al.*, 2005). However, these genes all act within engulfing cells, and it is unclear how they are activated by external signals, no receptor for the pathway being known.

The receptor in the second pathway, involving *ced-1/ -6/ -7*, is encoded by *ced-1* (Figure 1.12). CED-1 is a homologue of human scavenger receptors, which have been implicated in phagocytosis of apoptotic human cells (Zhou *et al.*, 2001). It localises to cell membranes and contains an extracellular EGF-like-repeat-containing extracellular domain, a transmembrane domain, and a novel intracellular domain. Although no ligand has yet been identified, CED-1 is known to function in engulfing cells, and clusters around cell corpses. CED-7 is required for this clustering (Zhou *et al.*, 2001). A membrane-localised homologue of human ABC transporters that mediate ATP-dependent translocation of substrates across membranes, CED-7 is required within engulfing cells, and is also the only gene known to be required within dying cells to mediate phagocytosis (Wu and Horvitz, 1998b). The adapter protein CED-6, a homologue of human GULP, binds to the intracellular domain of CED-1, a region required not for apoptotic cell recognition but for engulfment (Liu and Hengartner, 1998; Su *et al.*, 2002). This pathway converges with CED-2/ -5/ -10/ -12 at CED-10, to co-ordinate reorganization of the actin cytoskeleton (Kinchen *et al.*, 2005). However, again, the signal present on the apoptotic cell required to activate the CED-1 receptor is unknown.

Intriguingly, two studies have suggested that engulfment genes may play a role in promoting cell death (Reddien *et al.*, 2001; Hoeppner *et al.*, 2001). In weak *ced-3* or *ced-4* mutants, in which some cells that would normally undergo programmed cell death are able to survive, mutations in engulfment genes allow increased cell survival (Reddien *et al.*, 2001; Hoeppner *et al.*, 2001). This death-promoting activity seems to arise from the engulfing cell, as mosaic analyses inducing expression of CED-1 only in engulfing cells rescues the extra survival seen in *ced-1:ced-3* mutants. It does however depend upon the existence of some CED-3 activity in the dying cell (Reddien *et al.*, 2001). In addition, mutants in engulfment genes in a wild-type background cause a low level of failure in cell death. These results suggest that engulfment genes may promote the irreversibility of the cell

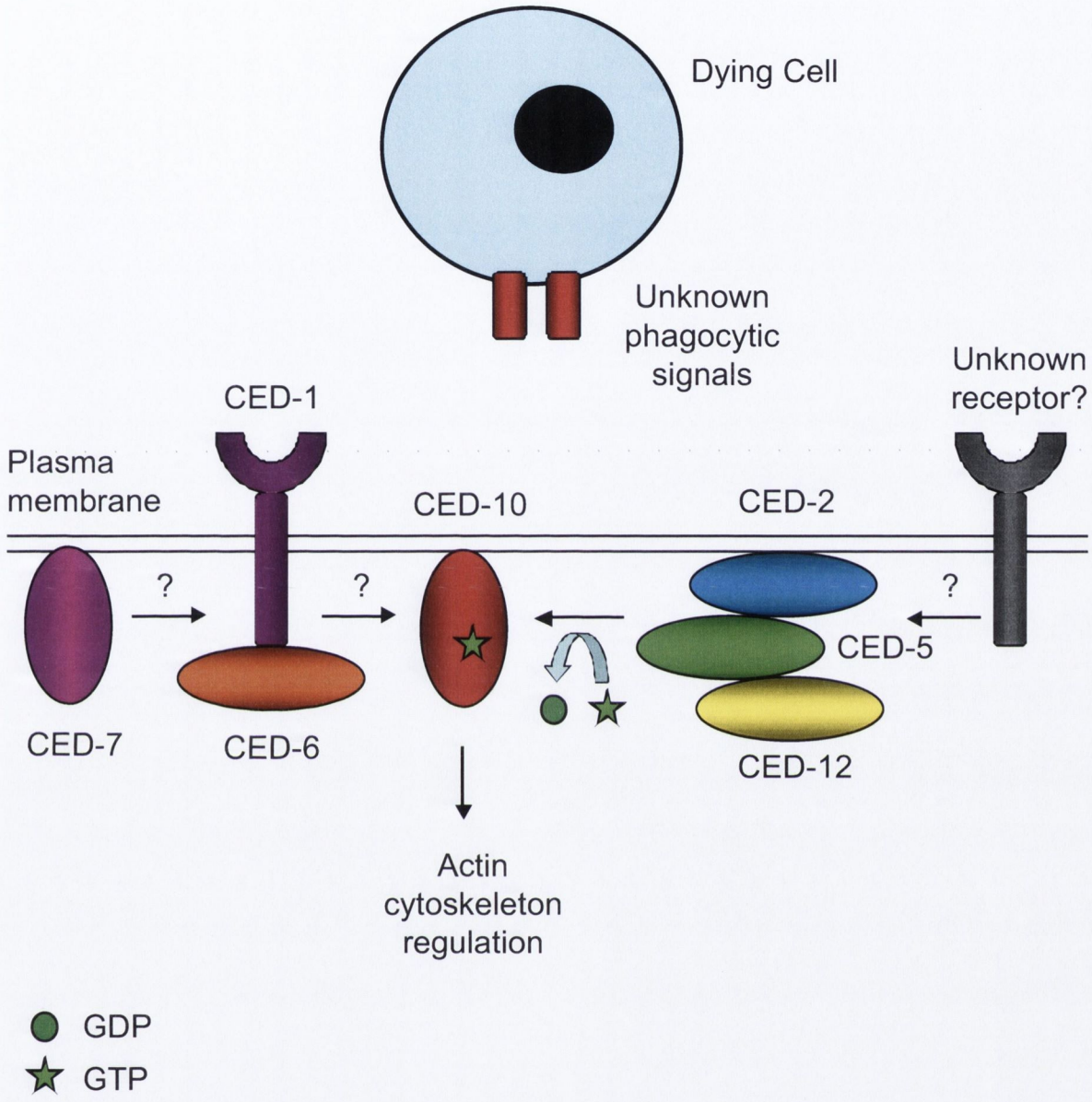

Figure 1.12

Phagocytosis in *C. elegans*.

Phagocytosis of dead cells involves two pathways that converge at CED-10. The CED-1 receptor may recognise an unknown ligand on dying cells. It is able to bind to CED-6. CED-7, an ABC transporter homologue, is also required in this pathway, which leads to the downstream activation of the Rac homologue CED-10, which regulates the actin cytoskeleton. In the second pathway, ligation of an unknown receptor may lead to the recruitment to the plasma membrane of CED-5 and CED-12 by CED-2. CED-5/CED-12 act as a bi-partite GEF for CED-10.

death process in at least some cases, though how this might occur, and how cell death can be reversed once CED-3 is activated, is not understood.

In human cells, a confusing variety of molecules have been implicated as "eat-me" signals on apoptotic cells, and as receptors on phagocytes, without a clear understanding of how these various molecules and pathways interact (Savill and Fadok, 2000; Lauber *et al.*, 2004). The best known of the "eat me" signals is the phospholipid phosphatidylserine, which translocates from the inner to the outer plasma membrane of apoptotic cells in a caspase-dependent manner (Fadok *et al.*, 1992; Martin *et al.*, 1995; Martin *et al.*, 1996b). The mechanism responsible for this phenomenon is still unclear, but it has been suggested that the ABC1 transporter is able to direct this translocation and is also required in phagocytic cells, acting therefore similarly to its *C. elegans* homologue, CED-7 (Hamon *et al.*, 2000). Other "eat-me" signals are only poorly characterized, and include changes in surface sugars, binding sites for "bridging" molecules such as complement C1q, oxidised low-density lipoproteins, and the Ig superfamily member ICAM-3. Recently, the phospholipid lysophosphatidylcholine was found to be released from apoptotic cells in a caspase-3-dependent manner, mediating attraction of phagocytic cells (Lauber *et al.*, 2003). This is the first reported example of an apoptotic "find-me" signal for phagocytes requiring caspase activity in the dying cell.

In contrast, we have a better knowledge of the phagocyte receptors that recognise human cell corpses (Savill and Fadok, 2000). Phagocyte surface CD14 and β_2 integrins may be able to tether to apoptotic cells and recruit the CrkII-DOCK180-Rac1 signalling module that is also activated in *C. elegans*. In addition, several scavenger receptors have been implicated in the detection of dying cells, including SREC and CD91, both homologous to *C. elegans* CED-1. At least one of these scavenger receptors, CD36, may be able to interact with GULP, the homologue of CED-6. There does also appear to be a receptor specific for detection of phosphatidylserine, but the identity of this receptor is as yet unknown (Fadok *et al.*, 2000). However, exposure of phosphatidylserine might also cause the ligation of phagocyte CD36, CD68, CD14, or LOX-1, or the binding of a "bridging" receptor.

1.8.4 Caspase substrates in *C. elegans*

If knowledge of the roles of caspase substrates in the demolition phase of apoptosis is confused in the human system, it is an entirely blank slate in the nematode. How CED-3 co-ordinates downstream events is almost entirely unknown. Although cleavage of a few proteins has been shown *in vitro*, including CED-9 and CED-3 itself (Xue and Horvitz, 1995; Xue and Horvitz, 1997; Kim *et al.*, 2004), the physiological relevance of these proteolytic events (with the exception of CED-3 autoproteolysis) is unclear. We also know little about many other aspects of CED-3 activation and activity, such as its manner of binding to CED-4 and its sub-cellular localization. Given the intensive study of cell death in the nematode and the contribution that this work has made to our understanding of cell death, these gaps are surprising.

With all the additional complexities that exist in studying apoptosis in the human system, there is a lot of value in returning to the *C. elegans* model to study the execution phase of cell death. The core death machinery in the worm is well-defined, and a single caspase is essential for all cell deaths. This is a significant advantage in studying caspase substrates. A single caspase is likely to cleave fewer cellular proteins than the panoply of caspases active during apoptosis in mammalian cells. Despite this, worm cells still die showing most of the characteristic apoptotic changes occurring in human cells. The necessary cleavage events must therefore still be occurring within this smaller set of substrates, suggesting that it might be easier to identify the important proteins from among the substrate pool. The lack of additional caspases also makes it easier to study substrates without the issue of redundancy, whereby several caspases may cleave the same protein, or different proteins with similar functions. The ability to compare *C. elegans* with human caspase substrates would also allow the identification of those substrate cleavages that have been conserved through evolution, increasing the likelihood of spotting critical cleavage events.

C. elegans remains an extremely genetically tractable model. The availability of a variety of mutants, and the ease with which genes may be knocked down by RNAi, facilitates the inactivation or alteration of caspase substrates for analyses into their possible function. It is also comparatively facile to generate transgenic animals, making it possible to overexpress non-cleavable or truncated substrates in order to

investigate their roles in the death programme. Using these techniques, cell death can be studied in the worm in a physiological setting. Apoptotic events can be studied in a natural context, and the effects of cell death regulation on a whole organism can be seen. There are also two apoptotic programmes occurring, somatic developmental death and physiological or environmentally-induced germline cell death, allowing the study of different apoptotic pathways. The reproducible nature of developmental PCDs and the availability of phagocytic mutants to prevent corpse removal makes it relatively easy to identify effects increasing or decreasing the number of cells dying in the organism.

1.9 THESIS AIMS

1.9.1 Overall aims

Because activated caspases are the downstream effectors of all apoptotic pathways, understanding which proteins are cleaved by caspases and how these cleavages affect protein function is crucial to understanding how important downstream events such as phagocytosis are regulated. While in human cells we are aware of many caspase substrates but often have little idea of their functions, in *C. elegans* there are almost no CED-3 substrates known. However, *C. elegans* has many advantages, as well as a long history, as a model organism in which to study programmed cell death. Studying CED-3 activity, identifying its substrates and examining the functional outcomes of their cleavage could therefore be a very useful way to increase our knowledge of the important events of the execution phase of apoptosis, in mammalian as well as worm cells.

This study therefore addressed the characterization of the CED-3 enzyme, and the identification and functional analysis of its substrates. To achieve this, we first aimed to purify and characterize recombinant CED-3, to learn more about its enzymatic activity and to generate sufficient enzyme to use in a substrate identification screen. The next aim of the project was to use a proteomic approach involving 2D SDS-PAGE and mass spectrometry to identify substrates of recombinant CED-3 in *C. elegans* extracts. In this way, we hoped to identify caspase substrates that are conserved between worms and man. We then aimed to validate that these proteins are genuine substrates of CED-3, and to identify their cleavage sites. Finally, an important aim of the study was to functionally

analyse substrate proteins in both human and *C. elegans* cells, to define the role of their cleavage during programmed cell death.

1.9.2 Chapter III: Generation and characterization of recombinant CED-3

The aim of this first phase of the project was to generate sufficient quantities of recombinant CED-3 for use in proteomic analysis. To achieve this, we tried a range of methods, including expression in both bacterial and human cells, refolding of insoluble enzyme, and *in vitro* transcription/ translation. We ultimately achieved a sufficient yield of protease by expressing GST-CED-$3^{221-503}$ in bacterial cells under low temperature conditions. This enzyme showed a similar DEVD peptide substrate preference to human caspase-3, although it was more promiscuous than that enzyme, and was able to cleave the *C. elegans* substrates CED-3 and CED-9.

1.9.3 Chapter IV: Proteomic identification of CED-3 substrates

The aim of the second part of this study was to use recombinant CED-3 to identify its substrates in *C. elegans*, and to confirm that these proteins are genuine substrates of CED-3. We developed a system to generate soluble protein extracts from populations of *C. elegans*, and added recombinant CED-3 to these to allow it to cleave substrate proteins. CED-3-treated extracts were analysed first by 1D SDS-PAGE and then by 2D SDS-PAGE, and a subset of the proteome was found to undergo CED-3-dependent alteration. Mass spectrometry was used to find the identity of these altered proteins, and 22 identifications were obtained. The wide range of cellular roles played by these substrate proteins suggests that CED-3 kills cells by targeting multiple cellular functions. We then used Western blotting and *in vitro* substrate synthesis analysis to validate our screen by showing that four substrates genuinely undergo CED-3-mediated proteolysis. We then identified cleavage sites in three substrate proteins, FTT-2, TBB-2 and CRT-1.

1.9.4 Chapter V: Functional analysis of CED-3 substrates

The third part of this work aimed to identify functional roles of the cleavage of CED-3 substrates. We made constructs for the generation of transgenic nematodes able to over-express wild-type and cleavage-resistant FTT-2, TBB-2 and CRT-1, but none of these nematode lines had an overt apoptotic phenotype. We then confirmed that the human homologues of FTT-2, TBB-2 and CRT-1 are

cleaved by caspases. Over-expression of FTT-2, CRT-1 and human calreticulin had no effect on apoptosis, while knockdown of alpha-tubulin with siRNAs induced a low level of spontaneous cell death but had no effect on the kinetics or morphology of apoptotic cells treated with several stimuli. We then found that in apoptotic cells, calreticulin can be detected on the cell surface, where it has been reported to act as a ligand for phagocytes (Gardai *et al.* 2005). This translocation proved to be a general feature of apoptosis, and is inhibited by the over-expression of Bcl-2 or by inhibition of caspases with z-VAD-fmk, suggesting that it might be caused by caspase-mediated cleavage of calreticulin. Calreticulin may therefore represent a conserved caspase substrate which translocates to the surface of dying cells, where it induces cell engulfment.

CHAPTER II

Materials and Methods

2.1 REAGENTS

2.1.1 Chemicals and general reagents

The peptides z-VAD-fmk, Ac-DEVD-AFC, Ac-LEHD-AFC, Ac-IETD-AFC and Ac-YVAD-AFC were all purchased from Bachem (UK). 17 cm IPG strips (pH 3-6 and pH 5-8), easymelt agarose and Bio-Lyte ampholytes™ were purchased from Biorad (UK). TPCK and DCI were purchased from Merck (UK). Unless otherwise indicated, all other reagents were purchased from Sigma (Ireland) Ltd.

2.1.2 Enzymes

Unless otherwise stated, enzymes were obtained from New England Biolabs (NEB, UK).

2.1.3 Antibodies

The following antibodies were obtained from the indicated sources:

α-FLAG M2	Sigma Aldrich
α-His	Novagen
α-GST	BD Pharmingen
α-CED-3 B1	Generated by this laboratory
α-CED-3 p17	Generated by this laboratory
α-CED-3 C20	Santa Cruz Biotechnology
α-caspase 2	BD Transduction Laboratories
α-caspase 3	BD Transduction Laboratories
α-caspase 6	Upstate Biotechnology
α-caspase 7	BD Pharmingen
α-caspase 8	Apotech
α-caspase 9	Oncogene Research products
α-caspase 10	Upstate Biotechnology
α-actin	ICN Biomedicals
α-alpha-tubulin	ICN Biomedicals
α-beta-tubulin	ICN Biomedicals
α-XIAP	BD Transduction Laboratories
α-calreticulin (pAb)	Affinity Bioreagents
α-calreticulin (mAb)	BD Transduction Laboratories

α-mouse-HRP Jackson Laboratories

α-rabbit-HRP Jackson Laboratories

α-mouse-AlexaFluor488 Molecular Probes

α-rabbit-AlexaFluor488 Molecular Probes

2.2 PURIFICATION AND MANIPULATION OF NUCLEIC ACIDS

2.2.1 Bacterial strains

E. coli strain DH5α was used to amplify plasmid DNA.

2.2.2 Preparation of competent bacteria

Bacteria competent for DNA transformation were typically prepared by the Inoue method (Inoue *et al.,* 1990). DH5α bacteria were streaked onto LB agar (10 g/ L tryptone (BD), 5 g/ L yeast extract (BD), 10 g/ L NaCl, 15 g/ L agar (BD)). Single colonies were used to inoculate overnight 3 ml cultures in liquid LB (10 g/ L tryptone (BD), 5 g/ L yeast extract (BD), 10 g/ L NaCl). The following day, overnight cultures were diluted into 50 ml of SOB medium (2 % tryptone (BD), 0.5 % yeast extract (BD), 10 mM NaCl, 2.5 mM KCl, 10 mM $MgCl_2$, 10 mM $MgSO_4$) to give an OD_{600} of 0.1 AU. Cultures were grown at room temperature to an $0D_{600}$ of 0.4 - 0.6 AU. Cells were then harvested by centrifugation at 2,500 g for 10 minutes. After resuspension in 20 ml of transformation buffer (10 mM Pipes, 55 mM $MnCl_2$, 15 mM $CaCl_2$, 250 mM KCl, pH 6.7), cells were incubated for 10 minutes on ice. Centrifugation was repeated and cells resuspended in a further 4 ml of transformation buffer. DMSO was added to a 7 % final concentration and the cells incubated for 10 minutes on ice. Cells were then divided into 200 μl aliquots and frozen at –70 °C.

2.2.3 Transformation of competent bacteria

Plasmid DNA was transformed into competent bacteria by heat shock. Bacteria were thawed and 50 μl dispensed into 13 ml culture tubes. 1 μl of plasmid was added and cells incubated on ice for 30 minutes. Cells were then heat-shocked for 40 seconds at 42 °C and transferred to ice for 2 minutes. 450 μl of LB was added to the cells followed by incubation in a 37 °C shaker incubator at 220 rpm for 1 hour. 20 μl was then plated on LB agar with an appropriate antibiotic and incubated overnight at 37 °C.

2.2.4 Plasmid purification

(i) Miniprep procedure

Single colonies from plates of transformed bacteria were inoculated into 3 ml of LB with antibiotic and grown in a 37 °C shaker incubator overnight. 1 ml of each culture was pelleted at 20,800 g for 1 minute in a microfuge. Cell pellets were resuspended in 100 μl of buffer P1 (50 mM Tris-HCl, pH 8, 10 mM EDTA) and bacteria were lysed with 200 μl of buffer P2 (0.2 M NaOH, 1 % SDS) for 1 minute on ice. 200 μl of buffer P3 (3 M KAc, pH 5.5) was added and incubated for 3 - 5 minutes on ice to precipitate genomic DNA. Precipitated DNA was removed by a 15 minute centrifugation at 20,800 g. Plasmid DNA was precipitated by adding 0.7 x volumes of isopropanol and incubating for 20 - 30 minutes at room temperature. DNA was pelleted for 10 minutes at 20,800 g and washed in 1 ml of 70 % ethanol. Centrifugation was repeated and the pellet air-dried. DNA was then solubilized in 20 μl of 0.5 x TE (10 mM Tris-HCl, 1 mM EDTA, pH 8).

(i) Midiprep procedure

50 μl of a 3 ml bacterial culture was inoculated into 50 ml of LB with antibiotic and grown in a 37 °C shaker incubator overnight. The following day, the culture was pelleted at 5000 g for 15 minutes. The cell pellet was resuspended in 4 ml of buffer P1. Bacteria were lysed with 4 ml of buffer P2 for 1 minute on ice. 4 ml of buffer P3 was added and incubated for 3 - 5 minutes on ice to precipitate genomic DNA. Precipitated DNA was removed by 15 minutes centrifugation at 15,000 g. The supernatant was then passed through a Qiagen Q100 column equilibrated with 4 ml of Qiagen QBT buffer (750 mM NaCl, 50 mM MOPS, pH 7.0, 15 % isopropanol, 0.15 % Triton X-100). DNA bound to the column was washed with 2 x 10 ml volumes of Qiagen QC buffer (1 M NaCl, 50 mM MOPS, pH 7, 15 % isopropanol) and then eluted from the column with 5 ml of Qiagen QF buffer (1.25 M NaCl, 50 mM Tris-HCl, pH 8.5, 15 % isopropanol). Plasmid DNA was precipitated from the eluate by adding 0.7 x volumes of isopropanol and incubating for 20 - 30 minutes at room temperature. DNA was pelleted for 20 - 30 minutes at 15,000 g, washed in 2 x 1 ml volumes of 70 % ethanol, and pelleted for 10 minutes at 15,000 g. The pellet was air-dried and solubilized in 200 μl of 0.5 x TE.

2.2.5 Agarose gel electrophoresis

DNA yield was typically assessed by electrophoresis through agarose gels alongside a ladder of marker DNA fragments of known sizes. Agarose suspensions of 0.6 % or 1 % agarose were prepared in TAE (40 mM Tris-HCl, pH 8, 1 mM EDTA), melted by microwaving, and solidified in gel casting rigs. DNA was diluted in loading buffer and electrophoresed through the gel at 50 V. Gels were incubated an ethidium bromide solution for 20 minutes and visualised in a Biorad Gel Doc 2000 system.

2.2.6 DNA quantitation

DNA was accurately quantitated by spectrophotometry. Double-stranded DNA was diluted 1:200 in ddH_2O and triplicate readings of $OD_{260/280}$ measured in a quartz cuvette using a Bio-Rad spectrophotometer.

2.2.7 Genecleaning procedure

(i) Genecleaning from solution

Genecleaning was conducted primarily to generate ultra-pure DNA for cloning. To purify nucleic acids from solution, 3 x volumes of 6 M NaI were added to the DNA followed by 5 µl/ µg silica (100 mg/ml suspension in 3 M NaI). The suspension was incubated under rotation at room temperature for 10 minutes to allow DNA to bind to the silica. The silica-bound DNA was pelleted for 5 seconds at 20,800 g and washed in 5 x 500 µl volumes of wash buffer (10 mM Tris-HCl, pH 7.5, 50 mM NaCl, 2.5 mM EDTA, 50 % ethanol). The silica pellet was finally air-dried for 5 minutes and DNA eluted into ddH_2O or 0.5 x TE.

(ii) Genecleaning from agarose gels

For purification of nucleic acids from agarose gels, the gels were stained with ethidium bromide, visualized under UV and the required DNA band excised. A 3 x volume of 6 M NaI was added to each gel slice and incubated at 55 °C until the gel was melted. 5 µl/ µg silica was added and the genecleaning procedure continued as described above.

2.2.8 Restriction digests

DNA was digested using restriction endonucleases, following the manufacturers instructions (NEB UK).

2.2.9 DNA ligation reactions

For gene cloning, DNA fragments were ligated following endonuclease digestion. Typically, 200 ng of digested vector was incubated with a 2:1 molar ratio of digested insert DNA. DNA was brought to 8.5 μl with ddH_2O and incubated for 5 minutes at 45 °C to melt re-annealed DNA ends. T4 DNA ligation buffer was added according to manufacturers instructions, followed by T4 DNA polymerase. Ligation reactions were incubated for 1 – 4 hours at 16 °C.

2.2.10 PCR

PCR reactions were carried out to amplify genes for cloning, and to confirm successful insertion of a gene into a vector. PCR reaction volumes were typically 100 μl. The DNA polymerase used for amplification was Taq (Qiagen), at 2.5 units per reaction. Other reaction constituents were:

- 100 - 500 ng of Qiagen-purified template DNA
- Taq buffer from a 10 x stock supplied by the manufacturer
- 200 μM dATP, dTTP, dCTP, dGTP
- 100 - 200 nM forward and reverse oligonucleotide primers, typically incorporating restriction sites for cloning purposes

Reactions were then put through a PCR programme involving:

-	initial denaturing:	3 minutes 94 °C	
-	30-35 cycles of:	*denaturation*	1 minute 94 °C
		annealing	1 minute 55 - 60 °C
		elongation	1 minute/ kB 72 °C
-	final elongation:	10 minutes 72 °C	

2.2.11 Site-directed mutagenesis

Site-directed mutagenesis was carried out using the Quickchange kit (Stratagene). Primers were designed to incorporate the desired mutation in both forward and reverse strands. Reactions were carried out in a 25 μl volume. The enzyme used was the Pfu Turbo polymerase. Reactions were assembled as follows:

- 0.75 μl of template plasmid DNA at 50 ng/ μl
- 2.5 μl Pfu buffer from 10 x stock
- 2.5 μl dNTPs at 2.5mM
- 0.75 μl forward and reverse primers at 10 μM

Typically an aspartic acid residue was mutated to a glutamic acid residue by mutation of the coding GAT or GAC sequence to GAG. All plasmids were verified by DNA sequencing.

2.3 PROTEIN PRODUCTION

2.3.1 Induction of fusion proteins in bacteria

(i) Induction of His-tagged proteins

His-tagged proteins were expressed from the pET15b and pET45b vectors, which encode an N-terminal His^6 tag and contain a T7-driven promoter sequence. To express His-tagged proteins for purification, plasmids encoding the tagged protein were transformed into *E. coli* BL21 DE3 pLysS bacteria that contain an inducible T7 polymerase gene. Transformed bacteria were inoculated to 3 ml cultures in LB with antibiotic. After overnight growth in a 37 °C shaker incubator, cultures were diluted to between 50 ml and 5 L in LB with antibiotic, to give an OD_{600} of 0.1. Cultures were then incubated in a 37°C shaker incubator until bacteria reached an OD_{600} of 0.4 - 0.6. IPTG was then added to a final concentration of 600 μM -1mM. Cultures were incubated at 25 - 37 °C in a shaker incubator, typically for 3 hours. After induction, cells were pelleted at 5000 g for 10 minutes.

(ii) Induction of FLAG-tagged proteins

Flag-tagged protein was expressed from the pET3a vector as described above.

(iii) Induction of GST-tagged proteins

GST-tagged protein was expressed from the pGEX4TK2 vector, which encodes an N-terminal GST tag. Plasmids encoding the tagged protein were transformed into DH5α bacteria. Bacteria were cultured as described above and expression induced with 100 μM IPTG. Bacteria were incubated and harvested as described above.

2.3.2 Purification of fusion proteins expressed in bacteria

(i) Purification of His-tagged proteins

Pellets of bacteria induced to express His^6-tagged protein were frozen at –20 °C for 1 hour or overnight. Cells were then thawed and resuspended in TM lysis buffer (50 mM Tris-HCl, pH 8.5, 10 mM β-mercaptoethanol, 1 mM PMSF, 2 µg/ ml aprotonin, 10 µg/ ml leupeptin) at 2 % of the original culture volume. For His-CED-3 room temperature inductions, cells were lysed in CED-3 lysis buffer (100 mM Tris-HCl, pH 8, 100 mM NaCl, 0.5% NP40, 1 mM PMSF, 2 µg/ ml aprotonin, 10 ug/ ml leupeptin) at 4 % of the original culture volume. Resuspended bacteria were lysed by sonication using 6 x 30 second pulses at 58 W in a Branson sonifier. Insoluble material was removed by centrifugation at 15,000 g for 15 minutes. Supernatant was then incubated with 2.5 - 50 µl/ ml Ni-NTA agarose (Qiagen) on a rotating platform at 4 °C for 4 hours or overnight. Purified protein conjugated to resin was washed in 3 x 1 ml volumes of wash buffer (20 mM Tris-HCl, pH 8.5, 10 mM β-mercaptoethanol, 10 % glycerol, 20 mM imidazole) and finally resuspended to a 50 % slurry in protease reaction buffer (PRB; 50 mM HEPES, pH 7.4, 75 mM NaCl, 0.1 % CHAPS, 2 mM DTT). Protein was eluted from resin by incubation with equal volumes of PRB containing 100 - 500 µM imidazole, rotating for 30 minutes per elution at 4 - 37 °C.

(ii) Purification of FLAG-tagged proteins

Bacteria induced to express FLAG-tagged protein were lysed as described above. α-FLAG agarose was generated by incubation of protein A/G agarose with 10 µg of α-FLAG M2 antibody (in 200 ml PBS) for 2 hours at 4 °C. α-FLAG agarose was added to bacterial supernatants and incubated under rotation at 4 °C overnight. Protein was then washed and resuspended as above.

(iii) Purification of GST-tagged proteins

Bacteria induced to express GST-tagged proteins were brought up in NETN buffer (20 mM Tris-HCl, pH 8, 100 mM NaCl, 1 mM EDTA, 0.5 % NP40) at 2 % of the original culture volume. Cells were lysed by sonication as described above. Protein was captured from cell supernatants on 10 - 20 µl/ ml glutathione sepharose resin under rotation at 4 °C overnight. Purified protein was then washed in 4 x 1 ml volumes of PBS and 1ml of PRB, and finally brought up to a 50 % slurry in PRB. Protein was then eluted by incubation

in 3 x 0.5X volumes of PRB containing l0 mM glutathione, under rotation at room temperature.

2.3.3 Preparation of purified inclusion bodies

To prepare purified bacterial inclusion bodies, cells were induced to express His-tagged proteins and then lysed by sonication, as described above. The insoluble fraction remaining after centrifugation was resuspended in 80 ml of 50 mM Tris-HCl, pH 7.5, and rotated at room temperature for 30 minutes. Following centrifugation at 15,000 g for 15 minutes, protein was resuspended in a further 80 ml of 50 mM Tris-HCl, pH 7.5, and rotated at room temperature for 30 minutes. Protein was finally pelleted at 15,000 g for 15 minutes.

2.3.4 Refolding of insoluble proteins from inclusion bodies

To solubilize insoluble protein, purified inclusion bodies were resuspended at 20 mg/ ml in denaturing buffer (50 mM Tris-HCl, pH 7.5, 20 mM DTT, 6 M guanidine-HCl) and incubated on a rotating platform at room temperature for 6 hours. The solution was then centrifuged at 20,800 g for 15 minutes to remove residual insoluble material. Refolding was carried out in buffers supplied with the FoldIt™ Protein Refolding Kit (Hampton Research, USA). Buffer additives were mixed according to manufacturers instructions to give 16 different refolding conditions. 50 µl of protein at 20 mg/ ml or 2 mg/ ml, as appropriate, was added drop-wise to 950 µl of each buffer. Reactions were rotated at 4 °C for 12 hours. To remove refolding additives, 350 µl of each reaction was dialysed in 3.5 kD MWCO microdialysis units (Pierce) against 350 ml of PRB (without CHAPS/ DTT) at 4 °C for 10 hours. Dialysis was repeated against a further 350 ml of PRB (without CHAPS/ DTT) at 4 °C overnight and finally against 35 ml PRB at 4 °C for 3 hours.

2.3.5 Preparation of protein from HEK293T cells

Transiently transfected HEK293T cells were lysed in IP lysis buffer (150 mM NaCl, 50 mM Tris-HCl, pH 8, 1 % NP40, 1 mM PMSF, 1 µg/ ml aprotonin, 10 µg/ ml leupeptin) using 1 ml/ 10 cm culture plate. Lysates were centrifuged at 20,800 g for 15 minutes to remove insoluble material. His-tagged protein was captured from the supernatant with Ni-NTA agarose (50 µl/ 10 cm culture plate) at 4 °C overnight. Purified protein was washed in 3 x 1 ml volumes of

wash buffer (20 mM Tris-HCl, pH 8.5, 10 mM β-mercaptoethanol, 10 % glycerol, 20 mM imidazole) and resuspended to a 50 % slurry in PRB.

2.3.6 *In vitro* protein synthesis in *E. coli* HY lysates

Recombinant protein was synthesised using a coupled *in vitro* transcription and translation system based on *E. coli* high yield lysates containing T7 polymerase (Roche). Plasmids were used in their native forms and also linearised by digestion with the Pst1 endonuclease (NEB). Reactions were set up on a 100 µl scale:

24 µl HY lysate
20 µl reaction mix
20 µl amino acid mix
2 µl methionine
10 µl reconstitution buffer
1 µl Qiagen-pure template plasmid DNA
ddH_20 to 100 µl

Reactions were incubated at 30 °C for 5 hours. For purification of His-tagged proteins, reactions were brought up to 500 µl with lysis buffer (50 mM Tris-HCl, pH 8.5, 10 mM β-mercaptoethanol, 1 mM PMSF, 2 µg/ ml aprotonin, 10 µg / ml leupeptin) and incubated with 30 µl Ni-NTA agarose at 4 °C for 4 hours. Purified protein was washed in 3 x 500 µl of wash buffer/ 20 mM imidazole and resuspended in PRB as described above.

2.3.7 *In vitro* protein synthesis in rabbit reticulocyte lysates

Radiolabelled recombinant proteins were synthesised using a coupled *in vitro* transcription and translation system based on rabbit reticulocyte lysates depleted of amino acids (TNT, Promega). Proteins were labelled with ^{35}S methionine (10 mCi/ ml, Amersham). Reactions were set up on a 25 µl scale:

12.5 µl rabbit reticulocyte lysate
1 µl TNT reaction buffer
1 µl amino acid mix (without methionine)
2 µl ^{35}S methionine
1 µg Qiagen-pure template plasmid DNA

1 µl RNAsin

1 µl T7 polymerase

ddH_20 to 25 µl

Reactions were incubated at 30 °C for 2 hours.

2.4 PROTEIN ANALYSIS

2.4.1 Fluorimetric analysis of enzymatic activity

Protease activity levels were measured by the rate of hydrolysis of fluorogenic peptide substrates. Substrates used were the tetrapeptides DEVD, IETD, LEHD, and YVAD conjugated to the fluorescent peptide AFC. Release of AFC was monitored in an automated fluorimeter (Tecan) using an excitation wavelength of 430 nm and an emission wavelength of 535 nm. Hydrolysis assays were set up on a 50 - 100 µl scale in PRB with 50 µM substrate. Fluorescence readings were taken every 2 minutes for 1 - 2 hours and free AFC plotted against time for rate comparison.

2.4.2 SDS-PAGE electrophoresis

Proteins were typically subjected to sodium dodecyl sulphate polyacrylamide gel electrophoresis (SDS-PAGE) for analysis. SDS-PAGE was carried out as detailed in Sambrook and Maniatis (Sambrook and Maniatis, 1989). Protein samples were denatured by boiling for 7 minutes in SDS loading buffer (2 % SDS, 50 mM Tris-HCl, pH 6.8, 10 % glycerol, 2.5 % β–mercaptoethanol) and loaded onto 10 - 15 % polyacrylamide gels. Electrophoresis was carried out at 55 V through the stacking gel, and 75 V through the separating gel.

2.4.3 Coomassie Blue staining

Proteins were visualized by staining with Coomassie Blue. Following electrophoresis, SDS-PAGE gels were incubated in Coomassie Blue staining solution (45 % methanol, 10 % acetic acid, 0.25 % Coomassie Brilliant Blue) for 2 hours or overnight. Gels were then incubated in destain solution (45 % methanol, 10 % acetic acid) to remove background staining.

2.4.4 Immunoblotting

For Western blotting analysis, proteins were transferred from SDS-PAGE gels onto Whatman nitrocellulose membrane overnight at 35 mA in transfer buffer (39 mM glycine, 48 mM Tris-HCl, pH 8.3, 0.037 % SDS, 20 % methanol). Blots were blocked in blocking buffer (10 mM Tris-HCl, pH 8, 150 mM NaCl, 0.05 % Tween, 5 % non-fat dried milk, 0.05 % NaN_3) for 30 - 60 minutes. Blots were then rotated for 2 hours at room temperature in primary antibody diluted at 1:500 - 1:1000 in blocking buffer. After 3 x 10 minute washes in TBST (10 mM Tris-HCl, pH 8, 150 mM NaCl, 0.05 % Tween), blots were rotated for 1 hour at room temperature in horseradish peroxidase-conjugated secondary antibodies (Jackson Labs) diluted 1:1000 in blocking buffer (without NaN_3). Washing was repeated, and proteins were then incubated in Supersignal West Peroxide and Enhancer solutions (Pierce) to provide chemiluminescent substrate. Proteins were visualised by exposing the blots to autoradiography film (HyperfilmMP, Amersham). Before incubation with a second primary antibody, blots were incubated for 10 mins in 0.2 M NaOH.

2.4.5 Fluorography

Methionine-labelled proteins were resolved by SDS-PAGE electrophoresis and visualised by enhanced fluorography using Amplify reagent (Amersham). Gels were fixed in fixative solution (45 % methanol, 10 % acetic acid) for 2 hours followed by incubation for 25 minutes in Amplify and vacuum drying onto blotting paper (Whatman) for 2 hours at 80 °C. Gels were exposed to autoradiography film (HyperfilmMP, Amersham) at –70 °C for 12 - 48 hours.

2.4.6 2-dimensional SDS-PAGE

(i) Isoelectric focusing

Samples were brought up to 400 µl in 2D solubilization buffer (8 M urea, 4 % CHAPS, 100 mM DTT, 0.05 % SDS, 0.5 % pI 3 - 10 ampholytes, 0.03 % bromophenol blue) and passively rehydrated into 17 cm immobilized pH gradient (IPG) strips (BioRad) overnight at room temperature. Isoelectric point focusing (IEF) was performed in a BioRad Protean IEF Cell using the following conditions:

Linear voltage ramp to 500 V over 1 hour

5 hours at 500 V

Linear voltage ramp to 3500 V over 5 hours

12 hours at 3500 V

(ii) Second dimension electrophoresis

Following IEF, IPG strips were incubated for 5 - 7 minutes in reducing buffer (6 M urea, 375 mM Tris-HCl, pH 8.8, 2 % SDS, 20 % glycerol, 2 % DTT) followed by a 5 - 7 minute incubation in alkylating buffer (6 M urea, 375 mM Tris-HCl, pH 8.8, 2 % SDS, 20 % glycerol, 2.5 % IAA). The IPG strips were then mounted on 12 % SDS-PAGE gels using easy-melt agarose (BioRad) and electrophoresed at 37.5 mA / gel in a BioRad Protean II xi electrophoresis cell.

2.4.7 MS-compatible silver staining

Gels were stained using a modified version of the EMBL mass spectrometry-compatible silver-staining procedure (Mortz *et al.*, 2001). Gels were fixed in 50 % methanol/ 10 % acetic acid for 30 minutes. They were then washed in 50 % methanol for 10 minutes followed by 3 x 10 minute washes in ddH_2O. Gels were sensitized in 0.002 % Na_2S_2O, for 1 minute. After 2 rinses in ddH_2O, gels were stained in 0.1 % $AgNO_3$ for 20 minutes. Following 2 more rinses in ddH_2O, gels were developed in 0.04 % formalin/ 2 % Na_2CO_3. Gel development was stopped by addition of 5 % acetic acid, and gels were then transferred to and stored in 1 % acetic acid.

2.4.8 Trypsin digestion for MALDI-TOF mass spectrometry

For protein identification by mass spectrometry, silver-stained protein spots were manually excised from gels and transferred to 1 % acetic acid. Gel pieces were destained by oxidation of silver following 5 minutes room temperature shaking at 800 rpm in 15 mM K_3FeCN_6/ 50 mM $Na_2S_2O_3$. The gel pieces were then washed for 5 x 5 minutes in 500 µl of 50 % methanol/ 10 % acetic acid, shaking at 800 rpm at 22 °C. Samples were incubated in 50 mM NH_4HCO_3 for 5 minutes, shaking as above. After 5 minutes dehydration in acetonitrile, gel pieces were dried in a SpeedVac (ThermoSavant). Trypsin for digestion (Boehringer, sequencing grade) was solubilized to 100 µg/ ml in 1 mM HCl and further diluted to 25 µg/ ml in 25 mM NH_4HCO_3/ 0.1 % n-octylglucoside prior to digestion. 2 µl of trypsin was then added directly to each gel piece and allowed to penetrate for 5 minutes. A further 10 µl of 25 mM NH_4HCO_3/ 0.1 % noctylglucoside was then added to each sample and digestion allowed to

proceed for 12 - 16 hours at 37 °C. Following digestion, peptides were extracted twice from the gel pieces into 45 μl of 66 % acetonitrile/ 0.1 % trifluoro-acetic acid (TFA) in a sonicating water bath. Peptides were then dried down in a speed-vac and resolubilized into 5 % formic acid in a sonicating water bath.

2.4.9 MALDI-TOF mass spectrometry

Proteins excised from 2D gels and digested by trypsin as above were identified by matrix-assisted laser desorption and ionization (MALDI-TOF) mass spectrometry. The instrument used was a Voyager DE Pro MALDI mass spectrometer. 0.5 μl of digested sample was applied to a Teflon-coated 96-well MALDI target plate (Applied Biosciences) followed by 0.5 μl of a 10 mg/ml matrix solution made up of α-cyano-4-hydroxy-cinnamic acid in 60 % acetonitrile/ 0.1 % TFA. Samples were fully air-dried before analysis in positive reflector mode. Instrument settings for acquiring peptide fingerprint data were:

20 kV accelerating voltage
0.002 % guide wire
76.5 % grid
125 nsec delay
peptide gating 750 - 30000 m/z

Data from about 1000 laser shots was collected for each sample. Spectra were deisotoped and internally calibrated based on the known m/z values of autolytic tryptic peptides. Peptide mass data was submitted to MASCOT and MS-Fit search engines for protein identification based on comparison with theoretical trypsin digests of proteins in the NCBI database. Database searches were usually restricted to C. *elegans* proteins, and assumed carbamidomethylation of cysteine residues and possible oxidation of methionine residues. Permitted mass tolerance was 50 ppm.

2.5 HUMAN CELL CULTURE-BASED METHODS

2.5.1 Cell culture conditions

All cell cultures were maintained at 37 °C and 5 % CO_2. Human embryonic kidney (HEK) 239T cells were grown in DMEM (Gibco) supplemented with 10 % fetal calf serum (FCS) and 2 mM L-glutamine (Gibco). The HeLa and Jurkat T lymphocyte cell lines were cultured in RPMI (Gibco) supplemented with 5 % fetal calf serum (FCS) and 2 mM L-glutamine. CEM.neo and CEM.Bcl-2 stably-transfected T lymphoblastoma cell lines were grown in RPMI supplemented with 10 % fetal calf serum (FCS) and 2 mM L-glutamine. Cells were passaged every 2 - 3 days. Passage of adherent cells was conducted by trypsinization of cells with Trypsin-EDTA (Gibco) (0.25 % Trypsin, 1 mM EDTA, in Hank's balanced salt solution) at 37 °C. Cells were then treated with fresh medium to inactivate trypsin, and pelleted for 5 minutes at 250 g to remove EDTA. The cell pellet was resuspended in culture medium and transferred to new plates.

2.5.2 Transient transfection

(i) Transfection using calcium phosphate precipitation

HEK 293T cells were plated at 2 x 10^6 cells/ plate on 10 cm tissue culture plates (Sarstedt) the day prior to transfection. For transfection, 50 ng - 10 μg Qiagen-pure filter-sterilized DNA was diluted to 200 μl with sterile ddH_2O and 50 μl of 2.5 M $CaCl_2$ added. This mixture was then added drop-wise to 250 ml of HEPES-buffered saline (HBS; 280 mM NaCl, 10 mM KCl, 1.5 mM Na_2HPO_4, 12 mM dextrose, 50 mM HEPES, pH 7.1). Precipitates were allowed to form for 20 - 30 minutes followed by addition to cell monolayers. Cells were allowed to express proteins for 24 - 48 hours.

(ii) Transfection using Genejuice reagent

HeLa cells were plated at 2 x 10^5 cells/ well in 6-well tissue culture plates or 2 x 10^6 cells/ plate on 10 cm tissue culture plates on the day preceding transfection. 2 μl/ well or 10 μl/ plate of GeneJuice transfection reagent (Novagen) was diluted to 100 μl with RPMI, incubated 10 minutes, and added dropwise to 50 ng - 5 μg Qiagen-pure filter-sterilized DNA. After a 20 minute incubation, this mixture was added to cell monolayers. Cells were incubated for 24 - 48 hours to allow protein expression.

(iii) Transfection of siRNAs using Oligofectamine

HeLa cells were plated at 10^5 cells/ well in 6-well tissue culture plates. The following alpha-Tubulin oligos were used for transfection: Oligo 1, 5'- AAG TCC AAG CTG GAG TTC TCC-3'; Oligo 2, 5'-AAG GTA CAG AGA GCT GTG TGC-3'. For each well of cells to be transfected, 4 μl of Oligofectamine reagent (Invitrogen) was added dropwise to 16 μl RPMI and incubated for 5 minutes. 10 μl of each siRNA oligo at 20 μM was diluted to 100 μl with RPMI and the Oligofectamine/ RPMI mixture added drop-wise, followed by a 20 minute incubation for complex assembly. Cells were washed with RPMI and 880 μl RPMI was added to each well. 120 μl/ well of each transfection mixture was added to cells and incubated for around 6 h. 1 ml of RPMI containing 10% FCS and 4 mM L-glutamine was then added to each well and cells were incubated for a total of 72 h before further analysis.

2.5.3 Induction of apoptosis

Apoptosis was induced by incubation with the indicated concentrations of actinomycin D, daunorubucin, etoposide (VP-16), tumour necrosis factor with cyclohexamide (TNF/CHX), *N*-tosyl-l-phenylalanine chloromethyl ketone (TPCK), or 3,4-Dichloroisocoumarin (DCI). Adherent cells were typically plated at 10^5 cells/ well in 6-well plates, or 1 - 2 x 10^6 cells/ plate in 10 cm plates, on the day before treatment. Suspension cells were treated at a concentration of 10^6 cells/ ml.

2.5.4 FACS analysis

To quantitate apoptosis, cells were pelleted for 5 minutes at 800 g and brought up in annexin V binding buffer (10 mM Hepes-NaOH, pH 7.4, 150 mM NaCl, 5 mM KCl, 1 mM $MgCl_2$, 1.8 mM $CaCl_2$) containing annexin V-FITC at 1 μg/ ml. Propidium iodide was added just prior to analysis to a final concentration of 10 μg/ ml. Cell fluorescence was measured on a flow cytometer (FACSCalibur, Becton Dickinson, CA) using CellQuest software.

2.5.5 Light and UV microscopy

Cells were visualised by Hoffman modulation and DIC microscopy at 4 - 100 x magnification. Microscopes used were an Olympus BX51, for Hoffman modulation, and an Olympus IX71, for DIC microscopy. For analysis of fluorescence, cells were examined at 60 x or 100 x magnification on an Olympus IX71 UV microscope using appropriate filters (Mason Technologies).

2.5.6 Immunostaining for analysis by FACS

Cells were pelleted for 5 minutes at 800 g and washed with 1 ml PBS pH 7.2 containing 3 % BSA and 0.05 % NaN_3. This was followed by a 15 minute incubation in the same buffer. Primary antibodies were diluted in PBS/ 3 % BSA/ 0.05 % NaN_3 to concentrations between 1:100 and 1:400, and a 100 μl volume of the antibody solution was added to cells. Cells were then incubated for 1 hour followed by washing three times in PBS/ 3 % BSA/ 0.05 % NaN_3. Secondary antibody was diluted to 1:500 in PBS/ 3 % BSA/ 0.05 % NaN_3 and 100 μl added to cells followed by incubation for 1 hour. Cells were washed another three times in PBS/ 3 % BSA/ 0.05 % NaN_3 and fixed for 15 minutes in PBS/ 3% PFA, or left unfixed. Cells were then pelleted, brought up in PBS pH 7.2, and fluorescence was analysed by flow cytometry as described above.

2.5.7 Immunostaining for analysis by microscopy

Cells were plated on glass coverslips followed by transfection or treatment. Before staining, cells were washed three times with 2 ml PBS pH 7.2 followed by 15 minutes fixation in 3% PFA/ PBS pH 7.2. Cells were then rehydrated in three 15 minute washes with 2 ml of PBS pH 7.2 and permeabilized for 15 mins with 0.15 % TX-100 in PBS pH 7.2. Blocking was carried out for 30 mins using PBS pH 7.2 containing 2 % BSA and 0.05 % NaN_3. Primary antibodies were diluted in PBS/ 2 % BSA/ 0.05 % NaN_3 to 1:100 and a 100 μl volume added onto coverslips. Cells were incubated for 1 hour and then washed three times for 10 mins in PBS/ 2 % BSA/ 0.05 % NaN_3. Secondary antibody was diluted to 1:1500 in PBS/ 2 % BSA/ 0.05 % NaN_3 and 100 μl added to cells followed by incubation for 1 hour. Cells were washed another three times as before and coverslips mounted on glass slides using mounting medium. Fluorescence was then analysed by UV microscopy.

2.5.8 Cell lysate preparation

To make cell lysates for SDS-PAGE analysis, cells were pelleted at 800 g, washed in PBS pH 7.2, and brought up at 2 x 10^7 cells/ ml in SDS-PAGE loading buffer or IP lysis buffer (50 mM Tris-HCl, pH 8.0, 150 mM NaCl, 0.1% NP-40). Cells lysed with IP lysis buffer were incubated for 10 minutes on ice, pelleted for 10 minutes at 10,000 g, and supernatant removed to a fresh tube follwed by addition

of an equal volume of 2x SDS-PAGE lysis buffer. Lysates were then incubated for 7 minutes at 93 °C and analysed by SDS-PAGE.

2.5.9 Preparation of Jurkat cell-free extract

Approximately 5 x 10^8 cells were pelleted at 400 g and washed twice with 50 ml phosphate-buffered saline, pH 7.2 (PBS; 137 mM NaCl, 2.7 mM KCl, 4.3 mM Na_2HPO_4, 1.4 mM KH_2PO_4). Cells were transferred to a 2 ml Dounce-type homogeniser in 1 ml of cell extract buffer (CEB; 20 mM Hepes-KOH, pH 7.5, 10 mM KCl, 1.5mM $MgCl_2$, 1mM EDTA, 1mM EGTA, 1mM DTT, 100 μM PMSF, 10 μg/ml leupeptin, 2 μg/ml aprotinin) and pelleted at 800 g. Two volumes of CEB were added and cells were allowed to swell on ice for 20 minutes. The cells were then lysed by 20 - 30 strokes of a B-type pestle. These crude extracts were centrifuged at 15,000 g for 15 minutes to remove debris and the resulting supernatant was retained. The final cell-free extracts (CFE) were frozen in 50 μl aliquots at –70°C. CFE concentrations were determined using the Biorad Protein Assay and were typically ~30 mg/ ml.

2.5.10 Assembly of cell-free reactions

Cell-free reactions were typically set up in 100 μl reaction volumes. All were assembled on ice as follows:

Control:	50 μl CFE
	50 μl CEB
Cytochrome c/dATP-treated:	50 μl CFE
	30 μl CEB
	10 μl bovine cytochrome *c* (500 μg/ml)
	10 μl dATP (10 mM).
CED-3-treated:	50 μl CFE
	16.7 μl CEB
	33.3 μl GST-CED-$3^{221-503}$

Reactions were incubated at 37 °C for 120 minutes and samples taken at indicated timepoints.

2.6 NEMATODE CULTURE-BASED METHODS

2.6.1 *C. elegans* culture conditions

(i) Growth on NGM plates

N2 and MT3970 strains of *Caenorhabditis elegans* were obtained from the *C. elegans* Genetics Centre (CGC). Worm populations were routinely maintained at 20 °C on nematode growth medium (NGM; 3 g/ L NaCl, 16 g/ L Bacto-agar, 2.5 g/ L Bacto-peptone, 5 μg/ ml cholesterol, 1 mM $MgSO_4$, 1 mM $CaCl_2$, 25 mM KPO_4, pH 6.0) seeded with overnight cultures of *E. coli* OP50 bacteria. Populations were maintained in an exponential growth phase by transfer of agar chunks from saturated plates to fresh NGM/ OP50 plates.

(ii) Growth in liquid cultures

To generate large populations of nematodes, worms were grown on OP50 bacteria in liquid cultures. 3 ml overnight cultures of OP50 bacteria were diluted to 3 L in LB and grown overnight in a 37 °C shaker incubator. Bacteria were then pelleted for 10 minutes at 3000 g. Pellets were resuspended in 250 ml of S medium (composed of: 1 L S basal: 6.5 mM K_2HPO_4, 43.5 mM KH_2PO_4, 0.1 M NaCl, 5 μg/ml cholesterol; 10 ml 1 M potassium citrate, pH 6.0: 905 mM tri-potassium citrate monohydrate, 95 mM citric acid monohydrate; 10 ml trace metals solution: 5 mM EDTA, 2.5 mM $FeSO_4.7H_20$, 1 mM $MnCl_2.4H_2O$, 1 mM $ZnSO_4.7H_2O$, 0.1 mM $CuSO_4.5H_20$). Four saturated plates of nematodes were then washed into the OP50 suspension. Cultures were incubated at 20 °C in a shaker incubator at 350 rpm for 5 days or until all bacteria had been consumed.

2.6.2 *C. elegans* extract preparation

Worms were harvested from 250 ml liquid cultures by centrifugation at 500 g for 5 minutes. The nematode pellet was washed twice in 50 ml of 100 mM NaCl. To remove residual bacteria and debris, worms were added to 20 ml of 60 % sucrose and centrifuged for 5 minutes at 5000 g. Worms were then removed from the sucrose and washed in 100 mM NaCl. Following centrifugation at 500 g, the pelleted worms were resuspended in 2 volumes of extract buffer (20 mM HEPES-KOH, pH 7.5, 10 mM KCl, 1.5 mM $MgCl_2$, 1 mM

EDTA, 1 mM EGTA, 1 mM DTT, 100 mM PMSF, 10 μg/ ml leupeptin, 2 μg/ ml aprotonin). Resuspended worms were lysed by sonication, using 4 x 30 second pulses at 3 W. Insoluble material was pelleted for 15 minutes at 15,000 g and soluble supernatant retained. Final extracts (CeCFE) were frozen in 100 μl aliquots at –70°C. CeCFE concentrations were determined using the Biorad Protein Assay and were typically ~30 mg/ ml.

2.6.3 Assembly of reactions in *C. elegans* CFE

Recombinant CED-3 was added to soluble *C. elegans* extract at a 1:3 dilution unless otherwise indicated. Reactions were incubated for two hours at 37 °C to facilitate CED-3-dependent proteolysis. Cell-free reactions were then either assessed by immunoblotting, or subjected to two-dimensional electrophoresis.

2.6.4 Isolation of embryos from *C. elegans*

To prepare isolated embryos from mixed populations of C. *elegans,* worms were first washed from cleared NGM/ OP50 plates into M9 buffer (3 g/ L KH_2PO_4, 6 g/ L Na_2HPO_4, 5 g/ L NaCl, 1 mM $MgSO_4$), and pelleted for 5 mins at 500 g. Pelleted worms were brought up in a 5 x volume of 2.5 M NaOH/ 5 % NaOCl to dissolve adult and larval material. The worms were vortexed occasionally and monitored visually under 4 x magnification. Once embryos appeared relatively free of contaminating material, a 20 x volume of M9 buffer was immediately added to the embryo suspension and embryos pelleted for 2 minutes at 400 g. Embryos were then washed again in M9 buffer and pelleted for 5 minutes at 200 g. The final embryo preparations were brought up in a 2 x volume of M9 buffer.

2.6.5 *C. elegans* embryonic extract preparation

C. elegans embryos were isolated as above. Embryos were pelleted at 1000 g and all supernatant removed. The embryo pellet was then sonicated using brief low power pulses until all embryos were disrupted. Insoluble material was pelleted for 15 minutes at 15,000 g. The soluble supernatant was decanted and stored at –70 °C. Embryonic CeCFE protein concentration was determined using the Biorad Protein Assay.

2.6.6 Treatment of temperature-sensitive mutant strains

In order to inactivate temperature-sensitive mutant proteins, isolated embryos were prepared as described and incubated at 25 °C for 4 hours.

2.6.7 Confocal microscopy

Confocal microscopy was performed with a laser scanning microscope (Olympus FV1000) using a 488 nm Argon laser (green fluorescence), a 543 nm HeNe laser (red fluorescence) and a 405 nm LD laser (Hoechst fluorescence). FluoView 1000 V.1. Application Software was used.

2.6.8 Hoechst staining of embryos

To stain DNA, embryos were first fixed in 70 % ethanol/ M9 for 10 minutes. Worms were then pelleted and brought up in 20 nM Hoechst (bisBenzimide) in M9. Following a wash in M9 buffer, embryos were mounted on glass slides with a 4 % agarose coating, and visualised by fluorescence microscopy.

2.6.9 MitoTracker staining of embryos

To visualize mitochondria in *C. elegans* embryos, NGM agar was prepared containing Mitotracker CMX-Ros (Molecular Probes) at a final concentration of 0.4 μg / ml. Populations of *C. elegans* were grown on NGM/ MitoTracker until plates were cleared of bacteria. Nematodes were then washed from the plates with M9 buffer and embryos were isolated as described. Following incubation at 20 °C or 25 °C for 0 - 4 hours, embryos were mounted in M9 buffer on glass slides and observed by confocal microscopy.

CHAPTER III

Purification and characterization of recombinant CED-3 protease

3.1 CHAPTER INTRODUCTION

ced-3 was identified in early genetic screens as one of three genes essential for developmental programmed cell death in *C. elegans* (Ellis and Horvitz, 1986). On cloning *ced-3,* its gene product proved homologous to a human enzyme, ICE, responsible for the proteolytic maturation of the cytokine interleukin-1 β (Yuan and Horvitz, 1993; Miura *et al.*, 1993). Homology between the two enzymes was strongest in the region containing the catalytic residues of ICE, and the catalytic QACRG site itself was entirely conserved. This suggested that CED-3 might act, like ICE, as a cysteine protease, and that this activity might be required during cell death. Over-expression of ICE in mammalian cells was sufficient to initiate apoptosis, strengthening this theory. The discovery that many cellular proteins undergo proteolysis during apoptosis, in certain cases contributing directly to characteristic apoptotic events, has confirmed the importance of proteolysis in producing the apoptotic phenotype (Fischer and Schulze-Osthoff, 2003).

ICE and CED-3 are the founder members of the caspase (cysteine-dependent aspartate-specific protease) family. Since then, many other members of the human caspase family have been identified (Lamkanfi *et al.*, 2002). All caspases, including CED-3, share a requirement for an active site cysteine residue, a cleavage site tetrapeptide motif containing an aspartate residue at the P1 position, and activation by separation of two catalytic subunits. However, the human caspase family, numbering 12 members, has become substantially diversified. Members can be divided in terms of function, as some are involved in regulating inflammation while others regulate cell death. They also differ in substrate specificity, with three specificity subgroups recognising distinct tetrapeptide motifs. In addition, it is possible to divide the family into those that initiate proteolytic cascades, upon activation by upstream signals, and those that execute cell death by cleaving other cellular substrate proteins. How then, with just one essential caspase, CED-3, can programmed cell death occur in *C. elegans* with a phenotype so similar to that seen in human cells? CED-3 must be both activated by upstream signals, and able to cleave the downstream proteins required to cause the death of the cell. How CED-3 is able to combine both initiator and activator functions within one enzyme is unclear. In addition, the downstream proteins it cleaves and the role of these cleavage events are almost entirely unknown.

3.2 CHAPTER SUMMARY

The aims of this first phase of the study were two-fold. Firstly, as a step towards our broader goal of identifying substrates of CED-3, we sought to prepare sufficient quantities of active recombinant CED-3 for proteomic screening. We then also aimed to characterize the enzymatic activity of CED-3, and its relationship with human caspases, in order to better understand how this enzyme is able to act alone in catalysing programmed cell death in the worm, and how these functions have been shared and adapted among the human caspases.

The first approach taken to purify CED-3 was to express the enzyme in *E. coli*, a strategy that has been successful in the purification of several mammalian caspases. We obtained a plasmid encoding the full length CED-3 sequence in the pET3a vector, and then cloned truncated CED-3 sequences into the pET15b vector to produce N-terminally His^6-tagged CED-3 subunits. However, upon expression of these proteins in *E. coli* BL21 cells, we found that they were highly insoluble and sequestered within bacterial inclusion bodies. Attempting to refold the enzyme into an active conformation from these inclusion bodies produced insufficient active enzyme for our purposes.

We therefore looked to other means of purifying CED-3. A commercial *in vitro* transcription/ translation system also failed to synthesize sufficient protease. Attempts to express His^6-tagged CED-3 in human HEK293T cells allowed us to purify small amounts of enzyme, but again, not at sufficient levels to make large-scale proteomic analyses viable. This resulted in a return to bacterial expression systems, to determine whether changes in expression conditions might be more successful in generating a fraction of soluble and active protease. Using low temperature protein inductions and a modified lysis buffer, we were able to purify small quantities of active CED-3, both the full-length enzyme and a truncation lacking the CED-3 pro-domain. Induction conditions were optimized and culture volumes increased, producing sufficient amounts of purified enzyme for initial characterizations and for the preparation of a polyclonal antibody. However, it was not possible to elute the enzyme from the purification resin, leading us to examine other modifications that might improve protein purification.

Because GST tags often improve protein solubility, we cloned CED-$3^{221-503}$ into pGEX4TK2 to express CED-3 with an N-terminal GST tag in place of its pro-domain. This protein proved more soluble than earlier CED-3 preparations, and it was also successfully eluted from the glutathione-sepharose purification resin. The ability of GST-CED-$3^{221-503}$ to auto-process, and the concentration of active sites in our preparation, was assessed. We validated the ability of GST-CED-$3^{221-503}$ to cleave both peptide substrate analogues and its only known protein substrates, CED-3 and CED-9. GST- CED-$3^{221-503}$ therefore seemed suitable for use in the subsequent proteomic screen for *C. elegans* substrate proteins. We also used purified GST- CED-$3^{221-503}$ to compare the activity of CED-3 to that of caspase-3, its closest human homologue, against four tetrapeptide substrate analogues. Both enzymes showed a distinct preference for an aspartic acid residue at the P4 position, although CED-3 was substantially more promiscuous, consistent with its role as sole executioner caspase in *C. elegans*.

3.3 RESULTS

3.3.1 Induction of CED-3 as a His^6-tagged fusion protein in *E. coli*

Our first approach to purifying the CED-3 protease was to express it as a fusion protein in *E. coli*. Expression in bacteria is a common means of producing recombinant proteins, and several caspases have been successfully synthesized using this method (Stennicke and Salvesen, 1999b; Garcia-Calvo *et al.*, 1999). Some, including caspase-3 and caspase-7, have been expressed as full-length polyhistidine-tagged proteins (Stennicke and Salvesen, 1997). Others, such as caspase-6 and caspase-8, have been expressed without their pro-domains, as this region of the protein can lead to aggregation and therefore insolubility (Srinivasula, 1996; Stennicke and Salvesen, 1997; Thornberry *et al.*, 1997). Another approach has been to express separate polyhistidine-tagged subunits, which can then be recombined to produce an active enzyme (Thornberry *et al.*, 1997). CED-3 itself has been expressed in *E. coli*, albeit in small quantities only detectable by highly-sensitive silver staining (Xue and Horvitz, 1995; Xue *et al.*, 1996; Xue and Horvitz, 1997; Shaham, 1998).

To produce a full-length CED-3 fusion protein, we obtained a construct encoding the full length CED-3 ORF with a C-terminal FLAG protein tag (Dr. Shai Shaham, Rockefeller University, New York). We also decided to create constructs encoding CED-3 without its pro-domain (residues 221-503), and each catalytic subunit separately (residues 221-374, and residues 375-503), to maximise the chance of obtaining active enzyme. These truncated sequences were cloned into the pET15b vector, adding N-terminal polyhistidine tags to each protein (Figure 3.1).

These constructs were transformed into *E. coli* DE3 pLysS bacteria, which contain an IPTG-inducible T7 polymerase. Cultures of the transformed cells were treated with IPTG to drive transcription of CED-3 from the T7 promoter. Successful expression of each protein was confirmed by subjecting bacterial lysates to SDS-PAGE followed by staining with Coomassie Blue (Figure 3.2). Cells were then lysed by sonication, and lysates incubated with Ni-NTA resin to purify the His^6-tagged proteins. However, despite several attempts, we were not successful in recovering detectable CED-3 protein from any culture, as assessed by SDS-PAGE analysis and enzyme activity assays (Figure 3.2 and data not shown). SDS-PAGE analysis of the soluble and insoluble lysate fractions revealed that, in each case,

the induced protein was present in the insoluble fraction, rendering it inaccessible for purification (Figure 3.2). This was not entirely unexpected, as several mammalian caspases including caspase-1, caspase-2, caspase-8 and caspase-9 are insoluble in bacteria and as a consequence are difficult to purify (Ramage *et al.*, 1995; Stennicke and Salvesen, 1999b).

We then pursued various strategies to improve the solubility of the induced CED-3 in bacterial cells, including altering the incubation time after addition of IPTG, and changing the incubation temperature. Recombinant CED-3 was induced for 60, 30 and 15 minutes, and at room temperature for 3 hours and overnight. However, none of these changes increased the proportion of soluble protein produced (data not shown). We therefore attempted to utilize the insoluble CED-3 to recover active enzyme.

3.3.2 Refolding CED-3 from bacterial inclusion bodies

Although the insolubility of recombinant CED-3 in bacterial lysates had precluded its direct purification, the CED-3 present in the insoluble fraction still represented a rich source of CED-3 protein. It is possible to solubilize proteins from inclusion bodies by using strong chaotropic agents to fully denature and therefore release the proteins, then allowing them to refold into their native conformation (Rudolph and Lilie, 1996; De Bernardez Clark, 1998; Middelberg, 2002). However, the outcome of this process in yielding reasonable quantities of successfully refolded protein is dependent on a variety of factors, mostly involving the refolding buffer conditions. To maximise the chance of successful refolding, we utilized a refolding system to screen a variety of refolding conditions. Using a factorial combination of variables known to affect protein refolding (including protein concentration, pH, ionic strength, divalent cation concentration, ionic additive, non-ionic additive, chaotrope, reducing/ oxidising agent, detergent, and PEG) sixteen different refolding buffers were screened to find optimal refolding conditions for the renaturation of CED-3 (Chen and Gouaux, 1997) (Figure 3.3).

The purity of His^6-CED-$3^{221-503}$ in the inclusion bodies was assessed by SDS-PAGE followed by Coomassie staining. Recombinant CED-3 appeared to represent over 90 % of the protein content of the insoluble fraction (data not shown). Inclusion bodies were further washed in cell lysis buffer and subjected to

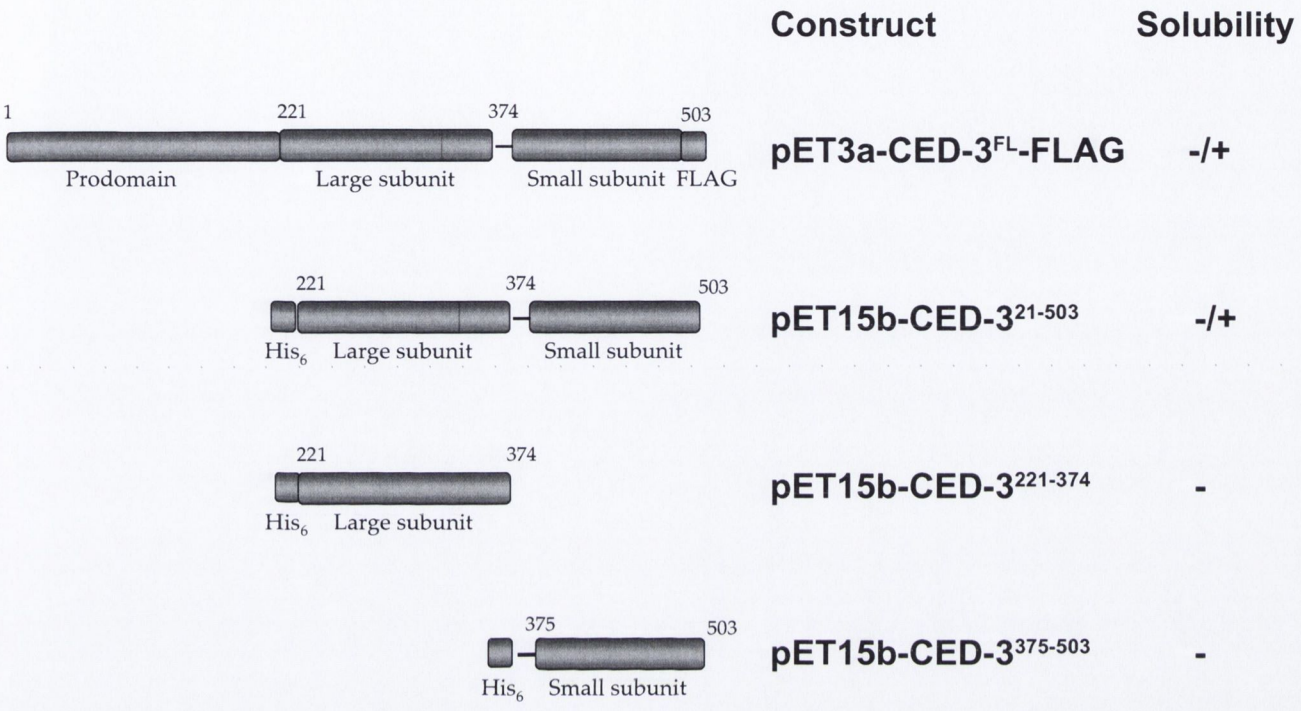

Figure 3.1

His^6-tagged CED-3 constructs generated for bacterial expression and purification of CED-3

Schematic representation of His^6- and FLAG-tagged constructs used for expression and purification of the CED-3 protease. pET3a-CED-3^{FL}-FLAG encoding the full length CED-3 sequence with a C-terminal FLAG tag was obtained from Dr. Shai Shaham. Truncated sequences encoding CED-3$^{221-503}$, CED-3$^{221-374}$ and CED-3$^{375-503}$ were cloned into the pET15b expression vector for expression of N-terminal His^6-tagged protein. Proteins were expressed in *E. coli* and their solubility assessed. -, indicates insolubility. -/+, indicates partial solubility.

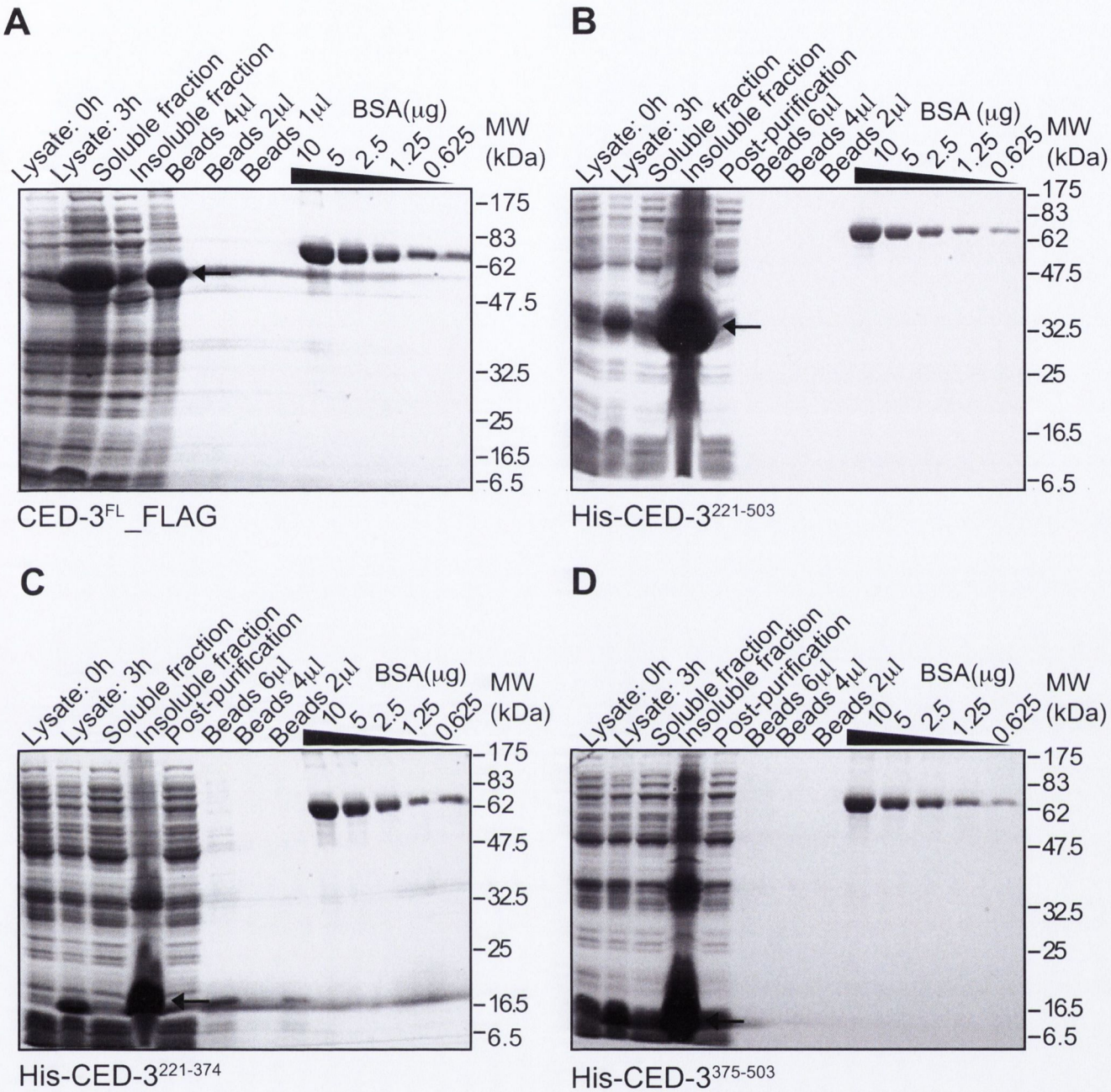

Figure 3.2

Expression from CED-3 constructs in *E. coli*

pET3a-CED-3^{FL} (A), pET15b-CED-3$^{221-503}$ (B), pET15b-CED-3$^{221-374}$ (C), and pET15b-CED-3$^{375-503}$ (D) plasmids were transformed into *E. coli* bacteria. Expression of CED-3 was induced by the addition of 600 µM IPTG to the bacterial cultures followed by 3 hours incubation under rotation at 37 ^{o}C. Cells were lysed by sonication and soluble supernatants incubated with α-FLAG agarose (A) or Ni-agarose beads (B - D). Samples of bacteria before and after IPTG addition (0.5 ml of culture), soluble and insoluble post-lysis fractions (20 µl), and beads (4, 2, 1 µl (A); 6, 4, 2 µl (B - D)) were ran on 12% SDS-PAGE gels and stained with Coomassie Blue protein stain. Arrows indicate the induced CED-3 proteins.

A

#	Buffer	Salt	PEG (% w/v)	GHCl	Cation/ chelator	Polar/ Non-polar Additives	DTT	Lauryl maltoside	Redox system
1	Tris pH8.2	275mM	0.055%	-	EDTA	-	1mM	-	-
2	MES pH6.5	11mM	-	550mM	MgCl/CaCl	-	-	0.3mM	GSH/GSSG
3	MES pH6.5	11mM	0.055%	550mM	EDTA	L-Arg/Sucrose	-	-	GSH/GSSG
4	Tris pH8.2	275mM	-	-	MgCl/CaCl	L-Arg/Sucrose	1mM	0.3mM	-
5	MES pH6.5	275mM	-	-	MgCl/CaCl	Sucrose	-	-	GSH/GSSG
6	Tris pH8.2	11mM	0.055%	550mM	EDTA	Sucrose	1mM	0.3mM	-
7	Tris pH8.2	11mM	-	550mM	MgCl/CaCl	L-Arg	1mM	-	-
8	MES pH6.5	275mM	0.055%	-	EDTA	L-Arg	-	0.3mM	GSH/GSSG
9	MES pH6.5	275mM	0.055%	550mM	MgCl/CaCl	Sucrose	1mM	-	-
10	Tris pH8.2	11mM	-	-	EDTA	Sucrose	-	0.3mM	GSH/GSSG
11	Tris pH8.2	11mM	0.055%	-	MgCl/CaCl	L-Arg	-	-	GSH/GSSG
12	MES pH6.5	275mM	-	550mM	EDTA	L-Arg	1mM	0.3mM	-
13	Tris pH8.2	275mM	-	550mM	EDTA	-	-	-	GSH/GSSG
14	MES pH6.5	11mM	0.055%	-	MgCl/CaCl	-	1mM	0.3mM	-
15	MES pH6.5	11mM	-	-	EDTA	L-Arg/Sucrose	1mM	-	-
16	Tris pH8.2	275mM	0.055%	550mM	MgCl/CaCl	L-Arg/Sucrose	-	0.3mM	GSH/GSSG

B

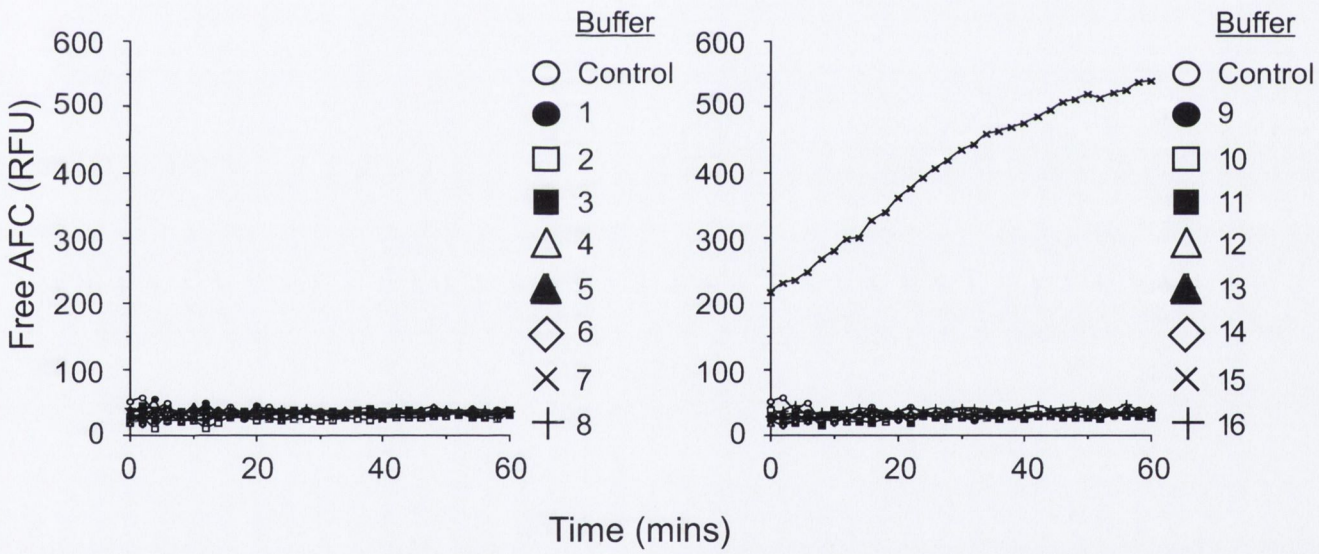

Figure 3.3

Refolding CED-3$^{221-503}$ using a range of buffer conditions

(A) Overview of the renaturation system. A range of buffers factorially screen conditions influencing protein refolding to select the optimal environment for protein renaturation. Abbreviations: MES (2-morpholinoethanesulfonic acid), PEG (polyethylene glycol), GHCl (guanidine hydrochloride), EDTA (ethylene diamine tetraacetic acid), L-Arg (L-arginine), DTT (dithiothreitol), GSH (L-glutathione reduced), GSSG (L-glutathione oxidised).

(B) DEVD-ase activity of refolded CED-3. Inclusion bodies containing insoluble CED-3 were purified and solubilized in GHCl. 50 μl of CED-3 was then added to 950 μl of each buffer to a final concentration of 1 mg/ ml (buffers 5 - 8 and 13 - 16) or 0.1mg/ml (1- 4 and 9 - 12). Reactions were incubated for 12 h followed by dialysis against PRB. The activity of 90 μl of refolded CED-3 against Ac-DEVD-AFC was tested. Note that buffer 15 was the only buffer that succeeded in recovering active CED-3.

additional rounds of sonication in order to lyse any remaining bacteria and remove residual soluble protein. The inclusion bodies were then solubilized in 6 M guanidine-HCl, a strong denaturing agent. After solubilization, denatured CED-$3^{221-503}$ was incubated overnight in 16 different refolding buffers (see Figure 3.3 A). Following dialysis into a buffer designed to optimize caspase activity, the ability of CED-$3^{221-503}$ from each refolding condition to hydrolyse the fluorogenic substrate analogue DEVD-AFC was measured.

Of the 16 refolding buffers, only buffer 15 appeared to produce active CED-3 enzyme (Figure 3.3 B). Refolding products were also subjected to SDS-PAGE, and Coomassie staining confirmed that buffer 15 had yielded the most soluble protein (data not shown). This buffer contained MES pH 6.5, 11 mM salt, EDTA, sucrose, and L-arginine. We then prepared a larger quantity of the buffer and repeated the reaction on a 1 L scale. However, this larger reaction repeatedly failed to yield any detectable enzymatic activity (data not shown). Repeating the screen using full length CED-3 also failed to yield any active enzyme. We were therefore forced to conclude that this method was not suitable to produce the preparative quantities of CED-3 that we required for our analysis.

3.3.3 *In vitro* transcription and translation in bacterial lysates

We then turned to an *in vitro* method of protein synthesis. A coupled *in vitro* transcription/ translation system was selected, in which expression is driven from T7 promoters by T7 polymerase in modified high-yield bacterial lysates, and translation occurs at bacterial ribosomes (Figure 3.4 A). We used the system to express CED-3^{FL} and CED-$3^{221-503}$ from our bacterial expression constructs, using both native and linearized plasmid. Reactions were incubated for 5 hours to allow maximum transcription and translation. The reaction products were then analysed by SDS-PAGE followed by Coomassie Blue staining and Western blotting.

Although Coomassie staining of the ITT reactions did not reveal any expressed proteins, other than the GFP control, Western blotting analysis did indicate that low levels of both CED-3^{FL} and CED-$3^{221-503}$ were expressed (Figure 3.4 B and data not shown). The pET15b-CED-$3^{221-503}$ synthesis reaction resulted in detection of a His-reactive band at the expected size of ~32 kDa, and a lower-intensity band at ~17 kDa, consistent with some auto-processing to release the

His^6-tagged large catalytic subunit. However, while the CED-3^{FL} reaction yielded some FLAG-reactive protein at the predicted size of 56 kDa, prominent bands at 35/ 40 kDa were difficult to explain. At least one band might be consistent with removal of the 24 kDa prodomain (Figure 3.4 B).

The CED-$3^{221-503}$ reaction was repeated and the protein purified onto Ni-NTA resin. A 100 μl reaction yielded ~0.5 μg of purified CED-$3^{221-503}$ as estimated by Coomassie Blue staining (Figure 3.4 C). Western blot analysis of lysate before and after the capture process suggested that this capture was relatively inefficient (data not shown). Assessment of the DEVDase activity of purified CED-$3^{221-503}$ yielded a final level of 4000 RFU free AFC after 2 hours (Figure 3.4 D). Although this was a substantial improvement over earlier CED-3 purification attempts, it was still a considerably lower yield than required for our experiments, rendering the ITT system non-viable. We therefore explored further methods of protein production.

3.3.4 Expression of CED-3 in a human cell line

Although CED-3 had proven highly insoluble in bacterial cells, this seemed less likely to be the case in human cells, which do not form inclusion bodies. There already existed evidence that this system can be useful in the purification of caspases; human caspase-1, caspase-3 and caspase-9 have previously been successfully purified from human cell lines (Ceretti *et al.*, 1992; Thornberry *et al.*, 1992; Nicholson *et al.*, 1995; Li *et al.*, 1997). We used human embryonic kidney (HEK) 293T cells to express CED-3, as this cell line is highly amenable to plasmid transfection using calcium phosphate and has previously been successfully used to purify proteins in our laboratory.

Sequences encoding CED-3^{FL} and CED-$3^{221-503}$ were cloned into the mammalian expression vector pcDNA3, using primers that incorporated a C-terminal and an N-terminal His^6 tag, respectively. Two clones of each construct were transiently transfected into HEK 293T cells alongside plasmids encoding His-ubiquitin and His-caspase-9 as controls, and cells were allowed to express recombinant proteins for 24 hours. Cells were then lysed in a mild detergent lysis buffer, and the His-tagged proteins purified onto Ni-NTA agarose. Purified proteins were then analysed by Western blotting and DEVD-AFC hydrolysis assays.

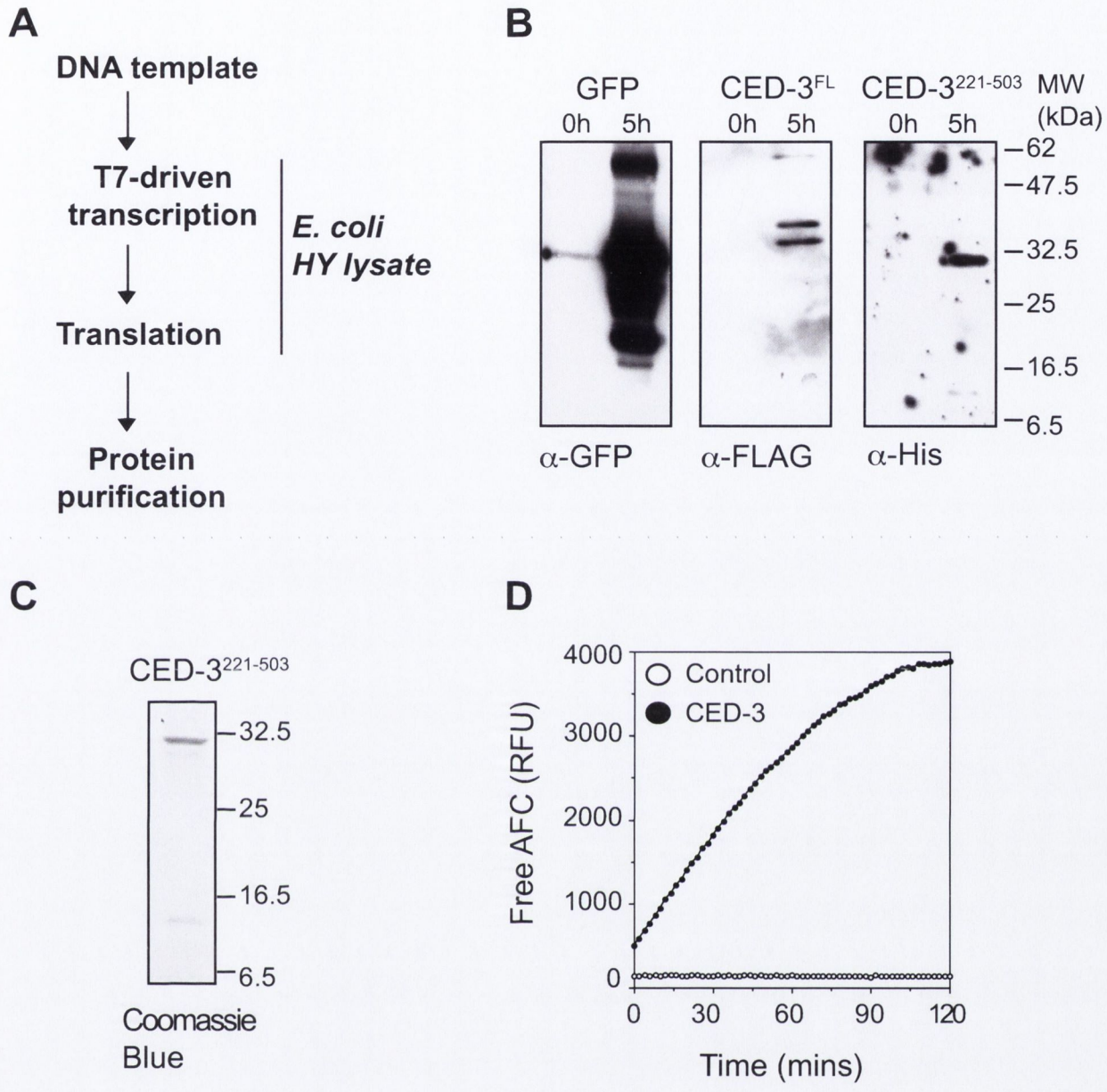

Figure 3.4

Expression of CED-3 using an ITT system

(A) Schematic representation of the Roche HY lysate Rapid Translation System. Plasmid template is added to an *E. coli* lysate. Transcription is driven by bacterial T7 RNA polymerase and translation occurs at bacterial ribosomes.

(B) Efficiency of protein expression assessed by Western blotting. 0 h and 5 h samples of lysates incubated with plasmid templates were ran on a 12% SDS-PAGE gel, and subjected to Western blot analysis to detect GFP, FLAG and His. Each lane shows 4μl of lysate.

(C) Purified CED-$3^{221-503}$. CED-$3^{221-503}$ synthesized in 100μl HY lysate was captured onto 30 μl Ni-NTA agarose and analysed by SDS-PAGE and Coomassie blue staining.

(D) Activity of purified CED-$3^{221-503}$. The activity of 30 μl of CED-$3^{221-503}$ beads against Ac-DEVD-AFC was tested over two hours.

As anticipated, expression of CED-3 proved toxic and induced widespread apoptosis in transfected cells (Figure 3.5 A). Expression and purification of CED-$3^{221-503}$ was detected by Western blotting, with protein bands at 32 kDa and 17 kDa in evidence (Figure 3.5 B). Protein purified from cells transfected with CED-$3^{221-503}$ and CED-3^{FL} displayed DEVD-AFC hydrolysis activity, suggesting the purification of active enzyme (Figure 3.5 C).

However, once again, the levels of CED-3 activity obtained were low, and repeating the experiment on the scale required to produce sufficient quantities of active enzyme was prohibitive. We therefore returned to the bacterial expression system, to determine whether further optimisation and larger scale cultures might yield higher levels of soluble protein.

3.3.5 Low temperature induction of recombinant CED-3

As CED-3^{FL} had previously been expressed and purified from bacterial lysates, albeit at low levels, we decided to further explore modifications to our expression protocol that might lead to production of more soluble protein. Bacterial culture sizes could then be scaled-up to maximise the CED-3 available for purification. We decided to express CED-3^{FL} at room temperature, and lyse cells in a modified lysis buffer containing NP40 detergent. These modifications were designed to increase the proportion of soluble CED-3 in bacterial cells, and to encourage its solubilization on cell lysis.

Using this modified protocol, we were still unable to detect purified protein by Coomassie Blue staining (Figure 3.6 A). However, using Western blotting analysis, some purified FLAG-tagged CED-3 was visible (Figure 3.6 B). We therefore tested both lysates and purification matrix in DEVD-AFC hydrolysis assays. Unclarified lysate had a high level of DEVDase activity, although most of this activity appeared to be removed upon centrifugation to remove insoluble material (Figure 3.6 C). However, a significant level of activity could still be purified onto α-FLAG agarose (Figure 3.6 D). This suggested that our modifications were indeed aiding solubility and CED-3 purification.

We then repeated the experiment to express CED-$3^{221-503}$, and produced a higher level of enzyme activity using the same conditions (data not shown). The

expression and purification procedure was therefore repeated with a culture volume of 5 L rather than 500 ml, and conditions that had been optimised further. These additional modifications included a 3 hour induction period at 25 °C, with lysis in an increased buffer volume (4% rather than 2 % of the original culture volume) and purification onto 500 μl of Ni-NTA agarose.

Using SDS-PAGE analysis and Coomassie Blue staining, these conditions appeared to result in the purification of some CED-3, although due to a high level of background binding this was difficult to assess (Figure 3.7 A). However, using Western blotting with α-His and α-CED-3 antibodies, substantial quantities of purified CED-3 could be detected including significant production of the p17 subunit, suggesting that the enzyme was active and able to autoprocess (Figure 3.7 B). Consistent with this, CED-3 bound to Ni-NTA agarose beads exhibited robust DEVD-AFC hydrolysis rates (Figure 3.7 C). These levels of protease activity suggested that the optimized induction and purification protocol might be able to produce the preparative protein levels that were required for proteomic screening for CED-3 substrates.

The next stage of protease purification involved the elution of the purified protease from the Ni-NTA purification resin. To do this, we added the nickel-binding compound imidazole to the CED-3-bound resin at concentrations of 100 - 500 μM, and after 30 minute incubation periods collected the eluate fractions. However, we were unable to release any active CED-3 from the Ni-NTA agarose, as determined by DEVD-AFC hydrolysis assays and SDS-PAGE (Figure 3.7 C and data not shown). Despite altering the elution incubation times (up to 12 hours) and temperatures (between 4 and 37 °C), we remained unable to elute virtually any His^6-CED-3 (data not shown). As we required soluble protease to add to our *C. elegans* extracts, we continued to explore different means of obtaining soluble active CED-3.

3.3.6 Generating CED-3-specific polyclonal antibodies

Although we were unable to use purified His^6-CED-$3^{221-503}$ in our substrate screen, it did have the potential to act as an antigen to generate a CED-3-specific polyclonal antibody. Up to this point there was no reliable antibody recognising CED-3 available to us, and this would be an extremely useful reagent both in

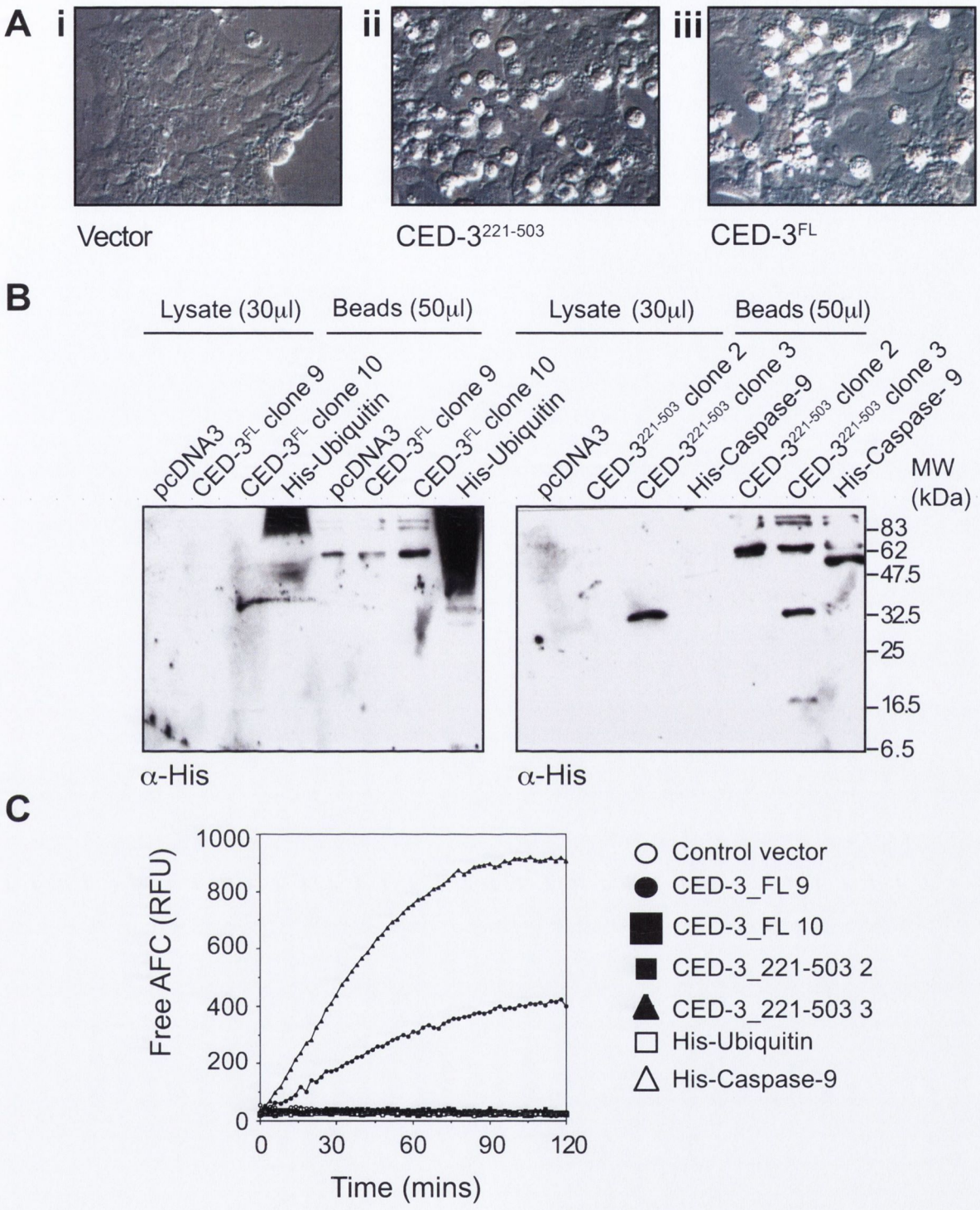

Figure 3.5

Expression of CED-3 in HEK 293T cells

(A) HEK 293T cells after transfection with CED-3 expression constructs. HEK 293T cells were transfected with 5 μg of pcDNA3 (i), pcDNA3-CED-$3^{221-503}$ (ii) and pcDNA3-CED-3^{FL} (iii). 24 h after transfection, CED-3-transfected cells showed high levels of cell death.

(B) Expression and purification of CED-3 from cell lysates. HEK 293T cells were transfected with 10μg of pcDNA3-CED-3^{FL}_His, pcDNA3-His_CED-$3^{221-503}$, pcDNA3-His-Ubiquitin and pcDNA3-His-Caspase 9, lysed 24 h after transfection, and proteins captured onto Ni-NTA agarose. 30μl of lysates and 50μl of beads were analysed by Western blotting for His^6.

(C) DEVDase activity of purified CED-3. 30μl samples of purified proteins conjugated to Ni-agarose beads were tested for activity against Ac-DEVD-AFC.

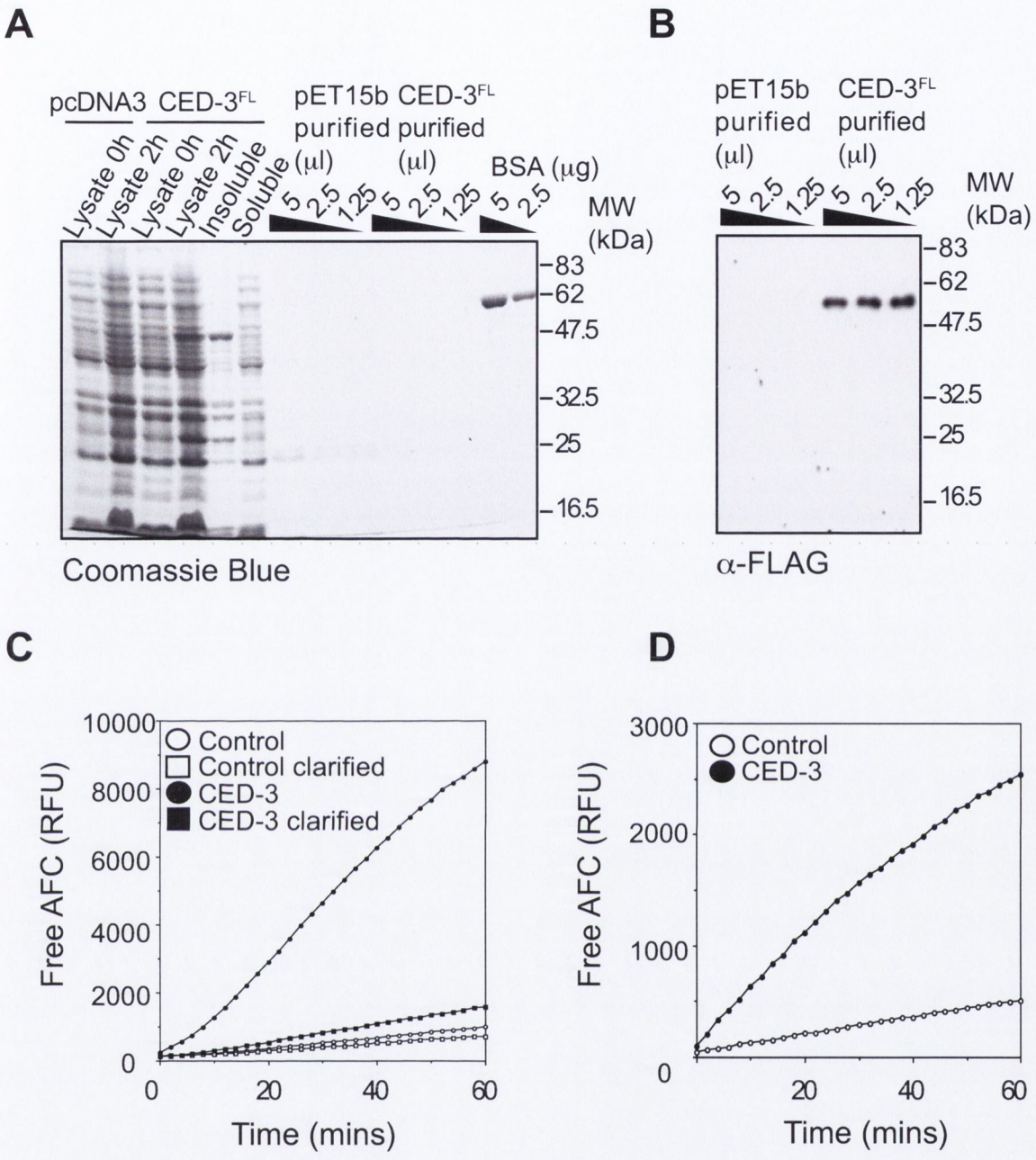

Figure 3.6

Expression of CED-3^{FL} at 25^{o}C

(A) Expression and purification of CED-3^{FL}. pET3a-CED-3^{FL} and control vector were transformed into *E. coli* BL21 cells. Expression was induced with 1mM IPTG followed by 2 hours incubation at 25^{o}C. Cells were lysed by sonication and clarified lysate incubated with α-FLAG-agarose for 9 hours. Samples of bacterial cultures before and after induction, soluble and insoluble lysate fractions, and purified CED-3^{FL} were ran on an SDS-PAGE gel and stained with Coomassie blue.

(B) Western blotting analysis of CED-3^{FL}. Purified CED-3^{FL} was probed with α-FLAG.

(C) and (D). Assessing CED-3^{FL} activity. Lysates before or after clarification by centrifugation (C) and purified CED-3^{FL} (D) were tested for activity against Ac-DEVD-AFC.

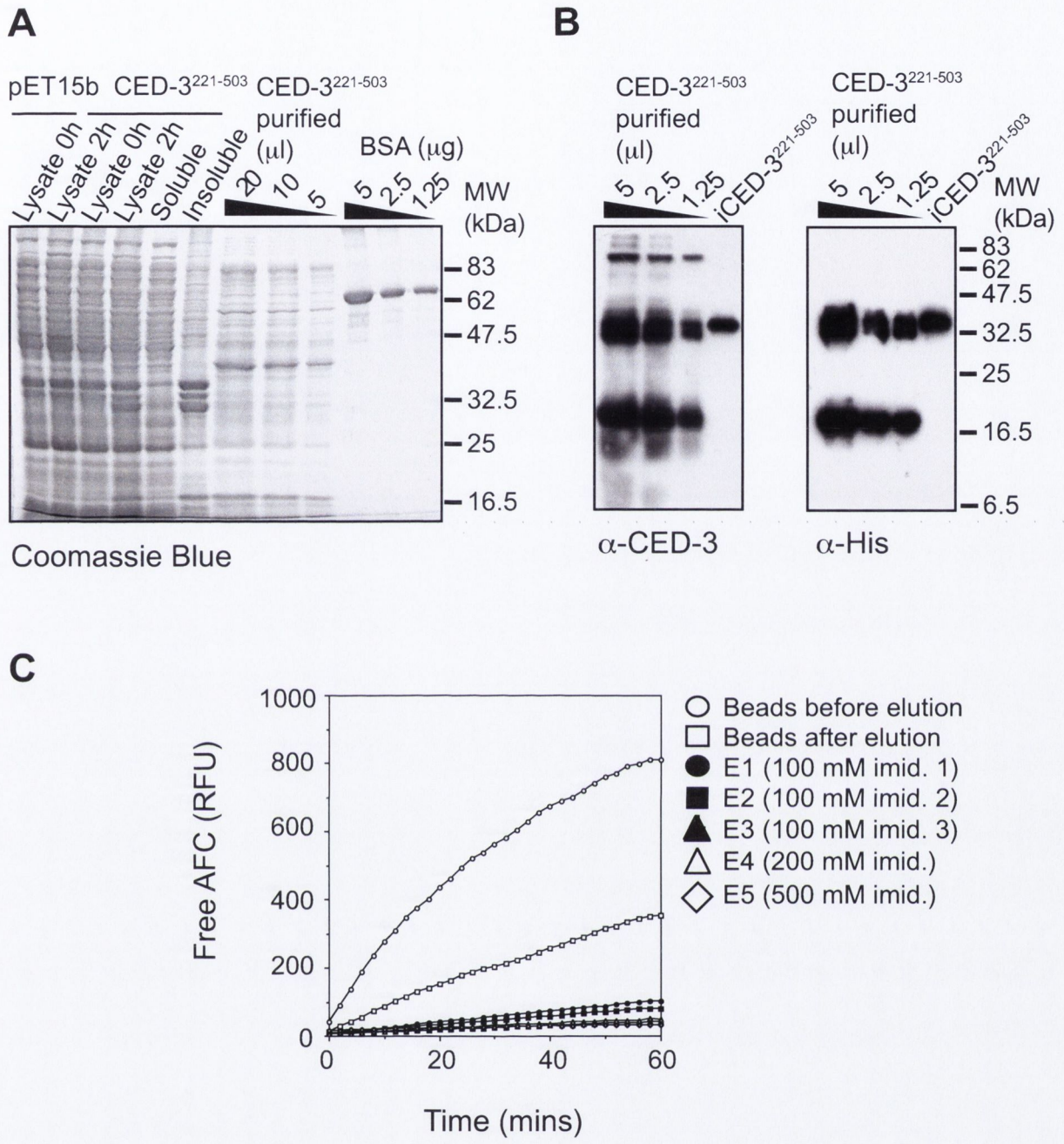

Figure 3.7

Expression of CED-3$^{221-503}$ at 25°C

(A) Expression and purification of CED-3$^{221-503}$. pET15b-CED-3$^{221-503}$ and control vector were transformed into *E. coli* BL21 cells. Expression was induced with 1 mM IPTG followed by 2 h incubation at 25 °C. Cells were lysed by sonication and clarified lysates were incubated with Ni-NTA agarose overnight. Samples of bacteria before and after induction, soluble and insoluble lysis fractions, and purified CED-3$^{221-503}$ were ran on an SDS-PAGE gel and stained with Coomassie blue. iCED-3$^{221-503}$ is insoluble CED-3 ran as a control. (B) Western blotting analysis of CED-3$^{221-503}$. Purified CED-3$^{221-503}$ was probed with α–His. (C) DEVDase activity of CED-3$^{221-503}$ eluates. CED-3$^{221-503}$ eluate fractions E1 - E5 were tested for activity against Ac-DEVD-AFC compared with beads before and after elution.

characterizing our recombinant CED-3 and in other studies examining the sub-cellular localization and expression pattern of CED-3 in *C. elegans* embryos.

We used two sources of recombinant CED-3 for the immunization of four rabbits (in collaboration with Harlan SeraLabs). Two rabbits were immunized with inclusion bodies prepared from cells induced to express His^6-$CED\text{-}3^{221\text{-}503}$ at high levels, containing over 90 % CED-3 (experiments A1 and A2). Two further rabbits were immunized with purified His^6-$CED\text{-}3^{221\text{-}503}$ conjugated to Ni-NTA agarose that had been shattered by sonication (experiments B1 and B2).

Three interim serum samples and the terminal bleed antisera were tested against recombinant His^6-$CED\text{-}3^{221\text{-}503}$ by Western blotting to determine antibody sensitivity, using an α-His antibody as a control. All antisera recognised recombinant CED-3, with three, A1, A2, and B2, detecting as little as 10 ng of CED-3 protein, a sensitivity comparable to that of the α-His monoclonal antibody (Figure 3.8). These antibodies were used subsequently in the study to analyse CED-3 auto-processing, and its presence in *C. elegans* extracts.

3.3.7 Expression and purification of GST-$CED\text{-}3^{221\text{-}503}$

The next strategy adopted to encourage both solubility and elution of recombinant CED-3 was to tag the N-terminus of the truncated 221-503 sequence with glutathione-S-transferase (GST), an extremely hydrophilic protein. Being a long and very soluble protein tag, we hypothesized that the addition of GST to CED-3 might encourage solubility of the whole protein. The GST tag can also be captured on glutathione-sepharose and efficiently eluted using free glutathione.

We cloned the $CED\text{-}3^{221\text{-}503}$ sequence into the pGEX4TK2 vector encoding an N-terminal GST tag (Figure 3.9 A). This construct was then transformed into *E. coli* DH5α cells and expression induced by the addition of IPTG under a range of conditions. The most successful conditions for purifying active CED-3 were those already described in the induction and purification of His^6-$CED\text{-}3^{221\text{-}503}$. Using a 3 hour 25 °C induction, followed by detergent lysis in 4 % culture volume, and purification onto 500 µl of glutathione-sepharose, substantial quantities of protein consistent in size with GST-$CED\text{-}3^{221\text{-}503}$ and its processed products were purified and could be observed by staining with Coomassie Blue (Figure 3.9 B). This

purified protein could also be eluted from the glutathione-sepharose resin. We found that the addition of 10 mM glutathione in three 30 minute elutions at room temperature produced maximum levels of eluted CED-$3^{221-503}$ (Figure 3.9 B).

We further characterized the purified soluble GST-CED-$3^{221-503}$ by Western blotting. Antibodies directed towards the GST tag, and against individual catalytic subunits, were used alongside Coomassie Blue staining (Figure 3.10 A, B). Coomassie Blue stained a 61 kDa band consistent in size with GST-CED-$3^{221-503}$, as well as a 46 kDa band consistent with removal of the small catalytic subunit, a doublet at 26/ 29 kDa most likely representing free GST, and a 17 kDa band possibly corresponding to the large catalytic subunit. Consistent with this analysis, the α-GST antibody detected similar 61 kDa and 46 kDa bands, and the 26/ 29 kDa doublet. The α-p17 antibody reacted weakly against the 61 kDa band, and also detected the 46 kDa band. A reactive band at 17 kDa appeared likely to be the large catalytic subunit. The p15 antibody detected the 61 kDa but not the 46 kDa band, confirming the prediction that this 46 kDa protein lacks the p15 subunit. There was also a poorly resolved reactivity below the 16.5 kDa marker, consistent with the p15 subunit with and without the 2 kDa linker region. This analysis therefore suggested that substantial auto-proteolysis was occurring, with the recombinant CED-3 showing high levels of activity and cleaving specifically at the predicted inter-domain proteolytic sites (Figure 3.10 B).

3.3.8 Determining the active site concentration of GST-CED-$3^{221-503}$

Once GST-CED-$3^{221-503}$ had been purified, we then assessed the concentration of active GST-CED-$3^{221-503}$ within the preparation. We did this using an active site titration method (Stennicke and Salvesen, 1999b). GST-CED-$3^{221-503}$ was incubated with a range of concentrations of the poly-caspase inhibitor z-VAD-fmk for 30 minutes, before addition at a 1:10 final CED-3 dilution to a 100 μl reaction containing 50 μM DEVD-AFC. Concentrations of z-VAD-fmk that were used ranged from no inhibitor, to a concentration established to fully inhibit GST-CED-$3^{221-503}$ under these conditions (0.1 μM). Proteolysis of the peptide substrate was assessed by the release of free AFC (Figure 3.11 A). Rates of DEVD-AFC hydrolysis were calculated for each reaction and plotted against z-VAD-fmk concentration (Figure 3.11 B). A linear equation was fitted to the plot, and this was used to calculate the concentration at which z-VAD-fmk fully inhibited all the CED-

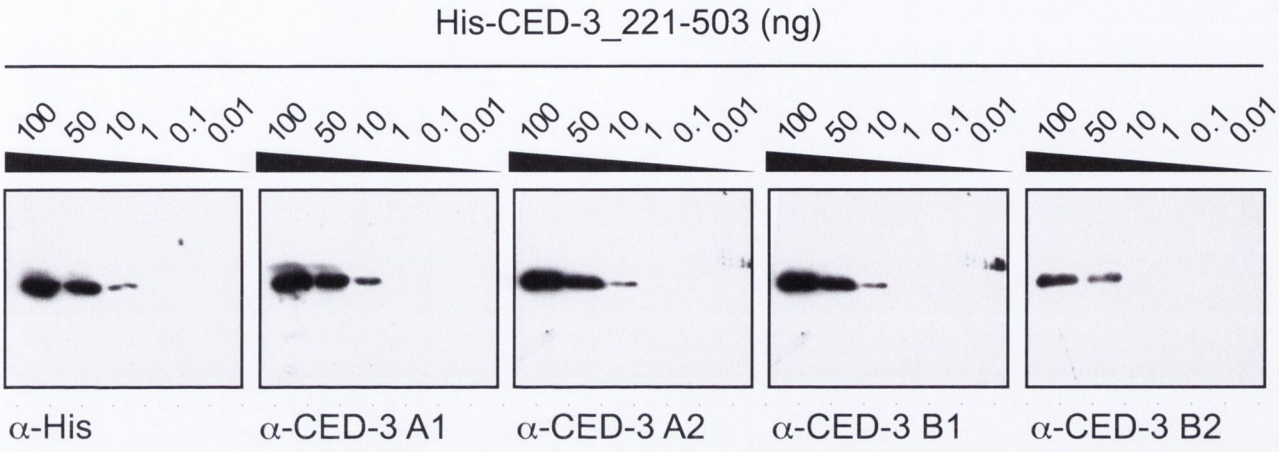

Figure 3.8

Generation of a polyclonal antibody against CED-$3^{221-503}$

Purified CED-$3^{221-503}$ was used to immunise rabbits for the production of polyclonal antisera. Two samples of CED-$3^{221-503}$ in bacterial inclusion bodies, and two samples of CED-$3^{221-503}$ coupled to Ni-NTA agarose (broken into fragments by sonication) were used for immunisation of four rabbits (A1, A2, A3, A4). The resulting antisera were tested against recombinant His-CED-$3^{221-503}$ on Western blots to determine antibody sensitivity. Results shown were obtained with terminal bleed antisera, alongside a control monoclonal antibody recognising the His^6 tag.

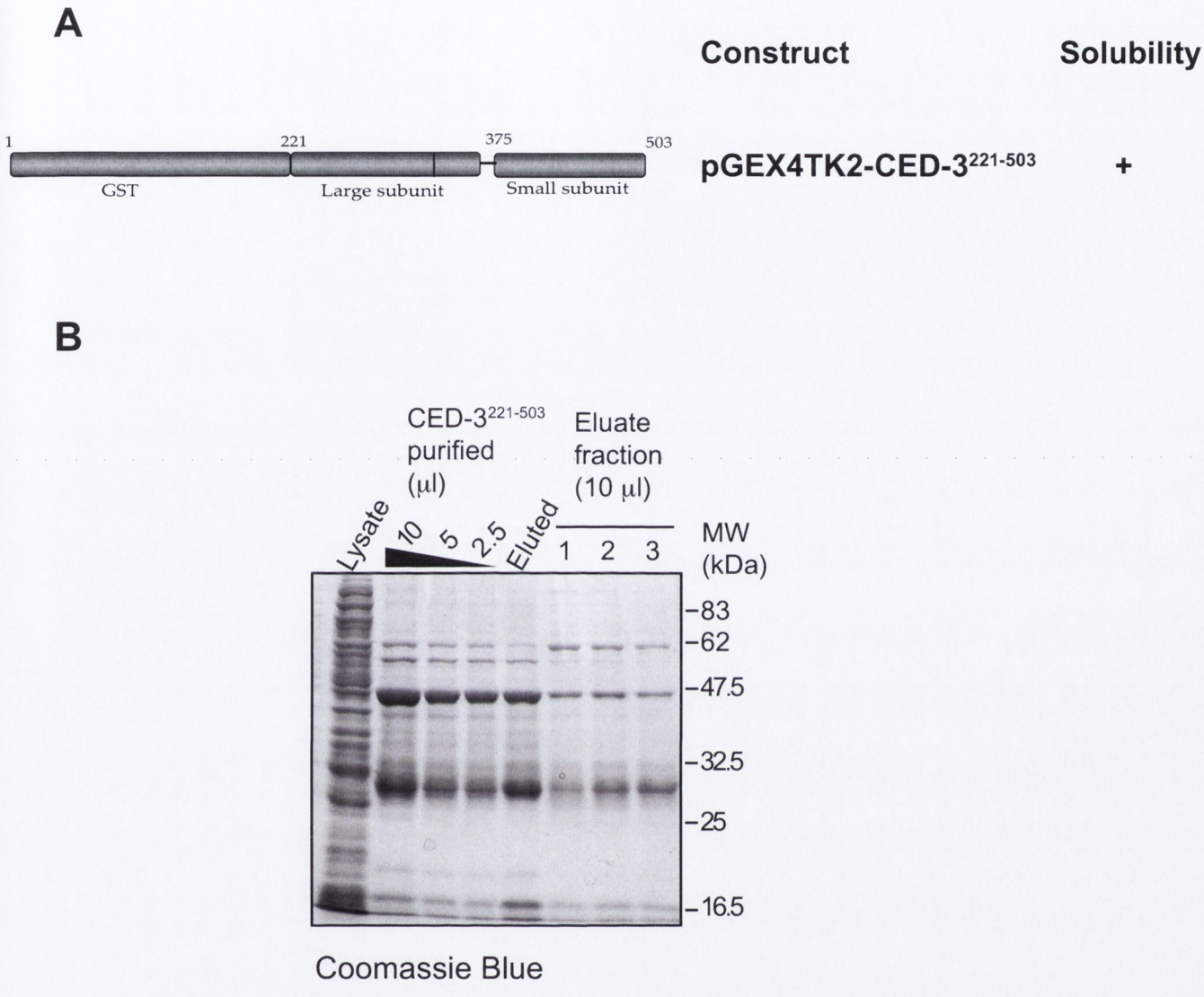

Figure 3.9

Induction of GST-CED-3$^{221-503}$

(A) Schematic representation of the GST-CED-3$^{221-503}$ expression construct. CED-3$^{221-503}$ was cloned into pGEX4TK2 to produce an N-terminally GST-tagged protein.

(B) Purified GST-CED-3$^{221-503}$. Samples of bacterial lysate after GST-CED-3$^{221-503}$ induction (1 ml of culture), GST-CED-3$^{221-503}$ purified onto glutathione-sepharose beads (10, 5, and 2.5 μl), glutathione-sepharose beads after elution with glutethione (10 μl), and GST-CED-3$^{221-503}$ eluate fractions (10 μl), were ran on SDS-PAGE gels and analysed by Coomassie Blue staining.

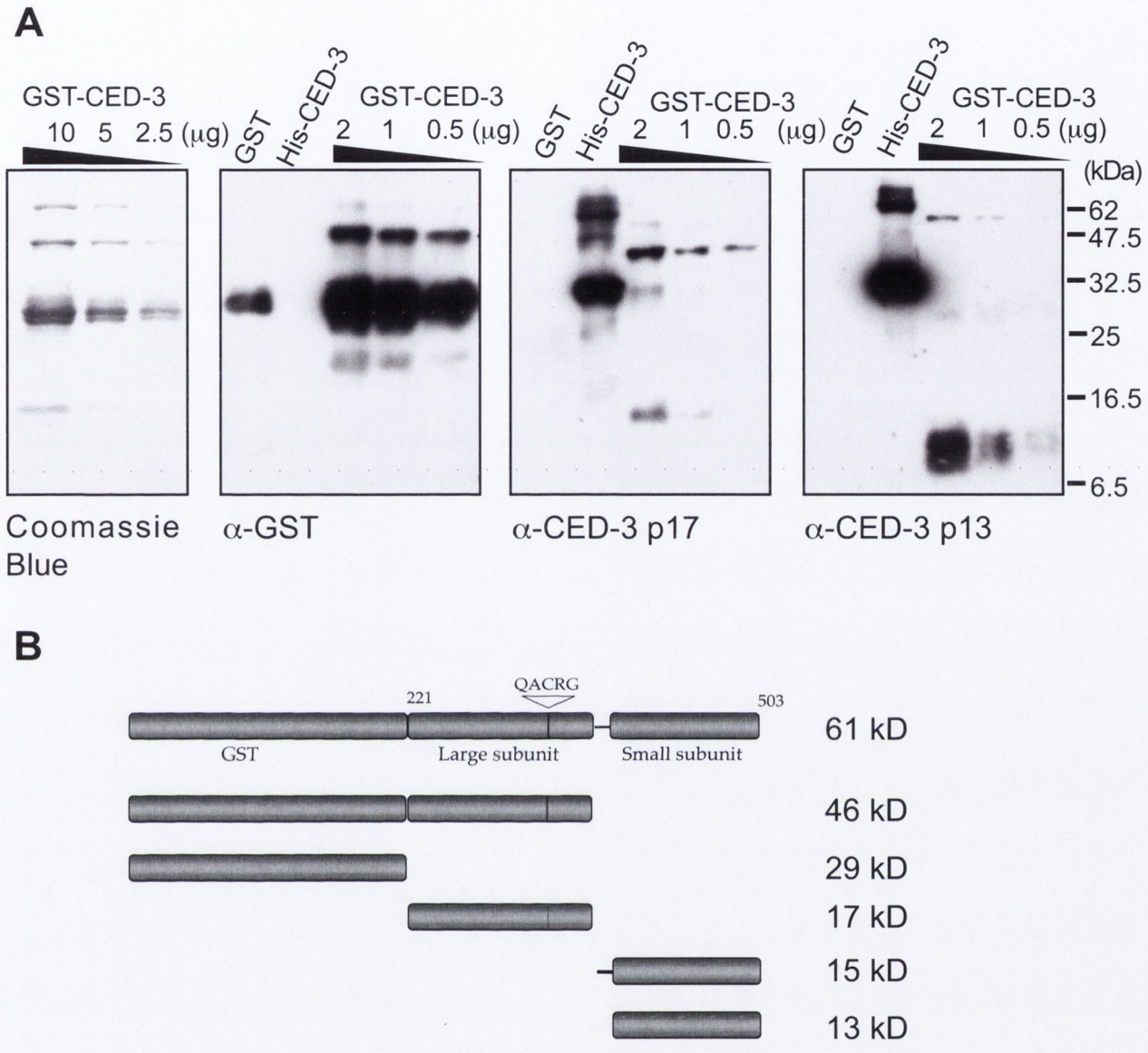

Figure 3.10

Western blotting analysis of purified GST-CED-$3^{221-503}$

(A) Purified GST-CED-$3^{221-503}$. Samples of GST-CED-$3^{221-503}$eluate, GST and His-CED-$3^{221-503}$ were ran on SDS-PAGE gels and analysed by Western blotting. Blots were probed for CED-3 p17, CED-3 p13 and GST.

(B) Schematic representaion of GST-CED-$3^{221-503}$ and processed products. Bands detected by Western blotting are consistent with auto-processing of GST-CED-3 to liberate the small and large subunits.

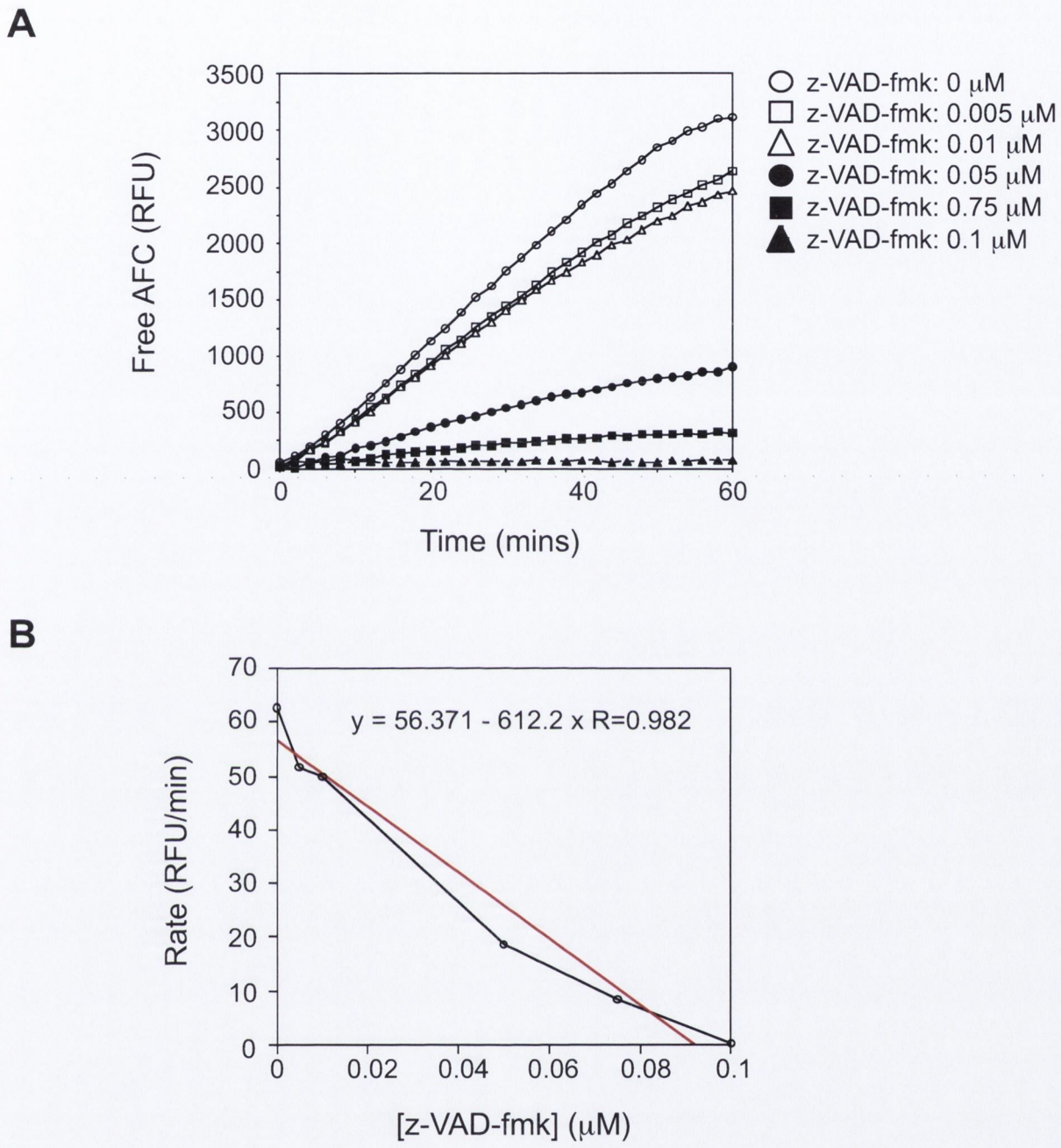

Figure 3.11

Active site titration of GST-CED-3$^{221-503}$

(A) Establishing hydrolysis rates after incubation of CED-3 with z-VAD-fmk. GST-CED-3 was incubated with a range of concenrations of the poly-caspase inhibitor z-VAD-fmk. The CED-3/ z-VAD reactions were then added at a 1:10 CED-3 dilution to 0.05 μM DEVDE-AFC, and peptide hydrolysis measured by the release of free AFC.

(B)Hydrolysis rates as a function of z-VAD-fmk concentration. Peptide hydrolysis rates at each z-VAD concentration were plotted against z-VAD concentration. The concentration at which full CED-3 inhibition is acheived represents the concentration of CED-3 active sites present.

3 present (92 nM). This concentration therefore represented the concentration of CED-3 active sites present in the reaction. Given that the enzyme was used in these reactions at a 1:10 dilution, and that there are two active sites present in each CED-3 heterotetramer, we were able to calculate that the concentration of active GST-CED-$3^{221-503}$ molecules in the original preparation was ~410 nM.

3.3.9 Comparing the activity of GST-CED-$3^{221-503}$ and caspase-3 against peptide substrates

We then tested the ability of recombinant GST-CED-$3^{221-503}$ to cleave different fluorogenic peptide substrate analogues. We used a range of peptides based on different caspase cleavage consensus tetrapeptide motifs, to gain a better idea of the substrate specificity of CED-3. We also compared this specificity profile with that of human caspase-3, the primary human executioner caspase and the human caspase family member most closely-related by sequence to CED-3.

GST-CED-$3^{221-503}$ displayed typical caspase activity and was able to cleave the fluorogenic peptides to release free AFC moieties (Figure 3.12 A). The highest degree of activity was displayed against DEVD-AFC, confirming previous results (Thornberry *et al.*, 1997). This was also the preferred substrate of caspase-3, suggesting that the two enzymes may form part of the same specificity sub-family, also including the human executioner caspase-7 (Figure 3.12 B).

Significant levels of proteolysis against IETD and LEHD were also observed, to a much greater degree than that catalysed by caspase-3, suggesting that CED-3 is more promiscuous than its human relative. However, neither enzyme showed any significant activity against YVAD-AFC, a preferred substrate for caspase-1.

3.3.10 Testing the activity of GST-CED-$3^{221-503}$ against protein substrates

In order to determine whether recombinant GST-CED-$3^{221-503}$ was active against protein substrates, we synthesized ^{35}S-methionine-labelled CED-3^{FL} and CED-9, both known to be substrates of CED-3 (Xue and Horvitz, 1995; Xue *et al.*, 1996; Xue and Horvitz, 1997). We incubated both proteins with a range of concentrations of purified soluble GST-CED-$3^{221-503}$ for 2 hours at 37 °C. Reaction products were then subjected to SDS-PAGE followed by fluorography. Both

substrates were cleaved by all concentrations of GST-CED-$3^{221-503}$ tested (Figure 3.13 A).

Cleavage reactions were then repeated in the presence of a *C. elegans* soluble protein extract, in order to determine the concentration of GST-CED-$3^{221-503}$ that would be required to cleave substrate proteins in the protein-rich environment of our substrate screen conditions. The presence of these additional proteins did appear to reduce the efficiency with which GST-CED-$3^{221-503}$ cleaved CED-3 and CED-9 (Figure 3.13 A). The pattern of cleavage products observed was also modified. The enzyme dilution selected for screening purposes was 1:3 of the CED-3 stock preparations, as the lowest concentration that seemed to cleave substrates with full efficiency.

We went on to test the ability of z-VAD-fmk to inhibit the proteolysis of CED-3 and CED-9, to confirm that this proteolysis was specific and caspase-mediated. A range of concentrations of z-VAD-fmk was incubated with GST-CED-$3^{221-503}$ for 15 minutes before addition to the substrate proteins and analysis as before. Full inhibition of CED-3 was observed at all concentrations tested (Figure 3.13 B).

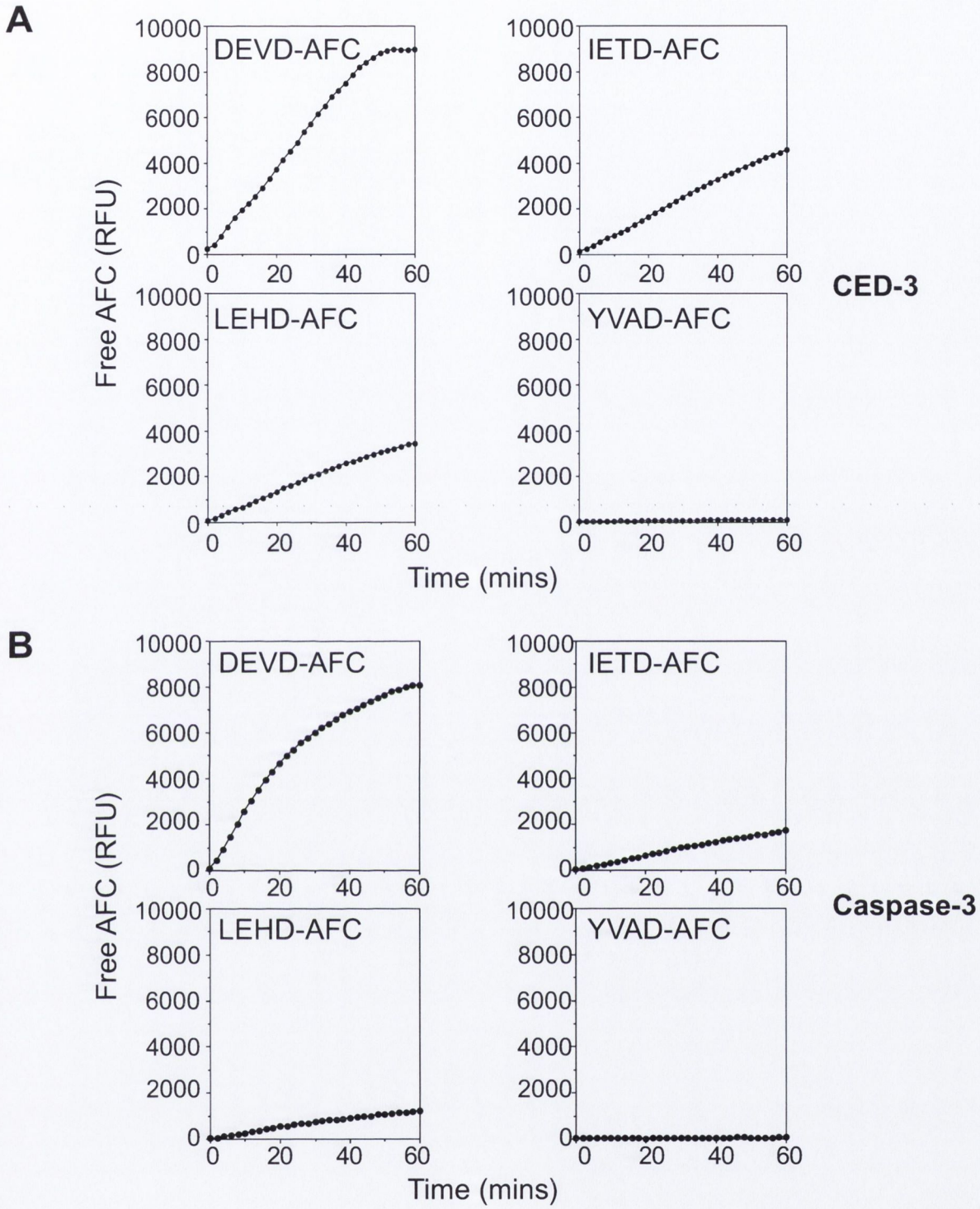

Figure 3.12

Comparing the activity of GST-CED-3$^{221-503}$ and human caspase-3 against a range of peptide substrates

(A) Testing the activity of GST-CED-3$^{221-503}$ against different peptide substrates. The fluorogenic peptides Ac-DEVD-AFC, Ac-IETD-AFC, Ac-LEHD-AFC, and Ac-YVAD-AFC were tested as substrates for purified GST-CED-3$^{221-503}$. 10 μl of GST-CED-3$^{221-503}$ was used in 100 μl hydrolysis assays with 50 μM peptide.

(B) Testing the activity of human caspase-3 against different peptide substrates to compare with the activity of CED-3. The fluorogenic peptides Ac-DEVD-AFC, Ac-IETD-AFC, Ac-LEHD-AFC, and Ac-YVAD-AFC were tested as substrates for recombinant caspase-3. 10 μl of caspase-3 was used in 100 μl hydrolysis assays with 50 μM peptide.

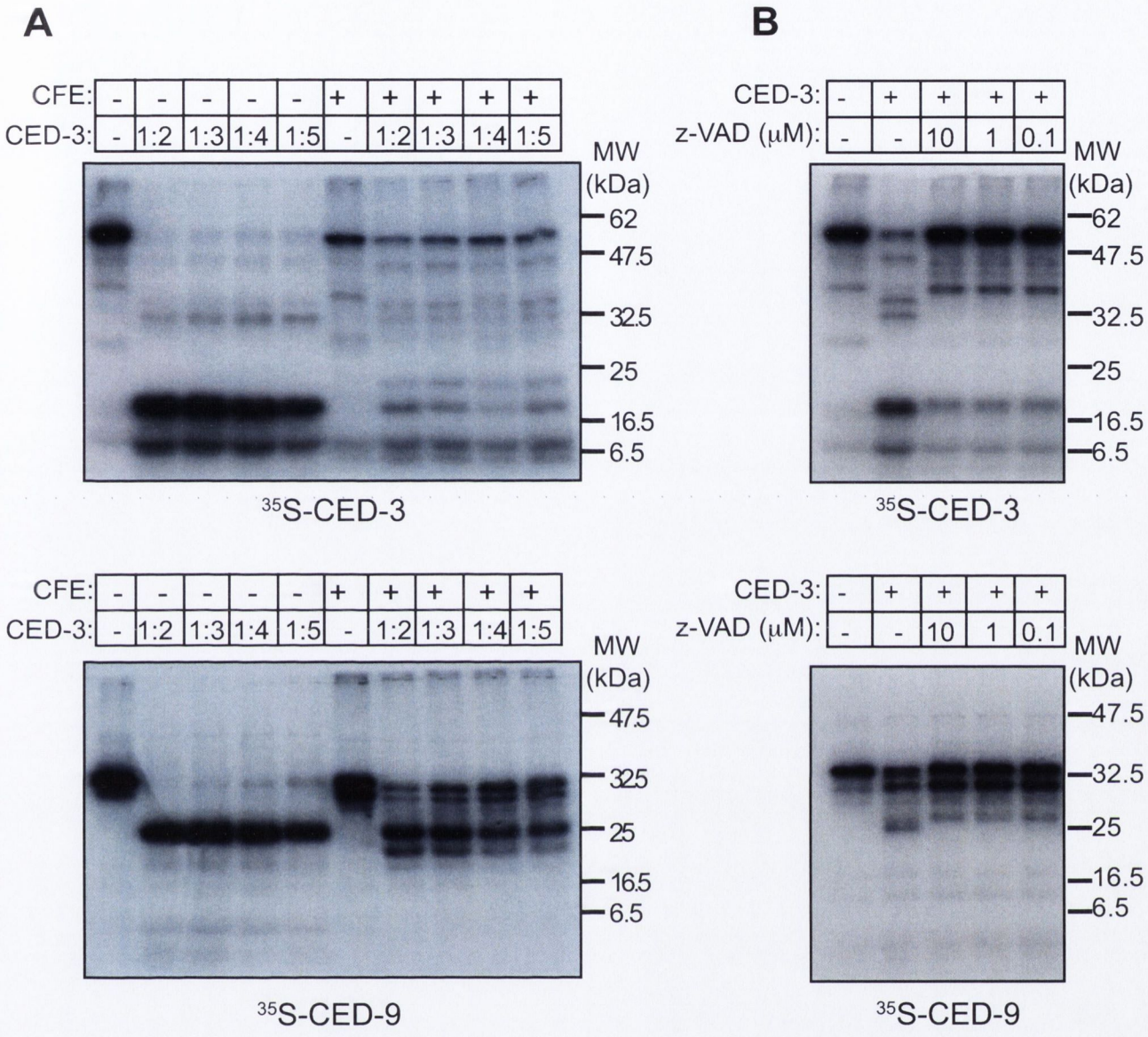

Figure 3.13

Activity of GST-CED-3$^{221-503}$ against CED-3 and CED-9

(A) Testing the activity of GST-CED-3$^{221-503}$ against ^{35}S-Met-labelled CED-3 and CED-9. A titration of GST-CED-3 was incubated with ^{35}S-Met-CED-3 and ^{35}S-Met-CED-9 in PRB for 2 h. In a replicate set of reactions, 6.35 mg/ ml *C. elegans* CFE was also included. (B) Testing the ability of z-VAD-fmk to inhibit GST-CED-3 activity. GST-CED-3 was pre-incubated with z-VAD-fmk at 10, 1, and 0.1 μM for 15 mins. This GST-CED-3 was then added at a 1:10 dilution to ^{35}S-Met-CED-3 and ^{35}S-Met-CED-9 and incubated for 2 h. Reaction products were analysed by SDS-PAGE and enhanced fluorography.

3.4 DISCUSSION

3.4.1 Summary

To purify recombinant CED-3 we tested a number of approaches. Our initial strategy, to express CED-3 as a polyhistidine-tagged fusion protein in bacteria, proved difficult as all CED-3 truncations tested proved highly insoluble. We then attempted to refold CED-3 from inclusion bodies into an active conformation. However, yields of active protease produced were too low for our purposes. An *in vitro* transcription/ translation system based upon bacterial lysates was also examined, but again, yields of protease activity were insufficient. A mammalian cell expression system was next tested, but resulted in only low levels of CED-3 production. Returning to a bacterial expression system we found that, by using low temperature inductions, a modified lysis buffer, and a significantly scaled-up culture volume, we were able to purify sufficient CED-3. Addition of a GST tag to the N-terminus of a truncated CED-3 construct also improved solubility and allowed the protein to be eluted from the purification resin. We were therefore able to produce active recombinant CED-3 in sufficient quantities for the substrate screen. Purified GST-CED-$3^{221-503}$ proved have a substrate specificity similar to but more promiscuous than that of human caspase-3 and was able to cleave *C. elegans* protein substrates in a z-VAD-fmk-inhibitable fashion.

3.4.2 Purification of CED-3

Expression in bacteria is commonly used as a simple means to purify recombinant proteins for biochemical analysis. Although we eventually succeeded in purifying recombinant CED-3 from bacterial lysates, it was certainly not straightforward, and the process was severely hampered by the sequestration of CED-3 within bacterial inclusion bodies. This is, in fact, a relatively common problem encountered with this technique (Rudolph and Lilie, 1996; De Bernardez Clark, 1998; Middelberg, 2002). Although many foreign proteins are tolerated well by bacterial cells, others are actively packaged into inclusion bodies; this may happen particularly when the expressed protein is toxic or expressed at extremely high levels. Protein aggregation and incorporation into inclusion bodies may also occur passively if the protein is by nature hydrophobic or insoluble, or if it requires specific factors such as chaperones to fold into a soluble conformation.

Insolubility has been encountered on expression of human caspases in bacterial cells, particularly those with long pro-domains such as caspase-8, caspase-9 and caspase-1, and it is possible that long pro-domains encourage aggregation of the protein (Stennicke and Salvesen, 1999b). However, in the case of CED-3, removal of the pro-domain did not improve its solubility. There were also no obviously hydrophobic regions in the sequence of CED-3 that might lead to aggregation. In an effort to counteract the solubility problems, we also expressed individual CED-3 subunits in bacteria, but each proved insoluble. This left the possibility that high levels of CED-3 expression were causing bacteria to actively sequester the protein. Indeed, reducing induction incubation temperature and therefore slowing the production of protein did encourage the solubilization of a small proportion of expressed CED-3, suggesting that high levels of expression were one reason for the packaging of the latter into inclusion bodies.

Incorporation of a GST tag in place of the CED-3 pro-domain also improved solubility. GST is a highly hydrophilic protein, and may force some CED-3 into solution rather than forming aggregates. We were initially concerned that the addition of a large (29 kDa) tag might alter the enzymatic properties of CED-3. However, the substrate specificity profile of GST-CED-$3^{221-503}$ proved almost identical to that of His-CED-$3^{221-503}$, its activity could be fully inhibited by z-VAD-fmk, was able to auto-process, and it cleaved the known substrates CED-3 and CED-9 in the predicted pattern, suggesting that GST-CED-$3^{221-503}$ was acting in a manner similar to that of native CED-3.

3.4.3 CED-3 is relatively promiscuous

We then went on to examine the substrate specificity of CED-3. In our analysis of different peptide substrates, CED-3 proved able to cleave three out of the four peptides tested, to varying degrees of efficiency. The DEVD-AFC peptide was clearly the optimal sequence of those tested, and is also the preferred peptide for the human executioner caspases, caspase-3 and caspase-7, suggesting that CED-3 is most closely related to these caspases in terms of activity. However, there was also significant proteolysis against IETD-AFC and LEHD-AFC, substrates efficiently cleaved by the third executioner caspase, caspase-6, and the initiator caspases, caspase-8, -9 and -10. In comparison to caspase-3, CED-3 therefore appears relatively promiscuous in its ability to cleave different peptides.

This agrees with a previous study using a combinatorial peptide screen to determine caspase substrate site specificities (Thornberry *et al.*, 1997) in which CED-3 was comparatively promiscuous in its preference for residues at the P2 position. However, our analysis suggests that CED-3 might also be more promiscuous in its preferences at the P4 position, and, unlike caspase-3, is able to cleave at branched-chain aliphatic residues.

As CED-3 acts as the only executioner in the worm and must cleave all necessary substrates, this comparative promiscuity might enable the caspase to cleave a wider range of substrates and so co-ordinate all the downstream effects of apoptosis. In humans, the executioner caspases caspase-3 and caspase-7 have a different preference from the caspase-6 executioner, and each one is more specific than CED-3. Why have these different substrate specificities been divided among different caspases in humans? It may be that having specialised executioner caspases with different substrate preferences allows an even broader range and larger overall number of substrates to be proteolysed. In humans, the increased complexity of the organism means that downstream events in apoptosis must be more complex and subject to more regulation. For example, the existence of a more complex immune system necessitates the existence of mechanisms for maintaining immunological silence. Caspases mediate the cleavage of several proteins that act as peptide-binding "danger signals" when released intact during necrosis (Basu *et al.*, 2000). Phagocytosis of dying cells is also accomplished by specialised immune cells, which must be attracted to the dying cell and also induced to produce cytokines that prevent inflammation (Meagher *et al.*, 1992; Sauter *et al.*, 2000). Apoptotic mammalian cells in addition appear to undergo more extensive blebbing and formation of apoptotic bodies than worm cells (our unpublished observations).

There is also the possibility that having several executioner caspases allows redundancy during the execution phase. In *C. elegans*, CED-3 is absolutely required for programmed cell death, and virtually no cell deaths occur in its absence. No caspase redundancy appears to exist. However, if CED-3 activity is completely blocked and no programmed cell deaths take place, the resulting worm is almost completely normal in its morphology and behaviour (Ellis and Horvitz, 1986). Human caspase-3 is the closest human homologue of CED-3, both in

terms of sequence identity and substrate specificity, as we and others have shown (Thornberry *et al.*, 1997). It is also a functional equivalent, as it appears to be the major executioner caspase and required for almost all apoptotic substrate cleavages in cell-free extracts. Extracts immuno-depleted of caspase-3 exhibit cleavage of almost no substrates, the exceptions being a few caspase-6-specific substrates such as lamin A, and some substrates such as PARP that are cleaved redundantly by caspase-3 and caspase-7 (Slee *et al.*, 2001; Ruchaud *et al.*, 2002).

In caspase-3 knockout mice, a sub-population of neurons fail to undergo cell death (Kuida *et al.*, 1996; Woo *et al.*, 1998). This failure in apoptosis leads to the accumulation of large numbers of supernumerary cells in the developing mouse brain. Like cells that survive in a CED-3 mutant, these cells are able to achieve a terminally differentiated state (Kuida *et al.*, 1996; Avery and Horvitz, 1987). Interestingly, a large percentage of the cells dependent upon CED-3 for programmed cell death are the sisters of neuronal cells, and adopt a neuronal phenotype if their death is suppressed (Avery and Horvitz, 1987), again linking the functions of the two enzymes. In this respect, the null phenotypes of the two related caspases are similar. However, there are also profound differences. In caspase-3-null mice, the additional neurons lead to multiple ectopic cell masses in the brain, and distortions in the development of other brain regions. The mutant mice are non-viable, and die either early during development or at 1-3 weeks after birth (Kuida *et al.*, 1996). Blocking caspase activity is therefore much more damaging in mammals than in the worm, and it is not surprising that mechanisms exist to ensure that apoptotic death is completed in higher organisms. Other cell populations from these caspase-3 null mutants, when tested with various apoptotic stimuli, proved just as sensitive to undergoing apoptosis as wild-type cells. This suggested that in most cell types, there is some redundancy in caspase activity that allows cells to undergo apoptosis even in the absence of the major executioner caspase. Human cell lines lacking caspase-3 are also able to undergo apoptosis, albeit with an altered morphology and slower kinetics. This redundancy may have evolved therefore to prevent, as far as possible, the detrimental effects of deregulated apoptosis. However, in mammals, even without the presence of caspases, cells will still undergo cell death, but in a damaging necrotic manner. Once mitochondria have released cytochrome c, the point of no return is passed; even the inhibition of caspases will not prevent cell death, but

this death will occur by necrosis, releasing many damaging cellular constituents and inflammatory mediators into the cell's surroundings (Kroemer and Martin, 2005; Basu *et al.*, 2000). Caspase redundancy may help prevent this, allowing apoptosis to occur even when one executioner caspase is missing or inhibited, for example due to mutation. This is not the case in post-mitotic cells such as neurons, though, that are absolutely dependent on caspases for their death, as seen in the caspase-3 null phenotype (Kuida *et al.*, 1996; Woo *et al.*, 1998). This in turn may prevent the adventitious death of cells that cannot be replaced.

Redundancy between caspase-3 and caspase-7 becomes particularly apparent in double-knockout mice lacking both these caspases (Lakhani *et al.*, 2006; Adrain and Martin, 2006). The phenotype of these mice is substantially more severe than that of mice lacking either caspase alone, having substantial defects in both cardiomyocytes and neuronal cells. In addition, thymocytes and fibroblasts from the knockout mice are resistant to several apoptotic stimuli and features of apoptosis. Substantial redundancy does therefore seem to exist, to help ensure that cell death occurs when and how it is appropriate.

3.4.4 CED-3 can also act as an initiator caspase

As the only caspase required in the worm, the function of CED-3 must extend beyond that of an executioner. It must also act in a way similar to the mammalian initiator caspases, in responding to upstream signals that lead to the downstream execution process. Human "initiator" caspases possess long pro-domains with protein-interaction motifs that mediate binding to adapter proteins, which cluster in response to upstream signals, leading to caspase auto-activation. They then activate downstream executioner caspases, which possess inter-domain cleavage sites similar to the (I/L/V)XXD consensus motif for the upstream caspases, allowing efficient activation. Like the initiator caspases, CED-3 also possesses a long pro-domain, with a CARD domain homologous to that of caspase-9. It also binds to an adapter molecule, CED-4, which oligomerizes to cause CED-3 auto-activation.

However, the auto-activation of CED-3 is sufficient to initiate downstream events in the worm, as no other caspase seems to be required to act as an executioner. Although it can cleave the substrates preferred by initiator caspases, LEHD and

IETD, its internal cleavage sites, $NFVD^{220}$, $DSVD^{374}$, $DNRD^{388}$, are most similar to its optimal DEVD/DETD motif, favoured by executioner caspases (Xue *et al.*, 1996). There has been a suggestion that other caspases might be expressed in the worm, raising the possibility that a proteolytic activation cascade might exist (Shaham, 1998). These potential caspases have been named CSP-1, CSP-2 and CSP-3. Transcription of two of these caspases was detected by Northern blotting, and one of the caspases exhibited proteolytic activity *in* vitro - a splice isoform of CSP-1, CSP-1B, that seemed able to cleave itself, CED-3 and CSP-2B. CED-3 was also able to cleave CSP-2B. This raises the possibility that CED-3 might act in a manner similar to human initiator caspases, triggering a proteolytic activation cascade; and also, that there might exist a second type of initiator caspase, as in humans. However, expression of these caspases has not been detected at the protein level, genetic screens have failed to identify a role for these proteases in the cell death process. The evidence therefore continues to suggest that CED-3 is able to act as the sole initiator and executioner caspase in the worm.

3.4.5 CED-3 does not cleave the substrates of inflammatory caspases

Some laboratories have phylogenetically grouped CED-3 with human caspase-1, -4 and –5, which are involved in inflammatory processes (Lamkanfi *et al.*, 2002). However, in our study, CED-3 showed virtually no activity against the YVAD-AFC peptide that is cleaved efficiently by these caspases, suggesting that its activity is fundamentally different. Other studies have suggested that CED-3 can only poorly cleave IL-1β and caspase-1, both good substrates for caspase-1 (Xue *et al.*, 1996). These differences reflect the highly different functions of CED-3 and the inflammatory caspases.

However, we cannot rule out entirely a role for CED-3 in the innate immune system of *C. elegans*. Worm cells lacking CED-3 or CED-4 appear to have a defective immune response and a reduced lifespan on infection with pathogenic bacteria (Aballay and Ausubel, 2001). Cells of *ced-3* mutant worms are also susceptible to the spread of vaccinia virus in comparison to wild-type worms (Liu *et al.*, 2006). By analogy with human inflammatory caspases, it is possible that CED-3 is able to cleave peptides with anti-microbial activity, causing their activation and/ or release. It is of interest that promoter-tagging studies suggest

that CED-3 may be expressed in intestinal cells of the adult worm, the point at which pathogenic organisms are most likely to enter (Shaham *et al.*, 1999).

3.4.6 Caspases in *Drosophila melanogaster*

When examining the evolution of the caspase family from worms to man, an interesting comparison can be made with the apoptotic pathways of the more complex invertebrate, *Drosophila melanogaster*, which may represent a mid-point in evolution. In *Drosophila*, there appears to have evolved a differentiation between initiator and executioner caspases, and some functional specialisation, though not to the degree seen in humans. Three executioners are present, DCP-1, drICE and DECAY (Kumar and Doumanis, 2000; Song *et al.*, 1997; Fraser *et al.*, 1997; Dorstyn *et al.*, 1999a). There are also two long pro-domain caspases, DRONC and DREDD (Kumar and Doumanis, 2000; Dorstyn *et al.*, 1999b; Chen *et al.*, 1998). DRONC appears to be required for cell death, and its oligomerization and auto-activation are driven by the Apaf-1 homologue DARK (Rodrigues *et al.*, 1999; Kanuka *et al.*, 1999; Zhou *et al.*, 1999). However, DREDD appears to play a role in the innate immune system and is activated downstream of Toll receptor activation in response to Gram-negative bacteria (Leulier *et al.*, 2000; Stoven *et al.*, 2000). It cleaves the NF-κB homologue Relish, which regulates the expression of anti-microbial genes. *Drosophila* caspase activation has also been implicated in the regulation of cell migration and differentiation, and it may be that additional roles such as these for *C. elegans* CED-3 await discovery (Arama *et al.*, 2003; Geisbrecht and Montell, 2004; Kumar, 2004).

3.4.7 Predicting CED-3 substrates

Given that we know something about the substrate site specificity of CED-3, might it not be possible to identify CED-3 substrates by screening a *C. elegans* database for caspase cleavage motifs using a bioinformatics approach? A simple search of the human database, however, demonstrates that the large majority of proteins in fact contain DXXD motifs, while we know by 2D protein analysis that only a very limited subset of the human proteome is cleaved during apoptosis (Gerner *et al.*, 2000; Dr. Colin Adrain, pers. comm.). The addition of the relatively promiscuous CED-3 to human cell extracts also resulted in the cleavage of a very limited number of proteins as determined by 2D analysis (data not shown). There are

clearly additional factors that influence selection of substrates beyond the tetrapeptide cleavage site motif.

Although peptide hydrolysis assays provide information on substrate site preference, they do not assess the ability of the caspase to cleave that site within a protein context, or the efficiency at which substrates are cleaved *in vivo*. For example, caspase-1 and –4 share a very similar substrate specificity profile, but while caspase-1 efficiently cleaves pro-IL-1β *in vitro* this protein is cleaved very poorly, if at all, by caspase-4 (Alexander Luthi, pers. comm.). Also, caspase-3 and -7 appear to have very similar substrate specificities against peptide substrates but actually play distinct roles *in vivo*, where caspase-3 activity appears to be required for almost all substrate cleavages while caspase-7 plays a much more limited role (Slee *et al.*, 2001). One possibility is that caspase substrate site specificity extends beyond the tetrapeptide motif. Where peptide substrate screens have examined residues extending beyond the essential tetrapeptide moiety, they have found that some caspases have specific requirements for the residues following the P1 pr preceding the P4 position (Nicholson, 1999). This is also true of the aspartic-specific serine protease granzyme B, which requires a small amino acid at the P1' position, immediately following the P1 aspartate (Harris *et al.*, 1998).

It is undoubtedly true that the positioning and accessibility of the potential cleavage site sequence is critical in determining whether proteolysis of a protein can occur. There is little known about the proteolytic activity of CED-3 against protein substrates. *In vitro* studies against limited panels of proteins show that it is able to auto-process, and to cleave the *C. elegans* protein CED-9, the baculovirus caspase inhibitor p35, and the human proteins PARP, caspase-2 and caspase-3 (Xue *et al.*, 1996; Hugunin *et al.*, 1996; Xue and Horvitz, 1995; Xue and Horvitz, 1997). CED-3 was able to cleave most of the proteins tested in these studies, reflecting its promiscuity against peptide substrates. However, it did exhibit some specificity; it had little activity against caspase-1 and pro-IL-1β, and was unable to cleave the caspase-1 inhibitor CrmA, consistent with its inability to cleave the caspase-1 consensus peptide YVAD-AFC. However, the only potentially relevant substrate among these is CED-9, and the *in vivo* importance of this cleavage event is not clear. A recent screen for CED-3 substrates involving the co-expression of CED-3 with a translated library of *C. elegans* genes in yeast cells

has revealed two further candidate substrates, Y24D9A.2 and Y17G7B.15b (Kim *et al.*, 2004). Y24D9A.2 is a predicted transcription factor containing a SET domain, and Y17G7B.15b is a centaurin β homologue. However, the potential relevance of these cleavage events is again unclear.

3.4.8 Further work with recombinant GST-CED-3$^{221-503}$

Our knowledge of the protein substrates of CED-3 is therefore extremely limited and confined to *in vitro* analyses. This has surely been due in large part to the difficulties associated with identifying downstream elements of proteolytic pathways through genetic means, the difficulty of activating endogenous CED-3, and difficulty of purifying the recombinant enzyme. These barriers have resulted in a general lack of knowledge of the mechanisms involved in CED-3 regulation and activity. In this phase of this study, we have developed a method for generating relatively large amounts of recombinant CED-3 that can efficiently cleave peptides and protein substrates. This enzyme can be used to address some of these gaps in our knowledge, as discussed in this and subsequent chapters.

Our aim in the next phase of this project was to identify substrates of CED-3 using the recombinant enzyme in *C. elegans* lysates followed by 2D analysis. However, there are many other potential applications for recombinant CED-3. For example, the crystal structure of CED-3 has not been solved to date. Knowledge of this structure would help us to understand its mode of activation, interactions with CED-4, substrate preferences, and relationship with caspases in other species. Some of our methods for generating soluble CED-3 could be applied to the full length enzyme for this type of study. On the other hand, organism-level studies into CED-3 have been substantially hindered by the lack of antibodies directed against CED-3. This means that we don't know the sub-cellular localization or expression patterns of CED-3 during development, which would give us further insights into its regulation. During this study, we have generated several antibodies against CED-3, which could potentially be applied to this problem.

Comparisons between CED-3 and human caspases can shed a lot of light on cell death processes in both organisms. Adding CED-3 to human cell free extracts resulted in the cleavage of several proteins, including caspases, which are substrates for human caspases (data not shown). This suggests that substrate

cleavage events are likely to be conserved between the two species. We went on to identify and characterize CED-3 substrates in *C. elegans*, with the aim of discovering substrates conserved between humans and worms, and in this way hopefully gaining a further understanding of the demolition phase of apoptosis in both organisms. This analysis is discussed in the following chapter.

CHAPTER IV

Identification of CED-3 substrates by proteomic analysis

4.1 CHAPTER INTRODUCTION

The convergence point of all pathways leading to apoptosis is the activation of the caspase family of proteases (Creagh and Martin, 2001; Martin and Green, 1995). Caspase activation leads to the limited proteolysis of a subset of the proteome (Martin and Green, 1995; Fischer and Schulze-Osthoff, 2003). These cleaved proteins then effect the downstream cellular changes that occur during apoptosis. Substrate cleavage events ensure, among other things, the detachment of the cell from its neighbours, the shutdown of cellular processes, and the efficient packaging and disposal of the dead cell.

The nature and importance of many of these downstream events are clear. What is poorly understood, however, is how individual substrate cleavages contribute to these cellular changes. In very few cases have substrates been linked directly to an apoptotic event; more usually, possible roles of cleaved substrates are extrapolated from the usual function of the substrate protein. One problem in deciphering the importance of individual caspase cleavage events is indeed the plethora of caspase substrates identified. The major focus of many studies has been the identification of large numbers of substrates, often using high-throughput techniques, without examining the physiological meaning of these cleavages. This has made it hard to see the wood for the trees – researchers looking at lists of identified substrates to find those involved in downstream events are unable to distinguish between important and bystander substrate cleavage events.

The situation is very different in *C. elegans*. Despite the long history of studying programmed cell death in this organism, virtually no substrates are known for CED-3. Recombinant CED-3 has been shown to cleave *in vitro* synthesized CED-3 and CED-9, and more recently the proteins Y24D9A.2 and Y17G7B.15b (Xue *et al.*, 1996; Xue and Horvitz, 1997; Kim *et al.*, 2004). However, with the exception of CED-3 auto-proteolysis, the physiological relevance of these cleavage events, or whether they even occur in a cellular environment, is unclear. We therefore have no idea how CED-3 mediates downstream events in *C. elegans* programmed cell death. However, as well as learning how CED-3 co-ordinates cell death in the worm, the identification of caspase substrates in *C. elegans* would allow us to identify conserved caspase substrates, proteins that have remained targets for caspase-dependent proteolysis through evolution in organisms as divergent as

worms and humans. Given the conservation of many downstream apoptotic events between the two species, this subset of conserved substrates could well prove enriched in proteins that mediate important downstream cellular changes. The identification of CED-3 substrates could therefore inform us as much about the execution of apoptosis in human cells as in the worm. These were our aims in embarking upon the identification of CED-3 substrates described in this chapter.

4.2 CHAPTER SUMMARY

The first stage of the analysis involved developing a system to generate large volumes of soluble protein extracts from *C. elegans*. Populations of *C. elegans* were grown in liquid cultures until saturated, then pelleted and washed free of bacteria and debris by centrifugation through a sucrose solution. Worms were lysed by sonication in cell extract buffer and insoluble material was removed by centrifugation. The supernatant represents the *C. elegans* soluble proteome.

These extracts were incubated with GST-CED-$3^{221-503}$, and treated and untreated extracts subjected to 1D SDS-PAGE followed by staining with Coomassie Blue. No protein alterations were observed by 1D gel analysis, so we subjected extracts to 2D SDS-PAGE to separate proteins into discrete spots based on molecular weight and pI. Proteins were stained with silver nitrate, and a subset appeared reproducibly altered upon treatment with CED-3. These latter proteins were excised from gels, digested with trypsin, and identified by MALDI-TOF mass spectrometry. The 22 identified substrate proteins encompass a variety of functions, and include several homologues of known human caspase substrates.

We then attempted to generate extracts from ced-9^{ts} mutant embryos, to validate our substrate identifications using endogenous CED-3. However, due to major technical problems we were unable to use these embryonic extracts for 2D analysis. Instead, we confirmed two substrate cleavages by Western blotting of CED-3-treated extracts, and selected three conserved substrates for *in vitro* expression. The addition of recombinant CED-3 caused proteolysis of all three proteins, confirming that they were genuine CED-3 substrates. We then identified CED-3 cleavage sites in the three substrates by using site-directed mutagenesis to generate non-cleavable mutant proteins. In the next phase of the analysis, we examined potential functional roles of these three substrates during apoptosis.

4.3 RESULTS

4.3.1 Preparation of soluble protein extracts from *Caenorhabditis elegans*

Our initial plan had been to activate endogenous CED-3 in *C. elegans* cells and analyse subsequent protein changes in extracts prepared from these cells by 2D electrophoresis. However, there are no available *C. elegans* cell lines in which to induce programmed cell death, and our attempts to activate CED-3 in isolated embryos by incubation with a variety of pro-apoptotic stimuli were entirely unsuccessful at inducing programmed cell death (data not shown). We therefore decided to proceed by generating soluble protein extracts from *C. elegans*, and adding recombinant CED-3 to them.

The method we developed for deriving these worm extracts is outlined in Figure 4.1. Large populations of *C. elegans* were grown on OP50 bacteria in liquid cultures. These populations were non-synchronous and therefore represented worms at all developmental stages. Once the population was saturated and all bacteria had been cleared, worms were harvested by centrifugation. The worm pellet was then washed with 100 mM NaCl followed by centrifugation through a 60 % sucrose solution. Washed nematodes were collected from the top of the solution and washed again with 100 mM NaCl. In order to break open the tough extracellular cuticle and extract soluble proteins, the population was gently sonicated in a cell extract buffer until no intact worms could be seen by light microscopy. Soluble proteins were then separated from the insoluble fraction by further centrifugation.

4.3.2 Characterizing CED-3 activity in *C. elegans* extracts

We went on to examine the activity of recombinant CED-3 in our *C. elegans* extracts. There was a possibility that the presence of endogenous caspase inhibitors in the extract might prevent substrate cleavage by CED-3, rendering our analysis more difficult. To assess whether this might be the case, we added recombinant CED-$3^{221\text{-}503}$ to *C. elegans* extracts and incubated the reactions for 30 minutes. In comparison, we also incubated CED-$3^{221\text{-}503}$ without extract. CED-3 activity was then analysed in fluorimetry reactions by measuring the rate of DEVD-AFC hydrolysis (Figure 4.2 A).

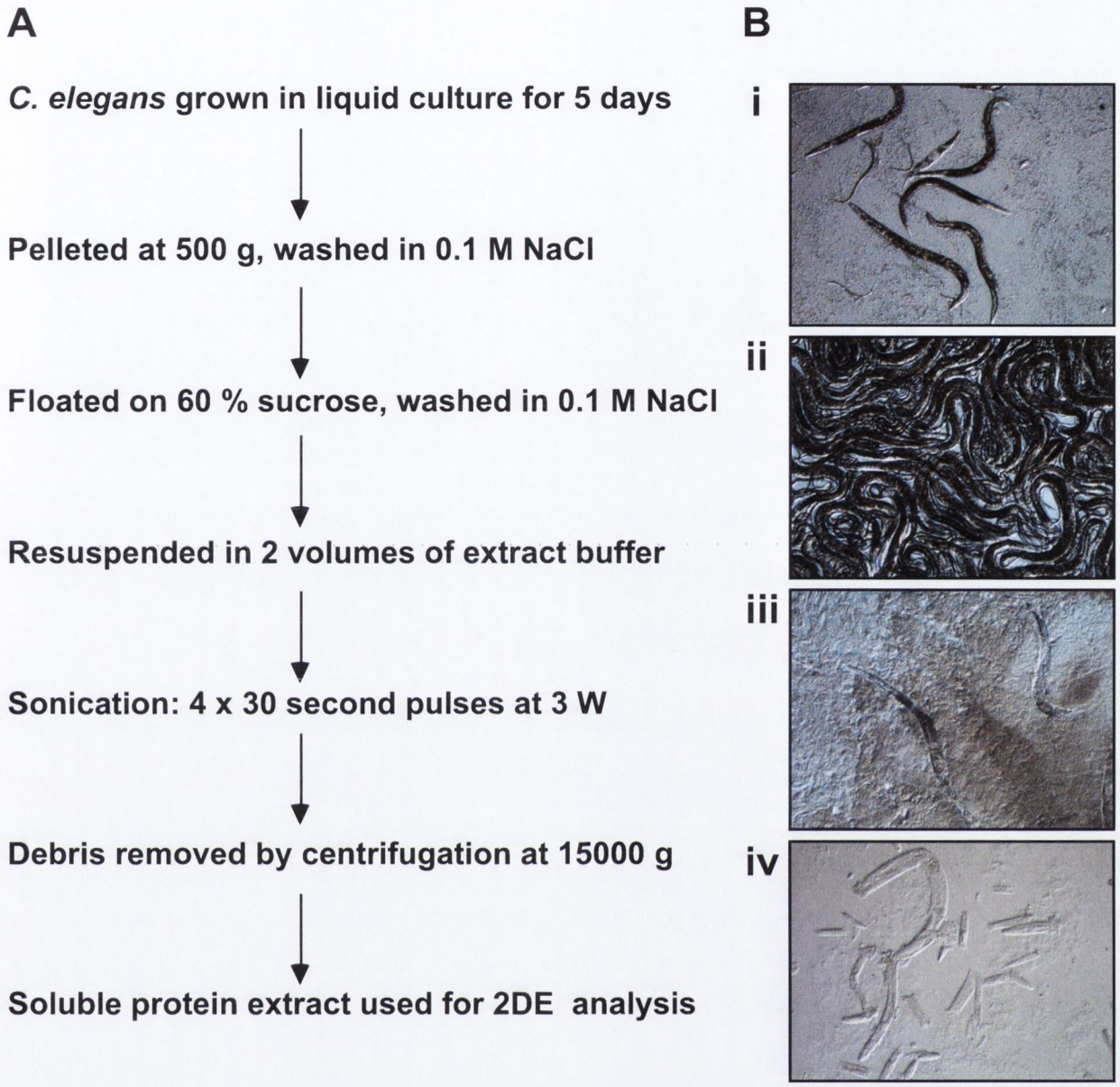

Figure 4.1

Preparation of *C. elegans* soluble protein extracts

(A) Schematic representation of the preparation of soluble protein extracts from *Caenorhabditis elegans*. Worms were grown on *E. coli* OP50 bacteria in liquid cultures until bacteria were cleared. The population was then packed and centrifuged through 60% sucrose. Worms were suspended in an isotonic extract buffer and sonicated. Cuticular and insoluble material was removed by centrifugation, and the supernatant used for analysis.
(B)(i) Mixed population of *C. elegans* in liquid culture
(ii) Packed worms prior to sonication
(iii) Insoluble material pelleted after sonication
(iv) Diluted insoluble material showing empty worm cuticles

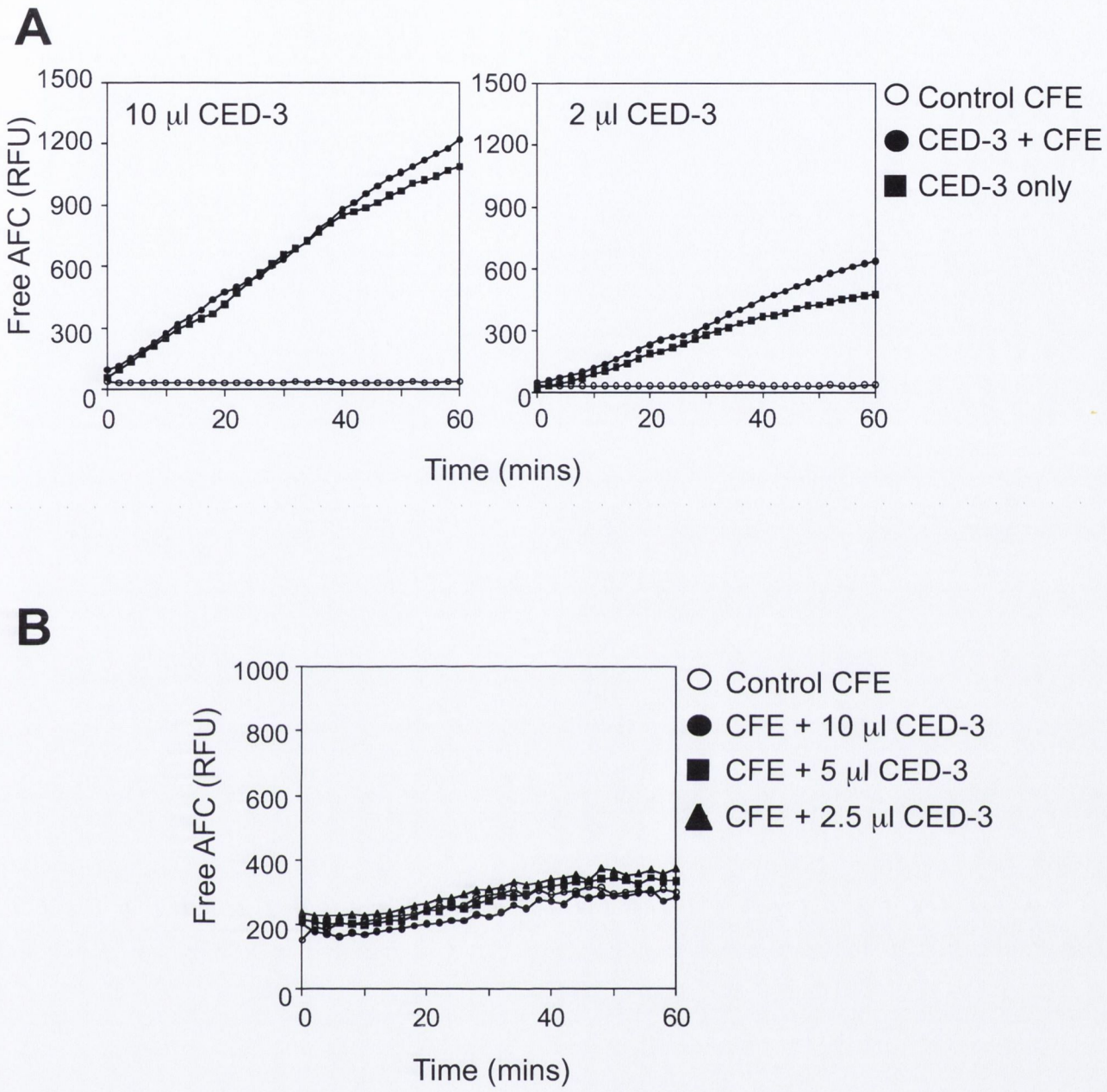

Figure 4.2

Incubation of CED-3 with *C. elegans* soluble protein extract

(A) Testing the effect of *C. elegans* soluble protein extract on CED-3 activity. 10 or 2 μl of His-CED-$3^{221-503}$ conjugated to Ni-NTA agarose was incubated for 30 minutes with 10 μl of *C. elegans* soluble protein extract in a total reaction volume of 20 μl, alongside parallel reactions without extract. 5 μl of each reaction was then added to a 200 μl reaction volume containing 50 μM DEVD-AFC. Activity of CED-3 was assayed by release of AFC. (B) CED-3 cannot stimulate activity of endogenous CED-3 in *C. elegans* soluble protein extracts. Extracts were incubated with 10, 5 and 2.5 μl of His-CED-$3^{221-503}$ conjugated to Ni-NTA agarose for 1 hour. His-CED-$3^{221-503}$ was then removed by pelleting and 5 μl of each reaction added to a 200 μl reaction volume containing 50 μM DEVD-AFC. Caspase activity was then measured by release of AFC.

The presence of *C. elegans* extracts appeared to slightly enhance the activity of CED-3, particularly at lower enzyme concentrations, suggesting against the presence of significant inhibitory activity. A possible explanation for the enhancement of CED-3 activity is that the presence of additional proteins and factors in the extracts may stabilise the CED-3 protein, especially at lower concentrations of the protease.

It was also possible that the addition of recombinant CED-3 might activate endogenous CED-3 present in the extract. To test this, we incubated samples of *C. elegans* extracts with a titration of recombinant His-CED-$3^{221-503}$ conjugated to Ni-NTA agarose for 1 hour at 37 °C. Beads were then removed from the reactions by centrifugation and the resulting extracts tested for DEVD-AFC hydrolysis activity (Figure 4.2 B). However, we detected no significant DEVDase activity in any of the extract samples, and untreated extracts behaved exactly the same as those incubated with CED-3. We therefore concluded that recombinant CED-3 is unable to activate endogenous CED-3 in these extracts.

4.3.3 Treatment of *C. elegans* extracts with GST-CED-$3^{221-503}$ and analysis by 1D SDS-PAGE

We then added GST-CED-$3^{221-503}$ to a sample of extract at a dilution of 1:3, capable of efficiently cleaving substrate proteins in a protein extract environment (Figure 3.13). The final protein concentration of the extract used in the reaction was 6.35 mg/ ml. In parallel, a sample of *C. elegans* extract at the same concentration was treated with buffer alone. The reactions were incubated for 2 hours at 37 °C. 100 μg samples of treated and untreated extracts were then electrophoresed through large-format 1D 12 % SDS-PAGE gels alongside a sample of GST-CED-$3^{221-503}$. The resulting protein gel was stained with Coomassie Blue (Figure 4.3).

There were no visible changes to the *C. elegans* proteome as assessed by this method. We hypothesized that this might be due to the lack of sensitivity of the Coomassie stain used, and a lack of protein band resolution on the 1D gel. To address these problems, we decided to repeat the analysis using 2D electrophoresis, to give a better resolution of individual proteins, and using silver nitrate staining to provide more sensitive protein detection.

4.3.4 Treatment of *C. elegans* extracts with GST-CED-3$^{221-503}$ followed by 2D SDS-PAGE analysis

We therefore treated samples of *C. elegans* extracts as above, followed by 2D SDS-PAGE. 400 μg samples of treated and untreated extracts were solubilized with 2D loading buffer and rehydrated into pI 5 - 8 and pI 3 - 6 IPG strips. The hydrated strips were subjected to isoelectric focusing followed by electrophoresis of the proteins through large-format 12 % second-dimension SDS-PAGE gels. Gels were stained with silver nitrate, developed, and protein profiles of untreated and CED-3-treated extracts were compared, as summarised in Figure 4.4.

A subset of the proteome was visibly altered on CED-3 addition (Figure 4.5 A, B). Some proteins present in untreated *C. elegans* extract disappeared upon CED-3 addition, while other protein spots were observed only after the addition of recombinant CED-3. In total, after a number of independent analyses, we were able to calculate that about 3 % of the protein spots visible on 2D SDS-PAGE gels were reproducibly altered on CED-3 treatment. This compares with around 5 % of the human proteome and around 2 % of the *Drosophila* proteome that were found to undergo caspase-dependent alterations in similar studies conducted on other species in our laboratory (Dr. Colin Adrain and Dr. Emma Creagh, pers. comm.) (Figure 4.6).

4.3.5 Identification of CED-3 substrates by mass spectrometry

The next stage of the analysis was to identify those proteins that appeared/disappeared upon addition of CED-3 to *C. elegans* extracts. To achieve this, we excised the appearing or disappearing proteins from gels and destained, fixed and dehydrated the gel samples. The proteins within the gel were then digested overnight with trypsin. These tryptic digest fragments were analysed by MALDI-TOF mass spectrometry. Peptide profiles from each protein were compared with theoretical tryptic digests of all *C. elegans* proteins in the NCBI database, using MS-Fit software, to obtain peptide fingerprint matches and therefore identify the protein in question (outlined in Figure 4.4). Identification of CED-3 substrates from four sets of pI 5 - 8 and pI 3 - 6 gels allowed us to compile a list of *C. elegans* CED-3 substrates (Table 4.1).

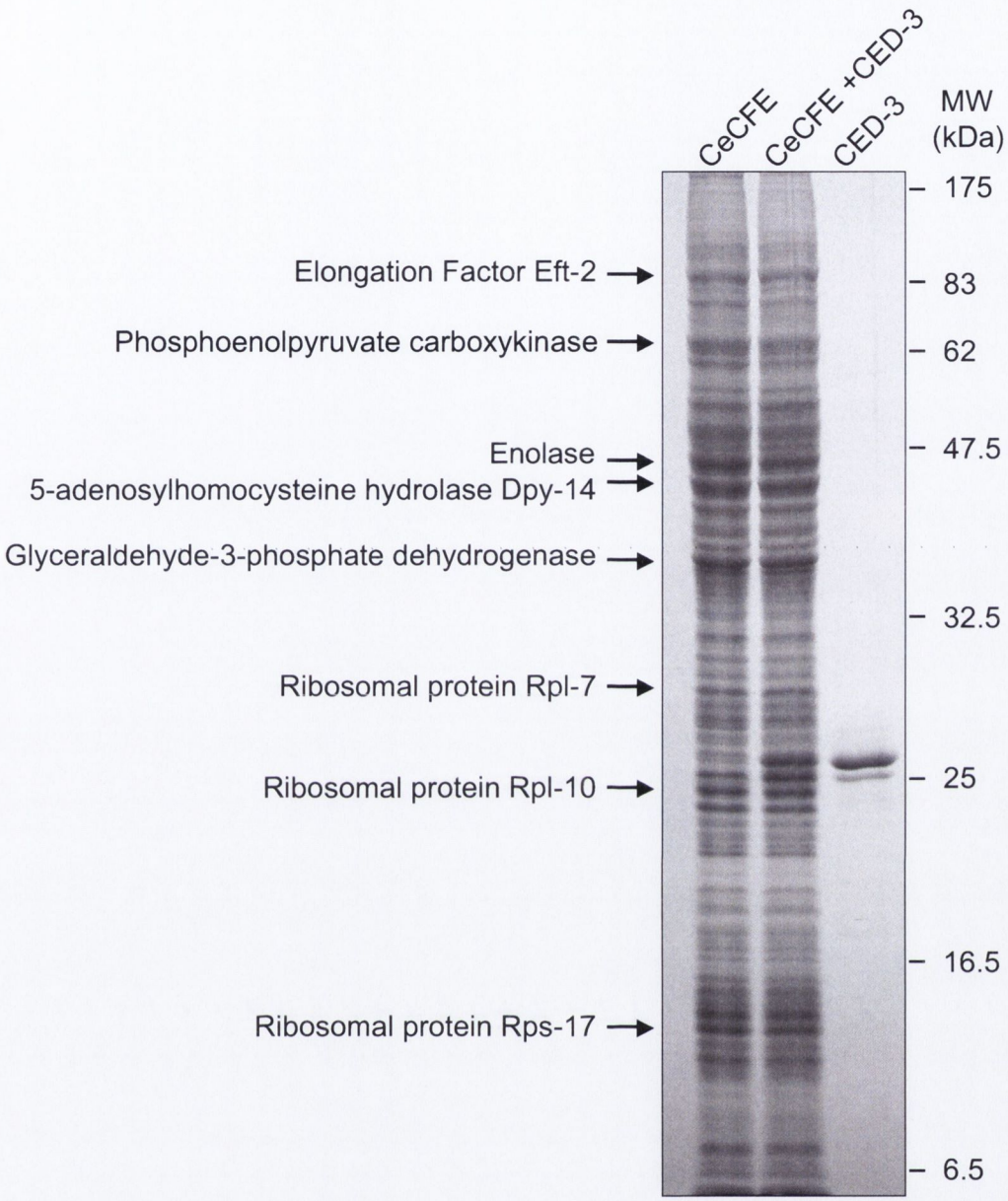

Figure 4.3

1DE analysis of *C. elegans* extract treated with GST-CED-3$^{221-503}$

CED-3 substrate cleavages are not detectable by 1D SDS-PAGE. *C. elegans* extract was diluted to 6.35 mg/ ml with extract buffer and treated with GST-CED-3$^{221-503}$ at a 1:3 final dilution of protease. After incubation for 2 hours at 37 ^{o}C, 100 μg of treated and untreated protein was loaded onto a large-scale 12% SDS-PAGE gel alongside an equivalent amount of CED-3 alone. The gel was stained with Coomassie Blue and examined for protein changes. Landmark proteins were identified by mass spectrometry and annotated.

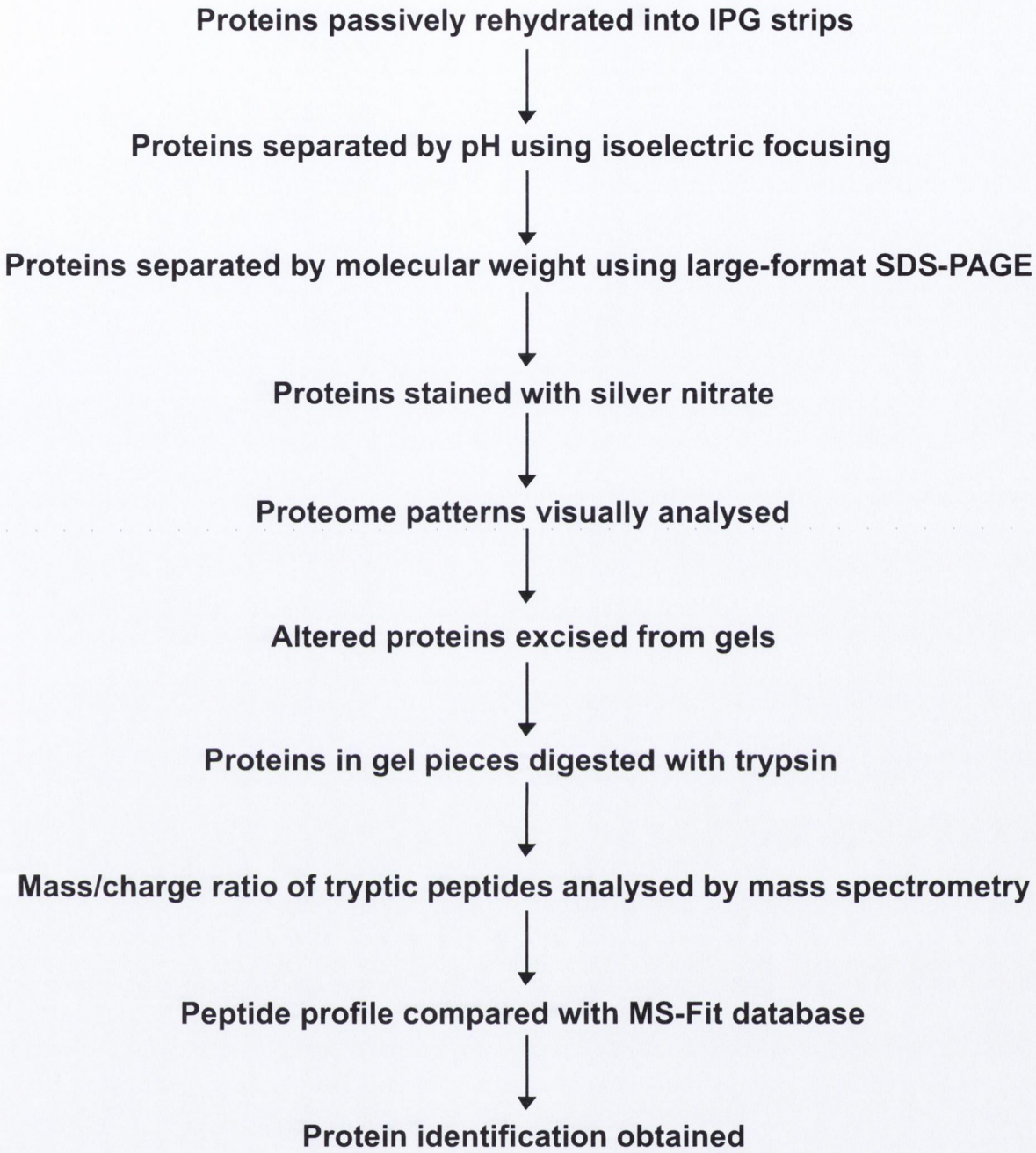

Figure 4.4

Identification of substrates using 2D SDS-PAGE and mass spectrometry

Schematic representation of the identification of CED-3 substrate proteins using 2DE and MS. *C. elegans* CFE treated with CED-3 or left untreated was rehydrated into immobilised pH gradient (IPG) strips and proteins distributed by pH along the strip by isoelectric focusing. Proteins were then separated by molecular weight on large format SDS-PAGE gels. Gels were stained with silver nitrate and changes in the protein profiles of CED-3-treated versus untreated extracts visually assessed. Altered protein spots were excised from gels and proteins were digested with trypsin. The mass/charge ratio of these tryptic peptides was then measured by MALDI-TOF MS, peptide m/z profiles compared with a database of theoretical protein digests, and protein identifications obtained.

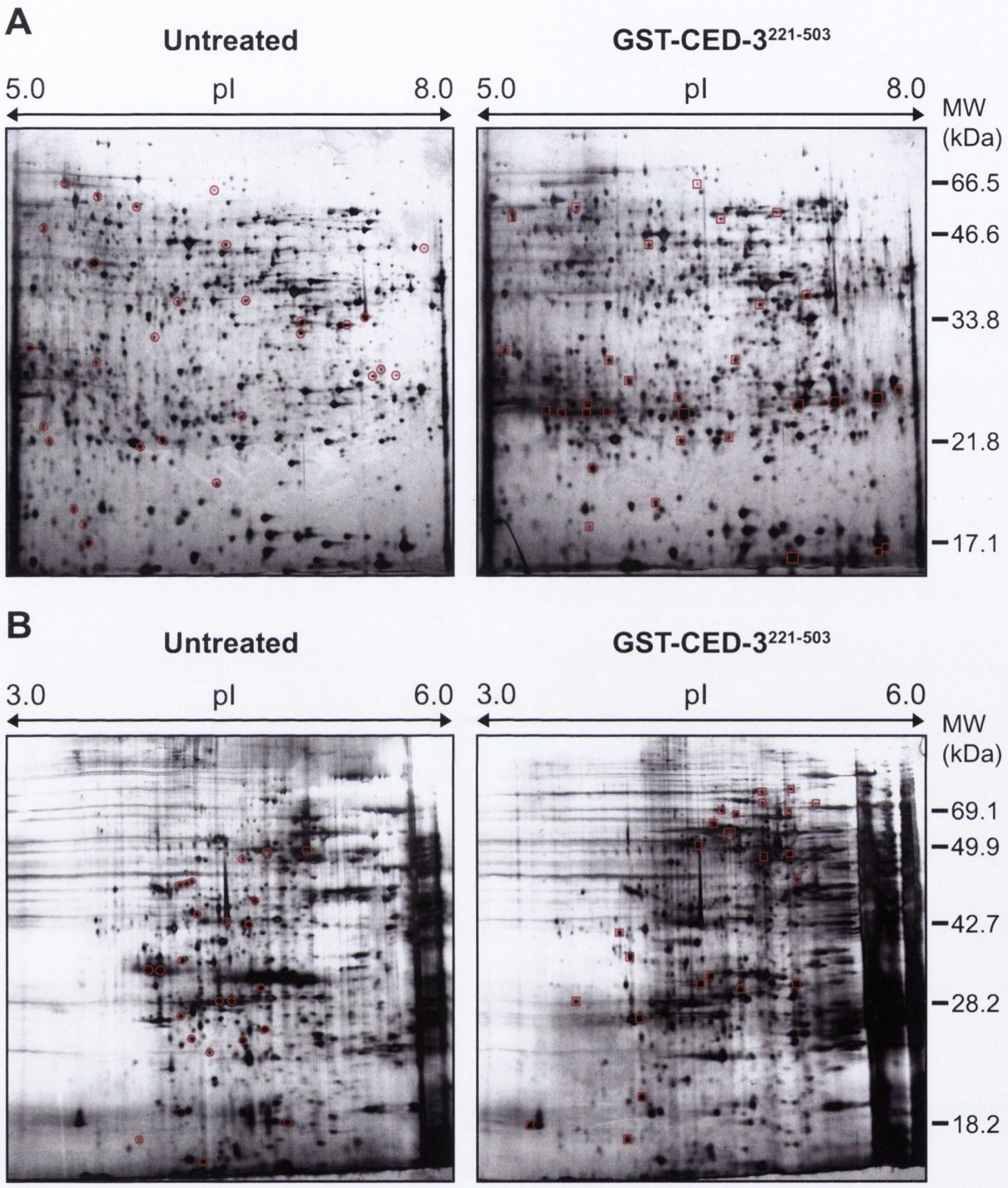

Figure 4.5

2DE analysis of *C. elegans* extract treated with rGST-CED-3$^{221-503}$

CED-3-mediated proteome alterations can be detected by 2D SDS-PAGE. *C. elegans* extract was diluted to 6.35 mg/ ml with extract buffer and treated with GST-CED-3$^{221-503}$ at a 1:3 final dilution of protease. After incubation for 3 hours at 37 ^{o}C, 400 μg of treated and untreated protein was loaded onto IPG strips with an immobilized pI 5 - 8 (A) or pI 3 - 6 (B) gradient. Strips were focused to acheive a final VH of 55000. Subsequent second-dimension electrophoresis was through a 12% SDS-PAGE gel. Spots disappearing/reduced from control gels after CED-3 treatment are marked with circles; spots appearing/increased on gels treated with CED-3 are marked with squares.

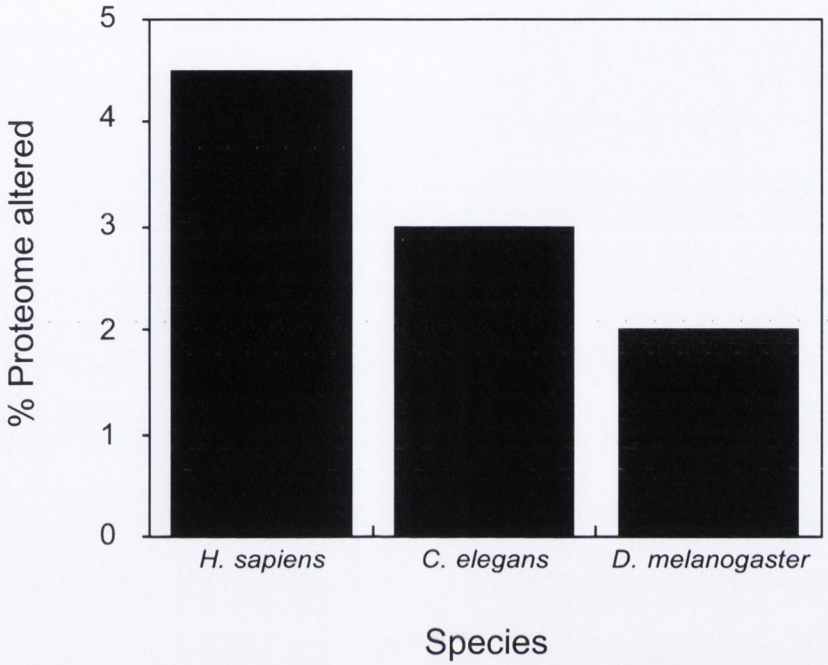

Figure 4.6

Percentage of the proteome cleaved by caspases in humans, *C. elegans*, and *D. melanogaster*

Caspases cleave a smaller proportion of the proteome in *C. elegans* than in humans, but a higher proportion than in *Drosophila*. 2D gels from human Jurkat CFE treated with cytochrome c/ dATP, *C. elegans* CFE treated with GST-CED-$3^{221-503}$, and extracts of cells from *D. melanogaster* treated with actinomycin D, were examined and numbers of protein changes occuring on caspase activation in each case were counted. The total number of proteins on 2D gels from each organism were also counted, and the percentage of the visible proteome cleaved by caspases in each case was calculated. *H. sapiens* data kindly provided by Dr. Colin Adrain. *D. melanogaster* data kindly provided by Dr. Emma Creagh.

Protein name	Accession no. (NCBI)	Protein function	MS coverage	Peptide matches
Actin (Act-1/-2/-3/-4)	gi:6628	Cytoskeletal	26.0%	11
Myosin light chain (Mlc-2)	gi:17569077	Cytoskeletal	69.0%	9
Tubulin beta-2 chain (Tbb-2)	gi:17552540	Cytoskeletal	56.0%	27
Tubulin alpha (Tba-2)	gi:17506073	Cytoskeletal	53.0%	20
ATP synthase α and β (Vba-13)	gi:17565854	ATP synthesis	58.0%	39
ATP synthase subunit 2 (Atp-2)	gi:25144756	ATP synthesis	57.0%	23
Aconitate hydratase (Aco-1)	gi:17568399	Metabolism	26.0%	19
Aconitase protein 2c (Aco-2)	gi:32564738	Metabolism	12.0%	8
Aldo-keto reductase	gi:17564128	Metabolism	40.0%	11
Transketolase	gi:17539652	Metabolism	35.0%	20
Aldo-keto reductase family 1 C1	gi:17550248	Metabolism	35.0%	10
Protein disulfide isomerase 3 (Pdi-3)	gi:17507915	Chaperone	15.0%	8
Stress-induced phosphoprotein 1	gi:17563052	Chaperone	50.0%	17
Calreticulin (Crt-1)	gi:17565428	Chaperone	25.0%	9
Chaperonin TCP-1 (Cct-4)	gi:17532603	Chaperone	26.0%	12
Aspartic protease precursor	gi:17560290	Proteolysis	28.0%	8
Aspartic protease 2 (Asp-2)	gi:32566657	Proteolysis	17.0%	5
Metalloenzyme	gi:32564249	Extracellular	15.0%	8
14-3-3 protein 2 (Ftt-2)	gi:17568359	Signalling	54.0%	18
Galectin (Lec-6)	gi:17556226	Signalling	37%	3
Nucleosome assembly 1-like 1 (Nap-1)	gi:17539540	DNA synthesis	36.0%	12
Ribosomal protein, small (Rps-12)	gi:17554772	Protein synthesis	80.0%	9

Table 4.1

Mass spectrometry identifications of CED-3 substrates

Substrates identified from pI 5 - 8 and pI 3 - 6 2D gels of *C. elegans* extract treated with GST-CED-$3^{221-503}$ were analysed by MALDI-TOF mass spectrometry. Identified substrates are shown with their NCBI accession numbers, functional classification, the % of protein coverage by the MS peptide fingerprint, and the number of specific peptides used to identify the protein.

In all, 22 CED-3 substrates were identified. These substrates can be divided into several broad functional categories - those involved in the cytoskeleton, ATP synthesis, metabolic processes, proteolysis, signalling pathways, DNA and protein synthesis, protein chaperoning, and extra-cellular functions. Eight of them are homologues of proteins known to be cleaved by human caspases – alpha-tubulin, beta-tubulin, myosin light chain, actin, nucleosome assembly protein 1-like 1, calreticulin, 14-3-3 protein 2, and aldo-keto reductase (Adrain *et al.*, 2006; Gerner *et al.*, 2000; Mashima *et al.*, 1997; Moretti *et al.*, 2002; Widmann *et al.*, 1998; Van Damme *et al.*, 2005; C. Adrain, pers. comm). The wide range of proteins identified suggests that CED-3 targets multiple cellular functions in order to kill the cell. Together, these newly-identified substrate proteins represent a blueprint for CED-3-mediated cell killing.

Examples of substrate proteins that disappear from control gels or appear as cleavage fragments on CED-3 addition are shown in Figure 4.7, and their corresponding mass spectrometry peptide profiles are represented in Figure 4.8. ATP synthase α and β subunits were repeatedly reduced in abundance on addition of CED-3 from the high molecular weight/ low pH region of pI 5 - 8 gels, and also on pI 3 - 6 gels (Figure 4.7 A). The spot was excised from control gels, and peptides derived from the whole sequence of the protein were observed (Figure 4.8 A). A spot identified as the tubulin β-chain appeared on pI 3 - 6 gels after CED-3 treatment (Figure 4.7 B). Peptides were obtained covering all of the protein with the exception of a small region at the C-terminus, suggesting cleavage at the extreme C-terminus, which contains many aspartic acid residues (Figure 4.8 B). Nucleosome assembly protein 1-like 1 virtually disappeared from pI 3 - 6 gels on CED-3 addition (Figure 4.7 C). Again, the protein was excised from control gels and peptide coverage was obtained over almost the whole protein (Figure 4.8 C). Calreticulin appears as a cleavage fragment on pI 3 - 6 gels, with no peptides detected over the N-terminal 80 amino acids, suggesting removal of this region (Figure 4.7 D; Figure 4.8 D). Finally the 14-3-3 protein FTT-2 disappears from control pI 3 - 6 gels on CED-3 treatment, and upon excision form control gels, identified by peptides covering almost the whole protein (Figure 4.7 E; Figure 4.8 E). In all these cases, the vast majority of neighbouring proteins are unaffected by CED-3 treatment, showing that the effect of CED-3 treatment is limited to specific substrate proteins.

The 22 proteins in Table 4.1 were identified as CED-3 substrates multiple times. However, there were other proteins that were altered on only one gel, or which showed only minor degrees of alteration upon CED-3 treatment. Some of these proteins were also identified by mass spectrometry. Other identifications made were of relatively low certainty, and might represent mis-identifications. While none of these proteins can be confidently categorised as CED-3 substrates and are therefore not listed in Table 4.1, among them are several homologues of known caspase substrates in other species. It is possible that at least some of them may prove to be genuine CED-3 substrates, and they are therefore included here as Appendix 1.

4.3.6 ced-9^{ts} mutant embryos as a source of endogenous active CED-3

A weakness of our analysis is that the use of recombinant CED-3 in extracts might not reflect the activity of endogenous CED-3 in whole cells. In addition, developmental cell death occurs mostly in embryos, and some in larvae, while our extract is composed of worms at all developmental stages, and might therefore not reflect the pool of proteins available to CED-3 *in vivo*. We therefore looked for a way in which we could use active endogenous CED-3 to validate that these substrate proteins are cleaved in an *in vivo* setting by the endogenous enzyme.

Mutant embryos lacking functional CED-9 undergo massive programmed cell death and developmental arrest (Hengartner *et al.*, 1992). In one mutant strain, containing the *ced-9* n1653 allele, the CED-9 protein is temperature-sensitive, losing its protective function at 25 °C. We decided to use embryos from this strain as a source of active CED-3, because the enzyme should become activated upon inactivation of CED-9 at the restrictive temperature, prompting massive programmed cell death. Analysis of the proteome of embryos incubated at the permissive and restrictive temperatures by 2D electrophoresis, we reasoned, should enable us to see which proteins are altered upon endogenous CED-3 activation and potentially validate the substrates already identified.

We started by characterizing the *ced-9^{ts}* mutant embryos, to confirm that embryos incubated at 25 °C do undergo loss of CED-9 function and programmed cell death. Firstly, embryos were isolated by treatment of worm populations with 2.5 M NaOH/

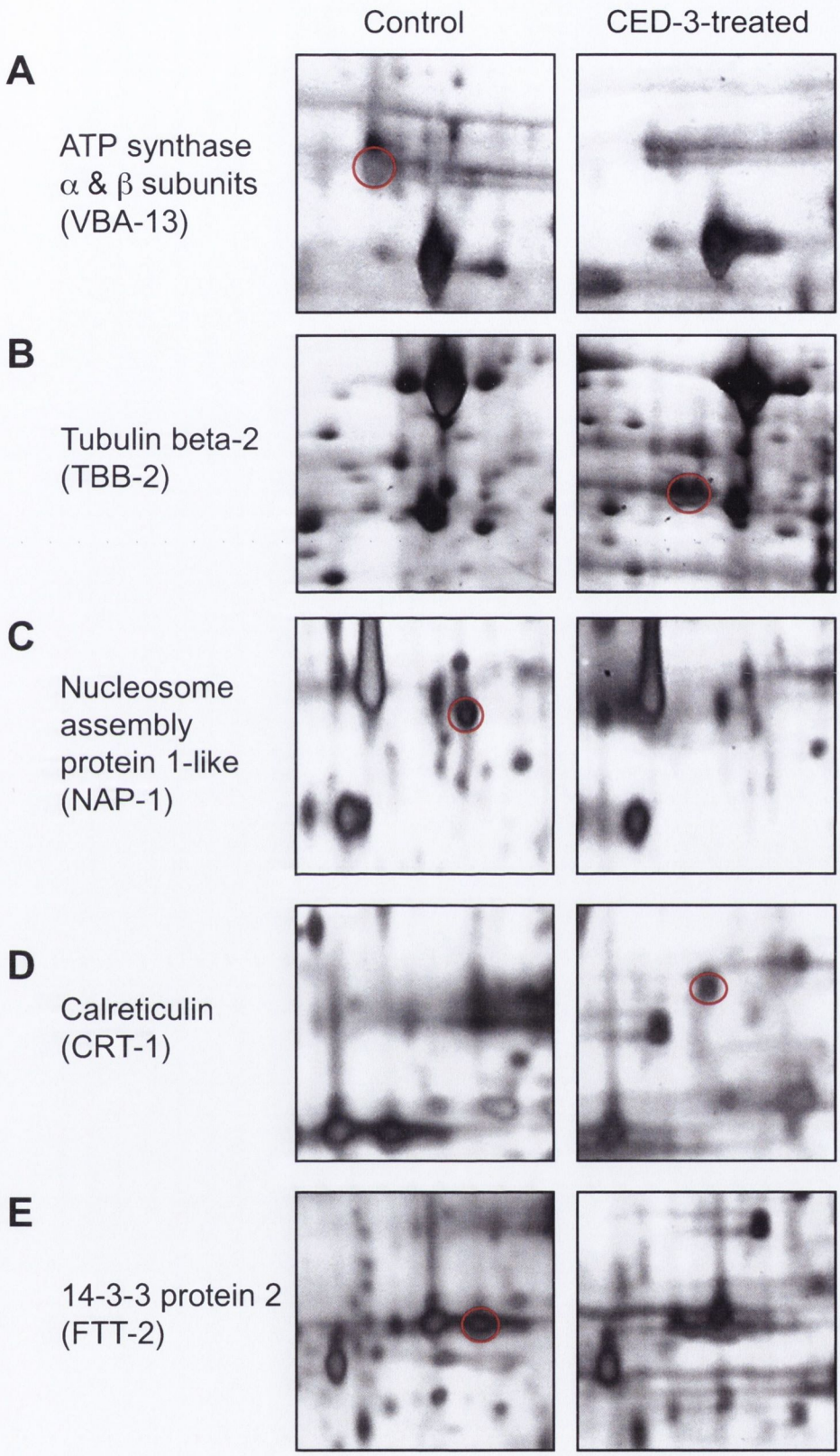

Figure 4.7

GST-CED-3$^{221-503}$ substrates on 2DE gels

Proteins showing alteration on 2D gels after treatment with recombinant CED-3. Protein identifications were obtained by MALDI-TOF mas spectrometry.

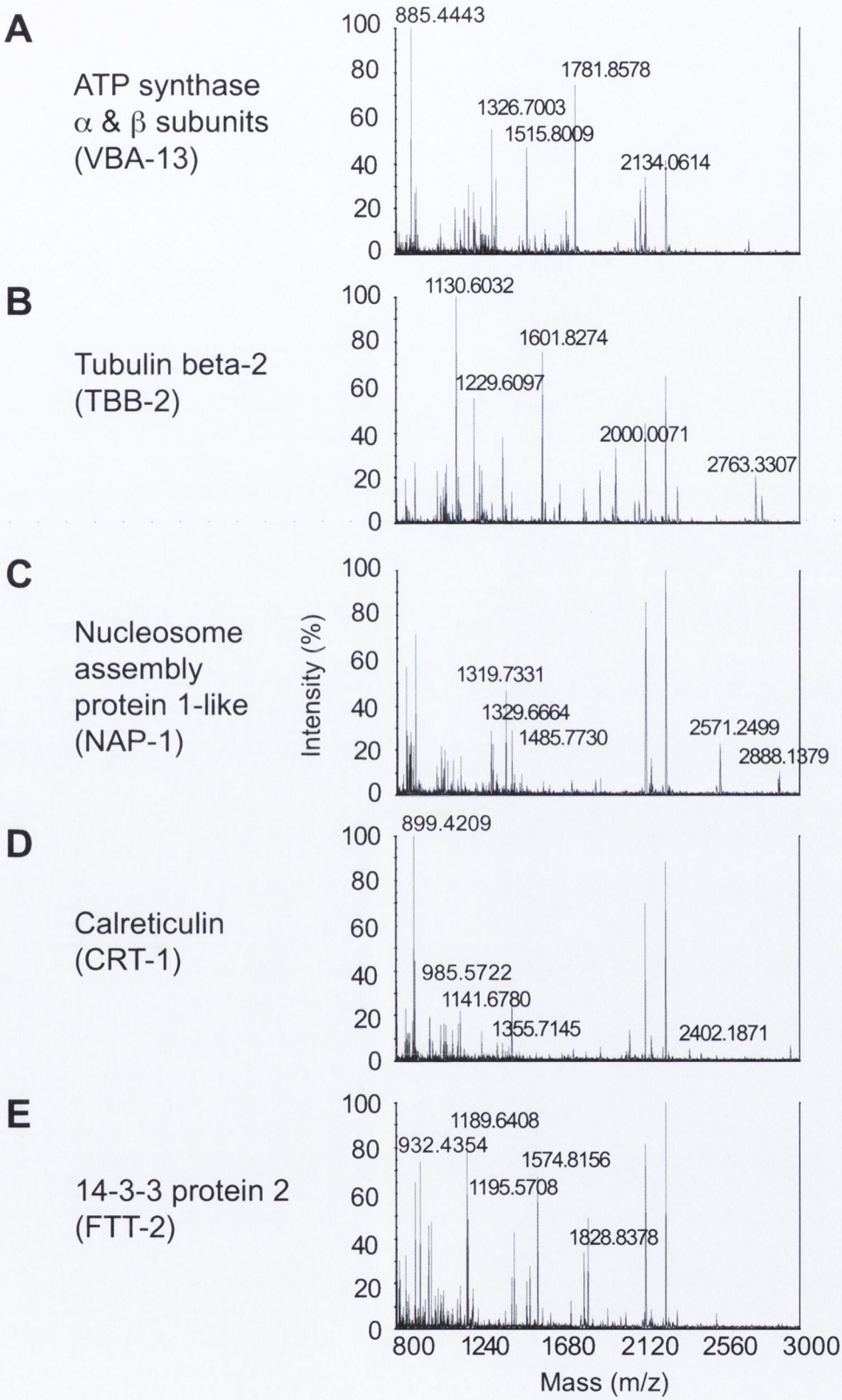

Figure 4.8

Peptide spectra of GST-CED-3$^{221-503}$ substrates

Peptide spectra obtained in MALDI-TOF mass spectromeric analysis of substrates depicted in Figure 4.7. The Y-axis shows the percentage intensity of each peptide peak. The X-axis shows the m/ z value of the peptides. Labels indicate the most prominent specific peaks from each protein.

5 % NaOCl to dissolve adult and larval material. Embryos were then incubated at 20 °C or 25 °C overnight and rates of hatching assessed (Figure 4.9 A). While virtually all wild-type embryos hatched into healthy larvae at both temperatures, viability of *ced-9*^{ts} embryos was reduced at 20 °C and further reduced at 25 °C. In addition, the larvae that did hatch from these embryos, most markedly at 25 °C, were defective in size, morphology and co-ordination, and the majority did not survive to adulthood (data not shown). These results indicated several things. It seems that even at 20 °C, there is some loss of ced-9 function and viability in the n1653 strain, which increases at higher temperatures. Also, it appears that not all cells in these mutants undergo programmed cell death at 25 °C, and that there is a range of phenotypes varying in severity. While some embryos became arrested during their development, presumably due to death of all or some cells, others were able to develop to adults. In the majority of embryos that hatched into larvae, there were substantial defects leading to a loss of viability, presumably caused by a degree of cell death; the uncoordinated phenotype may well have resulted from the death of neuronal cells. The differences in severity may have resulted from the ages of the individual embryos at the time at which they were elevated to the restrictive temperature.

These data suggested that loss of CED-9 in these mutants at 25 °C was indeed causing cell death. We then examined by light microscopy isolated N2 and *ced-9*^{ts} embryos that had been incubated for four hours at 20 °C or 25 °C. Prominent raised cell corpses were observed only in the *ced-9*^{ts} mutant embryos, to a higher degree following incubation at 25 °C (Figure 4.9B).

A recent study in our laboratory has suggested that CED-9 might be involved in mitochondrial remodelling (Delivani *et al.*, 2006). Transfection of human cells with *C. elegans ced-9* resulted in mitochondrial clustering and fusion, while neutralisation of CED-9 by the co-expression of EGL-1 led to mitochondrial fragmentation. We therefore looked to see whether *ced-9*^{ts} mutants show any mitochondrial abnormalities. Populations of N2 and *ced-9*^{ts} mutant *C. elegans* were grown on plates containing 0.4 μg/ ml Mitotracker CMX-Ros, a dye taken up by viable mitochondria. On clearance of all bacteria, populations were harvested and embryos isolated. The embryos were then incubated at 20 °C and 25 °C for two to four hours before examination by UV and confocal microscopy. We found

that wild-type embryos in almost all cases possessed brightly-stained mitochondria clustered around the nucleus of each cell (Figure 4.9 C, D). However, in *ced-9*^{ts} mutant embryos, mitochondrial staining was often severely disrupted (Figure 4.9 C, D). Staining was greatly reduced in the affected cells, appearing only in bright punctate spots. The disruption phenotype was seen at both temperatures, but numbers of affected embryos were elevated following incubation at 25 °C. This suggested that *ced-9*^{ts} embryos do undergo a temperature-dependent loss of CED-9 protein, and that this leads to mitochondrial disorganization. Interestingly, though, this mitochondrial disruption did not appear to be linked to cell death, as cells showing disturbed mitochondrial morphologies often appeared healthy in all other respects.

4.3.7 Production of embryonic extracts for 2DE analysis

Once we had established that CED-9 loss of function and programmed cell death would result from incubation of *ced-9*^{ts} embryos at 25 °C, we attempted to make embryonic lysates for 2DE analysis. We tested two methods initially. The first was to lyse a pellet of isolated embryos directly with 2D lysis buffer, measure the protein concentration, and load a sample onto IPG strips for 2D electrophoresis. In parallel, we subjected a separate preparation of pelleted embryos to gentle pulses of sonication until all embryos appeared disrupted. Insoluble material was then removed by centrifugation and protein content of the supernatant measured. However, both methods initially yielded very low concentrations of protein (data not shown). This appeared to result from incomplete lysis of the embryos, which we suspected was caused by the thick cuticle encasing each embryo. Lysis was improved in each case by adding a –70 °C freezing step followed by thawing at 37 °C, and by subjecting the directly lysed embryos to a short pulse of sonication. The resulting lysates were still low in protein concentration, possibly because the embryos did not pack tightly into a pellet, but did contain enough protein for use in 2D analysis.

However, following 2D electrophoresis and silver staining, embryonic extract proteins on the 2D gels appeared very poorly resolved compared with gels from mixed-stage protein extracts (Figure 4.10 A, B, D). Agarose gel electrophoresis revealed that both types of embryonic lysate contained a large amount of sheared DNA, which could account for the lack of success in protein resolution (data not

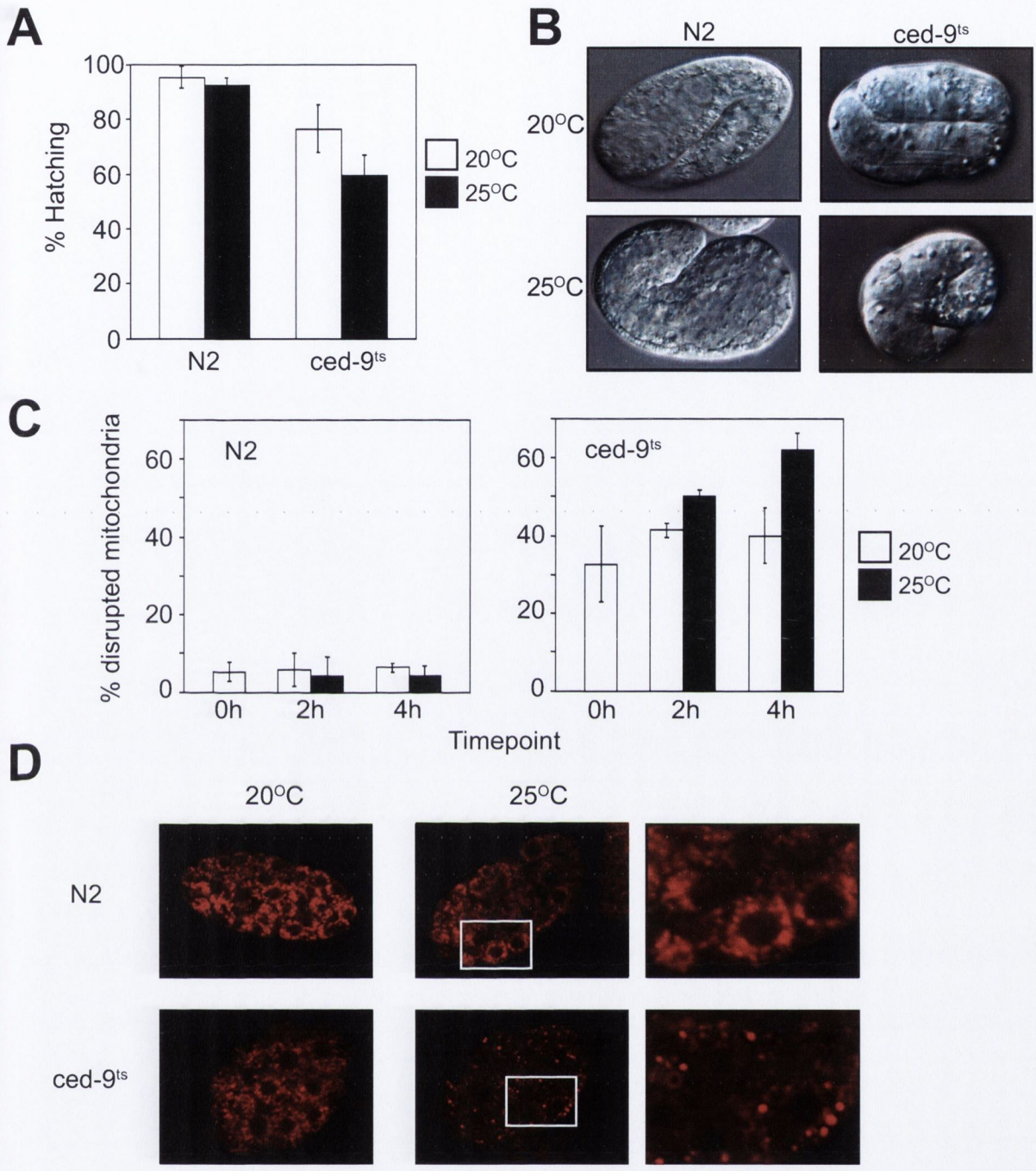

Figure 4.9

The phenotype of *ced-9^{ts}* mutant embryos

(A) Hatching rates of mutant (*ced-9^{ts}*) and wild type (N2) embryos. Embryos were isolated from N2 and *ced-9^{ts}* worms and incubated at 20 °C and 25 °C overnight. The percentage of embryos hatching into larvae following the incubation was assessed.

(B) Morphology of N2 and *ced-9^{ts}* embryos. Embryos were isolated from N2 and *ced-9^{ts}* worms and incubated at 20 °C and 25 °C for 4 h. Representative embryos are shown.

(C) Quantitative analysis of mitochondrial disruption in N2 and *ced-9^{ts}* embryos. Embryos were treated as above for 2 or 4 h and percentages of embryos exhibiting a disrupted mitochondrial phenotype were assessed.

(D) Morphology of mitochondria in N2 and *ced-9^{ts}* embryos. N2 and *ced-9^{ts}* worms were grown on NGM with 0.4 μg/ ml MitoTracker dye and embryos isolated after 2 days followed by incubation at 20 °C and 25 °C for 4 h. Images show representative mitochondria.

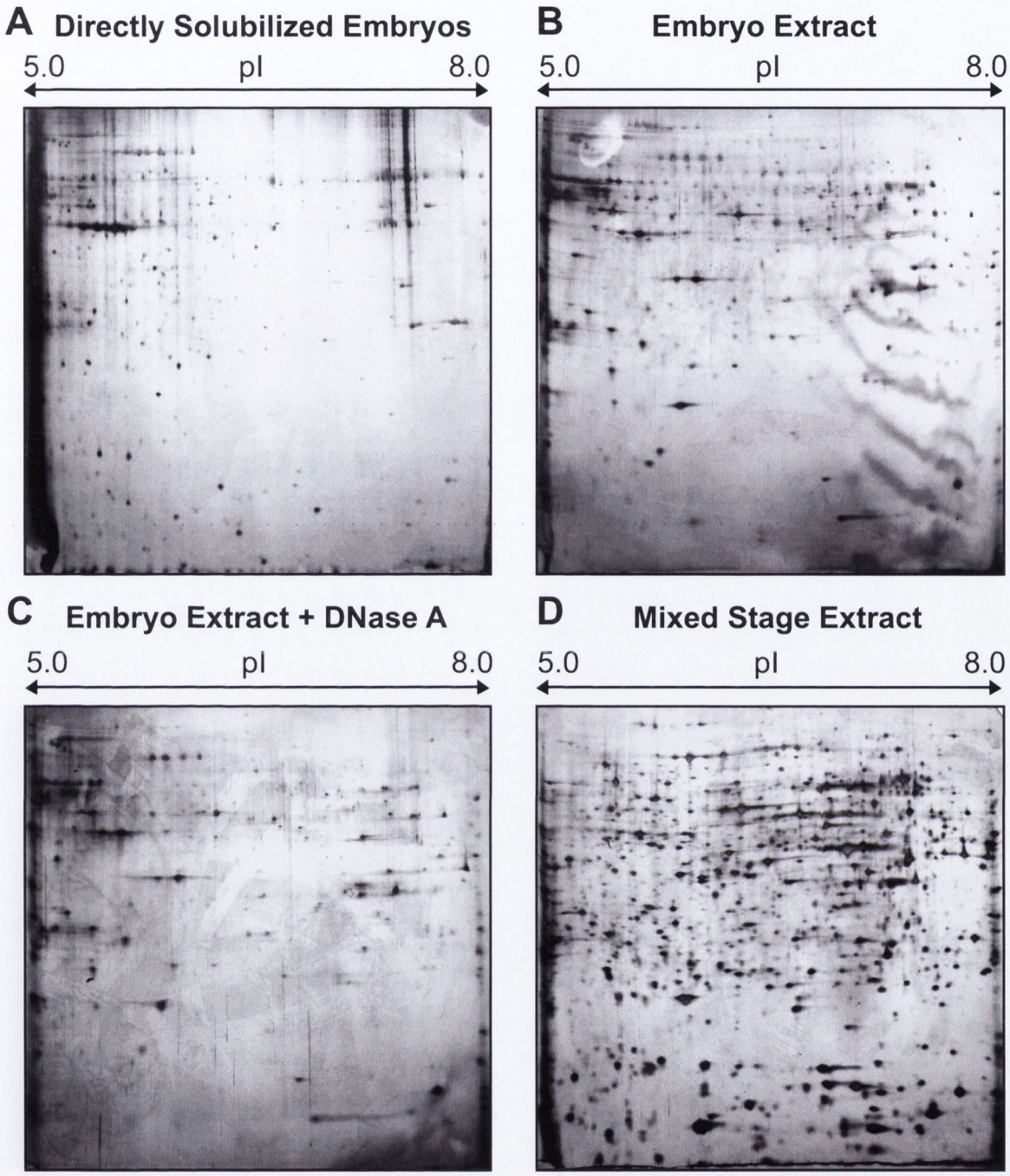

Figure 4.10

Protein extracts prepared from *C. elegans* embryos on 2DE gels

(A) Directly solubilized embryos. Embryos were isolated from populations of *C. elegans* and lysed in 2D loading buffer followed by sonication and one freeze/ thaw cycle. 100 μg of solubilized embryos were subjected to 2D electrophoresis and silver staining.

(B) Soluble protein extract from *C. elegans* embryos. Embryos were isolated from *C. elegans* followed by sonication until all embryos were disrupted. Insoluble material was pelleted and 100 μg of protein extract subjected to 2D electrophoresis and silver staining.

(C) Extract treated with DNase A. Embryonic extract prepared as above was treated with DNase A for 10 minutes prior to electrophoresis and silver staining.

(D) Mixed stage *C. elegans* extract. 100 μg of mixed stage *C. elegans* extract was subjected to 2D electrophoresis and silver staining for comparison.

shown). This DNA lysis may have resulted from the relatively harsh conditions required to lyse the embryos, combined with the large amount of DNA present in embryos. To resolve this issue, we tried incubating the soluble protein lysates with DNase A to reduce the DNA content, but this appeared to have no effect on protein resolution (Figure 4.10 C). Attempts to identify proteins from these gels by mass spectrometry were virtually all unsuccessful, due to the low levels of resolved protein contained in each spot. Due to these difficulties in analysing embryonic proteins by 2D electrophoresis, we reluctantly abandoned this means of validating our identified substrates.

4.3.8 Confirmation of substrate cleavages by Western blotting

We then decided to use Western blotting to determine whether at least some of our substrate proteins were genuinely cleaved by CED-3. This was problematic, as there are few antibodies available that are directed towards *C. elegans* proteins. We tested a panel of antibodies directed against human proteins to determine whether they could recognise their homologues in *C. elegans* extracts. Two of the antibodies, directed towards human β-tubulin and actin, did react against proteins at the size expected of their *C. elegans* homologues (data not shown). We therefore subjected samples of CED-3-treated and untreated *C. elegans* extracts to electrophoresis on 12 % 1D SDS-PAGE gels for Western blotting analysis with antibodies against β-tubulin and actin (Figure 4.11).

β-tubulin was readily detected in both the treated and untreated extracts. On addition of GST-CED-$3^{221-503}$, almost all full-length β-tubulin appeared to have undergone proteolysis after 30 minutes, to be replaced by a slightly lower molecular weight band. This is consistent with the mass spectrometry data suggesting that CED-3 removes only a small region of the β-tubulin C-terminus. Actin was also readily detected, but the full-length form of the protein appeared to undergo no reduction on CED-3 addition. However, lower molecular weight bands had become apparent by one hour after CED-3 addition, suggesting that actin cleavage might be a late and partial event during cell death. This is consistent with the 2D gel data, which showed only a reduction rather than a full disappearance in actin spot intensity after 2 hours of CED-3 treatment. And it is also consistent with 2D analyses in human cell-free extracts, in which actin appears to be partially proteolysed (Dr. Christopher Gerner and Dr. Colin Adrain,

pers. commun.). This Western blot analysis thus confirms that two of the proteins identified as CED-3 substrates are cleaved on addition of CED-3 to extracts.

4.3.9 Cleavage of CRT-1, TBB-2 and FTT-2 by CED-3 *in vitro*

Due to the limited availability of antibodies against our substrate proteins, we decided to synthesize three substrates *in vitro*, CRT-1, TBB-2 and FTT-2, incorporating a ^{35}S-methionine label, to confirm their cleavage by CED-3. These proteins were incubated for 2 hours at 37 °C with a titration of GST-CED-3$^{221-503}$ at 1:2, 1:4, 1:8 and 1:16 dilutions. In parallel, the known CED-3 substrates CED-3 and CED-9 were incubated with the same concentrations of GST-CED-3$^{221-503}$. The reactions were then electrophoresed through 12 % SDS-PAGE gels and proteins detected by fluorography (Figure 4.12).

All three proteins were confirmed to be CED-3 substrates. FTT-2 was cleaved to a slightly smaller molecular weight product, at all protease concentrations tested. TBB-2, as already indicated, was also only slightly reduced in size on treatment with CED-3, although it formed two discrete smaller fragments, indicating the presence of more than one cleavage site. All CED-3 dilutions appeared to result in full TBB-2 proteolysis; the 1:4 protease dilution also appeared to induce a degree of laddering. CRT-1 was robustly cleaved, although there was some full-length CRT-1 remaining at all protease dilutions, and the degree of proteolysis decreased with lower dilutions of CED-3. There were two prominent CRT-1 cleavage products formed, at around 30 kDa and 20 kDa.

The confirmation that these three proteins were all genuine CED-3 substrates suggests that our screen was accurate in identifying proteins that undergo CED-3-mediated proteolysis. However, it remained possible that under our assay conditions all proteins were being non-specifically proteolysed by CED-3. To exclude this possibility, we synthesized a variety of *C. elegans* proteins not identified as CED-3 substrates in our screen, to act as negative controls. These ^{35}S-methionine-labelled proteins were incubated with or without GST-CED-3$^{221-503}$ at a dilution of 1:3 for 2 hours at 37 °C. None of these proteins, FZO-1, CED-4, PAR-5, ICD-1 or ASP-1, showed significant proteolysis on addition of GST-CED-3$^{221-503}$ (Figure 4.13). Interestingly, one of the proteins tested, ICD-1, has been reported to be an inhibitor of programmed cell death in *C. elegans*, and it was

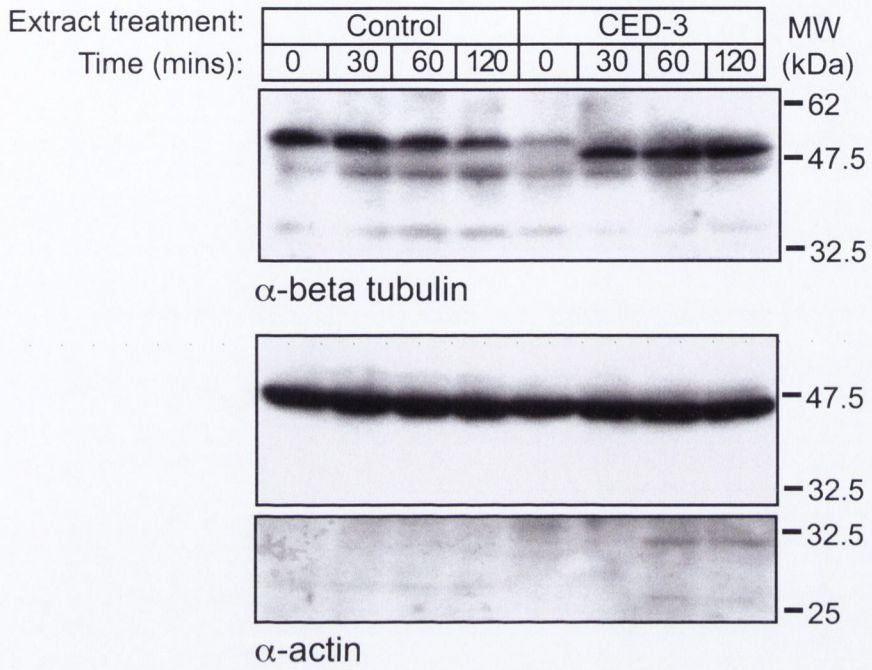

Figure 4.11

Western blotting analysis of actin and β-tubulin cleavage by CED-3 in extracts

Actin and β-tubulin are cleaved by CED-3 in cell extracts. *C. elegans* extracts were treated with a 1:3 dilution of GST-CED-$3^{221-503}$ for 2 hours at 37 ^{o}C. Samples of treated and untreated extracts were electrophoresed on 12 % SDS-PAGE gels and analysed by Western blotting with antibodies directed against actin and β-tubulin.

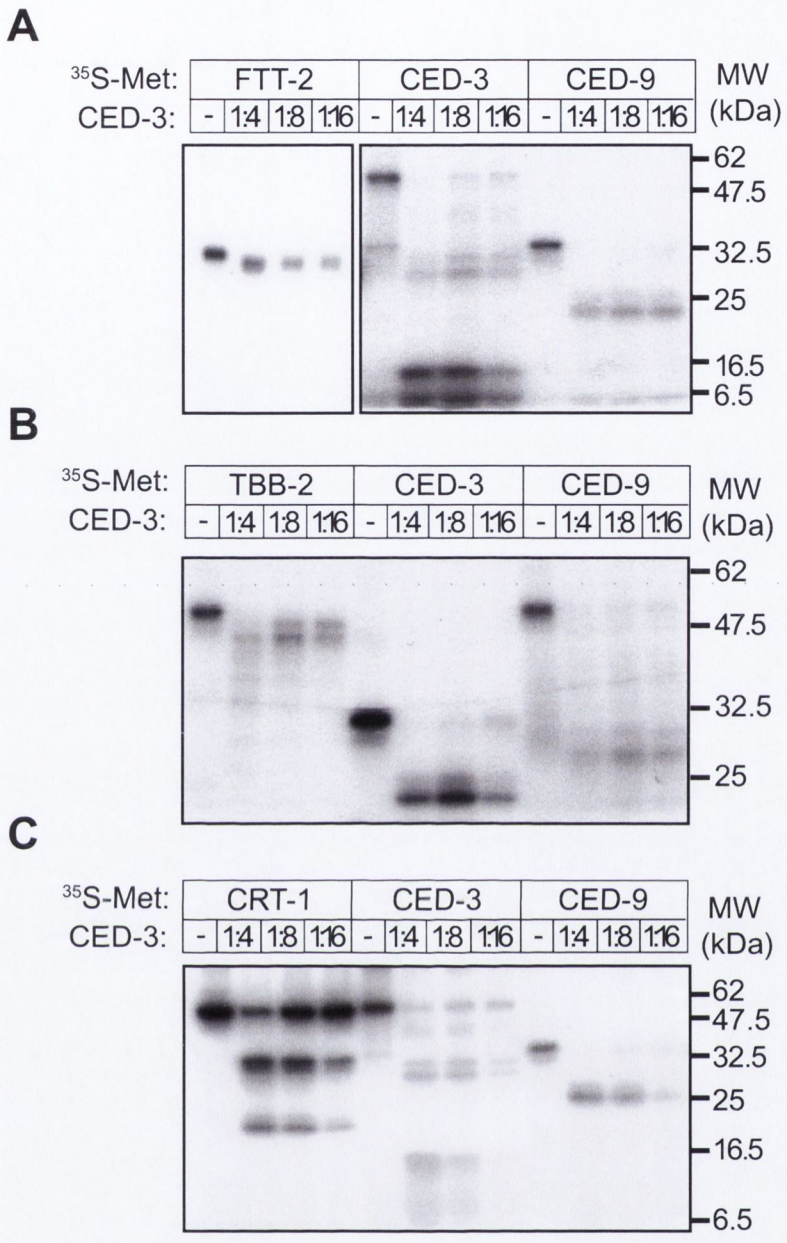

Figure 4.12

Confirmation of FTT-2, TBB-2 and CRT-1 cleavage by CED-3 *in vitro*

(A) FTT-2 is a CED-3 substrate. ^{35}S-methionine-labelled FTT-2 was incubated for 2 h with a titration of GST-CED-$3^{221-503}$ and subjected to SDS-PAGE followed by fluorography. ^{35}S-methionine-labelled CED-3 and CED-9 were treated in parallel as controls.

(B) TBB-2 is a CED-3 substrate. ^{35}S-methionine-labelled TBB-2, CED-3 and CED-9 were incubated for 2 h with a GST-CED-$3^{221-503}$ titration followed by SDS-PAGE and fluorography.

(C) CRT-1 is a CED-3 substrate. ^{35}S-methionine-labelled CRT-1, CED-3 and CED-9 were incubated for 2 h with a GST-CED-$3^{221-503}$ titration followed by SDS-PAGE and fluorography.

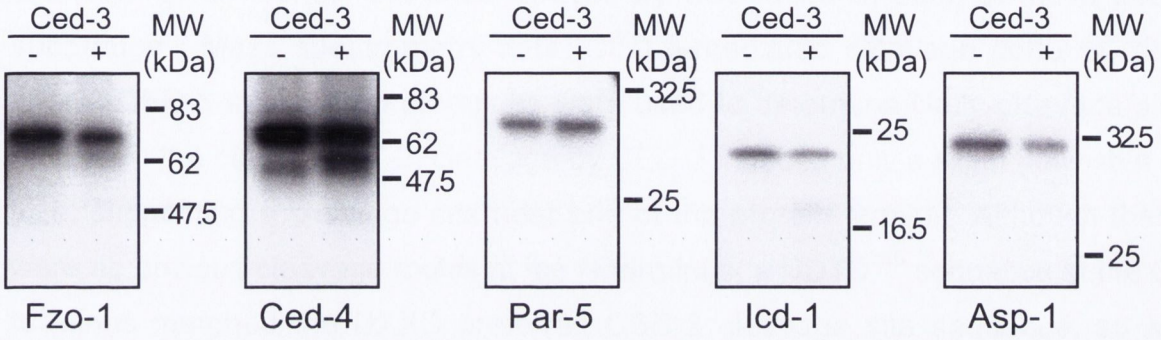

Figure 4.13

C. elegans* proteins not identified as substrates are not cleaved by CED-3 *in vitro

Negative control proteins are not cleaved by CED-3. ^{35}S-methionine-labelled FZO-1, CED-4, PAR-5, ICD-1 and ASP-1 were synthesized and incubated for 2 h with a 1:3 dilution of GST-CED-3$^{221-503}$. Reaction products were then subjected to SDS-PAGE and fluorography.

suggested in this report that it may be a substrate of CED-3 (Bloss *et al.*, 2003). However, in this assay, only a trace amount of ICD-1 cleavage could be detected despite the high concentration of CED-3 used against a single protein substrate. It therefore seems unlikely that ICD-1 is a physiological substrate of CED-3 in *C. elegans*.

4.3.10 Identification of CED-3 cleavage sites in CRT-1, TBB-2 and FTT-2

We went on to identify the sites cleaved by CED-3 within each of these three substrates. Mass spectrometry data, CED-3-mediated cleavage patterns, and known CED-3 substrate preferences were used to determine likely cleavage site motifs. In the case of FTT-2, cleavage by CED-3 induced only a slight downshift in size, suggesting a cleavage site near one of the protein termini. Although there were no obvious cleavage motifs at the N-terminus, a $DDTD^{240}$ sequence at the C-terminus matched the DXXD preferred CED-3 cleavage site sequence, so we decided to mutate D^{240} to glutamic acid using the Quickchange site-directed mutagenesis kit. The resulting mutant DNA sequence was transcribed and translated *in vitro*, incorporating a ^{35}S-methionine label. The labeled protein was then incubated alongside the wild-type protein for 2 hours at 37 °C with a titration of GST-CED-$3^{221-503}$ at 1:2, 1:4, 1:8 and 1:16 dilutions. The mutant protein underwent no proteolysis at any GST-CED-$3^{221-503}$ concentration, despite robust proteolysis of the wild-type protein at all GST-CED-$3^{221-503}$ dilutions, suggesting that this was indeed the tetrapeptide motif targeted by CED-3 (Figure 4.14 A).

CRT-1 cleavage resulted in the appearance of a protein spot on 2D gels that represented the protein without its N-terminal 80 amino acids. The CED-3 cleavage pattern *in vitro* suggested that the protein was cleaved into two fragments of approximately 20 kDa and 30 kDa. We therefore looked for cleavage motifs around the central region of the protein, a difficult task as CRT-1 is relatively rich in aspartic acids. However, structural analyses of the central P domain of rat calreticulin have identified an exposed loop region that contains an EEMD tetrapeptide site. In *C. elegans* calreticulin this site is largely conserved and is an optimal DXXD motif, $DEMD^{253}$. The similarity of this motif to the preferred peptide substrates of CED-3, coupled with its exposed location and the conservation of the P1, P2, and P3 sites in a mammalian species, suggested that it was a good candidate for the site of caspase-mediated cleavage. We targeted D^{253} for site-

directed mutagenesis to a glutamic acid residue, synthesized the mutant protein, and tested the ability of CED-3 to cleave it, as described above. Although CED-3 was still able to cleave this mutant it was at a substantially reduced efficiency relative to the wild-type protein, and generated different cleavage products. This suggested that other CED-3 target sites were undergoing proteolysis. We selected two further aspartic acid residues for mutagenesis, D^{225} and D^{182}, both within accessible structural regions and contained within tetrapeptides that appeared to be good candidates for CED-3 cleavage sites. The triple mutant protein was substantially resistant to CED-3-mediated proteolysis, although some residual cleavage still occurred at higher CED-3 concentrations (Figure 4.14 B).

In the case of TBB-2, mass spectrometry evidence had suggested that the CED-3 cleavage site must be located at the extreme C-terminus, and this was supported by the small decrease in size seen on addition of CED-3, by Western blotting and detection of radio-labelled protein. The C-terminus of TBB-2 is highly acidic and rich in aspartic acid residues. However, one motif, $DDVD^{435}$, appeared to closely match the CED-3 preferred tetrapeptide, so we mutated D^{435} to glutamic acid by site-directed mutagenesis. We synthesized the mutant protein *in vitro*, followed by incubation with CED-3 and analysis as described above. Proteolysis of the mutant protein was less efficient than that of the wild-type protein, and the cleavage fragment pattern was altered (data not shown). However, proteolysis was not abolished, and we therefore surmised that additional CED-3 target sites must exist. Mutation of two further aspartic acids within the C-terminal region, D^{404} and D^{417}, resulted in a mutant protein that was largely resistant to CED-3-mediated cleavage compared with the wild-type protein, although a degree of cleavage did occur, particularly at high concentrations of CED-3 (Figure 4.14 C).

4.3.11 Comparison of CED-3 cleavage sites in five substrate proteins

The identification of these cleavage sites therefore confirmed that recombinant CED-3 cleaves its substrate proteins at specific sites, within typical caspase cleavage site motifs (Figure 4.15 A, B). The identification of these 7 cleavage sites, along with the 5 cleavage sites already identified within CED-3 and CED-9 in other studies, gave us the opportunity to compare CED-3 cleavage motifs within several proteins and expand on the consensus arrived at through peptide substrate studies (Xue *et al.*, 1996; Xue and Horvitz, 1997) (Figure 4.15 B).

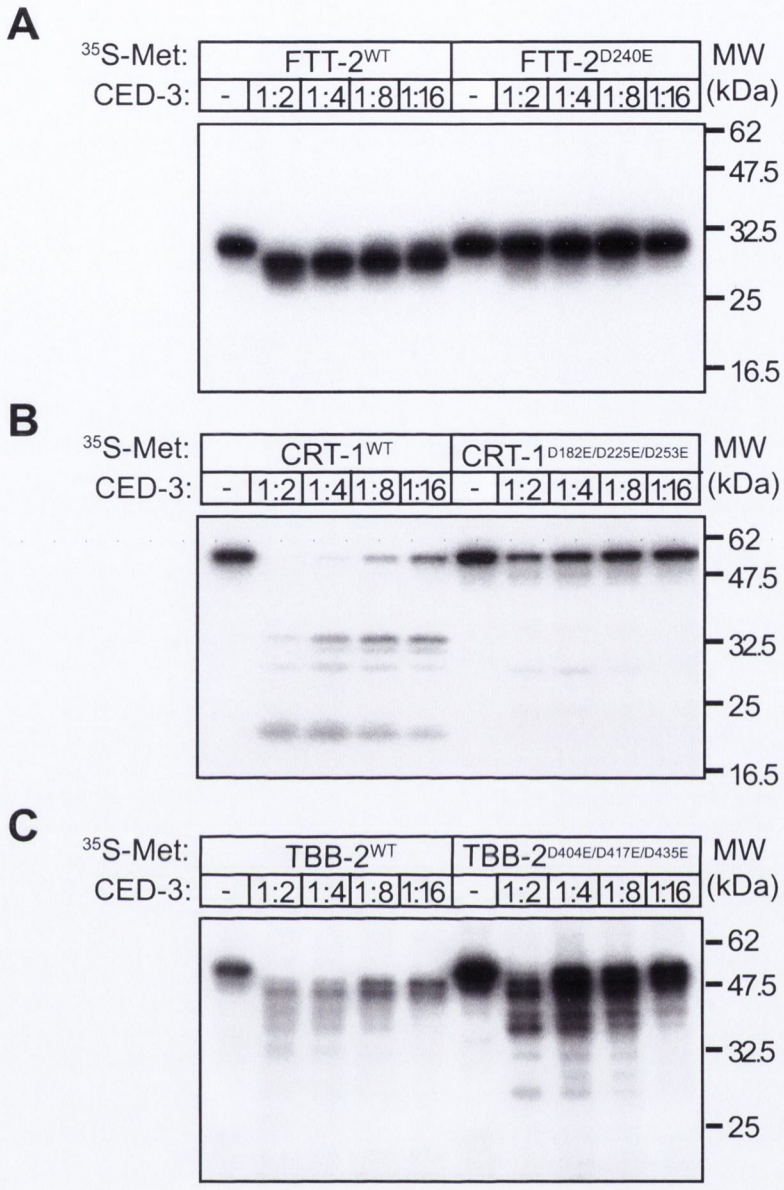

Figure 4.14

Identification and mutation of CED-3 cleavage sites in FTT-2, TBB-2 and CRT-1

(A) FTT-2 D^{240} is targeted by CED-3. Amino acid 240 of FTT-2 was mutated from aspartic acid to glutamic acid by *in vitro* site-directed mutagenesis. ^{35}S-methionine-labelled wild-type and mutant FTT-2 was incubated for 2 h with GST-CED-$3^{221-503}$ at 37 ^{o}C and subjected to SDS-PAGE followed by fluorography.

(B) CRT-1 D^{182}, D^{225}, and D^{253} are targeted by CED-3. Amino acids 182, 225 and 253 of CRT-1 were mutated from aspartic acids to glutamic acids. ^{35}S-methionine-labelled wild-type and mutant CRT-1 were synthesized and treated as above.

(C) TBB-2 D^{404}, D^{417}, and D^{435} are targeted by CED-3. Amino acids 404, 417 and 435 of TBB-2 were mutated from aspartic acids to glutamic acids. ^{35}S-methionine-labelled wild-type and mutant TBB-2 were synthesized and treated as above.

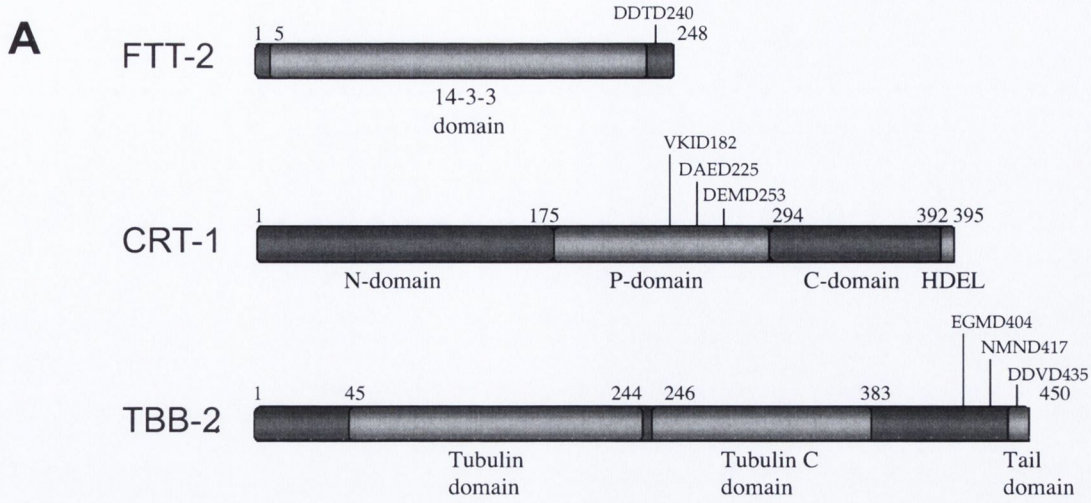

B

Substrate	Cleavage site				
	P4	**P3**	**P2**	**P1**	**P1'**
CED-3	N	F	V	D^{220}	A
	D	S	V	D^{374}	G
	D	N	R	D^{388}	G
CED-9	D	A	Q	D^{47}	L
	E	S	I	D^{67}	G
CRT-1	V	K	I	D^{182}	G
	D	A	E	D^{225}	A
	D	E	M	D^{253}	G
TBB-2	E	G	M	D^{404}	E
	N	M	N	D^{417}	L
	D	D	V	D^{435}	G
FTT-2	D	D	T	D^{240}	A
Consensus	**D**	**X**	**X**	**D**	**G**

Figure 4.15

Comparison between CED-3 cleavage sites

(A) Schematic representations of FTT-2, CRT-1 and TBB-2. Domains and CED-3 cleavage sites are indicated.

(B) Establishing a CED-3 cleavage site consensus. CED-3 cleavage sites identified in 5 CED-3 substrates - CED-3, CED-9, CRT-1, TBB-2, and FTT-2 - were aligned. A CED-3 cleavage site consensus motif based on these CED-3 target sites is indicated underneath.

On alignment of the 12 tetrapeptides, it was immediately noticeable that 7 sites contained an aspartic acid residue at the P4 position, confirming the evidence that this is the preferred residue at this position (Figure 4.15 B; Figure 3.12 A; Thornberry *et al.*, 1997). The remaining sites contained either an N, V or E residue at P4. Somewhat unexpectedly, there appeared to be no distinct preference for a glutamic acid residue at P3, which was suggested by previous studies with synthetic peptides (Thornberry *et al.*, 1997). There was also no clear consensus at the P2 position, although 5 of the 12 sites did contain a closely-related V or I residue. This is akin to the P2 residue within the readily-cleaved peptide substrate DEVD. Finally, we extended our consensus to include the P1' position beyond the P1 aspartate. We found that in 9 out of the 12 cases this position was occupied by a small amino acid – glycine, asparagine, or serine. In 6 of these sites the P1' residue was glycine, the smallest amino acid. This strongly suggests that CED-3 substrate site specificity extends beyond the tetrapeptide motif to include a preference for a small amino acid at the P1' position.

The identification of these cleavage sites within substrate proteins therefore both validated the ability of CED-3 to cleave substrates at specific caspase cleavage motifs in our assay, and has contributed to our knowledge of CED-3 substrate site specificity within whole proteins rather than just peptides. The generation of non-cleavable or cleavage-resistant mutant sequences also provided valuable reagents for analysing the functional effects of substrate cleavages, which is the subject of the following chapter.

4.4 DISCUSSION

4.4.1 Summary

The aim of this chapter was to identify substrates of the *C. elegans* caspase CED-3. We started by generating cell-free lysates from mixed-stage populations of *C. elegans*. CED-3 was added to these lysates and the subsequent reactions analysed by 1D SDS-PAGE and Coomassie staining. No alterations in the *C. elegans* proteome could be seen. We then analysed the reactions by 2D SDS-PAGE with silver staining, to achieve better protein resolution and more sensitive detection. Using this system we observed that about 3 % of the *C. elegans* proteome is altered following treatment with GST-CED-$3^{221-503}$. 22 of these altered proteins were then identified by MALDI-TOF mass spectrometry. The substrate proteins identified have a broad range of functions, and several are homologues of known human caspase substrates.

In order to determine whether these proteins are substrates of endogenous CED-3, we generated lysates from *ced-9* (n1653) embryos in which CED-9 function can be abolished by incubation at 37 °C, leading to CED-3 activation. These lysates could then be analysed by 2D SDS-PAGE and mass spectrometry. However, this approach proved impossible to carry out, due to problems with protein resolution. Instead, we confirmed cleavage of 2 substrates by Western blotting analysis on CED-3 treated lysates. We also synthesized 3 substrates *in vitro*, incorporating a ^{35}S-methionine label, and incubated them with CED-3 to demonstrate that all three were genuine CED-3 substrates. We finally identified CED-3 cleavage sites in the three proteins, and generated cleavage-resistant mutants. Comparison of these CED-3 cleavage sites with those already known suggested that CED-3 has an extended substrate site specificity of DXXDG.

4.4.2 2D SDS-PAGE as a means of protease substrate identification

Our initial analysis of the CED-3-treated lysates by conventional one-dimensional SDS-PAGE did not reveal any protein changes, while the same analysis by two-dimensional SDS-PAGE identified many proteome alterations. What does this signify? It suggests that CED-3, like all caspases, is a highly specific protease. Without such stringent substrate site requirements, a protease catalysing cell death through random proteolysis of multiple proteins would have left traces of its activity on a 1D gel. However, 2D electrophoresis provides dramatically better

protein resolution through the use of two separation dimensions. In addition, silver nitrate makes a far more sensitive protein stain than Coomassie Blue; Coomassie is typically able to detect 50-100 ng of protein, while silver stain is about 10-100-fold more sensitive. A typical pI 5-8 2D gel will also resolve significantly more proteins than a Coomassie-stained 1D gel, due to its larger separation area. 2D SDS-PAGE with silver staining is therefore a more sensitive means of detecting proteome changes.

However, there are also definite limitations to this means of analysis. In our study, only a small fraction of the ~19,000 proteins of the *C. elegans* proteome were visible on the silver-stained 2D gels, so that only the cleavage of relatively abundant proteins could be observed. There are several reasons why such a high percentage of the proteome cannot be visualised in our system. Although sensitive, silver staining is still only able to detect a fraction of the proteome. Other substrates will not be be resolved if they fall outside the pI 3 - 8 range covered by our IPG strips. Some proteins, particularly those with a high pI, will not enter the IPG strips, while other large proteins may be unable to enter the second dimension gel, and these proteins will therefore be excluded from our analysis. Further substrates that do successfully resolve may be missed due to overlap with another protein of similar molecular weight and pI. And although it is possible to estimate the percentage of the proteome cleaved using our analyses, it is likely that this percentage will be an over-estimate. Other proteins may be identified as substrates more than once, either because different isoforms appear at different positions on the gel, they appear on both pI 3-6 and 5-8 gels, both pro-form loss and fragment appearance are recorded, or two or more fragments are observed.

This last issue could be addressed by identifying all the protein changes observed on the 2D gels. However, there is again a sensitivity problem. MALDI-TOF mass spectrometry can only make a confident protein identification if enough protein is present in a sample. Small proteins can be difficult to identify as they often contain very few trypsin cleavage sites. In addition, an identification can only be made if the protein is present and correctly annotated within the databases screened. This means that many proteins that can be stained using silver nitrate cannot then be identified using mass spectrometry, explaining why only 22 of the proteins altered after CED-3 treatment of *C. elegans* protein extracts were

eventually identified. Out of the rest, many could not be successfully analysed by mass spectrometry, two proteins were bacterial contaminants, several represented GST-CED-3 itself or free GST from the enzyme preparation, and the rest were duplicate identifications of the same substrate, demonstrating how the percentage calculations could be misleading.

4.4.3 Comparing substrates cleaved in different organisms

As the problems associated with estimating the percentage of the proteome cleaved in this analysis also apply to other analyses in our laboratory of human and *Drosophila* substrates, it is still possible to make a valid comparison of these different studies. While around 3% of the *C. elegans* proteome appears to be altered on treatment with CED-3, based upon the percentage of protein changes observed out of the protein complement on a 2D SDS-PAGE gel, the same type of analysis in human cell extracts reveals around 5% of the proteome to be altered, and in *Drosophila melanogaster* extracts, around 2% of the proteome. As we expected a smaller percentage of the proteome to undergo cleavage in *C. elegans* than in human cells, due to the activity of only one as opposed to a family of caspases, this lower degree of proteome alteration in worms as opposed to human cells is consistent with our predictions. However, the decrease from 5% to 3% is not proportional with the expansion in number of the human caspase family. This is consistent with the involvement of a relatively small contingent of human caspases in cleaving substrate proteins. It has been suggested that caspase-3 mediates the majority of substrate cleavages in man, with caspase-7 and caspase-6 playing more minor roles, and the initiator caspases being specialised in cleaving other caspases only (Slee *et al.*, 2001). This would fit well with our data suggesting only a 40 % increase in the percentage of the proteome cleaved in humans despite a multiplication in active caspases in this system from one to twelve. It is also consistent with our data on CED-3 substrate cleavage sites in both peptides and proteins, which suggest that CED-3 is a relatively promiscuous caspase. It might therefore be expected to cleave a higher proportion of the proteome than any single human caspase.

In contrast, a higher percentage of the proteome was cleaved in *C. elegans* than in *D. melanogaster*, despite the latter organism having at least five caspases, three of which are executioners. This is unexpected, and it is possible that the reason

lies in differences in the way these two analyses were conducted. The *Drosophila* study involved the use of lysates prepared from cells treated with pro-apoptotic stimuli. It is often significantly more difficult to observe cleavage of even known caspase substrates in cell lysates as opposed to cell-free extracts (compare Figures 5.4 and 5.9 as an example). This may be due to the sequestration of protein substrates in areas of intact cells to which caspases cannot gain access, or the result of heterogeneity in the cell population, in which not all cells will undergo apoptosis synchronously. It is certainly true that this study of caspase substrates in the fly yielded fewer substrate proteins than the studies carried out in human and worm cell-free extracts, and this reasoning could therefore explain the lower degree of proteome alteration observed in *Drosophila*.

In these analyses, α-tubulin, actin, aldo-keto reductase and calreticulin were identified as caspase substrates in both humans and worms (Adrain *et al.*, 2006; Dr. Colin Adrain, pers. comm.). In published reports, myosin light chain, beta-tubulin, 14-3-3 proteins, and nucleosome assembly protein 1-like 1 also have homologues that are reported to be human caspase substrates (Moretti *et al.*, 2002; Widmann *et al.*, 1998; Van Damme *et al.*, 2005). The fact that 8 out of the 22 substrates identified have homologues that are also cleaved in human cells suggests both that our analysis has been accurate in identifying true caspase substrates, and also supports our initial premise, that a core of important substrates might be conserved between species due to their essential roles during programmed cell death. On the other hand, studies in our laboratory on the identification of caspase substrates in *Drosophila melanogaster* revealed no substrates conserved between flies and worms. However, this is likely due to the limited number of substrates identified in that study, as discussed above.

4.4.4 Artificial vs endogenous systems

A potential weakness of our analysis is that it relies entirely upon recombinant enzyme and cell-free lysates. Recombinant enzyme may not act in the same way as native protease, and it is difficult to know whether the concentration and activity level of the recombinant enzyme added is physiologically relevant. In cell-free lysates, substrate availability may be different to that found in intact cells. In addition, most developmental cell death occurs in embryos, and populations of worms growing in liquid culture are often low in embryonic content; worms can

begin to starve before the culture is fully saturated, leading to egg-laying defective hermaphrodites and an over-representation of dauers and L1 larvae. The protein pool present in these mixed-stage extracts could therefore be very different from that present in embryos, leading to the identification of substrates that may not be physiologically relevant.

Indeed, we had originally explored the possibility of inducing co-ordinate cell death in *C. elegans* cell lines or embryos, followed by 2D SDS-PAGE. However, it was soon apparent that there are no *C. elegans* cell lines available, and that there are no published biochemical means of inducing co-ordinate cell death in embryos. Testing a variety of stimuli used to induce apoptosis in human cells had no effect on *C. elegans* embryos. The impervious embryonic cuticle is likely to prevent these agents from gaining access to the cell. It is also likely that, unlike *C. elegans* germline cells, somatic cells of the embryo do not possess the machinery to respond to damaging agents by inducing cell death.

We then attempted to use *C. elegans ced-9* temperature-sensitive mutants as a genetic means of inducing CED-3 activation in embryonic cells. We showed that loss of CED-9 function is able to induce CED-3 activation, although not apparently in all cells. This could have been improved by using a developmentally-synchronized population of worms to generate a population of early embryos, in which most or all cells would be responsive to the loss of CED-9 function. However, a more intractable difficulty was the failure of embryonic proteins to resolve effectively on a 2D gel. There are many factors that can affect the ability of proteins to resolve on 2D gels, but the most likely explanation in our case was the presence of sheared DNA, as embryonic cells contain a high percentage of nuclear material, and the conditions required to lyse embryos due to their robust cuticles were necessarily harsh. Analysis on agarose gels showed that there was in fact a substantial amount of sheared DNA present in embryonic extracts. However, addition of nucleases and testing of different lysis conditions did not seem to significantly reduce this fraction of sheared DNA and we were forced to abandon this line of investigation.

As it therefore seemed that we would have to use an entirely artificial system, we tried as far as possible to ensure that the conditions used in our analysis were

physiologically relevant. Although we attempted to trigger endogenous CED-3 activation by the addition of small amounts of recombinant CED-3, and by the addition of cytochrome c and dATP, no CED-3 activation could be detected using these methods. We therefore titrated recombinant GST-CED-$3^{221-503}$ against known substrates in the presence of cell extracts, to choose conditions at which genuine substrates were cleaved, but not excessively. We ensured that the population of worms used to generate extracts did contain embryos, and also many early stage larvae, so that it could be expected to include physiologically relevant targets.

We then confirmed cleavage of several of these substrates by Western blotting and proteolysis of *in vitro* synthesized substrate proteins by CED-3 *in vitro*, validating the ability of our screen to identify genuine CED-3 substrates. Substrates identified also included proteins expressed at a variety of developmental stages, suggesting that we had been successful in representing all stages of nematode development, including those relevant to the context of cell death. Importantly, the substrates identified included several homologues of human caspase substrates, as discussed above. This also helps to validate our analysis, and emphasizes the conservation of events in the apoptosis demolition phase. It therefore confirms our rationale, that identifying substrates in *C. elegans* will enable us to spotlight those substrate cleavages that are conserved between different species.

4.4.5 Cytoskeletal substrates

Our analysis has shown that CED-3 targets a range of protein substrates, allowing it to coordinate the many events of cell death and ensure the demise of the cell. The functions of many of these proteins suggest ways in which their cleavage might affect the cell during apoptosis. One of the biggest categories of substrates identified is that of proteins involved in the cytoskeleton and its regulation. This is not surprising, as the cytoskeleton is highly dynamic during apoptosis and responsible for many important aspects of the apoptotic phenotype, such as detachment and rounding of the cell, plasma membrane blebbing, and apoptotic body formation (Moss and Lane, 2006).

Actin has previously been identified as a human caspase substrate both in our laboratory and in other published reports. There is some controversy over whether it is genuinely cleaved in cells undergoing apoptosis, but we have identified it as a caspase substrate in analyses of both worm and human cell extracts, suggesting that it does undergo proteolysis (Mashima *et al.*, 1997; Song *et al.*, 1997). Myosin light chain, a regulator of actin contraction, was also identified as a CED-3 substrate. The actin cytoskeleton is known to be involved in the process of apoptotic membrane blebbing, with myosin light chain (MLC) phosphorylation causing contraction of a cortical actin ring, leading to membrane movement. MLC phosphorylation can be induced by ROCK1, a caspase substrate that is activated by caspase-mediated cleavage (Coleman *et al.*, 2001; Sebbagh *et al.*, 2001). It is possible that caspase-mediated cleavage of actin and myosin also contributes to this process.

The role of the microtubule cytoskeleton in apoptotic membrane changes is less well understood (Moss and Lane, 2006). Alpha-tubulin has already been identified in our laboratory as a substrate of caspases and granzyme B, and the removal of its C-terminus by granzyme B has been shown to cause enhanced polymerization of microtubules (Adrain *et al.*, 2006). Recent reports have also suggested that changes in the microtubule cytoskeleton during apoptosis might contribute to apoptotic body formation, chromatin dispersal, and the transport of phagocytic ligands such as phosphatidylserine to apoptotic blebs (Moss *et al.*, 2006). It is possible that the cleavage of the C-terminal amino acids of alpha- and beta-tubulin might therefore alter microtubule dynamics and cellular transport through affecting polymerization rates.

4.4.6 ATP synthesis

Although early stages of apoptosis are energy-dependent and require the continued production of ATP, ATP synthesis is later shut down. It has been suggested that this is responsible for the externalisation of phosphatidylserine that leads to phagocytosis, and for the eventual loss of plasma membrane integrity (Gleiss *et al.*, 2002; Ricci *et al.*, 2004). Cleavage of a component of the mitochondrial complex I in human cells has been demonstrated to contribute to a loss in ATP synthesis function (Ricci *et al.*, 2004). However, a non-cleavable mutant of this protein only partially rescues from loss of mitochondrial function and

plasma membrane events. This shutdown could in fact be also be mediated by proteolysis and inactivation of ATP synthases, and subunits of the mitochondrial and the vacuolar ATP synthetases have been identified here as CED-3 substrates.

Of particular interest is the proteolysis of the vacuolar ATPase subunit VAB-13. The vacuolar ATP synthase is required in *C elegans* to prevent cell-cell fusion, and has been implicated in causing the intracellular acidification required for the progression of necrosis in *C. elegans* cells (Kontani *et al.*, 2005; Syntichaki *et al.*, 2005). In human cells, it also regulates the activity of matrix metalloproteinases (Maquoi *et al.*, 2003). Cleavage of one of its subunits could therefore have several potential effects in the dying cell – preventing necrosis, allowing changes in membrane properties, or up-regulating the expression of matrix metalloproteinases and therefore causing detachment from the substratum.

4.4.7 Metabolic proteins

The high proportion of metabolic proteins identified in our analysis probably reflects their abundance in the proteome and therefore on 2D gels. However, it is also conceivable that the cleavage of "housekeeping" proteins might represent a strategy to disable essential processes in the cell, rendering cell death irreversible and at the same time preventing the wastage of energy by continuing futile metabolic reactions.

4.4.8 Chaperone proteins

Four chaperone-type proteins were identified as substrates of CED-3 in our screen. Cleavage of proteins involved in stress responses might prevent the cell from mounting a futile protective response in cells undergoing apoptosis. However, there are other reasons why cleaving chaperone proteins during apoptosis might be beneficial to the cell. Several human heat shock proteins, including calreticulin, are able to bind to cellular peptides, and on their release from the cell, bind to receptors on APCs and deliver these peptides for re-presentation (Basu and Srivastava, 1999; Nair *et al.*, 1999). A specific immune response can then be mounted against these cellular antigens. Heat shock proteins can also deliver a non-antigen-dependent maturation signal to cells of the immune system (Basu *et al.*, 2000). Several of these chaperone proteins, including calreticulin, are released from necrotic cells, and their cleavage during

apoptosis might act to prevent this release and the mounting of an immune response in situations where death is physiological and an immune response is undesirable. Whether this type of mechanism might have any relevance in *C. elegans* is unclear.

Calreticulin has also been implicated in a range of other roles during cell death. Reports have suggested that it acts in a death-promoting or an inhibitory fashion, and it is also required for necrosis to occur in neurons of *C. elegans* (Liu *et al.*, 1994; Liu *et al.*, 1997; Nakamura *et al.*, 2000; Kageyama *et al.*, 2002; Xu *et al.*, 2001). Cleavage of calreticulin could therefore be involved in the amplification of the cell death process, or to prevent diversion of cells into a necrotic pathway during cell death. It has also been implicated in the phagocytosis of dead cells, with a recent report suggesting that it is exposed on the surface of apoptotic cells to act as a ligand for CD91 on macrophages, triggering phagocytosis (Gardai *et al.*, 2005). It is therefore possible that cleavage might be involved in this exposure and ligand activity of calreticulin during cell death, a matter investigated in the following chapter.

4.4.9 Proteases

Two *C. elegans* aspartic proteases were identified as substrates of CED-3. This was surprising, and raises the possibility that CED-3 might trigger a proteolytic activation cascade during cell death, with these aspartic proteases going on to cleave further cellular substrates. Both proteases are believed to be synthesized as zymogens, and cleavage might remove the short N-terminal pro-domain, leading to protease activation. Alternatively, cleavage might inactivate the protease – from the 2D data obtained, we know only that the full-length proteins are absent from gels following CED-3 treatment, so it is not possible to predict in which region of the proteases cleavage occurs. Some *C. elegans* aspartic proteases are known to be required for neurodegeneration induced by degenerin channel hyper-activation (Syntichaki *et al.*, 2002). Influxes of calcium in these dying cells activate proteases that may induce necrosis by causing undetermined substrate cleavages. Although one of our substrate proteases, ASP-2, has been ruled out of an involvement in this process, the other, an uncharacterized aspartic protease most similar to the *C. elegans* lysosomal aspartic proteases ASP-5 and

ASP-6, may be involved. Its cleavage might therefore disable a pathway leading to necrotic death of the cell.

4.4.10 Signalling proteins

In human cells, many signalling proteins are cleaved by caspases. Some of these cleavage events amplify pro-apoptotic signalling pathways, while others shut down survival signals. One substrate involved in signalling pathways that we identified here as a CED-3 substrate is a 16 kDa galectin (Hirabayshi *et al.*, 1996; Ahmed *et al.*, 2002). Galectins are carbohydrate-binding signalling molecules largely localized in the immune cells of mammals. Several galectins may play roles in the death of human cells. The closest human homologue to the galectin identified here is ecalectin, believed to be a chemoattractant for human eosinophils (Matsumoto *et al.*, 1998). Ecalectin is a short form of galectin-9, proposed itself to be a pro-apoptotic protein (Kashio *et al.*, 2003). This galectin is therefore a possible candidate for a cell death or immune regulator in *C. elegans*.

Another signalling molecule identified here as a substrate of CED-3 is FTT-2, a 14-3-3 protein. The 14-3-3 family of signalling adapter molecules is involved in a variety of signalling pathways with a relevance to cell death, including the sequestration of the BH3-only protein Bad in response to survival signals (Masters *et al.*, 2002; Zha *et al.*, 1996; Datta *et al.*, 1997; Datta *et al.*, 2000). It is also involved in the regulation of the cytoskeleton (Jin *et al.*, 2004). Cleavage of Ftt-2 and human 14-3-3 proteins might therefore activate apoptotic signals, or cause apoptotic cytoskeletal changes.

4.4.11 DNA and protein synthesis

Finally, we also identified two proteins involved in DNA synthesis and protein synthesis as substrates. Nucleosome assembly protein 1-like 1 in humans is similar to nucleosome assembly protein 1, a histone chaperone involved in nucleosome assembly and remodelling (Loyola and Almouzni, 2004). It has also been identified as a substrate of human caspases, and therefore represents a conserved apoptotic target (Van Damme *et al.*, 2005). Its cleavage might cause nucleasome remodelling, leaving DNA accessible to cleavage by nucleases.

A ribosome subunit, RPS-12, was also identified as a CED-3 substrate. A number of ribosomal proteins have been identified as substrates of human caspases, suggesting that this might be a general strategy for the cessation of unnecessary protein synthesis during cell death (Dr. Colin Adrain, pers. comm.). RPS-12 in *C. elegans* is required for embryonic and germline development, and for overall health of the organism.

4.4.12 Cleavage site specificity of CED-3

In the previous chapter, we attempted to gain an insight into the substrate specificity of CED-3 using a range of peptide substrate analogues. Following the identification of CED-3 cleavage sites in three substrates, FTT-2, TBB-2, and CRT-1, we are now able to compare genuine CED-3 substrate cleavage sites in a protein context, looking if necessary beyond the basic tetrapeptide sequence. This analysis has suggested that the preferred P4 residue is a D, with secondary cleavage sites possessing a N/V/E residue at the P4 position. There was no obvious consensus at the P3 position, but a preference for a V/I residue at P2. There also seemed to be a distinct preference for a smaller amino acid at the P1' position, after the P1 aspartic acid residue.

This certainly aligns CED-3 with the human executioner caspases-3 and -7, which both have a preference for a P4 aspartic acid. Again, however, there is a distinct promiscuity, especially in the P3, and also P2 cleavage site positions. The role of the P1' residue has been unclear, although studies in our laboratory have shown that the serine protease granzyme B is also dependent upon a small amino acid at this position (Dr. Colin Adrain, pers. comm.). This analysis in a whole protein context therefore suggests that the conclusions made about substrate specificity using peptide substrate analogues can still hold true in a protein context, but in proteins further important elements also come into play.

4.4.13 Advantages and disadvantages of biochemistry and genetics in the identification of substrates for proteases

It is likely that the lack of knowledge of substrates for CED-3 stems from a lack of biochemical analysis in the worm, and the difficulty of identifying protease substrates through genetics. This difficulty largely arises from the fact that the mutation of a single substrate among many is likely to create an extremely subtle

phenotype that could well be missed in mutational analysis, or due to redundancy will not create any phenotype at all. Although some groups have designed complex genetic screening techniques to find downstream elements of the cell death pathway in *C.elegans*, these methods seem to have borne little fruit. In contrast, our proteomic screen has identified a large number of substrates for CED-3.

However, once a downstream element has been identified by genetic analysis, there is already a mutant phenotype to give a clue as to the function of the gene during cell death, and an understanding that the gene under study is important in the process. In our biochemical analysis, it is difficult to tell which of the many identified substrates plays a role in the cell death pathway, and which are mere "bystander" cleavage events. Although we can infer from the normal function of each substrate protein, and from reports linking them to cell death, what their role in this process might be, these connections are still tenous and require substantial analysis to confirm them. With so many substrate proteins, this is rather a formidable task.

In this chapter, we selected three CED-3 substrates, FTT-2, TBB-2 and CRT-1, which seemed to hold the strongest potential as functionally important CED-3 substrates. We confirmed their cleavage by CED-3 and generated non-cleavable mutants. We then attempted to define roles for each of these substrates in downstream events of programmed cell death, and these analyses are described in the following chapter.

CHAPTER V

Functional characterization of CED-3 substrates

5.1 CHAPTER INTRODUCTION

Of the many human caspase substrates that have been identified, few are known to play significant roles in apoptotic events. There are three broad categories into which these significant substrates can be divided. Some, such as Bid, amplify caspase activation and accelerate the progression of cell death. Other proteins become activated themselves to contribute to the cell death process, such as PAK2, which is constitutively activated upon cleavage and contributes to changes in cellular morphology. A further category of proteins become inactivated, including ICAD (inhibitor of caspase-activated DNase), cleavage of which causes dissociation from CAD (caspase-activated DNase) which is then activated and able to cleave inter-nucleosomal DNA. However, many more substrate proteins appear to be "innocent bystanders" and play no role in apoptosis at all, merely possessing fortuitous caspase cleavage motifs.

Separating the important from the bystander caspase cleavage events is crucial to understanding how the demolition phase of apoptosis progresses. Our study aimed, as well as identifying substrates of the *C. elegans* caspase CED-3, to gain some understanding of the physiological role of these caspase cleavage events. The identification of conserved substrates could help to pinpoint proteins whose cleavage may be important for conserved features of apoptosis. However, we also speculated that *C. elegans* might be a useful model in which to study downstream events in apoptosis, due to its genetic tractability, the ease of RNAi analysis, and the existence of established assays for monitoring numbers and morphologies of dying cells. Using a combination of human cell and *C. elegans* assays we hoped to gain an understanding of the role that three conserved substrates might play during programmed cell death in both organisms.

5.2 CHAPTER SUMMARY

Our first approach to analysing the importance of cleavage events was to construct *C. elegans* expression plasmids, containing wild-type and cleavage-resistant *crt-1*, *tbb-2* and *ftt-2* genes under the control of heat-shock promoters. In collaboration with other groups, these constructs were used to generate transgenic nematode lines able to express the substrate proteins on elevation to a restrictive temperature. However, expression of CRT-1 and TBB-2 in either their wild-type or cleavage-resistant forms did not result in any alteration in apoptotic frequency,

timing, or morphology as assessed by examination of cell death in the anterior pharynx (Prof. Michael Hengartner, pers. comm.).

In parallel, we examined the role of these three substrates during death of human cells. Using Western blotting analysis and *in vitro*-synthesized ^{35}S-methionine-labelled proteins, we demonstrated that human calreticulin, 14-3-3 proteins, and alpha- and beta-tubulin are also caspase substrates. This suggested that as conserved caspase substrates, these proteins might play conserved roles during apoptosis. We tested whether transfection of *C. elegans crt-1* or *ftt-2* were able to modulate apoptosis in human cells. However, we could observe no effects on the rate or morphology of apoptosis in these cells. Use of RNAi against alpha-tubulin in HeLa cells caused some spontaneous apoptosis, and we noted microtubule condensation in HeLa cells undergoing programmed cell death. However, reductions in alpha-tubulin levels did not appear to affect cell morphology, membrane blebbing, or nuclear fragmentation during apoptosis.

During the course of this work, a report was published suggesting that calreticulin is exposed on the surface of cells undergoing apoptosis and acts as a ligand for phagocytic cells (Gardai *et al*, 2005). We confirmed this observation, and demonstrated that the phenomenon is a general feature of apoptosis, occurring in response to a range of stimuli. It seemed possible that the cleavage of calreticulin by caspases might influence this cell surface exposure. Indeed, pre-incubating CEM cells in the poly-caspase inhibitor z-VAD-fmk prevented the exposure of calreticulin, confirming that this event is caspase-dependent. In addition, cells stably expressing the anti-apoptotic protein Bcl-2 failed to expose calreticulin on treatment with apoptotic stimuli. To confirm that the surface change detected by our antibody was genuinely an increased exposure of calreticulin, we transfected HeLa cells with calreticulin followed by treatment with an actinomycin D. Although there was an increase in the degree of surface calreticulin, this increase was small and not proportional to the degree of calreticulin over-expression. However, treatment with an ER stress agent, brefeldin A, led to a large increase in surface calreticulin detection, suggesting that the cell surface changes observed are due to the exposure of calreticulin. These results therefore suggest that caspases cleave calreticulin in both worm and human cells, and lead to its exposure on the cell surface where it acts as a ligand for phagocytes.

5.3 RESULTS

5.3.1 Over-expression of CED-3 substrates in *C. elegans*

Our first approach in examining the functional role of CED-3 substrate cleavages was to over-express substrate proteins in *C. elegans* through the creation of transgenic strains. In order to do this, we cloned three substrate ORFs, *crt-1*, *ftt-2* and *tbb-2*, into *C. elegans* expression vectors. These vectors, pPD49_78 and pPD49_83, contain sequences from the promoter of the *C. elegans* heat shock gene *hsp-16*. Upon elevation to a higher temperature, these promoter elements are able to drive expression of downstream genes. So that we could assess the effects of both an excess of substrate protein and the presence of uncleaved substrate, we also cloned the CED-3-cleavage-resistant mutant sequences of each substrate into both vectors (Figure 5.1; Figure 4.13).

In collaboration with the laboratories of Prof. Michael Hengartner and Prof. Brent Derry, these 12 plasmids were used to make transgenic nematode strains containing stable chromosomally-integrated substrate sequences. The transgenic worms were heat-shocked to induce expression of the substrate sequences, and cell deaths in the anterior pharynx of L1 stage larvae were counted and examined to detect any modulatory effects that the over-expressed substrates had on the frequency or phenotype of dying cells. However, transgenic lines expressing *crt-1* and *tbb-2* ORFs did not show a significant or reproducible change in any aspect of cell death, and *ftt-2* transgenic lines have yet to be examined (Prof. Michael Hengartner and Prof. Brent Derry, pers. comm.). Although these nematode strains await further and more thorough analysis, it seemed that a different system would have to be used to examine in detail the roles that these CED-3 substrates might play in cell death.

5.3.2 Human homologues of Crt-1, Tbb-2 and Ftt-2 are cleaved during apoptosis

In parallel to these studies in *C. elegans*, we decided to test whether the cleavage of these three substrates, CRT-1, TBB-2, and FTT-2, was a conserved event in programmed cell death. To determine whether human homologues of these proteins are substrates for human caspases, we used Western blotting analysis in cell-free extracts derived from a human cell line. Jurkat cell extracts were either treated with cytochrome c and dATP to activate caspases, or left untreated.

Samples of these extracts were taken after 0, 15, 30, 60, 90 and 120 minutes of treatment and electrophoresed through 12 % SDS-PAGE gels.

Using antibodies directed against human alpha- and beta-tubulin, we found that both of these proteins are substrates for human caspases (Figure 5.2 A). Beta-tubulin was cleaved relatively late compared to the control substrate, caspase-3. Alpha-tubulin appeared to be cleaved much earlier in the time-course, being almost fully proteolysed after 15 minutes. A cleavage fragment marginally lower in molecular weight than full-length alpha-tubulin was detected. This small downshift in size was similar to that seen after the CED-3-mediated C-terminal cleavage of TBB-2. In order to determine the cleavage pattern of human beta-tubulin, the beta-5 isoform was synthesized *in vitro* incorporating a ^{35}S-methionine label, and incubated with Jurkat cell-free extracts treated as described. Cleavage products were evident after 60 minutes of incubation in activated extracts, and again represented a protein only slightly smaller than the full-length substrate (Figure 5.2 B). Alpha- and beta-tubulin are therefore both conserved as caspase substrates in *C. elegans* and man.

FTT-2 is related to a family of human proteins, the 14-3-3 proteins. We used antibodies against 4 family members to determine whether they were cleaved in Jurkat cell-free extracts (Figure 5.3). Three of these proteins, 14-3-3 beta, epsilon and tau, were indeed caspase substrates, while the fourth, 14-3-3 zeta, was not. The full-length form of 14-3-3 beta began to diminish relatively late in apoptosis, after 60 minutes, while proteolysis of 14-3-3 tau followed kinetics similar to the control substrate, caspase-2, and was almost complete by 30 minutes. A cleavage fragment of 14-3-3 epsilon was observed by 30 minutes. This fragment was, like the cleavage product of FTT-2, only a little lower in molecular weight than the full-length form, suggesting that it might be cleaved in a similar region. FTT-2 therefore represents the *C. elegans* member of a family of conserved caspase substrates.

We then tested whether human calreticulin was also a substrate for caspases. Western blotting analysis showed that the full-length form of calreticulin was substantially proteolysed by 60 minutes after caspase activation (Figure 5.4 A). Our antibody detected 2 cleavage products of about 20 kDa and 7 kDa after 60

Figure 5.1

***C. elegans* expression constructs encoding wild-type and cleavage-resistant TBB-2, FTT-2 and CRT-1**

Schematic representation of *C. elegans* expression constructs generated to express wild-type and cleavage-resistant CED-3 substrates in *C. elegans*. Two *C. elegans* expression constructs, pPD49_78 and pPD49_83, were used to drive expression of insert sequences from *hsp-16* promoter sequences. Wild-type and cleavage-resistant *tbb-2*, *ftt-2* and *crt-1* were cloned into each of these vectors to make a total of 12 expression constructs. These constructs were then transformed into *C. elegans* hermaphrodites.

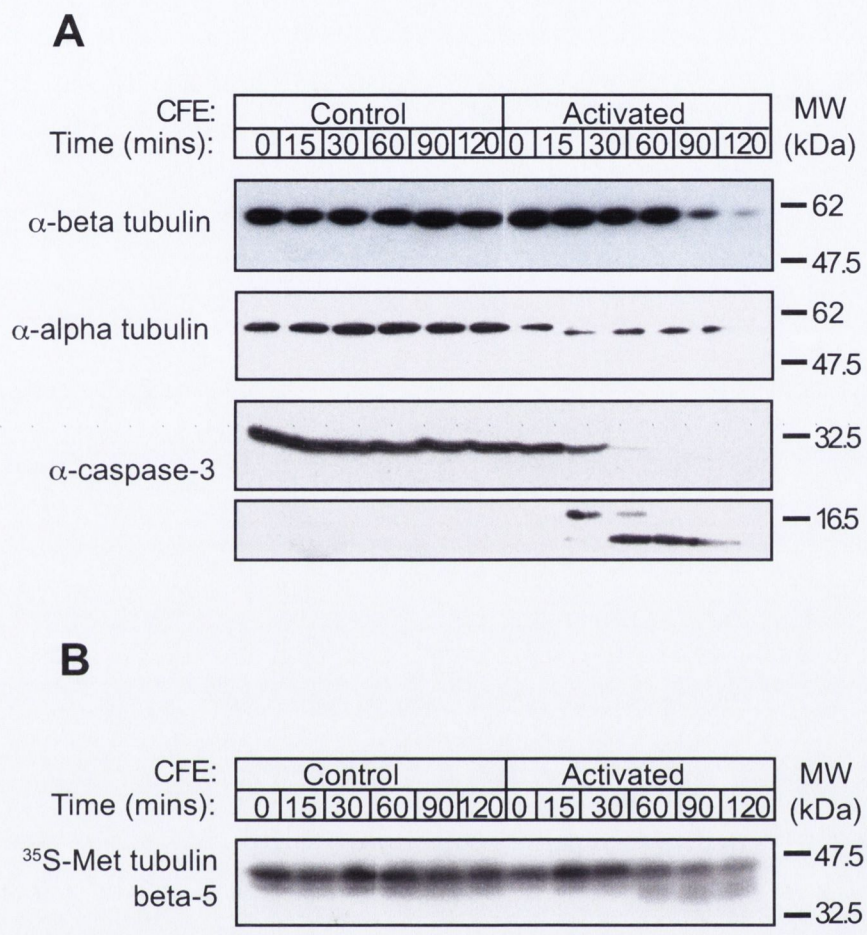

Figure 5.2

Both alpha-tubulin and beta-tubulin are substrates for human caspases

A) Cleavage of human alpha- and beta-tubulin in cell-free extract. Jurkat CFE was treated with buffer only or with cytochrome c/ dATP. Samples were taken at indicated timepoints and analysed by SDS-PAGE followed by Western blotting with antibodies directed against beta-tubulin, alpha-tubulin and caspase-3.

B)Cleavage of ^{35}S-methionine-labelled human tubulin beta-5 in cell-free extract. Human tubulin beta-5 was synthesized *in vitro* incorporating a ^{35}S-methionine tag, and incubated with control or cytochrome c/ dATP-treated Jurkat CFE. Samples were taken at the indicated timepoints and analysed by SDS-PAGE and fluorography.

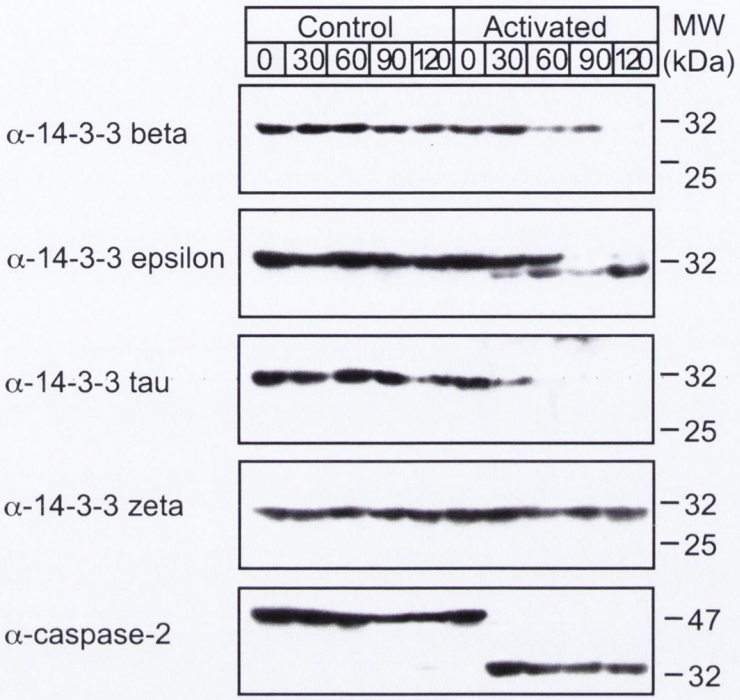

Figure 5.3

14-3-3 beta, epsilon and tau are substrates for human caspases

Cleavage of human 14-3-3 proteins in cell-free extract. Jurkat CFE was treated with buffer or with cytochrome c/ dATP. Samples were taken at indicated timepoints and analysed by SDS-PAGE followed by Western blotting with antibodies directed against 14-3-3 beta, 14-3-3 epsilon, 14-3-3 tau, 14-3-3 zeta and caspase-2.

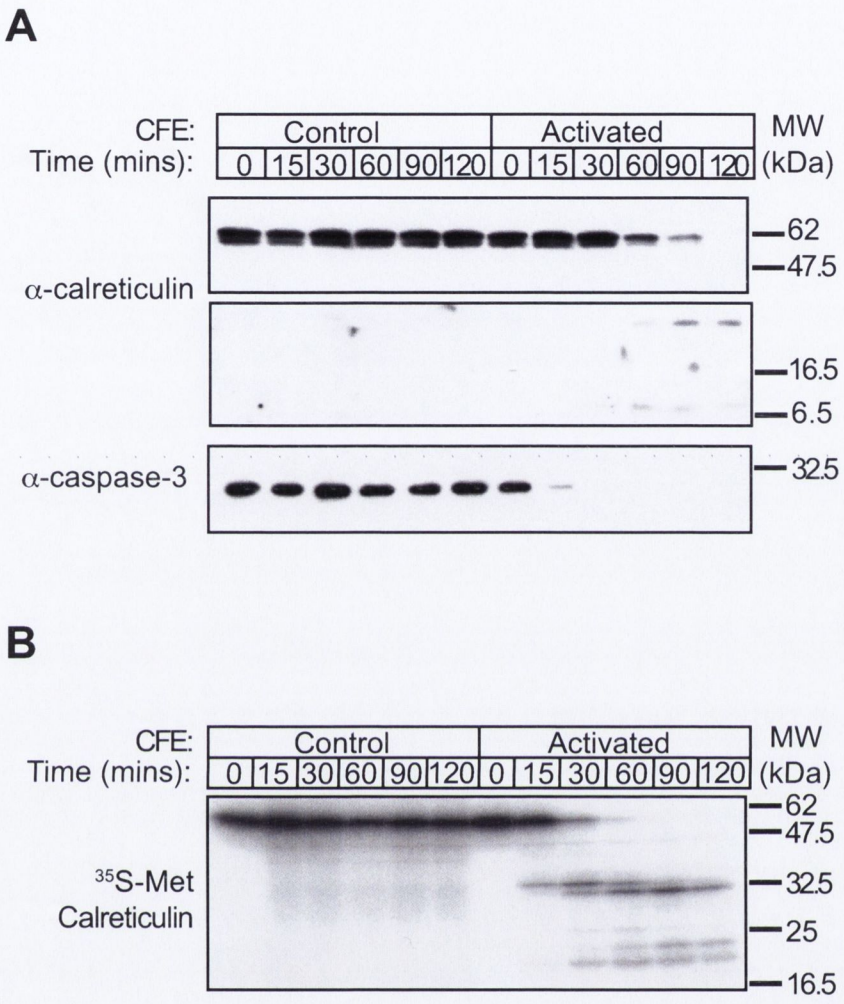

Figure 5.4

Calreticulin is a substrate for human caspases

A) Cleavage of human calreticulin in cell-free extract. Jurkat CFE was treated with buffer only or with cytochrome c/ dATP. Samples were taken at indicated timepoints and analysed by SDS-PAGE and Western blotting with antibodies against calreticulin and caspase-3. B) Cleavage of ^{35}S-methionine-labelled human calreticulin in cell-free extract. Human calreticulin was synthesized *in vitro* incorporating a ^{35}S-methionine tag and incubated with control or cytochrome c/ dATP-treated Jurkat CFE. Samples were taken at the indicated timepoints and analysed by SDS-PAGE and fluorography.

minutes. However, to better examine the cleavage pattern of human calreticulin, we also synthesized ^{35}S-methionine-labelled protein and incubated it with cytochrome c/ dATP-treated or untreated extracts. The results were analysed by SDS-PAGE and enhanced fluorography (Figure 5.4 B). Calreticulin cleavage was observed within 15 minutes of caspase activation, and at least 4 products of proteolysis were observed. This suggested that several sites for caspase-mediated cleavage exist within human calreticulin, leading to sequential proteolysis, akin to *C. elegans* CRT-1 in which there are at least 3 CED-3 cleavage sites. Calreticulin is therefore another example of a protein that is a caspase substrate in two divergent organisms.

5.3.3 Ftt-2 does not modulate apoptosis in human cells

These four proteins now identified as caspase substrates in both worms and man, alpha-tubulin, beta-tubulin, 14-3-3 proteins, and calreticulin, seemed good candidates for substrates that might play an important role in the downstream events characterizing apoptosis. We decided to test whether modulating levels of these proteins in human cells undergoing apoptosis might influence the rate or phenotype of cell death.

FTT-2 is highly conserved with human 14-3-3 proteins, showing an identity of 97.6 % with its closest human relative, 14-3-3 zeta. We therefore reasoned that, if cleavage of 14-3-3 proteins were an important event during apoptosis, the expression of cleavage-resistant or truncated FTT-2 in apoptotic human cells might influence the progression of cell death. To investigate this, we cloned wild-type and cleavage-resistant *ftt-2*, and a truncation mutant ending at D^{240}, into pcDNA3. These constructs were transfected into human HeLa cells, alongside control plasmids encoding the anti-apoptotic molecule Bcl-x_L, and the caspase inhibitor p35. Cells were then either left untreated or induced to undergo apoptosis by treatment with TNF/ CHX or daunorubicin. After treatment, dying cells were closely observed to detect any alterations in apoptotic morphology or the kinetics of cell death. The percentage of dead cells after 6 hours (TNF/ CHX) or 8 hours (daunorubicin and untreated) was assessed (Figure 5.5). In untreated cells, transfection with *ftt-2* constructs did not induce any cell death. In cells treated with TNF/ CHX or daunorubicin, there was no consistent enhancement or suppression of cell death upon transfection of any *ftt-2* construct. In contrast,

over-expression of Bcl-x_L robustly suppressed cell death under both these conditions, and p35 expression resulted in a reduction in the number of dying cells after treatment with TNF/ CHX. We therefore could not identify any role for caspase-mediated cleavage of 14-3-3 proteins during apoptosis in human cells.

5.3.4 Calreticulin does not modulate apoptosis in human cells

We then similarly analysed the effects of calreticulin over-expression on human cells. We cloned *C. elegans crt-1* wild-type and CED-3 cleavage-resistant ORFs into pcDNA3. We also cloned human calreticulin into the pcDNA3 vector. These constructs were transfected into HeLa cells alongside pcDNA3-Bcl-xl, and cells were then treated with TNF/ CHX or actinomycin D. Cell morphology was examined and numbers of dead cells counted after 6 hours treatment with TNF/ CHX or 8 hours treatment with actinomycin D (Figure 5.6). No differences in the phenotype of dying cells were observed. There did appear to be a low level of cell death induced upon over-expression of *C. elegans* and human calreticulin, and a slight enhancement of cell death induction on treament with both apoptotic agents tested. However, these effects were small and not reproducible, particularly when compared to the strong inhibitory activity of over-expressed Bcl-xl in both treatments. We were therefore unable to assign a specific role to caspase-mediated calreticulin cleavage during apoptosis in this system.

5.3.5 Knock-down of alpha-tubulin causes apoptosis

We also identified both alpha- and beta-tubulin as conserved substrates of *C. elegans* and human caspases. Alpha-tubulin had already been identified in our laboratory as a substrate of human caspases and the aspartate-specific serine protease granzyme B (Adrain *et al.*, 2006). During that earlier study, it had been noted that transfection of alpha-tubulin for transient over-expression studies had not led to any detectable increases in cellular alpha-tubulin levels. Transfection had also not resulted in any detectable incorporation of over-expressed alpha-tubulin into the microtubule cytoskeleton. Using a different approach to examine the potential role of tubulin in granzyme B-induced cell killing, reduction in tubulin levels by RNAi had led to a 20 - 30 % increase in spontaneous apoptosis of untreated cells. However, reduction of alpha-tubulin levels did not enhance the degree of apoptosis induced by de-granulation of cytotoxic natural killer (NK) cells.

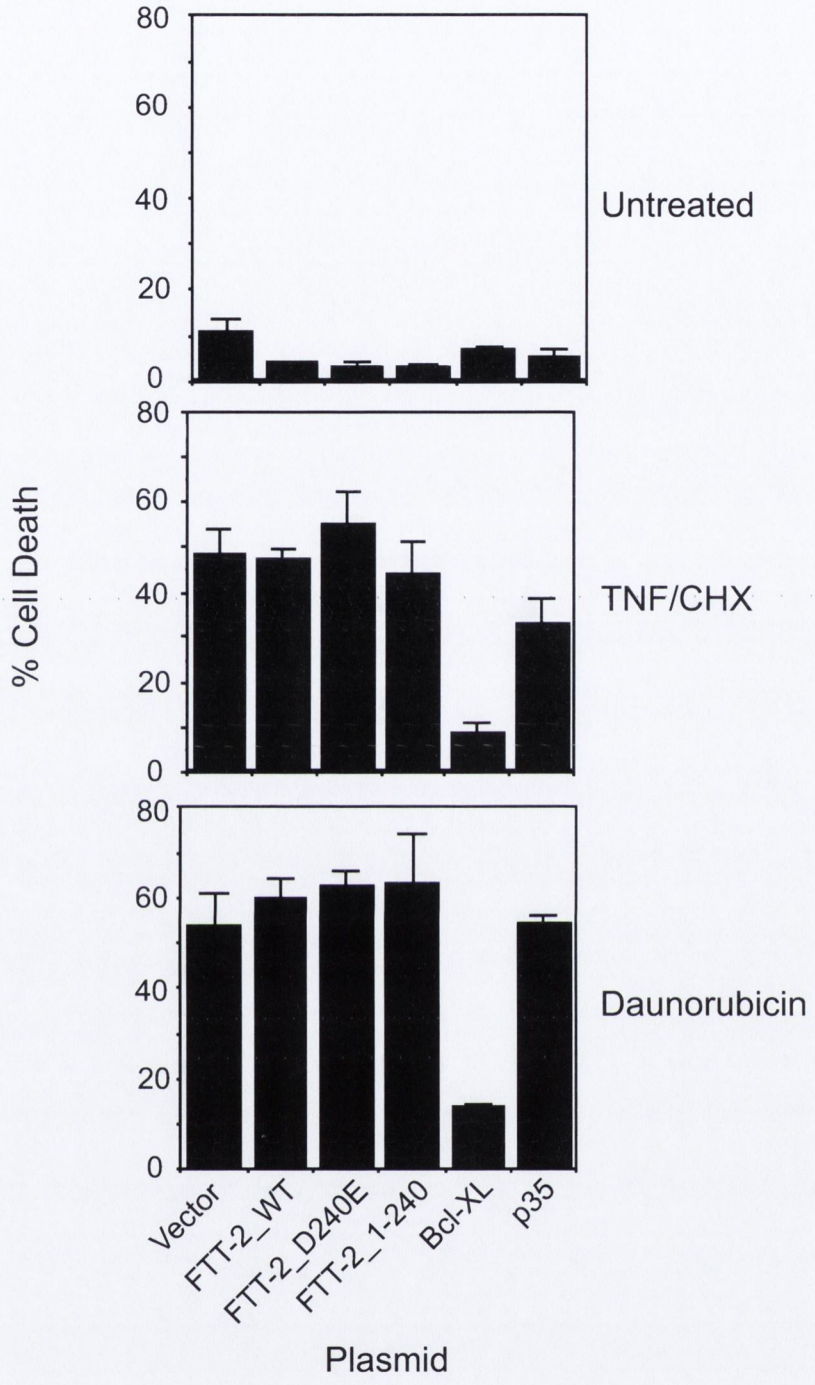

Figure 5.5

FTT-2 does not affect apoptosis in human cells

Expression of wild-type, cleavage-resistant or truncated FTT-2 does not affect apoptosis induced by TNF/CHX or daunorubicin. The wild-type *ftt-2* ORF, the D240E mutant sequence, or a truncated FTT-2 sequence ending at D^{240}, were cloned into pcDNA3. Each construct was transfected into HeLa cells, alongside vector alone and known apoptosis inhibitors Bcl-xl and p35, and cells were left untreated or apoptosis induced with TNF/CHX or daunorubicin. Percentages of cells dying were counted after 6 hours (TNF/ CHX) or 8 hours (Daunorubicin and untreated). Results represent at least 3 independent experiments.

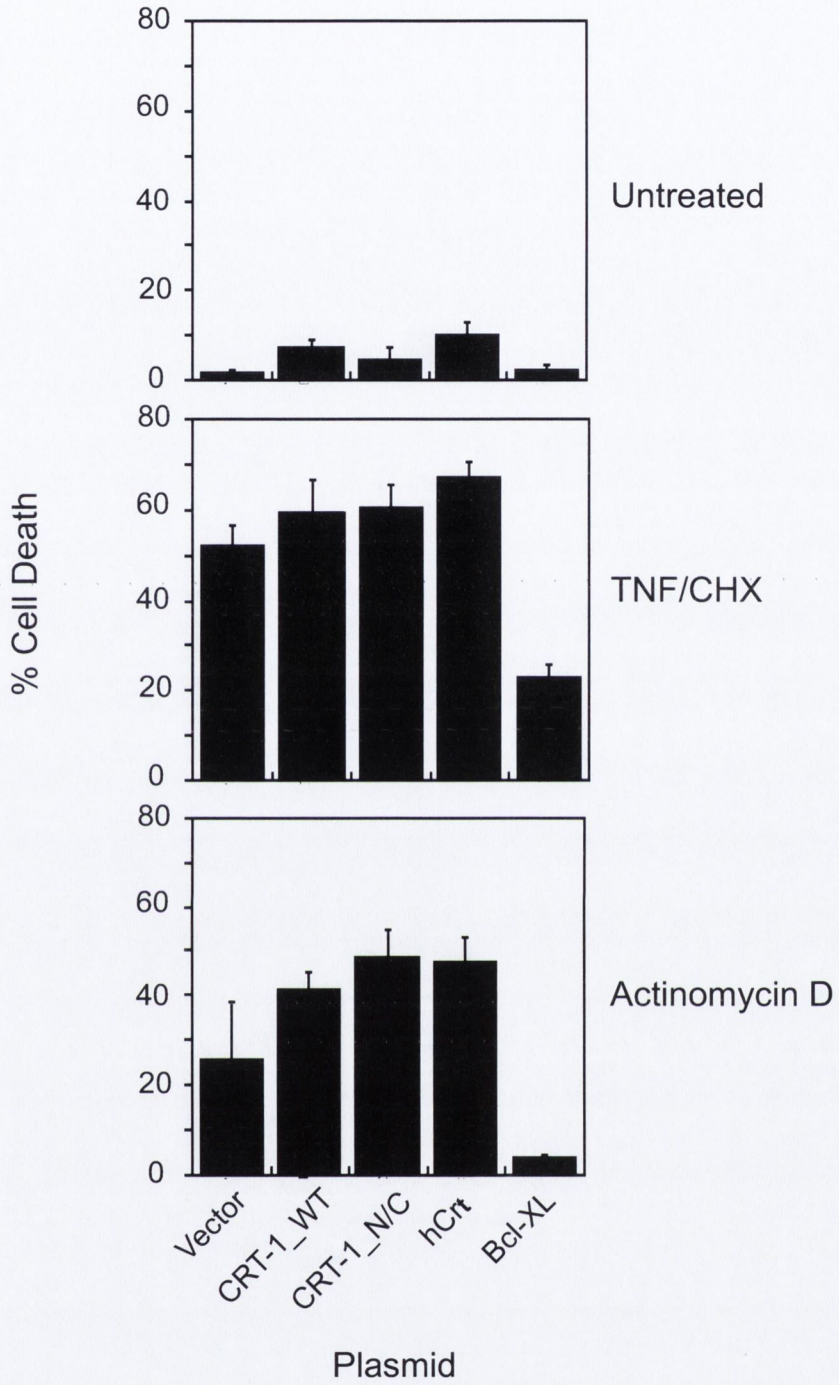

Figure 5.6

Calreticulin does not affect apoptosis in human cells

Expression of wild-type or cleavage-resistant CRT-1, or human calreticulin, does not affect apoptosis induced by TNF/CHX or actinomycin D. The wild-type and cleavage-resistant *crt-1* ORFs, and the human calreticulin ORF, were cloned into pcDNA3. Each construct was transfected into HeLa cells, alongside vector alone and the known apoptosis inhibitor Bcl-xl, and cells were left untreated or apoptosis induced with TNF/CHX and actinomycin D. Percentages of cells dying were counted after 6 hours (TNF/ CHX) or 8 hours (daunorubicin and untreated). Results represent at least 3 independent experiments.

We therefore used RNAi against alpha-tubulin to reduce cellular tubulin levels, and see whether this affected susceptibility to other apoptotic stimuli. Two different RNAi oligos were used, both of which had already been shown to substantially down-regulate expression of alpha-tubulin (Adrain *et al.*, 2006). Following transfection of 200 nM RNAi oligos, cells were incubated for 72 hours, and then treated with actinomycin D or daunorubicin. The percentage of dead cells in cultures left untreated or treated with either stimulus for 8 hours was assessed (Figure 5.7). Cells transfected with either alpha-tubulin oligo typically showed between 20 % and 30 % spontaneous cell death, confirming results in our earlier study (Adrain *et al.*, 2006). However, upon treatment with either daunorubicin or actinomycin D, there was no enhancement of cell death rates in cells with reduced levels of alpha-tubulin. There was also no obvious alteration in the morphology of dying cells. We therefore concluded that, although reduction in alpha-tubulin levels causes a degree of cell death, there is no consequent enhanced sensitivity to apoptotic stimuli, or any influence on the apoptotic phenotype.

5.3.6 Microtubule morphology is altered during apoptosis but reduction in alpha-tubulin levels does not affect nuclear fragmentation or apoptotic body formation

Our previous study showed that granzyme B-mediated removal of the alpha-tubulin C-terminus causes an increased rate of microtubule polymerization (Adrain *et al.*, 2006). The proteolysis of the same region by caspases might also mediate enhanced tubulin polymerization. It is not clear what the functional effects of microtubule polymerization during cell death would be, but reports have suggested that an altered microtubule cytoskeleton may be involved in chromatin dispersal and the formation of apoptotic bodies during late stages of apoptosis (Moss *et al.*, 2006). Although we saw no overt change in apoptotic cell morphology upon reducing alpha-tubulin levels by RNAi, we decided to examine more closely the morphology of microtubules during apoptosis and the effect of tubulin reduction on chromatin dispersal, plasma membrane blebbing, and apoptotic body formation, using immunofluorescence analyses.

HeLa cells plated on coverslips were transfected with RNAi oligos against alpha-tubulin, as before. After 72 hours, cells were left untreated, or treated with actinomycin D, for a further 8 hours. Cells were then fixed and stained with a

monoclonal antibody against alpha-tubulin, and with Hoechst, a DNA stain. Cells transfected with a control oligonucleotide showed an extensive network of filamentous microtubules throughout the cell (Figure 5.8). However, in cells undergoing apoptosis, microtubules appeared shortened and contracted and were mainly visible around the cell periphery. This is consistent with previous reports demonstrating altered microtubule morphology during apoptosis, and microtubule contraction upon treatment of cells with granzyme B (Moss *et al.*, 2006; Adrain *et al.*, 2006). In many of these apoptotic cells, formation of apoptotic bodies and nuclear fragmentation was clearly visible (Figure 5.8).

In cells transfected with RNAi oligos against alpha-tubulin, a majority of cells exhibited virtually no alpha-tubulin staining, as expected (Figure 5.8). However, the incidence of plasma membrane blebbing and apoptotic body formation appeared just the same in these as in apoptotic cells treated only with control oligos. In addition, chromatin dispersal as assessed by Hoechst staining also appeared to occur in a similar proportion of cells. It therefore seems that, at least in this cell type, these processes may not be dependent upon the presence of functional microtubules and would therefore not be influenced by cleavage of either alpha- or beta-tubulin.

5.3.7 Calreticulin is cleaved in cells undergoing apoptosis

During the course of this work, a report was published suggesting that calreticulin becomes exposed on the surface of cells during apoptosis, and acts as a recognition signal for phagocytic cells (Gardai *et al.*, 2006). As we had identified calreticulin as a conserved caspase substrate, we hypothesized that cleavage of calreticulin by caspases might influence its cell surface exposure. Because calreticulin is a highly conserved protein and is cleaved by caspases in both worm and human cells, it seemed that this mechanism might be able to operate in both organisms, as a conserved phagocytic signalling mechanism (Figure 5.9). We therefore investigated the cell surface exposure of calreticulin during cell death.

We started by establishing whether calreticulin is actually cleaved *in vivo*, in human cells induced to undergo apoptosis. HeLa cells were treated with three different apoptotic stimuli, actinomycin D, *N*-tosyl-l-phenylalanine chloromethyl ketone (TPCK) and 3,4-dichloroisocoumarin (DCI). 12 hours after treatment, cells

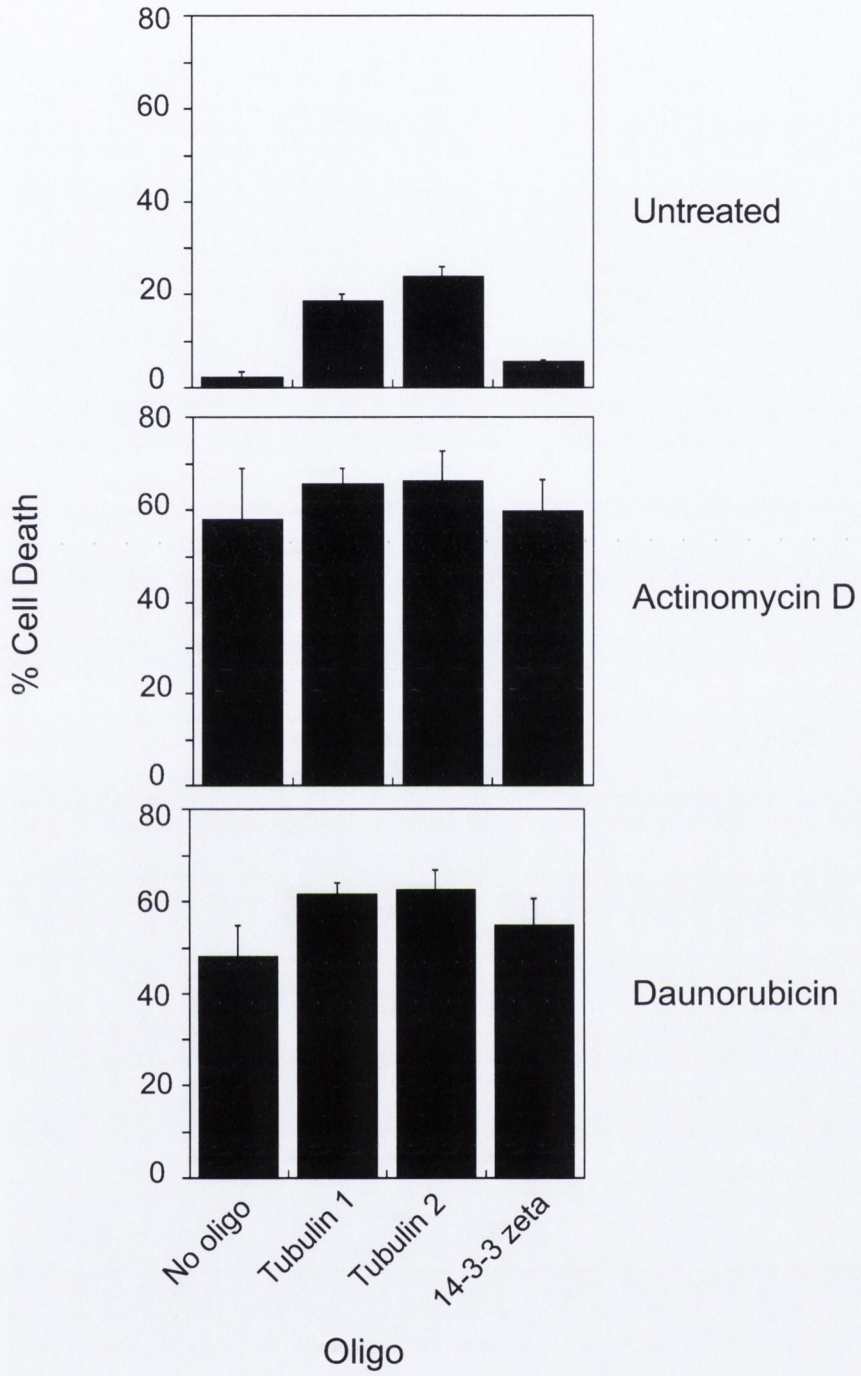

Figure 5.7

Knock-down of human alpha-tubulin induces a low level of apoptosis but does not affect death induced by apoptotic stimuli

Transfection of siRNAs against human alpha tubulin induces some spontaneous apoptosis but does not affect apoptosis induced by actinomycin D or daunorubicin. Two different siRNA oligonucleotides against alpha tubulin were transfected into HeLa cells and after 72 hours cells were left untreated or apoptosis induced with TNF/CHX and actinomycin D. Percentages of cells dying were counted after 8 hours of treatment. Results represent at least 3 independent experiments.

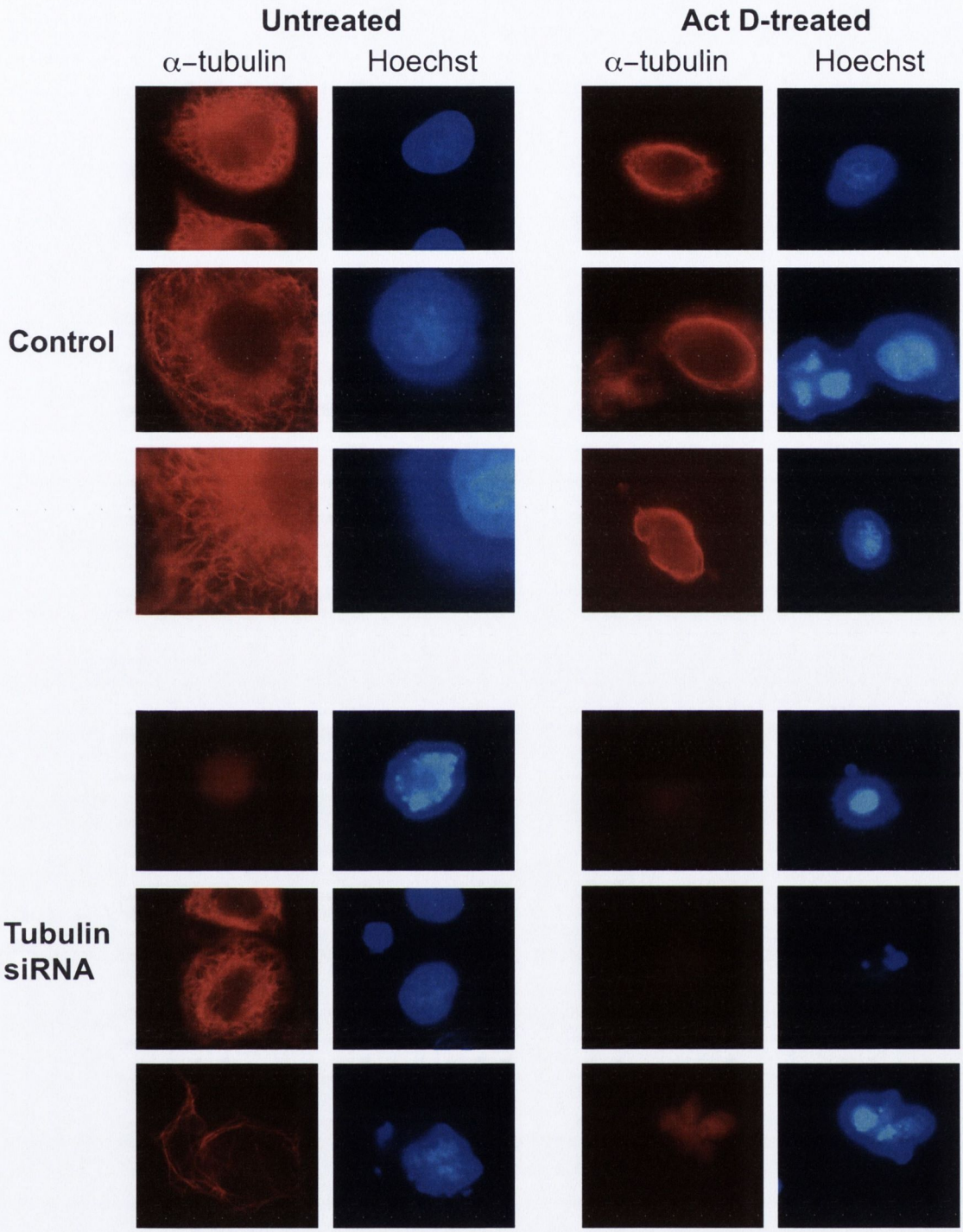

Figure 5.8

Knock-down of human tubulin does not affect apoptotic body formation or nuclear fragmentation in apoptotic cells

Transfection of siRNAs against human tubulin alpha does not affect the morphology of apoptotic cells. T wo different siRNA oligonucleotides against alpha tubulin were transfected into HeLa cells and after 72 hours cells were left untreated or apoptosis induced with actinomycin D. Images were taken using fluorescence microscopy after 8 hours of treatment. Results represent at least 3 independent experiments.

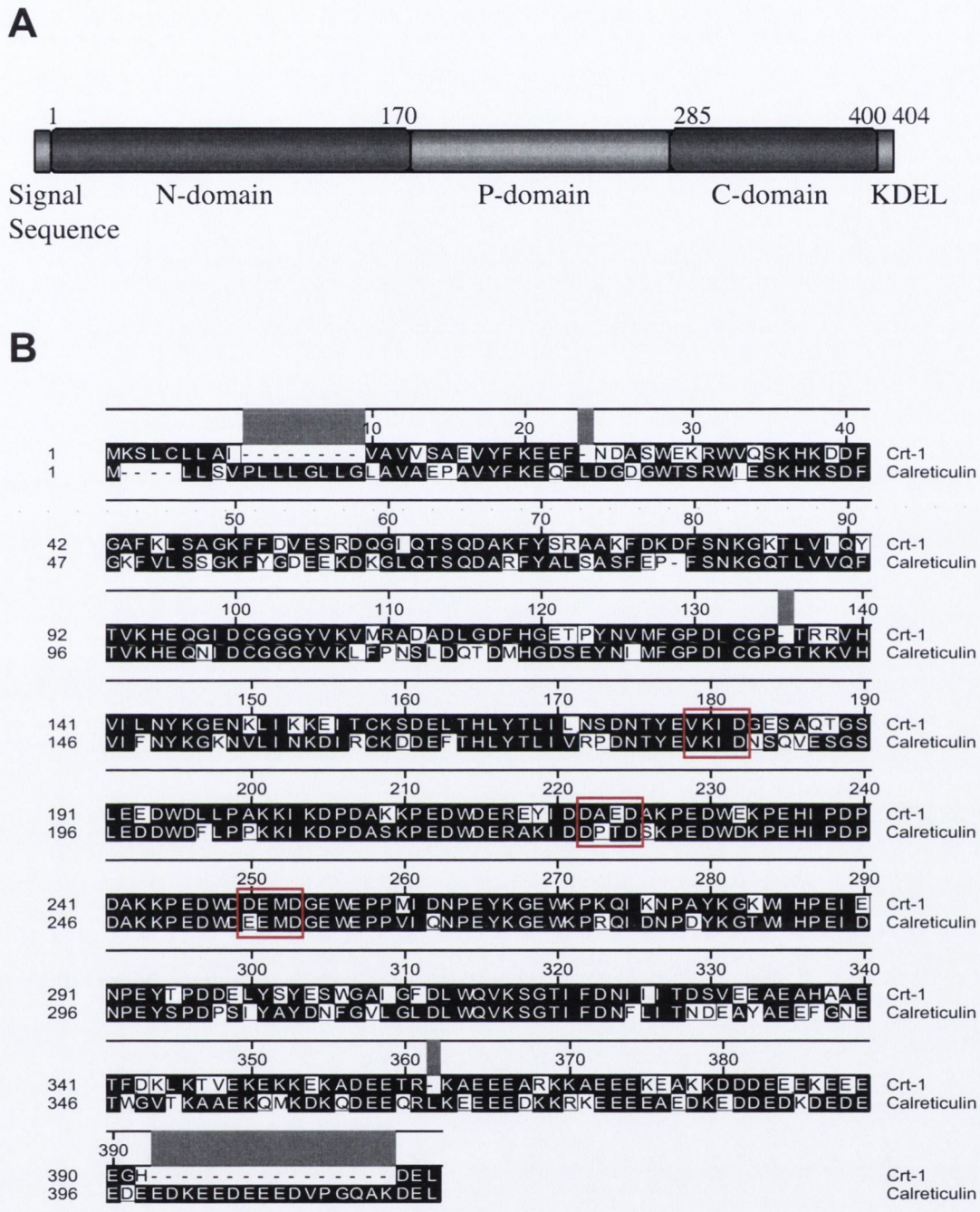

Figure 5.9

Domain structure and alignment of human and *C. elegans* calreticulin

(A) Schematic representation of human calreticulin. Human and worm calreticulin share the same domain structure.

(B) Alignment of human and *C. elegans* calreticulin. The two proteins share 60 % identity.

were collected and lysed in SDS-PAGE lysis buffer. Cell lysates were electrophoresed through 12 % SDS-PAGE gels, followed by Western blot analysis. Antibodies were used to detect two control caspase substrates, XIAP and capase-9, as well as calreticulin (Figure 5.10). Both XIAP and caspase-9 were substantially proteolysed after treatment with actinomycin D, and proteolysis was virtually complete upon treatment with TPCK and DCI. In contrast, there appeared to be no diminution of the full-length form of calreticulin upon any treatment. However, there was a cleavage fragment detected that appeared in all three treatments. This proteolysis product was at a size of about 30 kDa, consistent with the size of one of the bands appearing on the cleavage of ^{35}S-methionine-labelled calreticulin (Figure 5.4). This suggests that, although most of the cellular complement of calreticulin is protected from cleavage by caspases, possibly through its ER localization, a small fraction of this protein does undergo proteolysis during apoptosis.

5.3.8 Calreticulin is detected on the surface of cells treated with a range of apoptotic stimuli

We went on to confirm that calreticulin is exposed on the surface of cells undergoing apoptosis. CEM cells were treated with a range of apoptotic stimuli - actinomycin D, etoposide, TPCK and DCI – or left untreated. After 12 hours, the cells were harvested and a sample stained with annexin V, to detect surface exposure of phosphatidylserine, a phagocytic ligand and hallmark of apoptosis (Martin *et al.*, 1996b). The remaining cells were immunostained, without permeabilisation, using a polyclonal antibody directed against calreticulin. Cells were then analysed by flow cytometry (Figure 5.11). The majority of untreated cells were negative for annexin V staining and also for surface calreticulin. There was, however, a second smaller population representing cells positively stained for calreticulin. Upon exposure of cells to the apoptotic stimuli tested, this second population was greatly increased in size to include the majority of cells. The size of the second population was broadly proportional to the population of cells stained positively for surface phosphatidylserine. These results are therefore consistent with recent data suggesting that calreticulin is exposed on the surface of dying cells (Gardai *et al.*, 2006). They also extend the earlier observation, to demonstrate that this is a general apoptotic phenomenon, occurring in response to a range of different apoptotic stimuli.

5.3.9 z-VAD-fmk prevents the exposure of calreticulin on the surface of cells treated with actinomycin D

To establish whether caspase activity is required for the exposure of calreticulin on the surface of dying cells, CEM cells were pre-treated with 50 μM z-VAD-fmk for 30 minutes followed by treatment with 20 μM actinomycin D, for 12 hours. Cells were harvested and samples stained with annexin V to detect phosphatidylserine exposure. The remaining cells were immunostained with anti-calreticulin, and stained cells were analysed by flow cytometry (Figure 5.12). Z-VAD-fmk treatment substantially reduced the proportion of apoptotic cells as measured by the detection of exposed phosphatidylserine, from 56 % to 29 %. The percentage of cells with exposed cell surface calreticulin was also greatly decreased, from 75 % to 40 %. Caspase activity is therefore necessary for calreticulin exposure on the surface of dying cells.

5.3.10 Over-expression of Bcl-2 inhibits cell surface exposure of calreticulin in cells treated with actinomycin D

We also tested whether inhibition of caspase activation at the mitochondrial level could prevent the induction of cell surface exposure of calreticulin. CEM.neo and CEM.Bcl-2 cells stably expressing Bcl-2 were treated with actinomycin D for 12 hours. Cells were then harvested and samples stained with annexin V to quantify phosphatidylserine exposure. Remaining cells were stained with α-calreticulin and analysed by flow cytometry (Figure 5.13). As expected, exposure of phosphatidylserine was almost entirely blocked by over-expression of Bcl-2. The exposure of calreticulin was also almost entirely prevented. Apoptosome formation and caspase activation are therefore essential for the exposure of calreticulin on the cell surface following treatment with apoptotic stimuli.

5.3.11 Over-expression of calreticulin leads to increased calreticulin surface exposure on treatment with actinomycin D

A major concern that we had was whether the calreticulin antibody used was specifically detecting calreticulin, or instead recognising other changes in the apoptotic cell membrane. The antibody used for our immunostaining analyses was a polyclonal antibody, making it more prone to the non-specific detection of different proteins. To address the issue of antibody specificity, we used HeLa cells

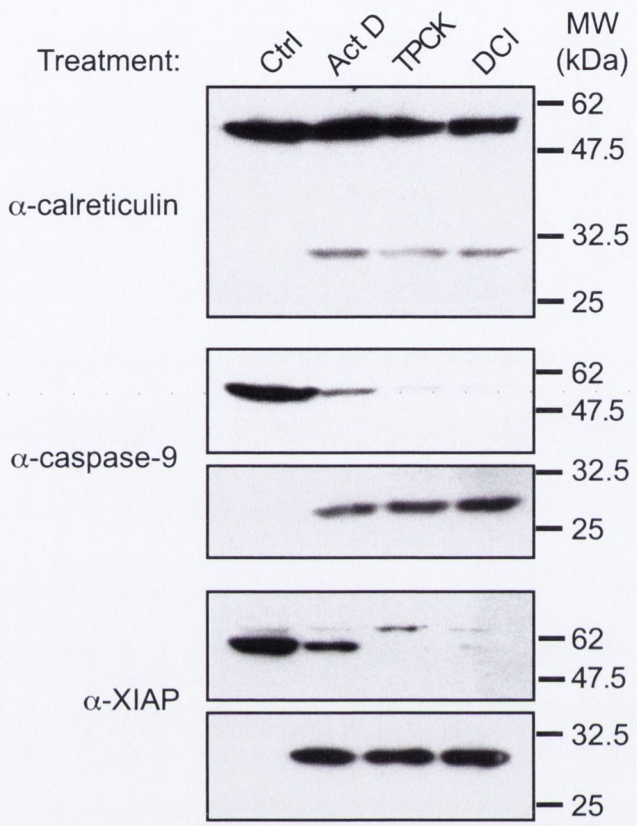

Figure 5.10

Calreticulin is cleaved in cell undergoing apoptosis

Calreticulin cleavage in apoptotic human cell lysates. HeLa cells were treated with 20 μM actinomycin, 75 μM TPCK, or 100 μM DCI, or left untreated. After 12 hours, cells were collected and lysed. Lysates were then analysed by SDS-PAGE followed by Western blotting with antibodies against calreticulin, caspase-9 and XIAP. Results represent at least 3 independent experiments.

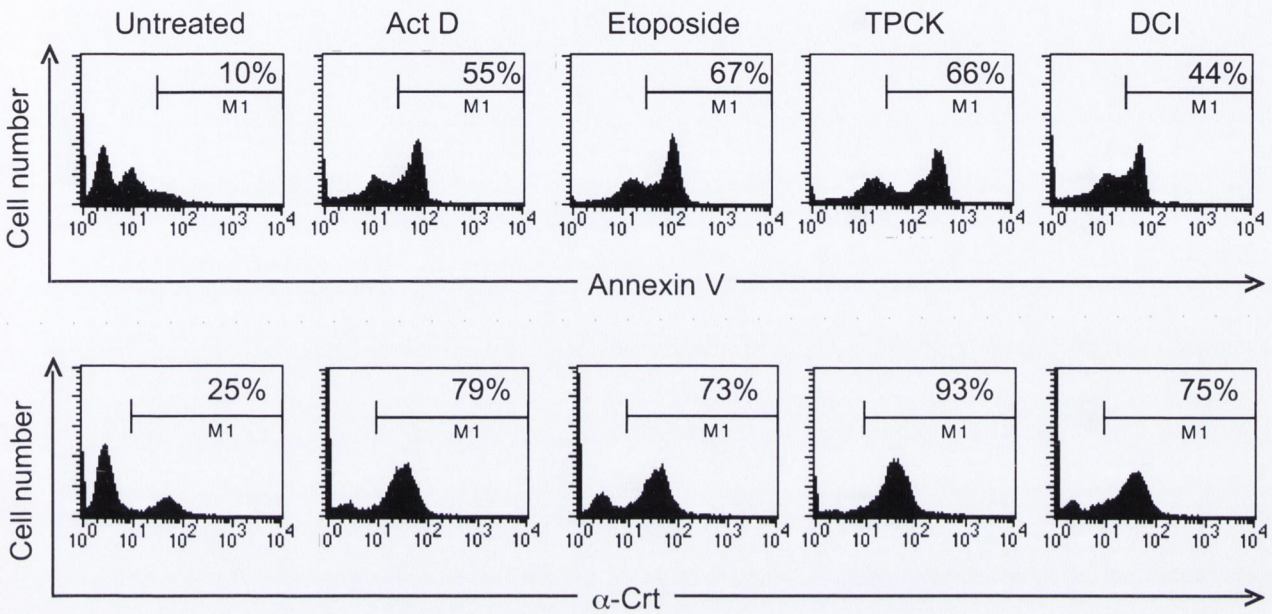

Figure 5.11

Calreticulin is exposed on the surface of apoptotic cells

Calreticulin exposure in cells treated with apoptotic stimuli. CEM cells were treated with 20 μM actinomycin D, 50 μM etoposide, 75 μM TPCK or 100 μM DCI, or left untreated. After 12 hours, cell samples were stained with annexin V or α-calreticulin, followed by flow cytometry. The upper panel represents cells stained with annexin V, and the lower represents cells stained with anti-calreticulin. Percentages of positively-stained cells are indicated on each graph. Results represent at least 3 independent experiments.

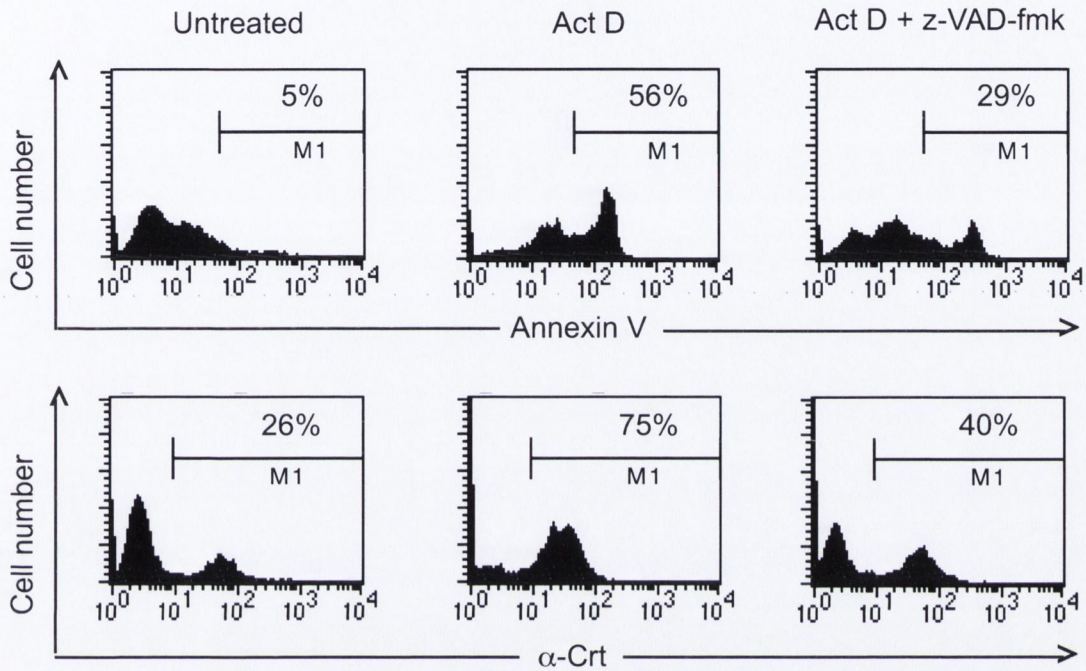

Figure 5.12

z-VAD-fmk blocks the exposure of calreticulin on the surface of cells treated with apoptotic stimuli

The poly-caspase inhibitor z-VAD-fmk prevents calreticulin exposure in cells treated with apoptotic stimuli. CEM cells were treated with 20 μM actinomycin D with or without a 30 minute pre-treatment with 50 μM z-VAD-fmk, or left untreated. After 12 hours, cell samples were stained with annexin V or α-calreticulin, followed by flow cytometry. The upper panel represents cells stained with annexin V, and the lower panel represents cells stained with anti-calreticulin. Percentages of positively-stained cells are indicated on each graph. Results represent at least 3 independent experiments.

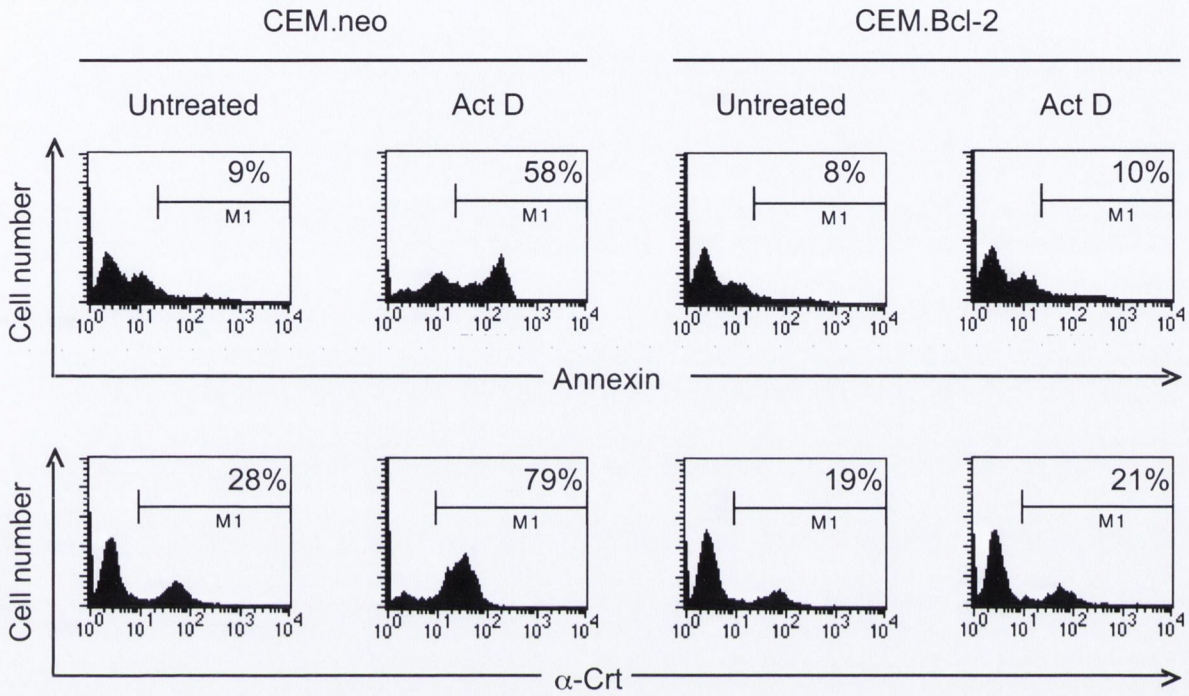

Figure 5.13

Bcl-2 blocks the exposure of calreticulin on the surface of cells treated with apoptotic stimuli

Over-expression of Bcl-2 prevents cell surface exposure of calreticulin in cells treated with actinomycin D. CEM.neo cells or CEM.Bcl-2 cells stably transfected with Bcl-2 were treated with 20 μM actinomycin D, or left untreated. After 12 hours, cell samples were stained with annexin V or α-calreticulin, followed by flow cytometry. The upper panel represents cells stained with annexin V, and the lower panel represents cells stained with anti-calreticulin. Percentages of positively-stained cells are indicated on each graph. Results represent at least 3 independent experiments.

transiently transfected with calreticulin to determine whether an increase in cellular calreticulin could lead to an increase in the amount of calreticulin exposed on the surface of the cell.

HeLa cells were transfected with pcDNA3-calreticulin and pcDNA-FLAG-calreticulin, and with vector and pcDNA3-FLAG-Mfn-2 as controls. 24 hours after transfection, cell lysates were prepared from transfected cells. Lysates were electrophoresed through 12 % SDS-PAGE gels and analysed by Western blotting with both monoclonal and polyclonal α-calreticulin antibodies (Figure 5.14 A). Both antibodies detected a large increase in calreticulin expression over endogenous levels in the transfected conditions. In addition, both antibodies detected an additional higher molecular weight band in lysates from FLAG-calreticulin-transfected cells. This indicated both that cells transfected with pcDNA3-calreticulin constructs were over-expressing calreticulin, and also that both antibodies were able to specifically detect calreticulin protein in a Western blotting context.

Transfected cells were also analysed by immunostaining for cell surface calreticulin. 24 hours after transfection, HeLa cells were either left untreated or treated with 20 μM actinomycin D for 12 hours. Cells were then harvested; floating and loosely-adherent cells were collected by pipette, while cells adhering firmly to the plate were briefly trypsinised. Harvested cells were pelleted followed by immunostaining for surface calreticulin (Figure 5.14 B). In healthy cells not treated with an apoptotic stimulus, there was no difference in levels of cell surface calreticulin between vector-transfected and calreticulin-transfected cells. However, upon treatment with the apoptotic stimulus actinomycin D, there was a small increase in the percentage of calreticulin-transfected cells with calreticulin exposed on their surface compared to vector-transfected cells. In the results shown in Figure 5.15 B, 30 % of calreticulin-transfected cells compared with 26 % of control cells have exposed calreticulin. Although this increase was relatively small, it was very reproducible, with an increase of about 10 % in positively-stained cells in each experiment. This suggests that over-expression of calreticulin is causing an increase in the detection of calreticulin cell-surface exposure by immunostaining, albeit not in proportion with the degree of over-

expression, strengthening our confidence in the previous results obtained using this antibody.

5.3.12 Over-expression of calreticulin leads to a substantial increase in calreticulin surface exposure on treatment with brefeldin A

While these results appeared positive, it was still of concern that the increase in calreticulin expression in calreticulin-transfected cells was not reflected in the degree of increase in calreticulin surface exposure. Calreticulin is largely ER-localized within the cell, and we speculated that the bulk of the over-expressed calreticulin was sequestered within the ER, inaccessible to caspases and therefore unable to translocate to the cell surface. We hypothesized that the use of an ER-stress-inducing apoptotic stimulus might induce an enhanced degree of calreticulin surface exposure by causing disruption of the ER compartment, and increased accessibility of calreticulin to caspases.

To test this, we transiently transfected HeLa cells with pcDNA3-calreticulin or pcDNA3 vector only. 24 hours after transfection, we either left cells untreated or treated them with 4 μg/ ml brefeldin A. The cells were then incubated for a further 36 hours to induce a substantial degree of cell death. At the end of this incubation period, cells were harvested as described by pelleting those floating in the culture medium, and subjecting adherent cells to a brief trypsinisation. These cells were then immunostained for cell surface calreticulin. Stained cells were analysed by flow cytometry (Figure 5.15). As seen previously, there was little difference in surface exposure of calreticulin between untreated vector-transfected or calreticulin-transfected cells. However, upon treatment with brefeldin A, a substantial difference was apparent. The population of positively-stained cells was increased by around 50 % in calreticulin-transfected cells. In the results shown in Figure 5.15, 40 % of brefeldin A-treated calreticulin-transfected cells exhibit surface staining for calreticulin, compared to 26 % of vector-transfected cells. This correlated much better with the degree of calreticulin over-expression seen by Western blotting. Brefeldin A did therefore seem to encourage the release of over-expressed calreticulin from the ER compartment. These results convincingly support the ability of the calreticulin polyclonal antibody used in our analysis to specifically detect calreticulin on the cell surface. It therefore validates our

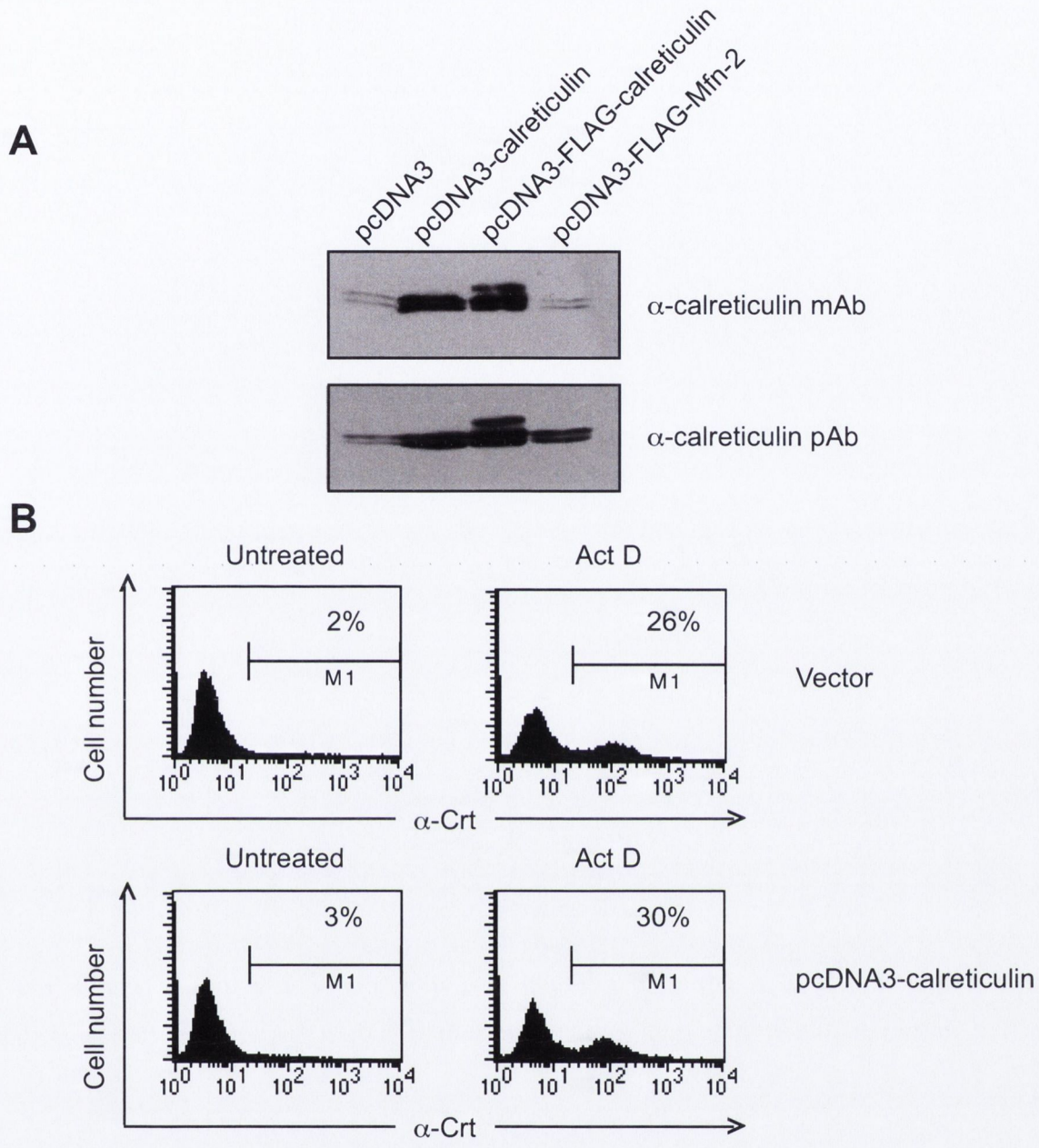

Figure 5.14

Over-expression of calreticulin in HeLa cells leads to a small increase in calreticulin exposure in response to actinomycin D

A) Over-expression of calreticulin confirmed by Western blotting. HeLa cells were transfected with vector plasmid only or with pcDNA3-calreticulin. 24 hours after transfection, cells were lysed and subjected to SDS-PAGE and Western blotting using a monoclonal and a polyclonal antibody directed against calreticulin.

B) Over-expression of calreticulin causes increased cell surface exposure in cells treated with actinomycin D. HeLa cells were transfected as above and, 24 hours after transfection, treated with 20 μM actinomycin D or left untreated. After 12 hours, floating cells were pelleted and adherent cells trypsinised for removal from the plate. Samples were stained with α-calreticulin followed by flow cytometry. The upper panel represent cells transfected with vector only, and the lower cells transfected with pcDNA3-calreticulin. Percentages of positively-stained cells are indicated on each graph. Results represent at least 3 independent experiments.

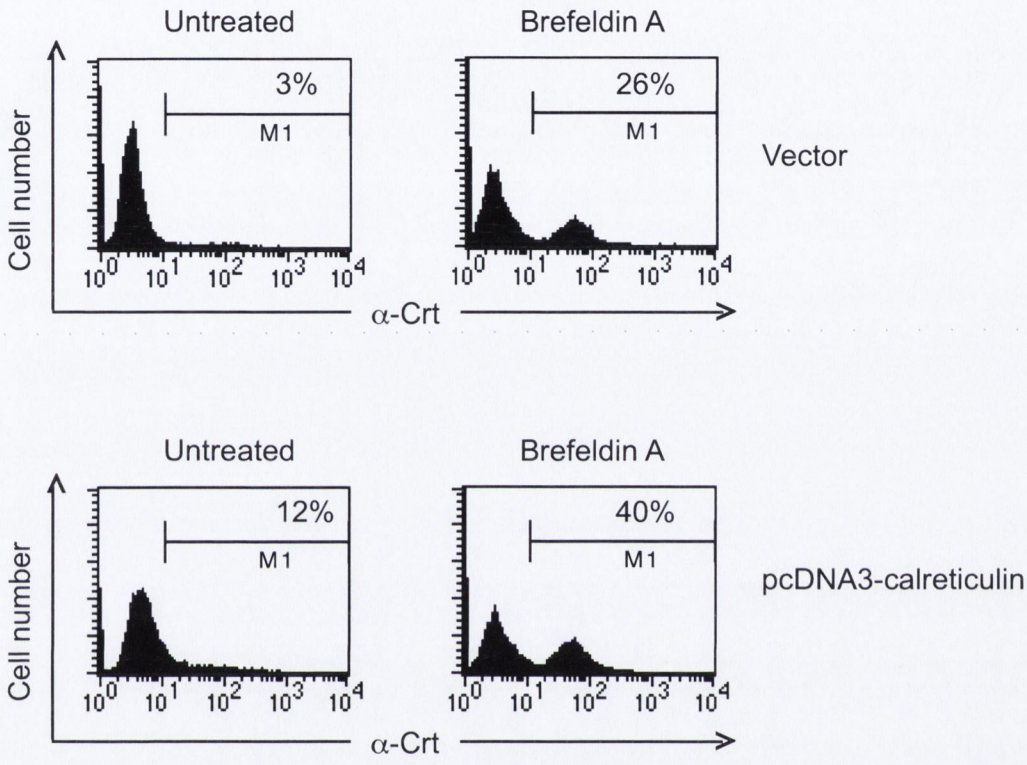

Figure 5.15

Over-expression of calreticulin in HeLa cells leads to substantially increased calreticulin exposure in response to brefeldin A

Over-expression of calreticulin causes increased cell surface exposure of calreticulin in cells treated with brefeldin A. HeLa cells were transfected with vector plasmid only or with pcDNA3-calreticulin. 24 hours after transfection, cells were treated with 4 μg /ml brefeldin A, or left untreated. After 36 hours, floating cells were pelleted and adherent cells trypsinised for removal from the plate. Samples were stained with α-calreticulin, followed by flow cytometry. The upper panel represent cells transfected with vector only, and the lower cells transfected with pcDNA3-calreticulin. Percentages of positively-stained cells are indicated on each graph. Results represent 2 independent experiments.

previous conclusions, that surface exposure of calreticulin is a general feature of apoptosis, and that caspase activity is crucial in mediating this phenomenon.

5.3.13 Caspase-mediated cleavage of calreticulin may lead to its cell surface exposure and role as a ligand for phagocytes

These results support a model outlined in Figure 5.16 for the conserved role of caspase-mediated cleavage of calreticulin in the induction of phagocytosis. Apoptotic signals lead to the activation of caspases. These active caspases are then able to cleave an accessible portion of the total cellular content of calreticulin. This cleavage encourages the translocation of calreticulin to the cell surface, possibly by preventing ER retention and retrieval mechanisms, and allowing calreticulin to associate with proteins trafficking to the cell surface. From its location at the plasma membrane where it is associated with other membrane proteins, it is able to bind to and activate scavenger receptors on the surface of phagocytes, leading to the consumption of the dying cell.

5.4 DISCUSSION

5.4.1 Summary

In this third phase of the study, we aimed to identify functional roles for caspase-mediated cleavage events. We selected three CED-3 substrates for analysis, FTT-2, TBB-2 and CRT-1. Wild-type and cleavage-resistant ORFs were cloned into *C. elegans* expression vectors, to create transgenic nematode lines. However, none of the lines generated showed an overt defect in the progression of apoptosis. We then confirmed that the human homologues of these proteins were also substrates for caspases. Using a human cell system, we investigated the effects of over-expressing FTT-2 and CRT-1 in cells treated with apoptotic stimuli. Again, no alterations in rates or morphology of apoptosis were found. Next, we examined the effects of reducing tubulin expression by RNAi. Reduction in alpha-tubulin levels led to a 20 - 30 % rate of spontaneous cell death, but did not influence susceptibility to apoptotic stimuli. As tubulin cleavage may increase microtubule polymerization rates, we looked at the morphology of microtubules in dying cells, and at the effects of RNAi against alpha-tubulin on nuclear fragmentation and apoptotic body formation. We observed a condensation of microtubules within dying cells; however, reductions in alpha-tubulin expression by RNAi did not affect nuclear or cellular morphology during apoptosis.

Following a report that calreticulin is exposed on the surface of apoptotic cells and acts as a phagocytic ligand (Gardai *et al.*, 2005), we used immunostaining to confirm that calreticulin can be detected on the surface of cells undergoing apoptosis. Moreover, this is a general phenomenon, occurring on treatment with several apoptotic stimuli. We also confirmed that a small proportion of cellular calreticulin is cleaved in cells undergoing apoptosis. We speculated that caspase-mediated cleavage of calreticulin might influence its surface exposure. Indeed, blocking caspase activation through over-expression of Bcl-2 or treatment with the caspase inhibitor z-VAD-fmk largely prevented translocation of calreticulin. Over-expressing calreticulin increased its surface translocation, particularly after treatment with the ER stress agent brefeldin A, confirming that our analyses specifically detected calreticulin exposure. These results suggest a model in which caspases cleave calreticulin, leading to its exposure on the surface of the cell, where it acts as a phagocytic ligand.

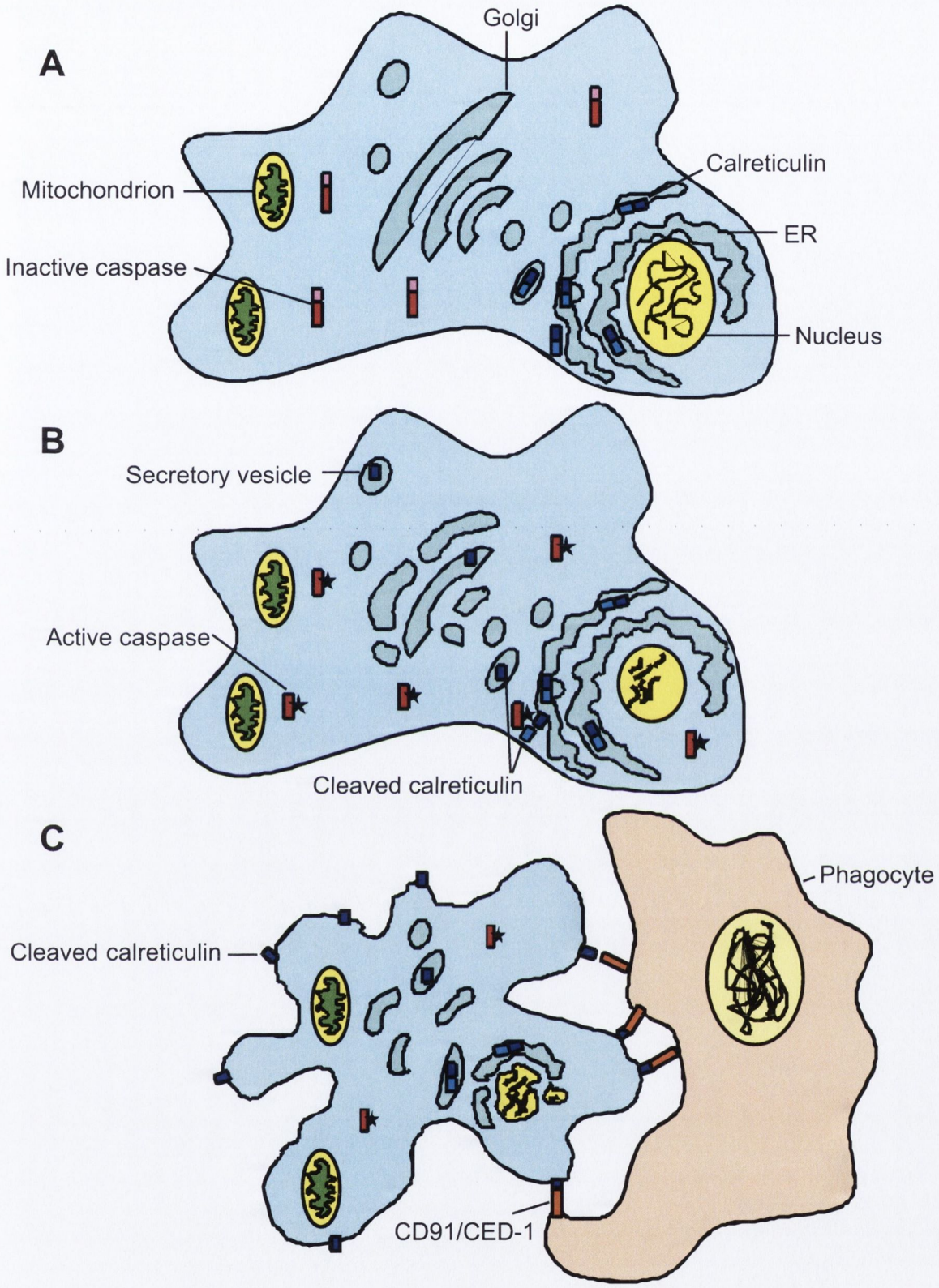

Figure 5.16

Apoptotic cell recognition through caspase-mediated cleavage of calreticulin

Schematic diagram showing how cleavage of calreticulin by caspases might result in apoptotic cell recognition by phagocytes in *C. elegans* and humans. In the healthy cell, calreticulin is largely localised to the ER (A). On activation of caspases, cytosolic calreticulin is cleaved and the N-terminal fragment is able to translocate through the secretory pathway to the plasma membrane (B). This cell surface calreticulin is finally recognised by CD91/CED-1 on phagocytic cells, stimulating phagocytosis of the dying cell (C).

5.4.2 Selection of substrates for analysis

With the identification of 22 substrates for CED-3, what rationale did we use in our selection of FTT-2, TBB-2 and CRT-1 for functional analysis? Firstly, the human homologues of each of these proteins were either known to be caspase substrates, or their CED-3 cleavage sites were conserved. This suggested that they might be conserved caspase substrates, and therefore more likely to be involved in the conserved events of the demolition phase of apoptosis. Each of the proteins had important cellular roles, disruption of which would be likely to affect the dying cells, and from which functional effects of cleavage could be inferred. Each also had previous links with apoptotic processes. These functions, in the context of the insights gained in this work, will be expanded upon in the next few paragraphs.

5.4.3 FTT-2 and the 14-3-3 protein family

FTT-2 and PAR-5 are the *C. elegans* members of a family that, in humans, is represented by at least seven proteins. 14-3-3 proteins act as dimers, and possess phosphopeptide binding sites that allow them to act in signalling cascades involving phosphorylation. On binding to phosphorylated proteins, they often sequester or anchor them at particular cellular locations. They are almost ubiquitously expressed in human cells, and have a range of roles. Many of these roles involve the regulation of the cell cycle and cytoskeletal dynamics, but there have also been published roles for 14-3-3 proteins in survival signalling pathways (Jin *et al.*, 2004; Masters *et al.*, 2002). One example is the binding of the BH3-only protein Bad to 14-3-3 proteins following its phosphorylation by Akt in response to cell survival signals (Zha *et al.*, 1996; Datta *et al.*, 1997; Datta *et al.*, 2000). 14-3-3 proteins also play roles in MAPK pro-survival signalling, in inhibiting ASK-1-mediated pro-apoptotic signalling, and in sequestering c-Abl in the cytosol until receipt of DNA damage signals (Xing *et al.*, 2000; Zhang *et al.*, 1999; Yoshida *et al.*, 2005). In fact, the inhibition of 14-3-3 proteins by peptide inhibitors can lead directly to cell death (Masters *et al.*, 2002). This involvement in survival signalling interested us on identifying FTT-2 as a CED-3 substrate, and led us to examine the cleavage of human 14-3-3 proteins by caspases, and the ability of FTT-2 to modulate apoptosis in human cells.

We found that 14-3-3 beta, epsilon and tau were caspase substrates in human cells. Proteolysis of 14-3-3 sigma and beta has already been documented (Nomura *et al.*, 2003; Widmann *et al.*, 1998). Cleavage of 14-3-3 sigma has been suggested to cause release of bound Bax (Nomura *et al.*, 2003). We found that FTT-2 is cleaved by CED-3 in the C-terminal region. These C-terminal amino acids of 14-3-3 proteins are believed to be highly disorganised, and it has been suggested that this highly acidic domain might occupy the positively-charged ligand-binding site, inhibiting peptide binding (Liu *et al.*, 1995). Indeed, removal of the C-terminal domain has been shown to cause increased binding to protein ligands including Raf-1 and the BH3-only protein Bad, and also binding to non-phosphorylated peptides (Truong *et al*, 2002). This suggested that cleavage of the C-terminus of 14-3-3 proteins by caspases might be able to alter its interactions with substrate proteins, possibly influencing the progression of apoptosis. As 14-3-3 proteins are highly conserved, we hypothesized that expression of FTT-2 would be able to mimic the influences of human 14-3-3 proteins on apoptosis. However, expression of either wild-type or non-cleavable FTT-2 had no effect on the percentage of cells undergoing cell death in response to TNF/ CHX or daunorubicin, activating the extrinsic and intrinsic caspase activation pathways, respectively. This suggested that either 14-3-3 proteins are not involved in downstream apoptotic events, or that *C. elegans* Ftt-2 is not able to functionally replace or alter these interactions in human cells.

Hypothesising that reduction in levels of 14-3-3 proteins might reveal an effect on apoptotic regulation, we used RNAi against several 14-3-3 isoforms in human cells. However, these RNAi constructs failed to reduce expression of their target proteins (data not shown), and we were therefore unable to gain any insights from this experiment. RNAi against FTT-2 expression in *C. elegans* caused a delay in phagocytosis of corpses (Prof. Brent Derry, pers. comm.). We believe that this may be caused by a failure to properly regulate the actin cytoskeleton during phagocytic cell uptake, but this is undergoing further analysis in collaboration with Dr. Derry's laboratory.

5.4.4 Alpha- and beta-tubulin

We identified several cytoskeletal proteins as CED-3 substrates, including the conserved caspase substrates alpha- and beta-tubulin. The execution phase of

apoptosis involves a high degree of cytoskeletal reorganisation, influencing dynamic events such as cell retraction, blebbing, fragmentation, packaging of cell contents, and exposure of signalling molecules, that require dramatic changes in the activity of the cytoskeleton (Moss and Lane, 2006). While the roles of actin and myosin in apoptotic changes have been widely studied, it is only recently that the roles of the tubulin-based microtubule skeleton have begun to be appreciated (Moss and Lane, 2006).

Microtubules are formed from dimers of alpha- and beta-tubulin, arranged head to tail to form protofilaments. They are dynamically unstable, and can extend or contract rapidly on polymerization or depolymerization of the tubulin dimers, a process controlled by GTP hydrolysis and the binding of microtubule-associated proteins (MAPs) (Nogales, 2001; Krebs *et al.*, 2005; Hirokawa, 1994). As well as forming structural elements, microtubules act as "tracks" for motor proteins that transport materials around the cell (Amos, 2000). They play important roles in cell motility and morphogenesis, intra-cellular transport, and chromosome separation during mitosis (Amos, 2000). Proteolysis of tubulin during apoptosis might be expected to disrupt the microtubule cytoskeleton and reduce cell viability. Indeed, our RNAi studies demonstrated that reduction in alpha-tubulin levels causes a 20% - 30% rate of spontaneous cell death. In addition, as previously reported, there was an increase in the number of cells with mitotic figures, suggesting an arrest in mitosis (Adrain *et al.*, 2006). This indicates that tubulin RNAi induces "mitotic catastrophe", in which the failure to complete mitosis activates a checkpoint leading to apoptosis (Martin and Cotter, 1990).

However, our results are in agreement with other recent reports suggesting that microtubules are not simply dismantled during cell death, but are present during the execution phase of apoptosis, with an altered morphology (Adrain *et al.*, 2006; Moss *et al.*, 2006). We found that in dying cells microtubules appear thickened and contracted. Another study has suggested that the interphase microtubule network is disassembled at the beginning of apoptosis, and that microtubules then reform with the contracted morphology that we observed (Moss *et al.*, 2006). Disruption of microtubules by treatment with the microtubule poison nocodazole in this study prevented chromatin accumulation in membrane blebs, cell fragmentation, and the transport of phagocytic signals to blebbing regions.

How might tubulin proteolysis contribute to these functions of the microtubule cytoskeleton during cell death? The acidic C-terminal domain of tubulin is extended in conformation, and accessible to attack by proteases (Nogales *et al.*, 1998; Serrano *et al.*, 1984; Sackett *et al.*, 1984). In *C. elegans*, the C-terminus of TBB-2 is the preferential substrate of the MEI-1/ MEI-2 katanin microtubule-severing complex, which regulates meiotic spindle microtubule function through tubulin cleavage (Lu *et al.*, 2004). The human alpha-tubulin C-terminus is cleaved by both the serine protease granzyme B and caspases at the same site, $VGVD^{438}$ (Adrain *et al.*, 2006). Experiments with the protease subtilisin have established that the tubulin C-terminus is critical in determining polymerization efficiency (Sackett *et al*, 1984). Subtilisin removes a small ~2 kDa region from the acidic C-terminus of alpha and beta tubulin. Cleaved tubulin can hydrolyse GTP and assemble into protofilaments, but the concentration required for polymerization is reduced 50-fold and the resulting microtubules are abnormal, forming sheets and twisted filaments (Sackett *et al*, 1984). Cleavage of tubulin *in vitro* by granzyme B also increases the rate of microtubule polymerization (Adrain *et al.*, 2006).

In addition, removal of the tubulin C-terminus disrupts many protein interaction sites. The MAPs Tau and MAP2 are unable to bind to tubulin without its C-terminus, and the beta-tubulin C-terminus is essential for the KinI depolymerising protein to mediate depolymerization and protofilament curling (Marya *et al.*, 1994; Paschal *et al.*, 1989; Moores *et al.*, 2002). The motor protein dynein also requires this region for interaction, and processivity of the kinesin motor protein is greatly reduced upon C-terminus removal (Paschal *et al.*, 1989). Altered tubulin polymerization dynamics caused directly by proteolysis, or indirectly through effects on MAP binding, could therefore play roles in chromatin dispersal and apoptotic body formation, while transport of materials such as phagocytic ligands to the periphery could result from altered motor protein activity.

Although in our study the loss of tubulin did not result in any apparent defects in cell fragmentation or chromatin dispersal, there are several possible reasons for this discrepancy between our results and those of Moss *et al.*. Different cell types were used in the two studies, which may have differential requirements for tubulin; our analysis used HeLa cells while most experiments conducted by Moss *et al.*

used A431 cells, which fragment to a greater degree (Moss *et al.*, 2006). Also, the latter study used confocal microscopy while we used UV, possibly allowing the observation of subtle morphological differences that we were unable to detect. It remains unclear what roles the microtubule cytoskeleton plays in apoptosis.

5.4.5 Calreticulin

Calreticulin, the third substrate that we analysed, is a multi-functional protein largely resident in the ER compartment (Michalak *et al.*, 1999). The structure of calreticulin includes a globular N-terminal domain, a central P high-affinity/low-capacity calcium-binding domain, and a C-terminal low-affinity/ high capacity calcium-binding domain. In the ER it acts as a buffer for cellular calcium, and plays a role in regulating calcium signalling processes. Calreticulin also acts as a chaperone for proteins that fold within the ER, having a lectin-like activity within its N and P domains, which act together as a functional protein-folding unit (Saito *et al.*, 1999). As well as its ability to chaperone nascent glycoproteins, it is now known that calreticulin has a polypeptide-binding capacity, and plays an important role in the loading of peptides onto MHC class I heavy chain-β_2M dimers in the ER (Sadasivan *et al.*, 1996).

In *C. elegans*, deletion mutants have demonstrated that calreticulin is required for fertility and stress responses. It also has a specific role to play in cells undergoing necrotic cell death. In a screen for mutations able to suppress necrotic cell death, multiple copies of calreticulin were identified (Xu *et al.*, 2001). Necrotic cell death induced by hyper-activated degenerin receptors is dependent upon increased levels of cytosolic calcium, and it is likely that the calcium allowed into cells through activated degenerin receptors triggers calcium-induced calcium release from the ER, and that calreticulin is required to maintain a sufficient store of calcium within this compartment.

We were interested in the identification of calreticulin as a caspase substrate, as it has been reported to have a range of functions in cell death. As well as its role in necrosis in *C. elegans*, there are numerous reports implicating calreticulin in various aspects of apoptosis, some of which present conflicting evidence. Studies have suggested that the presence of calreticulin protects cells from rapid increases in cellular Ca^{2+} and damage-induced apoptosis, while others believe

that calreticulin has a death-promoting activity (Liu *et al.*, 1994; Liu *et al.*, 1997; Nakamura *et al.*, 2000; Kageyama *et al.*, 2002). Calreticulin is also a constituent of the cytolytic granules contained in cytotoxic lymphocytes, and is released into target cells with granzymes (Dupuis *et al.*, 1993). It has been suggested that the role of calreticulin in this case is to regulate the activity of perforin, but an active role in the killing of cells has not necessarily been excluded (Dupuis *et al.*, 1993; Fraser *et al.*, 2000). It is clear that there are apoptotic defects in mice deficient in calreticulin; these mice die before birth exhibiting decreased cardiac cell mass, caused by increased apoptosis of cardiomyocytes, while 16% of embryos had defects in neural tube closure (Rauch *et al.*, 2000). However, it is not known whether these defects are caused by a direct role of calreticulin in apoptosis, or are a secondary result of loss of other calreticulin functions; fibroblasts isolated from these calreticulin-deficient mice show no defects in response to a range of apoptotic stimuli (Rauch *et al.*, 2000).

The peptide-binding activity of calreticulin may have an immunological function in cell death. Calreticulin is able to bind to cellular peptides and elicit an immune response through presenting these peptides to antigen-presenting cells (Basu and Srivastava, 1999; Nair *et al.*, 1999). The calreticulin-peptide complex binds to receptors, including but possibly not exclusively the scavenger receptor CD91, on the surface of APCs (Basu *et al.*, 2001; Walters and Berwin, 2005). These APCs re-present the bound peptides on MHC class I molecules to elicit an antigen-specific CTL response. As well as having this strong adjuvant activity, calreticulin is able to deliver a peptide-independent general maturation signal to cells of the immune system, although it is not clear which receptors are involved in this case (Basu *et al.*, 2000). During necrosis, release of calreticulin and other heat-shock proteins with associated peptides from the dead cell is therefore able to induce an immune response, through the maturation of immune cells, and the presentation of antigens from the damaged tissue to generate a specific antigen-directed immune response (Basu *et al.*, 2000). This release of calreticulin with bound peptides does not occur from cells undergoing apoptosis (Basu *et al.*, 2000). The presence of calreticulin in the extracellular milieu, bound to peptides, might therefore act as a danger signal, alerting the immune system to a potentially pathogenic situation. (Matzinger, 1994).

We hypothesised that cleavage of calreticulin during apoptosis might have one of several activities. It might promote cell death, by removing a protective activity or activating a death-promoting activity; it might prevent the diversion of cells into necrosis by disabling a necrotic death pathway; or it may abolish calreticulin's adjuvant or immunostimulatory activities, preventing the delivery of peptides to and activation of cells of the immune system following programmed cell death. We tested the first hypothesis by transfecting wild-type and cleavage-resistant calreticulin into human cells. However, other than a very mild toxicity, there was no indication in this assay of an important role for calreticulin in triggering or potentiating, or protecting from, apoptosis. There was also no indication in either the human cell assay or in transgenic nematodes (data not shown) that the presence of cleavage-resistant calreticulin led to an increase in necrotic characteristics during cell death – and it seemed unlikely that caspases would be able to gain access to this compartment to cleave calreticulin and prevent the release of calcium.

It was at this stage that a report was published suggesting that calreticulin is exposed on the surface of apoptotic cells to act as a ligand for phagocytic cells, inducing macropinocytosis and phagocytosis of dead cells through ligation of LRP/CD91 (Gardai *et al.*, 2005). A cell surface localisation for calreticulin is not a new concept, and has been described in many different cell types and contexts (White *et al.*, 1995; Arosa *et al.*, 1999; Ghiran *et al.*, 2003; Vance *et al.*, 2005). As calreticulin lacks a transmembrane domain it appears to bind *in cis* to several different cell surface receptors including CD91, CD59, CD69 and MHC class I (White *et al.*, 1995; Arosa *et al.*, 1999; Ghiran *et al.*, 2003; Vance *et al.*, 2005). The connection between calreticulin and phagocytosis is also not new; calreticulin has previously been implicated as part of a co-receptor complex with CD91 on phagocytes, able to bind to lectin- and collectin-like molecules such as C1q that themselves bind to the surface of apoptotic cells. (Ogden *et al.*, 2001; Vandivier *et al.*, 2002). However, the report by Gardai *et al.* for the first time suggested that calreticulin might be specifically exposed on the surface of apoptotic cells rather than phagocytes, and that instead of binding to CD91 to act as a co-receptor, it is able to act *in trans* as a ligand for the receptor.

As calreticulin is a substrate for caspases, and is exposed specifically in apoptotic cells, this immediately suggested to us that the two phenomena might be linked. Our initial exploration of the cleavage of calreticulin in apoptotic cells demonstrated that very little of the cell's complement of calreticulin undergoes cleavage by caspases. Although this was at first disconcerting, in the light of calreticulin's localisation it does make sense. Calreticulin is largely localised to the ER, where it is likely to remain inaccessible to caspases. However, there is a circulating portion of calreticulin that is located, not within the ER, but in other cellular locations, including calreticulin that is trafficked to the cell surface. This small fraction of calreticulin may be available for targeting by caspases. This degree of cleavage is also consistent with calreticulin's activation as a phagocytic ligand. If the aim of cleavage is to inactivate a particular function of the target protein, it might be important for the entire cellular complement of that protein to become proteolysed. However, if a protein is to be activated to perform a specific role, it might only be necessary for a small proportion of the cell's complement of that protein to become cleaved and perform that activated function.

We then established that caspase activity is indeed required for the exposure of calreticulin on the cell surface. How might calreticulin cleavage cause it to act as a phagocytic ligand? Calreticulin is maintained in the ER through two mechanisms, retrieval from post-ER compartments through recognition of its C-terminal KDEL motif, and retention within the ER through its C-terminal domain (Sonnichsen *et al.*, 1994). Studies have shown that even when highly over-expressed, to 50-100 times endogenous levels, calreticulin is virtually all maintained in the ER rather than following the secretory pathway, confirming the results we obtained in our over-expression analyses (Sonnichsen *et al.*, 1994). However, removal of the C-terminal domain or the KDEL signal leads to a 18% or a 29% release of calreticulin, respectively. Cleavage of calreticulin by caspases to remove both the KDEL signal and the C-terminal domain could mimic this effect, leading to calreticulin exposure on the cell surface. Notably, a monoclonal antibody recognising the C-terminus of calreticulin did not detect increased levels of surface calreticulin upon induction of apoptosis (data not shown), implying that this C-terminal region may be removed. In addition, the prominent calreticulin cleavage product detected on 2D gels represented the N-terminal portion of the protein.

Mutant calreticulin lacking its C-terminal residues 342-401 has an enhanced ability to bind to peptides, and is able to bind to proteins such as peptide-deficient HLA-A2 that can only be bound by full-length calreticulin under elevated temperature conditions (Rizvi *et al.*, 2004). It could therefore be that calreticulin with its C-terminus removed through cleavage by caspases undergoes a structural change enabling it to bind more tightly to proteins that are trafficking to the cell surface, or to allow it to associate with surface proteins and be retained on the cell surface. Calreticulin has previously been observed on the cell surface associated with LRP/CD91, MHC class I, and CD59 (Orr *et al.*, 2003; Arosa *et al.*, 1999; Ghiran *et al.*, 2003). A mutant calreticulin lacking the C-terminal domain also interacts more strongly with CFTR, and is translocated with it to the cell exterior (Harada *et al.*, 2006). An N-terminal fragment of calreticulin has been detected at the cell surface in association with CD69, and the domain of cell-surface calreticulin engaged in binding to thrombospondin is known to be at the N-terminus (Vance *et al.*, 2005; Goiciechea *et al.*, 2002). The binding of cleaved calreticulin to specific cell surface proteins could explain the patchy distribution of calreticulin on the surface of apoptotic cells seen by Gardai *et al.* This up-regulation of calreticulin on the cell surface might therefore reach a threshold required to activate phagocytosis. There is also the possibility that cleaved calreticulin might be better able to bind and activate the LRP/CD91 receptor.

Calreticulin might therefore be the first example of a phagocytic ligand directly activated by caspases. It may also be a phagocytic signal conserved between worms and man, and in support of this, the *C. elegans* phagocytic receptor CED-1, with no known ligand, is homologous to CD91 and other scavenger receptors. However, while we now know that the phenomenon of calreticulin exposure is certainly caspase-dependent, a direct link between caspase-mediated calreticulin cleavage and cell surface exposure is yet to be proven. It is hoped that future studies will solidify this hypothesis by the expression of wild-type and cleavage-resistant FLAG-tagged CRT-1 in cells, to determine whether lack of calreticulin cleavage abolishes its ability to undergo cell surface exposure.

5.4.6 Transgenic *C. elegans* lines

Given that tubulin and calreticulin seem to have important roles during apoptosis, why were there no visible apoptotic phenotypes in the transgenic nematode lines

expressing these cleavage-resistant substrates? In the case of tubulin, the wild-type protein is expressed to such high degrees that over-expression of cleavage-resistant tubulin is unlikely to be incorporated into the cytosol, and therefore is unlikely to have an effect on apoptotic events. Similarly, despite the presence of cleavage-resistant calreticulin, there will still be sufficient wild-type endogenous protein present to undergo cleavage and translocate to the cell surface. Expression of the cleavage-resistant proteins in null-mutant backgrounds might be more useful in producing cell death phenotypes.

However, it is also possible that there is sufficient redundancy within the events of the execution phase to render even these transgenic nematodes almost phenotypically normal. Our analysis has identified a wide range of caspase substrates, and it is likely that these are only the tip of the iceberg. In the case of a protein such as tubulin, where both alpha-and beta-tubulin are cleaved, and several other isoforms of each are present, it could be that, in order to see an effect of cleavage-resistant mutants on the tubulin cytoskeleton, all of these proteins would have to be replaced by non-cleavable mutants. In the case of calreticulin, other proteins may be able to bind redundantly to the same receptor, or different receptors and/or pathways may act redundantly, making it necessary to mutate several proteins to see an effect on phagocytosis. A lesson that we have learned from these studies is that the complexity of the apoptotic execution phase, and the sheer numbers of proteins cleaved by caspases even in an organism as simple as the worm, may make it extremely hard both to identify substrates that are important in apoptosis, and to study those substrates *in vivo*. Because of these considerations, it may be that the functional effects of cleavage of most caspase substrates will remain a mystery.

CHAPTER VI

Discussion

6.1 SUMMARY

The *C. elegans* caspase CED-3 is essential for the execution of all cell deaths in the nematode, and has played an important role in the study of programmed cell death. However, events downstream of CED-3 activation in *C. elegans* are very poorly understood, and virtually no substrates for this enzyme have been identified. Knowledge of what these substrates are, and an understanding of their role in the events that occur downstream of CED-3 activation, could help us to understand how cell death is regulated in the nematode, and could also enable us to identify caspase substrates that are conserved between species and play conserved roles during cell death.

The overall aim of this study was to gain a better understanding of how CED-3 coordinates downstream events in apoptosis, by identifying its substrates through a proteomic screening method, and by exploring the consequences of these proteolytic events. In order to do this, we first generated recombinant CED-3 for use in a proteomic substrate screen, and explored its ability to act in a specific and caspase-like fashion. In characterizing the activity of CED-3, we found it to possess a substrate specificity similar to but more promiscuous than human caspase-3, suggesting that the two enzymes are closely related, but also indicating how they are able to play different roles during the cell death process.

The data in Chapter IV show that this recombinant CED-3, when added to *C. elegans* extracts, is able to cleave a range of cellular substrates. CED-3 is able to cleave about 3 % of the worm proteome, compared to about 5 % of the human proteome cleaved by human caspases, suggesting that it has a broad activity but that the smaller proportion of proteins cleaved may contain fewer "innocent bystander" substrates. The 22 CED-3 substrate proteins identified encompass a range of functions, suggesting that CED-3 affects a wide range of cellular activities to mediate the downstream events of cell death. We also identified several homologues of known human caspase substrates, suggesting that caspase substrates may be conserved between species and that our identification of CED-3 substrates may shed light on which substrates of human caspases are important during apoptosis. We were also able to demonstrate that several of the CED-3 substrates can be cleaved by CED-3 *in vitro*, and identified their CED-3 cleavage sites, confirming that we have found genuine CED-3 substrates.

We also explored the functional effects of CED-3-mediated substrate cleavage. The data presented in Chapter V illustrates the difficulties inherent in studying functional roles of CED-3 substrates, due at least in part to the large numbers of substrates likely to be involved in each apoptotic event, as we were unable to identify any effect of the expression of non-cleavable substrates on cell death in *C. elegans*. We were also unable to detect any effect of the expression of FTT-2 or CRT-1, or the knockdown of alpha-tubulin, on apoptosis in human cells.

However, upon investigating the possible role of calreticulin in cell death, we were able to confirm reports that it is exposed on the surface of cells during apoptosis (Gardai *et al.*, 2005). We then showed that this event is caspase-dependent, and we propose a model whereby the caspase-mediated cleavage of calreticulin is able to cause its translocation to the cell surface, where it can act as a ligand for phagocytes.

6.2 CONCLUSIONS OF CHAPTER III

During the first phase of the project, we successfully purified large amounts of recombinant CED-3 protease, circumventing problems with protein insolubility and low levels of expression in several systems. We were then able to conclude that our recombinant CED-3 has specific caspase activity that is consistent with earlier reports (Thornberry *et al.*, 1997; Xue and Horvitz, 1995; Xue *et al.*, 1996; Xue and Horvitz, 1997). This production of CED-3 enzyme enabled us to conduct a proteomic substrate screen as outlined in Chapter IV, and it also enabled us to draw conclusions about the activity of the CED-3 enzyme, and how it is related to members of the human caspase family.

The substrate specificity of CED-3 is clearly very similar to that of human caspase-3, reflecting their relationship as primary executioner in each system. However, CED-3 is certainly more promiscuous, showing a high degree of activity against LEHD and IETD peptide sequences. This is consistent with its role as the only essential caspase in *C. elegans*, able both to auto-activate and to cleave all necessary cellular substrates.

These observations led us to ask why the functions of CED-3 have been divided into several specialised caspases in human cells. The consequences of inhibiting cell death are more profound in human cells than in those of *C. elegans*, as the phenotypes of CED-3 and caspase-3 null mutants show, leading potentially to a need for greater redundancy in caspase action in human cells (Ellis and Horvitz, 1986; Kuida *et al.*, 1996; Woo *et al.*, 1998; Lakhani *et al.*, 2006). In addition, the existence of several executioner caspases may enable a greater range of substrates to be cleaved in human cells, allowing the regulation of the more complex aspects of apoptosis in the human system, such as its interactions with the immune system.

This phase of the project has therefore achieved its aims in helping us to gain insights into the regulation of cell death by caspases in both *C. elegans* and human cells. The generation of this enzyme also enabled us to address our next aim, to identify the substrates of CED-3 through proteomic screening.

6.3 CONCLUSIONS OF CHAPTER IV

It is a true anomaly that, despite being the first caspase family member to be linked to the process of cell death, virtually no substrates for CED-3 have been identified to this point, and we have almost no idea how this protease is able to regulate downstream events in programmed cell death. In the second phase of this work, we used recombinant CED-3 and soluble protein extracts from populations of *C. elegans* to identify substrates of CED-3 using 2D electrophoresis and mass spectrometry. We identified 22 novel protein substrates of CED-3 using these techniques. Several of these proteins were homologues of known human caspase substrates, validating the ability of our screen to identify true caspase substrates, and suggesting that important caspase substrates may be conserved through evolution.

We were able to compare the percentage of the proteome cleaved by caspases in humans and *C. elegans*, finding that while human caspases appear to catalyse the proteolysis of around 5 % of the proteome, CED-3 is able to cleave around 3 %. This is in keeping with the existence of several apoptotic human caspases compared to the one acting in *C. elegans*; however, it is also consistent with the promiscuity of CED-3, enabling it to cleave a relatively high proportion of the proteome despite acting alone. It also validates our rationale in conducting a screen for CED-3 substrates, as we initially hypothesized that CED-3 might cleave a smaller proportion of the proteome than human caspases, and that this would reduce the number of functionless "bystander" cleavage events occurring.

The substrates identified encompass a wide range of cellular roles, suggesting that CED-3 is able to target multiple cellular functions to kill cells. Several cytoskeletal proteins are proteolysed, reflecting the important roles played by the cytoskeleton in mediating apoptotic phenomena such as membrane blebbing and apoptotic body formation. These cytoskeletal proteins include the known caspase substrates actin, myosin light chain, and tubulin (Adrain *et al.*, 2006; Gerner *et al.*, 2000; Mashima *et al.*, 1997; Moretti *et al.*, 2002). We also identified substrates involved in ATP synthesis, known to shut down during apoptosis, potentially influencing phosphatidylserine externalisation and loss of plasma membrane integrity; and substrates involved in metabolic processes, possibly ensuring the

loss of cell viability. Four chaperone-type proteins were found to be cleaved, potentially disabling the cells ability to undergo repair processes. One of these chaperones, the ER-localized protein calreticulin, also has several reported effects on cell death (Liu *et al.*, 1994; Liu *et al.*, 1997; Nakamura *et al.*, 2000; Kageyama *et al.*, 2002; Xu *et al.*, 2001; Basu *et al.*, 2000;Gardai *et al.*, 2005). Two aspartic protease were identified as substrates, raising the possibility of the existence of a proteolytic activation cascade in *C. elegans*, or the disablement of necrotic pathways. Two proteins involved in cell signalling were identified, including a 14-3-3 protein, a homologue of known cell death and cytoskeleton regulators, and human caspase substrates (Masters *et al.*, 2002; Zha *et al.*, 1996; Datta *et al.*, 1997; Datta *et al.*, 2000; Jin *et al.*, 2004; Widmann *et al.*, 1998). And finally, two proteins involved in DNA and protein synthesis were identified, suggesting that CED-3 may also act to shut down protein synthesis and alter chromatin structure.

We then validated the cleavage of several substrates by CED-3 *in vitro*, and identified CED-3 cleavage sites in three substrates. We can therefore be confident that the data presented here represents proteins that can genuinely be cleaved by the CED-3 protease. The identification of CED-3 target sites has also suggested that the DXXD specificity suggested by peptide substrates holds true in a protein context. CED-3 is relatively promiscuous at other residues within the tetrapeptide consensus, but has an extended specificity for a small amino acid residue at the P1' position.

This phase of the project therefore achieved its aims in identifying a novel panel of CED-3 substrates, including a range of different protein classes. These proteins represent a blueprint for CED-3-mediated killing, and further studies into these substrates can now determine their ability to influence events in cell death. They can also be used to identify those substrates whose cleavage has been conserved through evolution, and which are therefore more likely to play important roles during apoptosis.

6.4 CONCLUSIONS OF CHAPTER V

We next aimed to identify functional roles for CED-3-mediated cleavage events, to gain a more detailed insight into the way in which CED-3 mediates downstream events during apoptosis. Our failure to identify any cell death phenotype in transgenic nematodes expressing cleavage-resistant CRT-1 and TBB-2 emphasises the difficulty inherent in studying downstream elements of cell death. With many substrates undergoing caspase-mediated cleavage, the phenotype engendered by the mutation of any one substrate is likely to be subtle. It is also likely that redundancy among substrates makes the observation of a phenotype upon mutation of just one substrate difficult to observe. It is possible too that in the case of abundant substrates such as TBB-2 and CRT-1, there is sufficient endogenous protein available for cleavage by caspases to mediate cleavage-induced phenotypes despite the presence of a cleavage-resistant mutant.

We were able to establish that all three of our selected substrates, FTT-2, TBB-2 and CRT-1 are conserved caspase substrates, their homologues undergoing cleavage mediated by human caspases. Using over-expression and RNAi analyses in human cells, we were unable to identify functional roles for the cleavage of either FTT-2 or TBB-2. These substrates await more detailed analysis, and again illustrate the difficulty of identifying an effect of a single caspase substrate on apoptosis.

However, we were able to identify a potential role for the cleavage of calreticulin by caspases. Our results confirm a recent report that calreticulin translocates to the cell surface during apoptosis, where it can act as a ligand for CD91/LRP on phagocytes (Gardai *et al.*, 2005). We were also able to show that this translocation can be blocked by over-expression of the anti-apoptotic molecule Bcl-2, or treatment with the caspase inhibitor z-VAD-fmk, and that it is therefore caspase-dependent. We have proposed a model whereby the cleavage of calreticulin encourages its translocation to the cell surface, by the removal of ER retention or recovery signals that allow it to pass through the secretory pathway. Its enhanced ability to bind to proteins trafficking to the cell surface by the removal of its C-terminus may also aid its progression to the cell exterior. From the surface

it is then able to bind to CD91/LRP in humans, or possibly to its homologue CED-1 in worms, an interaction that might be enhanced by its cleavage.

We have still to confirm that cleavage of calreticulin is directly responsible for its cell surface relocalisation. To do this, we are involved in a collaborative effort to over-express FLAG-tagged wild-type and cleavage-resistant *C. elegans* CRT-1 in cells and investigate the ability of cleavage-resistant calreticulin to undergo translocation to the surface of these dying cells. However, we have made substantial progress in establishing the connection between cleavage of a protein by caspases and its role in a downstream apoptotic event, something that has rarely been done. This final chapter of our study has therefore been successful in achieving a functional understanding of a caspase cleavage event.

APPENDICES

APPENDIX I

Table A.1 Potential CED-3 substrate identifications

Protein name	Accession no. (NCBI)	Protein function	MS coverage	P
Tropomyosin	gi: 32563577	Cytoskeletal	61.0%	
Methyltetrahydrofolate reductase	gi: 25147441	Metabolism	13.0%	
Alcohol dehydrogenase	gi: 17562582	Metabolism	11.0%	
Bifunctional glyoxylate cycle protein	gi: 17561814	Metabolism	10.0%	
Phopsphoenolpyruvate carboxykinase	gi: 17508605	Metabolism	17.0%	
Enolase	gi: 17536383	Metabolism	58.0%	
Phosphomannomutase	gi: 38422344	Metabolism	37.0%	
Phosphoglycerate dehydrogenase	gi: 17532191	Metabolism	33.0%	
Protein disulfide isomerase-related P5	gi: 17549970	Chaperone	30.0%	
Protein disulfide isomerase 2	gi: 32566189	Chaperone	15.0%	
DAF-21 heat shock protein	gi: 17559162	Chaperone	13.0%	
Heat shock protein 1	gi: 17541098	Chaperone	18.0%	
Heat shock protein 3	gi: 17568549	Chaperone	30.0%	
Heat shock protein 4	gi: 17534771	Chaperone	18.0%	
Putative ER membrane protein	gi: 17542572	Putative	25.0%	
Putative secreted/extracellular protein	gi: 17534537	Putative	31.0%	
Serine protease precursor	gi: 32564813	Proteolysis	31.0%	
Guanine nucleotide-binding protein-like	gi: 17541222	Signalling	47.0%	
TCTP-like	gi: 17506817	Signalling	50.0%	
Nucleoside diphosphate kinase	gi: 17506807	DNA synthesis	41.0%	
Ribosomal protein, acidic	gi: 17506815	Protein synthesis	27.0%	
Translation elongation factor 1	gi: 17553634	Protein synthesis	46.0%	
eIF4A	gi: 17553942	Protein synthesis	28.0%	
eIF5A-1	gi: 17554954	Protein synthesis	26.0%	

APPENDIX II

Table A.2 Constructs generated by the author for use in this study

Plasmid name	Vector	Insertion sites	Primer numbers
pET15b-Ced-$3^{221-503}$	pET15b	NdeI/ Bam HI	1, 2
pET15b-Ced-$3^{221-374}$	pET15b	NdeI/ Bam HI	1, 3
pET15b-Ced-$3^{375-503}$	pET15b	NdeI/ Bam HI	4, 2
pcDNA3- Ced-3^{FL}-His	pcDNA3	Bam HI/ Xba I	5, 6
pcDNA3- His-Ced-$3^{221-503}$	pcDNA3	Bam HI/ Xba I	7, 8
pGEX4TK2-Ced-$3^{221-503}$	pGEX4TK2	Bam HI/ Sma I	9, 10
pAAV-p35	pAAV	Bam HI / Xho I	11, 12
pET45b-Ftt-2	pET45b	Kpn I / Xho I	13, 14
pcDNA3-Ftt-2	pcDNA3	Kpn I/ Xho I	15, 14
pcDNA3-Ftt-2^{D240E}	pcDNA3	Kpn I/ Xho I	15, 14
pcDNA3-Ftt-2^{1-240}	pcDNA3	Kpn I/ Xho I	15, 16
pET45b- Crt-1	pET45b	Kpn I/ Hind III	17, 18
pcDNA3- Crt-1	pcDNA3	Kpn I/ Eco RV	19, 20
pcDNA3- Crt-1 $^{D253E/D225E/D182E}$	pcDNA3	Kpn I/ Eco RV	19, 20
pcDNA3- FLAG-Crt-1	pcDNA3	Kpn I/ Eco RV	21, 20
pcDNA3- FLAG-Crt-1 $^{D253E/D225E/D182E}$	pcDNA3	Kpn I/ Eco RV	21, 20
pET45b-Tbb-2	pET45b	Kpn I/ Xho I	22, 23
pET21a-Asp-1	pET21a	Eco RI/ Xho I	24, 25
pET45b-Par-5	pET45b	Kpn I/ Xho I	26, 27
pPD49_78-Ftt-2	pPD49_78	Bam HI/ Kpn I	28, 29
pPD49_83-Ftt-2	pPD49_83	Bam HI/ Kpn I	28, 29
pPD49_78-Ftt-2^{D240E}	pPD49_78	Bam HI/ Kpn I	28, 29
pPD49_83-Ftt-2^{D240E}	pPD49_83	Bam HI/ Kpn I	28, 29
pPD49_78-Tbb-2	pPD49_78	Kpn I / Eco RV	22, 30
pPD49_83-Tbb-2	pPD49_83	Kpn I / Eco RV	22, 30
pPD49_78-Tbb-$2^{D435E/D417E/D404E}$	pPD49_78	Kpn I / Eco RV	22, 30
pPD49_83-Tbb-$2^{D435E/D417E/D404E}$	pPD49_83	Kpn I / Eco RV	22, 30
pPD49_78-Crt-1	pPD49_78	Kpn I/ Eco RV	17, 20
pPD49_83-Crt-1	pPD49_83	Kpn I/ Eco RV	17, 20
pPD49_78-Crt-1 $^{D253E/D225E/D182E}$	pPD49_78	Kpn I/ Eco RV	17, 20

pPD49_83-Crt-1 $^{D253E/D225E/D182E}$	pPD49_83	Kpn I/ Eco RV	17, 20
pcDNA3-Calreticulin	pcDNA3	Eco RI/ Xho I	31, 32
pcDNA3-FLAG-Calreticulin	pcDNA3	Eco RI/ Xho I	33, 32

APPENDIX III

Table A.3 Primers used by the author for generation of constructs used in this study

	Primer name	Primer sequence
1	CED-3_221-503MetF	5'-CGA CAT ATG GAT GCA CCA ACC ATA AGC-3'
2	CED-3_221-503StopR	5'-GTG GGA TCC TTA GAC GGC AGA GTT TCG-3'
3	CED-3_221-374StopR	5'-ACA GGA TCC GTC GAC AGA ATC CAA GAC-3'
4	CED-3_375-503MetF	5'-GTG CAT ATG GGA GTT CCT GCA TTT CTT CG-3'
5	CED-3_FL_His_F	5'-AGA GGA TCC GCC ATG ATG CGT CAA GAT AG-3'
6	CED-3_FL_His_R	5'-GGA TCT AGA TTA ATG GTG ATG GTG ATG ATG GAC GGC AGA GTT TCG-3'
7	His_CED-3_221-503_F	5'-AGA GGA TCC GCC ATG CAT CAT CAC CAT CAC CAT GAT GCA CCA ACC ATA AGC-3'
8	His_CED-3_221-503_R	5'-GGA TCT AGA TTA GAC GGC AGA GTT TCG-3'
9	GST_CED-3_MetF	5'-AGA GGA TCC GAT GCA CCA ACC ATA AGC-3'
10	GST_CED-3_StopR	5'-GGA CCC GGG TTA GAC GGC AGA GTT TCG-3'
11	ACp35MetF	5'-TTG GGA TCC GCC ATG TGT GTA ATT TTT CCG-3'
12	ACp35StopR	5'-GGG CTC GAG TTA TTT AAT TGT GTT TAA TAT TAC-3'
13	Ftt-2_MetF	5'-GTG GGT ACC ATG TCT GAC GGA AAG-3'
14	Ftt-2_StopR	5'-CCT CTC GAG TTA GTT GCC TCC CTC-3'
15	Ftt-2_MetF_2	5'-CAC GGT ACC GCC ATG CAT CAT CAC CAT CAC CAT TCT GAC GGA AAG-3'
16	Ftt-2_D240Stop_R	5'-CCT CTC GAG CTA ATC AGT GTC ATC GGT GGC-3'
17	Crt1_MetF	5'-GGA GGT ACC ATG AAA TCA CTC TGC-3'
18	Crt1_StopR	5'-TCC AAG CTT TTA GAG CTC ATC GTG TCC-3'
19	Crt1_MetF_2	5'-GGA GGT ACC GCC ATG AAA TCA CTC TGC-3'
20	Crt1_StopR_2	5'-TCC GAT ATC TTA GAG CTC ATC GTG TCC-3'
21	FLAG-CRT-1_MetF	5'-GGA GGT ACC GCC ATG GAC TAC AAG GAC GAC GAT GAC AAG AAA TCA CTC TGC-3'
22	Tbb2_MetF	5'-GAG GGT ACC ATG AGA GAG ATC GTC-3'
23	Tbb2_StopR	3'-CCA CTC GAG TTA TTG CTC CGA TTC-3'

24	ASP-1MetF	5'-GTG GAA TTC ATG CAG ACC TTC GTT TTG-3'
25	ASP-1StopR	5'-CCT CTC GAG TTA CAA TCC CTT GTG-3'
26	PAR-5MetF	5'-GTC GGT ACC ATG TCC GAT ACC GTG-3'
27	PAR5StopR	5'-CCA CTC GAG TTA GTT TCC AGC TTC-3'
28	Ftt-2_D240E_MetF	5'-GTG GGA TCC ATG TCT GAC GGA AAG-3'
29	Ftt-2_D240E_StopR	5'-CCT GGT ACC TTA GTT GCC TCC CTC-3'
30	Tbb2_StopR	5'–CCA GAT ATC TTA TTG CTC CGA TTC-3'
31	hCrtMetF	5'-GGT GAA TTC GCC ATG CTG CTA TCC GTG CCG-3'
32	hCrtStopR	5'-TGG CTC GAG CTA CAG CTC GCT CTT GGC-3'
33	FLAG-Crt_MetF	5'-CGC GAA TTC GCC ATG GAC TAC AAG GAC GAC GAT GAC AAG CTG CTA TCC GTG CCG CTG C-3'

APPENDIX IV

Table A.4 Point mutations generated by the author for use in this study

Plasmid name	ORF	Mutation	Primer numbers
pET45B-Crt-1^{D253E}	Crt-1	D253→E	34, 35
pET45B-Crt-1^{D225E}	Crt-1	D225→E	36, 37
pET45B-Crt-1^{D182E}	Crt-1	D182→E	38, 39
pET45b-Tbb-2^{D435E}	Tbb-2	D435→E	40, 41
pET45b-Tbb-2^{D417E}	Tbb-2	D417→E	42, 43
pET45b-Tbb-2^{D404E}	Tbb-2	D404→E	44, 45
pET45b-Ftt-2^{D240E}	Ftt-2	D240→E	46, 47
pcDNA3-calreticulin^{D258E}	Calreticulin	D258→E	48, 49
pcDNA3-calreticulin^{D232E}	Calreticulin	D232→E	50, 51
pcDNA3-calreticulin^{D187E}	Calreticulin	D187→E	52, 53
pcDNA3-calreticulin^{D31E}	Calreticulin	D31→E	54, 55
pcDNA3-calreticulin^{D71E}	Calreticulin	D71→E	56, 57

APPENDIX V

Table A.5 Primers used by the author for site-directed mutagenesis

	Primer name	Primer sequence
34	CRT1_D253E_F	5'-GAT GAC GAG ATG GAG GGA GAA TGG GAG-3'
35	CRT1_D253E_R	5'-CTC CCA TTC TCC CTC CAT CTC GTC ATC-3'
36	CRT1_D225E_F	5'-GAT GAT GCC GAG GAG GCC AAG CCA GAA G-3'
37	CRT1_D225E_R	5'-C TTC TGG CTT GGC CTC CTC GGC ATC ATC-3'
38	CRT-1_D182E_F	5'-GAA GTC AAG ATC GAG GGA GAA AGC GCC-3'
39	CRT-1_D182E_R	5'-GGC GCT TTC TCC CTC GAT CTT GAC TTC-3'
40	TBB2_D435E_F	5'-GAA GAC GAC GTC GAG GGA TAC GCT GAG-3'
41	TBB2_D435E_R	5'-CTC AGC GTA TCC CTC GAC GTC GTC TTC-3'
42	TBB-2_D417E_F	5'-G AGC AAC ATG AAC GAG CTC ATC TCA GAA TAC-
43	TBB-2_D417E_R	5'-G AGC AAC ATG AAC GAG CTC ATC TCA GAA TAC-
44	TBB-2_D404E_F	5'-GGA GAA GGA ATG GAG GAG ATG GAG TTC-3'
45	TBB-2_D404E_R	5'-GAA CTC CAT CTC CTC CAT TCC TTC TCC-3'
46	FTT-2_D240E_F	5'-ACC GAT GAC ACT GAG GCC AAC GAG ACA-3'
47	FTT-2_D240E_R	5'-TGT CTC GTT GGC CTC AGT GTC ATC GGT-3'
48	hCrt_D258_F	5'-GAT GAA GAG ATG GAG GGA GAG TGG GAA-3'
49	hCrt_D258_R	5'-TTC CCA CTC TCC CTC CAT CTC TTC ATC-3'
50	hCrt_D230_F	5'-GAT GAT CCC ACA GAG TCC AAG CCT GAG-3'
51	hCrt_D230_R	5'-CTC AGG CTT GGA CTC TGT GGG ATC ATC-3'
52	hCrt_D187E_F	5' -GAG GTG AAG ATT GAG AAC AGC CAG GTG-3'
53	hCrt_D187E_R	5' -CAC CTG GCT GTT CTC AAT CTT CAC CTC-3'
54	hCrt_D31E_F	5' -G TTT CTG GAC GGA GAG GGG TGG ACT TCC-3'
55	hCrt_D31E_R	5' -GGA AGT CCA CCC CTC TCC GTC CAG AAA C-3'
56	hCrt_D71E_F	5' -CAG ACA AGC CAG GAG GCA CGC TTT TAT G-3'
57	hCrt_D71E_R	5' -C ATA AAA GCG TGC CTC CTG GCT TGT CTG-3'

APPENDIX VI

Table A.6 Constructs obtained for use in this study

Plasmid name	Obtained from/ Made by
pET3a-Ced-3_FL_FLAG	Dr. Shai Shaham, Rockefeller University
pQE30-Ced-$3^{221-503}$	Dr. Victor Yu, University of Singapore
pET15b-Icd-1	Dr. Patrick Duriez, our laboratory
pET-Fzo-1	Dr. Patrick Duriez, our laboratory
pcRBG4-His-Ubiquitin	Dr. Emma Creagh, our laboratory
pcDNA3-His-Caspase-9	Dr. Helen Egan, our laboratory
pcDNA3-Bcl-xl	Petrina Delivani, our laboratory
pcDNA3-FLAG-Mfn-2	Petrina Delivani, our laboratory

REFERENCES

Aballay, A., and Ausubel, F. M. (2001). Programmed cell death mediated by ced-3 and ced-4 protects Caenorhabditis elegans from Salmonella typhimurium mediated killing. *Proc Natl Acad Sci U S A.* **98**, 2735-2739.

Acehan, D., Jiang, X., Morgan, D. G., Heuser, J. E., Wang, X., and Akey, C. W. (2002). Three-dimensional structure of the apoptosome: Implications for Assembly, Procaspase-9 Binding and Activation. *Mol Cell.* **9**, 423-432.

Adams, J. M., and Corey, S. (1998). The Bcl-2 Protein family: Arbiters of Cell Survival. *Science* **281**, 1322-1326.

Adrain, C., Slee, E. A., Harte, M. T., and Martin, S. J. (1999). Regulation of Apoptotic Protease Activating Factor-1 Oligomerization and Apoptosis by the WD-40 Repeat Region. *J Biol Chem.* **274**, 20855-20860.

Adrain, C., Brumatti, G., Duriez, P., Delivani, P., and Martin, S. J. (2006). The cytotoxic lymphocyte protease, granzyme B, targets the cytoskeleton and perturbs microtubule polymerization dynamics. *J. Biol. Chem.* **281**, 8118-8125.

Adrain, C., Brumatti, G., and Martin, S. J. (2006b). Apoptosomes: protease activation platforms to die from. *T.I.B.S.* **31**, 243-247.

Adrain, C., and Martin, S. J. (2006). Double knockout blow for caspases. *Science* **311**, 785-786.

Ahmed, H., Bianchet, M. A., Amzel, L. M., Hirabayashi, J., Kasai, K., Giga-Hama, Y., Tohda, H., and Vasta, G. R. (2002). Novel carbohydrate specificity of the 16-kDa galectin from Caenorhabditis elegans: binding to blood group precursor oligosaccharides (type 1, type 2, Talpha, and Tbeta) and gangliosides. *Glycobiology* **12**, 451-456.

Ahmed, S., and Hodgkin, J. (2000). MRT-2 checkpoint protein is required for germline immortality and telomere replication in C. *elegans. Nature* **403**, 159-164.

Ahmed, S., Alpi, A., Hengartner, M. O., and Gartner, A. (2001). C. *elegans* RAD5 /CLK-2 defines a new DNA damage checkpoint protein. *Current Biology* **11**, 1943-1944.

Amos, L. A. (2000). Focusing-in on microtubules. *Curr. Opin. Struct. Biol.* **10**, 236-241.

Arama, E., Agapite, J., and Steller, H. (2004). Caspase activity and a specific cytochrome c are required for sperm differentiation in *Drosophila*. *Dev. Cell* **4**, 687-697.

Arosa, F. A., de Jesus, O., Porto, G., Carmo, A. M., and de Sousa, M. (1999). Calreticulin is expressed on the cell surface of activated human peripheral blood T lymphocytes in association with major histocompatibility complex class I molecules. *J. Biol. Chem.* **274**, 16917-16922.

Ashkenazi, A., and Dixit, V. M. (1998). Death Receptors: Signaling and Modulation. *Science* **281**, 1305-1308.

Avery, L., and Horvitz, H. R. (1987). A cell that dies during wild-type *C. elegans* development can function as a neuron in a *ced-3* mutant. *Cell* **51**, 1071-1078.

Bakhshi, A., Jensen, J. P., Goldman, P., Wright, J. J., McBride, O. W., Epstein, A. L., and Korsmeyer, S. J. (1985). Cloning the chromosomal breakpoint of t(14;18) human lymphomas: clustering around JH on chromosome 14 and near a transcriptional unit on 18. *Cell* **41**, 899-906.

Barde, Y. A. (1989). Trophic factors and neuronal survival. *Neuron* **2**, 1525-1534.

Barry, M., Heibein, J. A., Pinkoski, M. J., Lee, S. F., Moyer, R. W., Green, D. R., and Bleackley R. C. (2000). Granzyme B short-circuits the need for caspase-8 activity during granule-mediated cytotoxic T-lymphocyte killing by directly cleaving Bid. *Mol Cell Biol.* **20**, 3781-3794.

Basu, S., and Srivastava, P. K. (1999). Calreticulin, a peptide-binding chaperone of the endoplasmic reticulum, elicits tumor- and peptide-specific immunity. *J. Exp. Med.* **189**, 797-802.

Basu, S., Binder, R. J., Suto, R., Anderson, K. M., and Srivastava, P. K. (2000). Necrotic but not apoptotic cell death releases heat shock proteins, which deliver a partial maturation signal to dendritic cells and activate the NF-κB pathway. *Int. Immunol.* **12**, 1539-1546.

Basu, S., Binder, R. J., Ramalingam, T., and Srivastava, P. K. (2001). CD91 is a common receptor for heat shock proteins gp96, hsp90, hsp70, and calreticulin. *Immunity* **14**, 303-313.

Bianchi, L., Gerstbrein, B., Frokaer-Jensen, C., Royal, D., Mukherjee, G., Royal, M. A., Xue, J., Schafer, W. R., and Driscoll, M. (2004). The neurotoxic MEC-4 (d) DEG/ENaC sodium channel conducts calcium: implication for necrosis initiation. *Nat. Neuroscience* **7**, 1337-1344.

Bloss, T. A., Witze, E. S, and Rothman, J. H. (2003). Suppression of CED-3-independent apoptosis by mitochondrial betaNAC in *Caenorhabditis elegans*. *Nature* **424**, 1066-1071.

Boldin M. P., Varfolomeev, E. E., Pancer, Z., Mett, I. L., Camonis, J. H., and Wallach, D. (1995). A Novel Protein that Interacts with the Death Domain of Fas/APO1 Contains a sequence Motif Related to the death domain. *J Biol Chem.* **270**, 7795-7798.

Borner, C. (2003). The Bcl-2 protein family: sensors and checkpoints for life-or-death decisions. *Mol. Immunol.* **39**, 615-647.

Bouillet, P. and Strasser, A. (2002). BH3-only proteins — evolutionarily conserved proapoptotic Bcl-2 family members essential for initiating programmed cell death . *J. Cell Sci.* **115**,1567-1574.

Bouillet, P., Metcalf, D., Huang, D. C. S., Tarlinton, D. M., Kay, T. W. H., Kontgen, F., Adams, J. M. and Strasser, A. (1999). Proapoptotic Bcl-2 relative Bim required for certain apoptotic responses, leukocyte homeostasis and to preclude autoimmunity. *Science* **286**,1735-1738.

Bouillet, P., Purton, J. F., Godfrey, D. I., Zhang, L. C., Coultas, L., Puthalakath, H., Pellegrini, M., Cory, S., Adams, J. M. and Strasser, A. (2002). BH3-only Bcl-2 family member Bim is required for apoptosis of autoreactive thymocytes. *Nature* **415**, 922 –926.

Cerretti, D. P., Koxlosky, C. J., Mosley, B., Nelson, N., Ness, K. V., Greenstreet, T. A., March, C. J., Kronheim, S. R., Druck, T., Cannizaro, L. A., Huebner, K., and Black, R. A. (1992). Molecular cloning of the interleukin-1β-converting enzyme. *Science* **256**, 97-100.

Certo, M., Moore, V. D. G., Nishino, M., Wei, G., Korsmeyer, S., Armstrong, S. A., and Letai, A. (2006). Mitochondria primed by death signals determine cellular addiction to antiapoptotic BCL-2 family members. *Cancer Cell* **9**, 351-365.

Chaudhary, D., O'Rourke, K., Chinnaiyan, A. M., and Dixit, V. M. (1997). The death inhibitory molecules CED-9 and CED-4L use a common mechanism to inhibit the CED-3 death protease. *J. Biol. Chem.* **273**, 17708-17712.

Chen, Z., Naito, M., Mashima, T., and Tsuruo, T. (1996). Activation of actin-cleavable interleukin Ibeta-converting enzyme (ICE) family protease CPP-32 during chemotherapeutic agent-induced apoptosis in ovarian carcinoma cells. *Cancer Res.* **56**, 5224-5229.

Chen, G.-Q and Gouaux, E. (1997). Overexpression of a glutamate receptor (GluR2) ligand binding domain in Escherichia coli: application of a novel protein folding screen. *Proc Natl Acad Sci U S A* **94**, 13431-13436.

Chen, P., Rodriguez, A., Erskine, R., Thach, T., and Abrams, J. M. (1998). Dredd, a novel effector of the apoptosis activators reaper, grim, and hid in Drosophila. *Dev. Biol.* **201**, 202-216.

Chen, L., Willis, S. N., Wei, A., Smith, B. J., Fletcher, J. I., Hinds, M. G., Colman, P. M., Day, C. L., Adams, J. M., and Huang, D. C. S. (2005). Differential targeting of prosurvival Bcl-2 proteins by their BH3-only ligands allows complementary apoptotic function. *Mol. Cell* **17**, 393-403.

Chinnaiyan, A. M., O'Rourke, K., Lane, B. R., and Dixit, V. M. (1997a). Interaction of CED-4 with CED-3 and CED-9: a molecular framework for cell death. *Science* **275**, 1122-1126.

Chinnaiyan, A. M., Chaudhary, D., O'Rourke, K., Koonin, E. V., and Dixit, V. M. (1997b). Role of CED-4 in the activation of CED-3. *Nature* **388**, 728-729.

Chipuk, J., Maurer, U., Green, D. R., and Schuler, M. (2003). Pharmacological activation of p53 elicits Bax-dependent apoptosis in the absence of transcription. *Cancer Cell* **4**, 371-381.

Chipuk, J., Kuwana, T., Bouchier-Hayes, L., Droin, N. M., Newmeyer, D. D., Schuler, M., and Green, D. R. (2004). Direct activation of Bax by p53 mediates mitochondrial membrane permeabilization and apoptosis. *Science* **13**, 1010-1014.

Chipuk, J., Bouchier-Hayes, L., Kuwana, T., Newmeyer, D. D., and Green, D. R. (2005). PUMA couples the nuclear and cytoplasmic proapoptotic function of p53. *Science* **309**, 1732-1735.

Chung, S., Gumienny, T. L., Hengartner, M. O., and Driscoll, M. (2000). A common set of engulfment genes mediates removal of both apoptotic and necrotic cell corpses in *C. elegans*. *Nat Cell Biol.* **2**, 931-937.

Clarke, A. R., Purdie, C. A., Harrison, D. J., Morris, R. G., Bird, C. C., Hooper, M. L., and Wyllie, A. H. (1993). Thymocyte apoptosis is induced by p53-dependent and independent pathways. *Nature* **362**, 849-852.

Cohen, P. L., and Eisenberg, R. A. (1991). Lpr and gld: single gene models of systemic autoimmunity and lymphoproliferative disease. *Ann Rev Immunol.* **9**, 243-269.

Coleman, M. L., Sahai, E. A., Yeo, M., Bosch, M., Dewar, A., and Olson, M. F. (2001). Membrane blebbing during apoptosis results from caspase-mediated activation of ROCK I. *Nat. Cell Biol.* **3**, 339-345.

Conradt, B. and Horvitz, H. R. (1998) The C. *elegans* protein EGL-1 is required for programmed cell death and interacts with the Bcl-2-like protein CED-9. *Cell* **93**, 519-529.

Conradt, B. and Horvitz, H. R. (1999). The TRA-1A sex determination protein of C. *elegans* regulates sexually dimorphic cell deaths by repressing the *egl-1* cell death activator gene. *Cell* **98**, 317 –327.

Coucouvanis, E., and Martin, G. R. (1995). Signals for death and survival: a two-step mechanism for cavitation in the vertebrate embryo. *Cell* **83**, 279-287.

Creagh, E. M., and Martin, S. J. (2001). Caspases: cellular demolition experts. *Biochem. Soc. Trans* **29**, 696-702.

Danial, N. N., Gramm, C. F., Scorrano, L., Zhang, C. Y., Krauss, S., Ranger, A. M., Datta, S. R., Greenberg, M. E., Licklider, L. J., Lowell, B. B., Gygi, S. P., and Korsmeyer, S. J. (2003). BAD and glucokinase reside in a mitochondrial complex that integrates glycolysis and apoptosis. *Nature* **424**, 952-956.

Datta, S. R., Dudek, H., Tao, X., Masters, S., Fu, H., Gotoh, Y. and Greenberg, M. E. (1997). Akt phosphorylation of BAD couples survival signals to the cell-intrinsic death machinery. *Cell* **91**, 231–241.

Datta, S. R., Katsov, A., Hu, L., Petros, A., Fesik, S. W., Yaffe, M. B., and Greenberg, M. E. (2000). 14-3-3 proteins and survival kinases cooperate to inactivate BAD by BH3 domain phosphorylation. *Mol. Cell* **6**, 41-51.

De Bernardez Clark, E. (1998). Refolding of recombinant proteins. *Curr. Op. Biotech.* 9, 157-163

Delivani, P., Taylor, R. C., Adrain, C., Duriez, P., and Martin, S. J. (2006). Role for CED-9 and Egl-1 as regulators of mitochondrial fission and fusion dynamics. *Mol. Cell* **21**, 761-773.

del Peso, L., Gonzalez-Garcia, M., Page, C., Herrera, R. and Nunez, G. (1997). Interleukin-3-induced phosphorylation of BAD through the protein kinase Akt. *Science* **278**,687 –689.

del Peso, L., Gonzalez, and Nunez, G. (1998). *Caenorhabditis elegans* EGL-1 disrupts the interaction of CED-9 with CED-4 and promotes CED-3 activation. *J. Biol. Chem.* **273**, 33495-33500.

del Peso, L., Gonzalez, V. M., Inohara, N., Ellis, R. E., and Nunez, G. (2000). Disruption of the CED-9:CED-4 complex by EGL-1 is a critical step for programmed cell death in *Caenorhabditis elegans. J. Biol. Chem.* **275**, 27205-27211.

Derry, W. B., Putze, A. P., and Rothman, J. (2001). *Caenorhabditis elegans* p53: role in apoptosis, meiosis, and stress resistance. *Science* **294**, 591-595.

Desagher, S., Osen-Sand, A., Montessuit, S., Magenat, E., Vilbois, F., Hochmann, A., Journot, L., Antonsson, B., and Martinou, J. C. (2001). Phosphorylation of Bid by casein kinases I and II regulates its cleavage by caspase-8. *Mol. Cell* **8**, 601-611.

Dorstyn, L., Read, S. H., Quinn, L. M., Richardson, H., and Kumar, S. (1999a). DECAY, a novel Drosophila caspase related to mammalian caspase-3 and caspase-7. *J Biol Chem.* **274**, 30778-30783.

Dorstyn, L., Colussi, P. A., Quinn, L. M., Richardson, H., and Kumar, S. (1999b). DRONC, an ecdysone-inducible Drosophila caspase. *Proc Natl Acad Sci U S A.* **96**, 4307-4310.

Driscoll, M., and Chalfie, M. (1991). The *mec-4* gene is a member of a family of *Caenorhabditis elegans* genes that can mutate to induce neuronal degeneration. *Nature* **349**, 588-593.

Dupuis, M., Schaerer, E., Krause, K.-H., and Tschopp, J. (1993). The calcium-binding protein calreticulin is a major constituent of lytic granules in cytolytic T lymphocytes. *J. Exp. Med.* **177**, 1-7.

Earnshaw, W. C., Martins, L. M., and Kaufmann, S. H. (1999). Mammalian Caspases: Structure, Activation, Substrates and Functions during apoptosis. *Ann Rev Biochem.* **68**, 383-424.

Ellis, H.M and Horvitz, H. R. (1986). Genetic control of programmed cell death in the nematode *C. elegans. Cell* **44**, 817-829.

Ellis, R.E and Horvitz, H. R. (1991a). Two *C. elegans.*genes control the programmed cell deaths of specific cells in the pharynx. *Development* **112**, 591-603.

Ellis, R.E, Jacobson, D. M., and Horvitz, H. R. (1991b). Genes required for the engulfment of cell corpses during programmed cell death in *C. elegans. Genetics* **129**, 79-94.

Ellis, G. C., Phillips, J. B., O'Rourke, S., Lyczak, R., and Bowerman, B. (2003). Maternally expressed and partially redundant β-tubulins in *Caenorhabditis elegans* are auto-regulated. *J. Cell Science* **117**, 457-464.

Enari, M., Sakahira, H., Yokoyama, H., Okawa, K., Iwamatsu, A., and Nagata, S. (1998). A caspase-activated DNase and its inhibitor, ICAD. *Nature* **391**, 43-50.

Epand, R. F., Martinou, J. C., Montessuit, S., Epand, R. M., and Yip, C. M. (2002). Direct evidence for membrane pore formation by the apoptotic protein Bax. *Biochem. Biophys. Res. Commun.* **298**, 744-749.

Fadok, V. A., Voelker, D. R., Campbell, P. A., Cohen, J. J., Bratton, D. L., and Henson, P. M. (1992). Exposure of phosphatidylserine on the surface of apoptotic lymphocytes triggers specific recognition and removal by macrophages. *J. Immunol.* **148**, 2207-2216.

Fadok, V. A., Bratton, D. L., Rose, D. M., Pearson, A., Ezekewitz, R. A. B., and Henson, P. M. (2000). A receptor for phosphatidylserine-specific clearance of apoptotic cells. *Nature* **405**, 85-90.

Ferri, K. F., and Kroemer, G. (2001). Organelle-specific initiation of cell death. *Nat Cell Biol.* **3**, 255-263.

Fesik, S. W. (2000). Insights into programmed cell death through structural biology. *Cell* **103**, 273-282.

Fire, A., Xu, S., Montgomery, M.K., Kostas, S.A., Driver, S.E., and Mello, C.C. (1998). Potent and specific genetic interference by double-stranded RNA in *Caenorhabditis elegans. Nature* **391**, 806-811.

Fischer, U., and Schulze-Osthoff, K. (2003). Many cuts to ruin: a comprehensive update of caspase substrates. *Cell Death Diff.* **10**, 76-100.

Fraser A. G., McCarthy N. J., and Evan G. I. (1997). drICE is an essential caspase required for apoptotic activity in Drosophila cells. *EMBO J.* **16**, 6192-6199.

Fraser, S. A., Karimi, R., Michalak, M. and Hudig, D. (2000). Perforin lytic activity is controlled by calreticulin. *J. Immunol.* **164**, 4150-4155.

Garcia-Calvo, M., Peterson, E. P., Rasper, D. M., Vaillancourt, J. P., Zamboni, R., Nicholson, D. W., and Thornberry, N. A. (1999). Purification and catalytic properties of human caspase family members. *Cell Death Differ.* **6**, 1054-1059.

Gardai, S. J., McPhillips, K. A., Frasch, S. C., Janssen, W. J., Starefeldt, A., Murphy-Ullrich, J. E., Bratton, D. L., Oldenborg, P., Michalak, M., and Henson, P. M. (2005). Cell-surface calreticulin initiates clearance of viable or apoptotic cells through trans-activation of LRP on the phagocyte. *Cell* **123**, 321-334.

Gartner, A., Milstein, S., Ahmed, S., Hodgkin, J., and Hengartner, M. O. (2000). A conserved checkpoint pathway mediates DNA damage-induced apoptosis and cell cycle arrest in C. *elegans. Mol. Cell* **5**, 435-443.

Geleziunas, R., Xu, W., Takeda, K., Ichijo, H., and Greene, W. C. (2001). HIV-1 Nef inhibits ASK1-dependent death signalling providing a potential mechanism for protecting the infected host cell. *Nature* **410**, 834-838.

Gerner, C., Frohwein, U., Gotzmann, J., Bayer, E., Gelbmann, D., Bursch, W., and Schulte-Hermann, R. (2000). The Fas-induced apoptosis analyzed by high throughput proteome analysis. *J. Biol. Chem.* **275**, 39018-39026.

Ghiran, I., Klickstein, L. B., and Nicholson-Weller, A. (2003). Calreticulin is at the surface of circulating neutrophils and uses CD59 as an adaptor molecule. *J. Biol. Chem.* **278**, 21024-21031.

Gleiss, B., Gogvadze, V., Orrenius, S., and Fadeel, B. (2002). Fas-triggered phosphatidylserine exposure is modulated by intracellular ATP. *FEBS Lett.* **519**, 153-158.

Glucksmann, A. (1951). Cell deaths in normal vertebrate ontogeny. *Biol. Rev.* **26**, 5986.

Goicoechea, S., Pallero, M. A., Eggleton, P., Michalak, M., and Murphy-Ullrich, J. E. (2002). The anti-adhesive activitiy of thrombospondin is mediated by the N-terminal domain of cell-surface calreticulin. *J. Biol. Chem* **277**, 37219-37228.

Goldstein, J. C., Waterhouse, N. J., Juin, P., Evan, G. I., and Green, D. R. (2000). The coordinate release of cytochrome c during apoptosis is rapid, complete and kinetically invariant. *Nat. Cell Biol.* **2**, 156-162.

Green, D. R. (2006). At the gates of death. *Cancer Cell* **9**, 328-330.

Gumienny, T. L., Lambie, E., Hartwieg, E., Horvitz, H. R., and Hengartner, M. O. (1999). Genetic control of programmed cell death in the *Caenorhabditis elegans* germline. *Development* **126**, 1011-1022.

Gumienny, T. L., Brugnera, E., Tosello-Trampont, A. C., Kinchen, J. M., Haney, L. B., Nishiwaki, K. *et al.* (2001). CED-12/ELMO, a novel member of the CrkII/DOCK180/Rac pathway, is required for phagocytosis and cell migration. *Cell* **107**, 27-41.

Hahne, M., Rimoldi, D., Schroter, M., Romero, P., Schreier, M., French, L. E., Schneider, P., Bornand, T., Fontana, A., Lienard, D., Cerottini, J., and Tschopp, J. (1996). Melanoma cell expression of Fas (Apo-1/CD95) ligand: implications for tumour immune escape. *Science* **274**, 1363-1366.

Hall, P. A., Coates, P. J., Ansari, B., and Hopwood, D. (1994). Regulation of cell number in the mammalian gastrointestinal tract: the importance of apoptosis. *J. Cell Sci.* **107**, 3569-3577.

Hall, D. H., Gu, G., Garcia-Anoveros, J., Gong, L., Chalfie, M., and Driscoll, M. (1997). Neuropathology of degenerative cell death in *Caenorhabditis elegans. J. Neuroscience* **17**, 1033-1045.

Hamon, Y., Broccardo, C., Chambenoit, O., Luciani, M.-F., Toti, F., Chaslin, S., Freyssinet, J.-M., Devaux, P. F., McNeish, J., Marguet, D., and Chimini, G. (2000). ABC1 promotes engulfment of apoptotic cells and transbilayer redistribution of phosphatidlyserine. *Nat. Cell Biol.* **2**, 399-406.

Han, J., Flemington, C., Houghton, A. B., Gu, Z., Zambetti, G. P., Lutz, R. J., Zhu, L. and Chittenden, T. (2001). Expression of *bbc3,* a proapoptotic BH3-only gene, is regulated by diverse cell death and survival signals. *Proc. Natl. Acad. Sci. USA* **98**,11318-11323.

Harada, K., Okiyoneda, T., Hashimoto, Y., Ueno, K., Nakamura, K., Yamahira, K., Sugahara, T., Shuto, T., Wada, I., Suico, M. A., and Kai, H. (2006). Calreticulin negatively regulates the cell surface expression of cystic fibrosis transmembrane conductance regulator. *J. Biol. Chem.* **281**, 12841-12848.

Harris, J. L., Peterson, E. P., Hudig, D., Thornberry, N. A., and Craik, C. S. (1998). Definition and redesign of the extended substrate specificity of granzyme B. *J. Biol. Chem.* **273**, 27364-27373.

Haslett, C. (1992). Resolution of acute inflammation and the role of apoptosis in the tissue fate of granulocytes. *Clin. Sci. (Colch)* **83**, 639-648.

Hedgecock, E. M., Sulston, J. E., Thomson, J. N. (1983). Mutations affectng programmed cell deaths in the nematode *Caenorhabditis elegans*. *Science* **220**, 1277-1279.

Heiben, J. A., Coping, I. S., Barry, M., Linkoski, M. J., Shore, C. C., Green, D. R., and Bleackley, R. C. (2000). Granzyme B-mediated cytochrome c release is regulated by the Bcl-2 Family Members Bid and Bax. *J Exp Med.* **192**, 1391-1401.

Hengartner, M. O., Ellis, R.E and Horvitz, H. R. (1992). C. *elegans* survival gene ced-9 protects cells from programmed cell death. *Nature* **356**, 494-499.

Hengartner, M. O. and Horvitz, H. R. (1994). C. *elegans* survival gene ced-9 encodes a functional homolog of the mammalian proto-oncogene Bcl-2. *Cell* **76**, 665-676.

Hirabayashi, J., Ubukata, T., and Kasai, K. (1996). Purification and molecular characterization of a novel 16-kDa galectin from the nematode *Caenorhabditis elegans*. *J. Biol. Chem.* **271**, 2497-2505.

Hirokawa, N. (1994). Microtubule organization and dynamics dependent on microtubule-associated proteins. *Curr. Opin Cell Biol.* **6**, 74-81.

Hockenberry, D., Nunez, G., Milliman, C., Schreiber, R. D., and Korsmeyer, S. J. (1990). Bcl-2 is an inner mitochondrial membrane protein that blocks programmed cell death. *Nature* **348**, 334-336.

Hoeppner, D. J., Hengartner, M. O., and Schnabel, R. (2001). Engulfment genes co-operate with *ced-3* to promote cell death in *C. elegans*. *Nature* **412**, 202-206.

Hofmann, E. R., Milstein, S., Boulton, S. J., Ye, M., Hofmann, J. J., Stergiou, L., Gartner, A., Vidal, M., and Hengartner, M. 0. (2002). *Caenorhabditis elegans* HUS-1 is a DNA damage checkpoint protein required for genome stability and EGL-1-mediated apoptosis. *Current Biology* **12**,1908-1918.

Hong, K., and Driscoll, M. (1994). A transmembrane domain of the putative channel subunit MEC-4 influencec mechanotransduction and neurodegeneration in *C. elegans*. *Nature* **367**, 470-473.

Horvitz, H. R., Shaham, S., and Hengartner, M. O. (1994). Genetics of programmed cell death in the nematode *Caenorhabditis elegans. Cold Spring Harbor Symp. Quant. Biol.* **LIX**, 377-385.

Hugunin, M., Quintal, L. J., Mankovich, J. A., and Ghayur, T. (1996). Protease activity of *in vitro* transcribed and translated *Caenorhabditis elegans* cell death gene (ced-3) product. *J. Biol. Chem.* **271**, 3517-3522.

Hu, Y., Benedict, M. A., Ding, L., Nunez, G. (1999). Role of cytochrome c and dATP/ATP hydrolysis in Apaf-1-mediated caspase-9 activation and apoptosis. *EMBO J.* **18**, 3586-3595.

Inoue, H., Nojima, H., and Okayama, I. I. (1990). High efficiency transformation of *Escherichia coli* with plasmids. *Gene* **96**, 23-28.

Irmler, M., Hofmann, K., Vaux, D., and Tschopp, J. (1997). Direct physical interaction between the *Caenorhabditis elegans* 'death proteins' CED-3 and CED-4. *FEBS Letters* **406**, 189-190.

Jacobson, M. D., Weil, M., and Raff, M. C. (1997). Programmed cell death in animal development. *Cell* **88**, 347-354.

Jeffers, J. R., Parganas, E., Lee, Y., Yang, C., Wang, J., Brennan, J., MacLean, K. H., Han, J., Chittenden, T., Ie, J. N., McKinnon, P. J., Cleveland, J. L., and Zambetti, G. P. (2003). Puma is an essential mediator of p53-dependent and -independent apoptotic pathways. *Cancer Cell* **4**, 321-328.

Jiang, X., and Wang, X. (2000). Cytochrome c promotes caspase-9 activation by inducing nucleotide binding to Apaf-1. *J. Biol. Chem.* **275**, 31199-31203.

Jin, J., Sith, F. D. *et al.* (2004). Proteomic, functional, and domain-based analysis of in vivo 14-3-3 binding proteins involved in cytoskeletal regulation and cellular organization. *Curr.Biol.* **14**, 1436-1450.

Kageyama, K., Ihara, Y., Goto, S., Urata, Y., Toda, G., Yano, K., and Kondo, T. (2002). Overexpression of calreticulin modulates protein kinase B/Akt signalling to promote apoptosis during cardiac differentiation of cardiomyoblast H9c2 cells. *J. Biol. Chem.* **277**, 19255-19264.

Kamer, I., Sarig, R., Zaltsman, Y., Niv, H., Oberkovitz, G., Regev, L., Haimovich, G., Lerenthal, Y., Marcellus, R. C., and Gross, A. (2005). Proapoptotic Bid is an ATM effector in the DNA damage response. *Cell* **122**, 593-603.

Kanuka, H., Sawamoto, K., Inohara, N., Matsuno, K., Okano, H., and Miura, M. (1999). Control of the cell death pathway by Dapaf-1, a Drosophila Apaf-1/CED4-related caspase activator. *Mol. Cell.* **4**, 757-769.

Kashio, Y., Nakamura, K., Abedin, M. J., Seki, M., Nishi, N., Yoshida, N., Nakamura, T., and Hirashima, M. (2003). Galectin-9 induces apoptosis through the calcium-calpain-caspase-1 pathway. *J Immunol.* **170**, 3631-3636.

Kayalar, C., Ord, T., Testa, M. P., Zhong, L. T., and Bredesen, D. E. (1996). Cleavage of actin by interleukin 1 beta-converting enzyme to reverse DNase I inhibition. *Proc. Natl. Acad. Sci. U S A.* **93**, 2234-2238.

Kerr, J. F., Wyllie, A. H., and Currie, A. R. (1972). Apoptosis: a basic biological phenomenon with wide-ranging implications in tissue kinetics. *Br. J. Cancer* **26**, 239-257.

Kim, S. Y., Valencia, M., Lee E. S., Park, D., Oh, M., Xue, D., and Park, W. J. (2004). Identification of CED-3 substrates by a yeast-based screening method. *Molecular Biotechnology* **27**, 1-6.

Kinchen, J. M., Cabello, J., Klingele, D., Wong, K., Feichtinger, R., Schnabel, H., Schnabel, R., and Hengartner, M. O. (2005). Two pathways converge at CED-10 to mediate actin rearrangement and corpse removal in *C. elegans*. *Nature* **434**, 93-99.

Kluck, R. M., Bossy-Wetzel, E., Green, D. R., and Newmeyer, D. D. (1997). The release of cytochrome c from mitochondria: a primary site for Bcl-2 regulation of apoptosis. *Science* **275**, 1132-1136.

Kontani, K., Moskowitz, I. P. G., and Rothman, J. H. (2005). Repression of cell-cell fusion by components of the *C. elegans* vacuolar ATPase complex. *Dev. Cell* **8**, 787-794.

Korsemeyer, S. J., Wei, M. C., Saito, M., Weiler, S., Oh, K. J., and Schlesinger, P. H. (2000). Pro-apoptotic cascade activates BID, which oligomerizes BAK or BAX into pores that result in the release of cytochrome *c*. *Cell Death Differ.* **7**, 1166-1173.

Kothakota, S., Azuma, T., Tang, J., Chu, K., McGarry, T. J., Kirschner, M. W., Koths, K., and Kwiatkowski, D. J. (1997). Caspase-3-generated fragments of gelsolin: effector of morphological change in apoptosis. *Science* **278**, 294-298.

Krebs, A., Goldie, K. N., and Hoenger, A. (2005). Structural rearrangements in tubulin following microtubule formation. *EMBO Reports* **6**, 227-232.

Kroemer, G., and Martin, S. J. (2005). Caspase-independent cell death. *Nat. Med.* **11**, 725-730.

Kuida, K., Zheng, T. S., Na, S., Kuan, C., Yang, D., Karasuyama, H., Rakic, P., and Flavell, R. A. (1996). Decreased apoptosis in the brain and premature lethality in CPP32-deficient mice. *Nature* **384**, 368-372.

Kumar, S., and Doumanis, J. (2000). The fly caspases. *Cell Death Differ.* **7**, 1039-1044.

Kumar, S. and Vaux, D. L. (2002). Apoptosis: a cinderella caspase takes centre stage. *Science* **297**, 1290-1291.

Kumar, S. (2004). Migrate, differentiate, proliferate, or die: pleiotropic functions of an apical "apoptotic caspase". *Scie STKE* **254**, pe49.

Kuwana, T., Mackey, M. R., Perkins, G., Ellisman, M. H., Latterich, M., Schneiter, R., Green, D. R., and Newmeyer, D. D. (2002). Bid, Bax and Lipids co-operate to form supramolecular openings in the outer mitochondrial membrane. *Cell* **111**, 331-342.

Kuwana, T., Bouchier-Hayes, L., Chipuk, J., Bonzon, C., Sullivan, B. A., Green, D. R., and Newmeyer, D. D. (2005). BH3 domains of BH3-only proteins differentially regulate Bax-mediated mitochondrial membrane permeabilization both directly and indirectly. *Mol. Cell* **17**, 525-535.

Lakhani, S. A., Masud, A., Kuida, K., Porter, G. A. Jr., Booth, C. J., Mehal, W. Z., Inayat, I., and Flavell, R. A. (2006). Caspases 3 and 7: key mediators of mitochondrial events of apoptosis. *Science* **311**, 847-851.

Lamkanfi, M., Declercq, W., Kalai, M., Saelens, X., and Vandenabeele, P. (2002). Alice in caspase land. A phylogenetic analysis of caspases from worm to man. *Cell Death Differ.* **9**, 358-361.

Lane, J. D., Lucocq, J., Pryde, J., Barr, F. A., Woodman, P. G., Allan, V. J., and Lowe, M. (2002). Caspase-mediated cleavage of the stacking protein GRASP65 is required for Golgi fragmentation during apoptosis. *J. Cell Biol.* **156**, 495-509.

Lauber, K., Bohn, E., Krober, S. M., Xiao, Y.-J., Blumenthal, S. G., Lindemann, R. K., Marini, P., Wiedig, C., Zobywalski, A., Baksh, S., Xu, Y., Autenrieth, I. B., Schulze-Ostoff, K., Belka, C., Stuhler, G., and Wesselborg, S. (2003). Apoptotic cells induce migration of phagocytes via caspase-3-mediated release of a lipid attraction signal. *Cell* **113**, 717-730.

Lauber, K., Blumenthal, S. G., Waibel, M. and Wesselborg, S. (2004). Clearance of apoptotic cells: getting rid of the corpses. *Mol. Cell* **14**, 277-287.

Leulier, F., Rodriguez, A., Khush, R. S., Abrams, J. M., and Lemaitre, B. (2000). The Drosophila caspase Dredd is required to resist gram-negative bacterial infection. *EMBO Rep.* **1**, 353-358.

Levine, A. J. (1997). p53, the cellular gatekeeper for growth and division. *Cell* **88**, 323-331.

Li, P., Nijhawan, D., Budihardjo, I., Srinivasula, S. M., Ahmad, M., Alnemri, E. S., and Wang, X. (1997). Cytochrome *c* and dATP-dependent formation of Apaf1 /Caspase-9 Complex initiates an apoptotic protease cascade. *Cell* **91**, 479-489.

Li, H., Zhu, H., Xu, C.-J., and Yuan, J. (1998). Cleavage of BID by caspase-8 mediates the mitochondrial damage in the Fas pathway of apoptosis. *Cell* **94**, 491-501.

Lindsten, T., Ross, A. J., King, A., Zong, W. X., Rathmell, J. C., Shiels, H. A., Ulrich, E., Waymire, K. G., Mahar, P., Frauwirth, K., et al (2000). The combined

functions of proapoptotic Bcl-2 family members Bak and Bax are essential for normal development multiple tissues. *Mol. Cell* **6**, 1389-1399.

Liu, D., Bienkowska, J., Petosa, C., Collier, R. J., Fu, H., and Liddington, R. (1995). Crystal structure data of the zeta isoform of the 14-3-3 protein. *Nature* **376**, 191-194.

Liu, H., Bowes, R. C., van de Water, B., Sillence, C., Nagelkerke, J. F., and Stevens, J. L. (1997). Endoplasmic reticulum chaperones GRP78 and calreticulin prevent oxidative stress, Ca^{2+} disturbances, and cell death in renal epithelial cells. *J. Biol. Chem.* **272**, 21751-21759.

Liu, N., Fine, R. E., Simons, E., and Johnson, R. J. (1994). Decreasing calreticulin expression lowers the Ca^{2+} response to bradykinin and increases sensitivity to ionomycin in NG-108-15 cells. *J. Biol. Chem.* **269**, 28635-28639.

Liu, Q. A., and Hengartner, M. O. (1998). Candidate adapter protein CED-6 promotes the engulfment of apoptotic cells in *C. elegans*. *Cell* **93**, 961-972.

Liu, W. H., Lin, Y. L., Wang, J. P., Liou, W., Hou, R. F., Wu, W. C., Liao, C. L. (2006). Restriction of vaccinia virus replication by a ced-3 and ced-4-dependent pathway in *Caenorhabditis elegans*. *Proc. Natl. Acad. Sci. USA* **103**, 4174-4179.

Liu, X., Kim, C. N., Yang, J., Jemmerson, R., and Wang, X. (1996). Induction of apoptotic program in cell-free extracts: requirement for dATP and cytochrome c. *Cell* **86**, 147-157.

Lockshin, R. A., and Zakeri, Z. (2001). Programmed cell death and apoptosis: origins of the theory. *Nat Rev Mol Cell Biol* **2**, 545-550.

Los, M., Mozoluk, M., Ferrari, D., Stepczynska, A., Stroh, C., Renz, A., Herceg, Z., Wang, Z. Q., and Schulze-Ostoff, K. (2002). Activation and caspase-mediated inhibition of PARP: a molecular switch between fibroblast necrosis and apoptosis in death receptor signalling. *Mol. Biol. Cell* **13**, 978-988.

Lowe, S. W., Schmitt, E. M., Smith, S. W., Osborne, B. A., and Jacks, T. (1993). p53 is required for radiation-induced apoptosis in mouse thymocytes. *Nature* **362**, 847-849.

Loyola, A. and Almouzni, G. (2004). Histone chaperones, a supporting role in the limelight. *Biochim. Biophys. Acta.* **1677**, 3-11.

Lu, C., Srayko, M., and Mains, P. E. (2004). The *Caenorhabditis elegans* microtubule-severing complex MEI-1/MEI-2 katanin interacts differently with two superficially redundant β-tubulin isotypes. *Mol. Biol. Cell* **15**, 142-150.

Luo, X., Budlhardjo, I., Zou, H., Slaughter, C. and Wang, X. (1998). Bid, a Bcl-2 interacting protein, mediates cytochrome *c* release from mitochondria in response to activation of cell surface death receptors. *Cell* **94**, 481-490.

Mancini, M., Machamer, C. E., Roy, S., Nicholson, D. W., Thornberry, N. A., Casciola-Rosen, L. A., and Rosen, A. (2000). Caspase-2 is localized at the Golgi complex and cleaves golgin-160 during apoptosis. *J. Cell Biol.* **149**, 603-612.

Mangahas, P. M., and Zhou, Z. (2005). Clearance of apoptotic cells in *Caenorhabditis elegans*. *Sem. Cell Dev. Biol.* **16**, 295-306.

Maquoi, E., Peyrollier, K., Noel, A., Foidart, J.-M. and Frankenne, F. (2003). Regulation of membrane-type 1 matrix metalloproteinase activity by vacuolar H^+-ATPases. *Biochem. J.* **373**, 19-24.

Martin, S. J., and Cotter, T. (1990). Disruption of microtubules induces an endogenous suicide pathway in human leukaemia HL-60 cells. *Cell Tissue Kinet.* **23**, 545-559.

Martin, S. J., and Green, D. R. (1995). Protease activation during apoptosis: death by a thousand cuts? *Cell* **82**, 349-352.

Martin, S. J., and Green, D. R. (1995b). Apoptosis and cancer: the failure of controls on cell death and cell survival. *Crit. Rev. Oncol. Haematol.* **18**, 137-156.

Martin, S. J., Reutelingsperger, C. P., McGahon, A. J., Rader, J. A., van Schie, R. C., LaFace, D. M., and Green, D. R. (1995). Early redistribution of plasma membrane phosphatidylserine is a general feature of apoptosis regardless of the initiating stimulus: inhibition by overexpression of Bcl-2 and Abl. *J. Exp. Med.* **182**, 1545-1556.

Martin, S. J., Amarante-Mendes, G. P., Shi, L., Chuang, T..-S., Casiano, C. A., O'Brien, G. A., Fitzgerald, P., Tan, E. M., Bokoch, G. M., Greenberg, A. H., and Green, D. R. (1996). The cytotoxic cell protease granzyme B initiates apoptosis in a cell-free system by proteolytic processing and activation of the ICE/CED-3 family protease, CPP32, via a novel two-step mechanism. *EMBO J.* **15**, 2407-2416.

Martin, S. J., Finucane, D. M., Amarante-Mendes, G. P., O'Brien, G. A., and Green, D. R. (1996b). Phosphatidylserine externalization during CD95-induced apoptosis of cells and cytoplasts requires ICE/CED-3 protease activity. *J. Biol. Chem.* **271**, 28753-28756.

Marya, P. K., Syed, Z., Fraylich, P. E., and Eagles, P. A. M. (1994). Kinesin and Tau bind to distinct sites on microtubules. *J. Cell Sci.* **107**, 339-344.

Mashima, T., Naito, M., Noguchi, K., Miller, D. K., Nicolson, D. W., and Tsuro, T. (1997). Actin cleavage by CPP32/apopain during the development of apoptosis. *Oncogene* **14**, 1007-1012.

Masters, S. C., Subramanian, R. R., Truong, A., Tang, H., Fujii, K., Zhang, H., and Fu, H. (2002). Survival-promoting functions of 14-3-3 proteins. *Biochem. Soc. Transact.* **30**, 360-365.

Matzinger, P. (1994). Tolerance, danger and the extended family. *Ann. Rev. Immunol.* **12**, 991-1045.

Meagher, L. C., Savill, J. S., Baker, A., and Haslett, C. Phagocytosis of apoptotic neutrophils does not induce macrophage release of thromboxane B2. *J. Leuk. Biol.* **52**, 269-273.

Medema, J. P., Scaffidi, C., Kischkel, F. C., Shevchenko, A., Mann, M., Krammer, P. H., and Peter M. E. (1997a). FLICE is activated by association with the CD95 death-inducing signaling complex (DISC). *EMBO J.* **16**, 2794-2804.

Meinl, E., Fickenscher, Thome, M., Tschopp, J., and Fleckenstein, B. (1998). Anti-apoptotic strategies of lymphotropic viruses. *Immunology Today* **19**, 474-479.

Metzstein, M. M., Hengartner, M. O., Tsung, N. Ellis, R. E., and Horvitz, H. R. (1996). Transcriptional regulator of programmed cell death encoded by *Caenorhabditis elegans* gene ces-2. *Nature* **382**, 545-547.

Metzstein, M. M., and Horvitz, H. R. (1999). The *C. elegans* cell death specification gene ces-1 encodes a small family zinc finger protein. *Mol. Cell* **4**, 309-319.

Michalak, M., Corbett, E. F., Mesaeli, N., Nakamura, K., and Opas, M. (1999). Calreticulin: one protein, one gene, many functions. *Biochem. J.* **344**, 281-292.

Middelberg, A. P. J. (2002). Preparative protein refolding. *Trends in Biotech.* **20**, 437-444.

Mittl, P. R. E., Di Marco, S., Krebs, J. F., Bai, X., Karanewsky, D. S., Priestle, J. P., Tomaselli, K., J., and Grutter, M. G. (1997). Structure of recombinant human CPP32 in complex with the tetrapeptide Acetyl-Asp-Val-Al-Asp fluoromethyl ketone. *J. Biol. Chem* **272**, 6539-6547.

Miura, M., Zhu, H, Rotello, R., Hartwieg, E. A., and Yuan, J. (1993). Induction of apoptosis in fibroblasts by IL-1β-converting enzyme, a mammalian homolog of the C. *elegans* cell death gene ced-3. *Cell* **175**, 653-660.

Moores, C. A., Yu, M., Guo, J., Beraud, C., Sakowicz, R., and Milligan, R. A. (2002). A mechanism for microtubule depolymerization by Kinl kinesins. *Mol. Cell* **9**, 903-909.

Moretti, A., Weig, H. J., Ott, T., Seyfarth, M., Holthoff, H. P., Grewe, D., Gillitzer, A., Boo-Flugel, L., Schomig, A., Ungerer, M., and Laugwitz, K. L. (2002). Essential myosin light chain as a target for caspase-3 in failing myocardium. *Proc. Natl. Acad. Sci. USA.* **99**, 11860-11865.

Mortz, E., Krogh, T. N., Vorum, H., and Gorg, A. (2001). Improved silver staining protocols for high sensitivity protein identification using matrix-assisted laser desorption/ionization-time of flight analysis. *Proteomics* **1**,1359-1363.

Moss, D. K., and Lane, J. D. (2006). Microtubules: forgotten players in the apoptotic execution phase. *Trends Cell Biol.* **16**, 330-338.

Moss, D. K., Betin, V. M., Malesinski, S. D., and Lane, J. D. (2006). A novel role for microtubules in apoptotic chromatin dynamics and cellular fragmentation. *J. Cell Sci.,* **119**, 2362-2374.

Muzio, M., Chinnaiyan, A. M., Kischkel, F. C., O'Rourke, K., Shevchenko, A., Ni, J., Scaffidi, C., Bretz, J. D., Zhang, M., Gentz, R., Mann, M., Krammer, P. H., Peter, M.E., and Dixit, V. M. (1996). FLICE, a novel FADD-homologous ICE /CED-3-like protease, is recruited to the CD95 (Fas / APO-1) death-inducing signaling complex. *Cell* **85**, 817-827.

Nagata, S. (1997). Apoptosis by death factor. *Cell* **88**, 355-365.

Nair, S., Wearsch, P. A., Mitchell, D. A., Wassenberg, J. J., Gilboa, E., and Nicchitta, C. V. (1999). Calreticulin displays in vivo peptide-binding activity and can elicit CTL responses against bound peptides. *J. Immunol.* **162**, 6426-6432.

Nakamura, K., Bossy-Wetzel, E., Burns, K., Fadel, M. P., Lozyk, M., Goping, I. S., Opas, M., Bleackley, C., Green, D. R., and Michalak, M. (2000). Changes in endoplasmic reticulum luminal environment affect cell sensitivity to apoptosis. *J. Cell Biol.* **150**, 731-740.

Nakano, K. and Vousden, K. H. (2001). *PUMA,* a novel proapoptotic gene, is induced by p53. *Mol. Cell* **7**,683 –694.

Nataraj, A., Pathak, S., Hopwood, V., McDonnell, T., and Ananthaswamy, H. (1994). bcl-2 oncogene blocks differentiation and extends viability but does not immortalize normal human keratinocytes. *Int. J. Oncology* **4**, 1211-1218.

Newmeyer, D., Farschon, D. M., and Reed, J. C. (1994). Cell-free apoptosis in *Xenopus* egg extracts: inhibition by Bcl-2 and requirement for an organelle fraction enriched in mitochondria. *Cell* **79**, 353-364.

Nicholson, D. W., Ali, A., Thornberry, N. A., Vaillancourt, J. P., Ding, C. K., Gallant, M., Gareau, Y., Griffin, P. R., Labelle, M., Lazebnik, Y. A., et al. (1995). Identification and inhibition of the ICE /CED-3 protease necessary for mammalian apoptosis. *Nature* **376**, 37-43.

Nicholson, D.W. (1999). Caspase structure, proteolytic substrates and function during apoptotic death. *Cell Death Diff.* **6**, 1028-1042.

Nishiwaki, K. (1999). Mutations affecting symmetrical migration of distal tip cells in *C. elegans*. *Genetics* **152**, 985-997.

Nogales, E., Wolf, S. G., and Downing, K. H. (1998). Structure of the $\alpha\beta$ tubulin dimer by electron crystallography. *Nature* **391**, 199-203.

Nogales, E. (2001). Structural insight into microtubule function. *Ann. Rev. Biophys. Biomol. Struc.* **30**, 397-420.

Nomura, M., Shimizu, S., Sugiyama, T., Narita, M., Ito, T., Matsuda, H., and Tsujimoto, Y. (2003). 14-3-3 interacts directly with and negatively regulates pro-apoptotic Bax. *J. Biol. Chem.* **278**, 2058-2065.

Norimura, T., Nomoto, S., Katsuki, M., Gondo, Y., and Kondo, S. (1996). p53-dependent apoptosis suppresses radiation-induced teratogenesis. *Nat Med* **2**, 577-580.

Oda, E., Ohki, R., Murasawa, H., Nemoto, J., Shibue, T., Yamashita, T., Tokino, T., Taniguchi, T. and Tanaka, N. (2000). Noxa, a BH3-only member of the Bcl-2 family and candidate mediator of p53-induced apoptosis. *Science* **288**, 1053 –1058.

Ogden, C. A., deCathelineau, A., Hoffman, P. R., Bratton, D., Ghebrehiwet, B., Fadok, V., and Henson, P. M. (2001). C1q and mannose binding lectin engaagment of cell surface calreticulin and CD91 initiates macropinocytosis and uptake of apoptotic cells. *J. Exp. Med.* **194**, 781-795.

Orr, A. W., Pedraza, C. E., Pallero, M. A., Elzie, C. A., Goicoechea, S., Strickland, D. K., and Murphy-Ullrich, J. E. (2003). Low density lipoprotein receptor-related protein is a calreticulin coreceptor that signals focal adhesion disassembly. *J. Cell Biol.* **161**, 1179-1189.

Paschal, B. M., Obar, R. A., and Vallee, R. B. (1989). Interaction of brain cytoplasmic dynein and MAP2 with a common sequence at the C terminus of tubulin. *Nature* **342**, 569-572.

Prasad, S., Soldatenkov, V. A., Srinivasarao, G., and Dritschilo, A. (1998). Identification of keratins 18, 19 and heat-shock protein 90 beta as candidate substrates of proteolysis during ionizing radiation-induced apoptosis of estrogen-receptor negative breast tumor cells. *Int J Oncol.* **13**, 757-764.

Ramage, P., Cheneval, D., Chvei, M., Graff, P., Hemmig, R., Heng, R., Kocher, H. P., Mackenzie, A., Memmert, K., Revesz, L., and Wishart, W. (1995). Expression,

Ruchaud, S., Korfali, N., Villa, P., Kottke, T. J., Dingwall, C., Kaufmann, S. H., and Earnshaw, W. C. (2002). Caspase-6 gene disruption reveals a requirement for lamin A cleavage in apoptotic chromatin condensation. *EMBO J.* **21**, 1967-1977.

Rudel T., and Bokoch G. M. (1997). Membrane and morphological changes in apoptotic cells regulated by caspase-mediated activation of PAK2. *Science* **276**, 1571-1574.

Rudolph, R., and Lilie, H. (1996). *In vitro* folding of inclusion body proteins. *FASEB J.* **10**, 49-56.

Sadasivan, B., Lehner, P. J., Ortmann, B., Spies, T., and Cresswell, P. (1996). Roles for calreticulin and a novel glycoprotein, tapasin, in the interaction of MHC class I molecules with TAP. *Immunity* **5**, 103-114.

Saito, Y., Ihara, Y., Leach, M. R., Cohen-Doyle, M. F., and Williams, D. B. (1999). Calreticulin functions *in vitro* as a molecular chaperone for both glycosylated and non-glycosylated proteins. *EMBO J.* **18**, 6718-6729.

Saito, M., Korsmeyer, S. J., and Schlesinger, P. H. (2000). BAX-dependent transport of cytochrome c reconstituted in pure liposomes. *Nat. Cell Biol.* **2**, 553-555.

Sackett, D. L., Bhattacharyya, B., and Wolff, J. (1984). Tubulin subunit carboxyl termini determine polymerization efficiency. *J. Biol. Chem.* **260**, 43-45.

Sakahira, H., Enari, M., and Nagata, S. (1998). Cleavage of CAD inhibitor in CAD activation and DNA degradation during apoptosis. *Nature* **391**, 96-99.

Salvesen, G. S. and Dixit, V. M. (1999). Caspase activation: the induced proximity model. *Proc. Natl. Acad. Sci. USA* **96**, 10964-10967.

Sattler, M., Yoon, H. S., Nettesheim, D., Wang, Y., Meadows, R. P., Harlan, J. E., Eberstadt, M., Yoon, H. S., Shuker, S. B., Chang, B., S., Minn, A. J. *et al.* (1997).

refolding and autocatalytic proteolytic processing of the interleukin-1 β-converting enzyme precursor. *J. Biol. Chem.* **270**, 9378-9383.

Rao, L., Perez, D., and White, E. (1996). Lamin proteolysis facilitates nuclear events during apoptosis. *J. Cell Biol.* **135**, 1441-1455.

Rauch, F., Prud'homme, J., Arabian, A., Dedhar, S., and St-Arnaud, R. (2000). Heart, brain, and body wall defects in mice lacking calreticulin. *Exp. Cell Res.* **256**, 105-111.

Reddien, P. W., and Horvitz, H. R. (2000). CED-2/CrkII and CED-10/Rac control phagocytosis and cell migration in *C. elegans*. *Nat. Cell Biol.* **2**, 131-136.

Reddien, P. W., Cameron, S., and Horvitz, H. R. (2001). Phagocytosis promotes programmed cell death in *C. elegans*. *Nature* **412**, 198-202.

Ricci, J. E., Munoz-Pinedo, C., Fitzgerald, P., Bailly-Maitre, B., Perkins, G. A., Yadava, N., Scheffler, I. E., Ellisman, M. H., and Green, D. R. (2004). Disruption of mitochondrial function during apoptosis is mediated by caspase cleavage of the p75 subunit of complex I of the electron transport chain. *Cell* **117**, 773-786.

Rizvi, S. M., Mancino, L., Thammavongsa, V., Cantley, R. L., and Raghavan, M. (2004). A polypeptide binding conformation of calreticulin is induced by heat shock, calcium depletion, or by deletion of the C-terminal acidic region. *Mol. Cell* **15**, 913-923.

Rodriguez, A., Oliver, H., Zou, H., Chen, P., Wang, X., and Abrams, J. M. (1999). Dark is a Drosophila homologue of Apaf-1 /CED-4 and functions in an evolutionarily conserved death pathway. *Nat. Cell Biol.* **1**, 272-279.

Rotonda, J., Nicholson, D. W., Fazil, K. M., Gallant, M., Gareau, Y., Labelle, M., Peterson, E. P., Rasper, D. M., Ruel, R., Vaillancourt, J. P., et al (1996). The three-dimensional structure of apopain/CPP32, a key mediator of apoptosis. *Nat. Struct. Biol.* **3**, 619-625.

Structure of Bcl-xL-Bak peptide complex: recognition between regulators of apoptosis. *Science* **275**, 983-986.

Sauter, B., Albert, M. L., Francisco, L., Larsson, M., Somersan, S., and Bhardwaj, N. (2000). Consequences of cell death: exposure to necrotic tumor cells, but not primary tissue cells or apoptotic cells, induces the maturation of immunostimulatory dendritic cells. *J Exp Med* **191**, 423-434.

Savill, J., Wyllie, A. H., Henson, J. E., Walport, M. J., Henson, P. M., and Haslett, C. (1989). Macrophage phagocytosis of aging neutrophils in inflammation. Programmed cell death in the neutrophil leads to its recognition by macrophages. *J. Clin. Invest.* **83**, 865-875.

Savill, J. and Fadok, V. (2000). Corpse clearance defines the meaning of cell death. *Nature* **407**, 784-788.

Schumaker, B., Hofmann, K., Boulton, S., and Gartner, A. (2001). The *C. elegans* homolog of the p53 tumor suppressor is required for DNA damage-induced apoptosis. *Current Biology* **11**, 1722-1727.

Schumacher, B., Schertel, C., Wittenburg, N., Tuck, S., Mitani, S., Gartner, A., Conradt, B., and Shaham, S. (2004). *C. elegans ced-13* can promote apoptosis and is induced in response to DNA damage. *Cell Death Differ.* **12**, 153-161.

Sebbagh, M., Renvoize, C., Hamelin, J., Riche, N., Bertoglio, J. and Breard, J. (2001). Caspase-3-mediated cleavage of ROCK I induces MLC phosphorylation and apoptotic membrane blebbing. *Nat. Cell Biol.* **3**, 346-352.

Serrano, L., Avila, J., and Maccioni, R. B. (1984). Limited proteolysis of tubulin and the localization of the binding site for colchicines. *J. Biol. Chem.* **259**, 6607-6611.

Seshagiri, S. and Miller, L. K. (1997). *Caenorhabditis elegans* CED-4 stimulates CED-3 processing and CED-3-induced apoptosis. *Current Biology* **7**, 455-460.

Shaham, S., and Horvitz, H. R. (1996). Developing *C. elegans* neurons may contain both cell protective and killer activities. *Genes Dev.* **10**, 578-591.

Shaham, S. (1998). Identification of multiple Caenorhabditis elegans caspases and their potential roles in proteolytic cascades. *J Biol Chem* **273**, 35109-35117.

Shaham, S., Reddien, P. W., Davies, B., and Horvitz, H. R. (1999). Mutational analysis of the Caenorhabditis elegans cell-death gene ced-3. *Genetics.* **153**, 1655-1671.

Shi, Y. (2002). Mechanisms of caspase activation and inhibition during apoptosis. *Mol. Cell* **9**, 459-470.

Slee, E. A., Adrain, C. and Martin, S. J. (1999a). Serial killers: ordering caspase activation events in apoptosis. *Cell Death Differ* **6**, 1067-1074.

Slee, E. A., Harte, M. T., Kluck, R. M., Wolf, B. B., Casiano, C. A., Newmeyer, D. D., Wang, H. G., Reed, J. C., Nicholson, D. W., Alnemri, E. S., Green, D. R., and Martin, S. J. (1999b). Ordering the cytochrome c-initiated caspase cascade: hierarchical activation of caspases-2, -3, -6, -7, -8 and –10 in a caspase-9 dependent manner. *J Cell Biol.* **144**, 281-292.

Slee, E. A., Adrain, C. and Martin, S. J. (2001). Executioner caspase-3, -6 and –7 perform distinct, non-redundant roles during the demolition phase of apoptosis. *J Biol Chem.* **276**, 7320-7326.

Sogn, Q., Wei, T., Lees-Miller, S. Alnemri, E., Watters, D., and Lavin, M. F. (1997). Resistance of actin to cleavage during apoptosis. *Procl. Nat. Acad. Sci. USA* **94**, 157-162.

Song Z, McCall K, and Steller H. (1997). DCP-1, a Drosophila cell death protease essential for development. *Science* **275**, 536-540.

Sonnichsen, B., Fullekrug, J., Van, P. N., Diekmann, W., Robinson, D. G., and Mieskes, G. (1994). Retention and retrieval: both mechanisms cooperate to maintain calreticulin in the endoplasmic reticulum. *J. Cell Sci.* **107**, 2705-2717.

Srinivasula, S. M., Ahmad, M., Fernandes-Alnemri, T., Litwack, G., and Alnemri, E. S. (1996). Molecular ordering of the Fas-apoptotic pathway: the Fas/APO-1 protease Mch5 is a CrmA-inhibitable protease that activates multiple Ced-3/ICElike cysteine proteases. *Proc. Natl. Acad. Sci. USA* **93**, 14486-14491.

Srinivasula, S. M., Ahmad, M., Fernandes-Alnemri, T., and Alnemri, E.,S. (1998). Autoactivation of procaspase-9 by Apaf-1-mediated oligomerization. *Mol Cell.* **1**, 949-957.

Stennicke, H. R, and Salvesen, G. S. (1997). Biochemical characteristics of caspases-3, -6, -7 and –8. *J Biol Chem.* **257**, 19-23.

Stennicke, H. R., and Salvesen, G. S. (1999a). Catalytic properties of the caspases. *Cell Death Differ.* ***6***, 1054-1059.

Stennicke, H. R., and Salvesen, G. S. (1999b). Caspases: preparation and characterization. *Methods* **17**, 313-319.

Stoven S, Ando I, Kadalayil L, Engstrom Y, and Hultmark D. (2000). Activation of the Drosophila NF-kappaB factor Relish by rapid endoproteolytic cleavage. *EMBO Rep.* **1**, 347-352.

Su, H. P., Nakada-Tsukui, K., Tosello-Trampont, A. C., Li, Y., Bu, G., Henson, P. M., and Ravichandran, K. S. (2002). Interaction of CED-6/GULP, an adapter protein involved in engulfment of apoptotic cells with CED-1 and CD91/low density lipoprotein receptor-related protein (LRP). *J. Biol. Chem.* **277**, 11772-11779.

Sulston, J. E. (1976). Post-embryonic development in the ventral cord of *Caenorhabditis elegans*. *Philos. Trans. R. Soc. London Ser. B* **275**, 287-298.

Sulston, J. E. and Horvitz, H. R. (1977). Post-embryonic lineages of the nematode, *Caenorhabditis elegans. Dev. Biol.* **56**, 110-156.

Sulston, J. E., Schierenberg, E., White, J. G., and Thomson, J. N. (1983). The embryonic cell lineage of the nematode *Caenorhabditis elegans. Dev. Biol.* **100**, 64-119.

Sutton, V. R., Davis, J. E., Cancilla, M., Johnstone, R. W., Ruefli, A. A., Sedelies, K., Browne, K. A., and Trapani, J. A. (2000). Initiation of apoptosis by granzyme B requires direct cleavage of Bid, but not direct granzyme B-mediated caspase activation. *J. Exp. Med.* **192**, 1403-1414.

Syntichaki, P., Xi, K., Driscoll, M., and Tavernarakis, N. (2002). Specific aspartyl and calpain proteases are required for neurodegeneration in *C. elegans*. *Nature* **419**, 939-944.

Syntichaki, P., Samara, C., and Tavernarakis, N. (2005). The vacuolar H^+-ATPase mediates intracellular acidification required for neurodegeneration in *C. elegans*. *Curr. Biol.* **15**, 1249-1254.

Tu, S., McStay, G. P., Boucher, L. M., Mak, T., Beere, H. M., and Green, D. R. (2006). In situ trapping of activated initiator caspases reveals a role for caspase-2 in heat shock-induced apoptosis. *Nat Cell Biol.* **8**, 72-77.

Thornberry, N. A., Bull, H. G., Calacay, J. R., Chapman, K. T., Howard, A. D., Kostura, M. J., Miller, D. K., Molineaux, S. M., Weidner, J. R., Aunins, J., Elliston, K. 0., Ayala, J. M., Casano, F. J., Chin, J., Ding, G. J.-F., Egger, L. A., Gaffney, E. P., Limjuco, G., Palyha, 0. C., Raju, S. M., Rolando, A. M., Salley, J. P., Yamn, T.-T., Lee, T. D., Shively, J. E., MacCross, M., Mumford, R. A., Schmidt, J. A, and Tocci, M. J. (1992). A novel heterodimeric cysteine protease is required for interleukin-1β processing in monocytes. *Nature* **356**, 768-774.

Thornberry, N. A., Rano, T. A., Peterson, E. P., Rasper, D. M., Timkey, T., Garcia-Calvo, M., Houtzager, V. M., Nordstrom, P. A., Roy, S., Vaillancourt, J. P., Chapman, K. T., and Nicoloson, D. W. (1997). A combinatorial approach defines

specificities of members of the caspase family and granzyme B. *J. Biol. Chem.* **272**, 17907-17911.

Thornberry, N. A., and Lazebnik, Y. (1998). Caspases: Enemies Within. *Science* **281**, 1312-1316.

Trent, C., Tsung, N., and Horvitz, H. R. (1983). Egg-laying defective mutants of the nematode *Caenorhabditis elegans. Genetics* **104**, 619-647.

Truong, A. B., Masters, S. C., Yang, H., and Fu, H. (2002). Role of the C-terminal loop in ligand interaction. *Prot. Struc. Func. Gen.* **49**, 321-325.

Vance, B. A., Harley, P. H., Backlund, P. S., Ward, Y., Phelps, T. L., and Gress, R. E. (2005). Human CD69 associates with an N-terminal fragment of calreticulin at the cell surface. *Arch. Biochem. Biophys.* **438**, 11-20.

Van Damme, P., Martens, L., Van Damme, J., Hugelier, K., Staes, A., Vandekerckhove, J., and Gevaert, K. (2005). Caspase-specific and nonspecific in vivo protein processing during Fas-induced apoptosis. *Nat. Methods* **2**, 771-777.

Vandivier, R. W., Ogden, C. A., Fadok, V. A., Hoffman, P. R., Brown, K. K., Botto, M., Walport, M. J., Fisher, J. H., Henson, P. M., and Greene, K. E. (2002). Role of surfactant proteins A, D, and C1q in the clearance of apoptotic cells in vivio and in vitro: calreticulin and CD91 as a common collectin receptor complex. *J. Immunol.* **169**, 3978-3986.

Vaux, D. L., Cory, S., Adams, J. M. (1988). Bcl-2 gene promotes haemopoietic cell survival and cooperates with c-myc to immortalize pre-B cells. *Nature* **335**, 440-442.

Walker, N. P. C., Talanian, R. V., Brady, K. D., Dang, L. C., Bump, N. J., Ferenz, C. R., Franklin, S., Ghayur, T., Hackett, M. C., Hammill, L. D., et al. (1994). Crystal structure of the cysteine protease interleukin-113-converting enzyme: a $(p20/p10)_2$ homodimer. *Cell* **78**, 343-352.

Walters, J. J., and Berwin, B. (2005). Differential CD91 dependence for calreticulin and *Pseudomonas* exotoxin-A for endocytosis. *Traffic* **6**, 1173-1182.

Wang, S., Miura, M., Jung, Y. K., Zhu, H., Li, E., and Yuan, J. (1998). Murine caspase-11, an ICE-interacting protease, is essential for the activation of ICE. *Cell* **92**, 501-509.

Watanabe-Fukunaga, R., Brannan, C. I., Copeland, N. G., Jenkins, N. A., and Nagata, S. (1992). Lymphoproliferation disorder in mice explained by defects in Fas antigen that mediates apoptosis. *Nature* **356**, 314-317.

Wei, M. C., Zong, W. X., Cheng, E. H., Lindsten, T., Panoutsakopoulou, V., Ross, A. J., Roth, K. A., MacGregor, G., R., Thompson, C. B., and Korsmeyer, S. J. (2001). Proapoptotic BAX and BAK: a requisite gateway to mitochondrial dysfunction and death. *Science* **292**, 727-730.

White, T. K., Zhu, Q., and Tanzer, M. L. (1995). Cell surface calreticulin is a putative mannoside lectin which triggers mouse melanoma cell spreading. *J. Biol. Chem.* **270,** 15926-15929.

Widmann, C., Gibson, S., and Johnson, G. L. (1998). Caspase-dependent cleavage of signaling proteins during apoptosis. A turn-off mechanism for anti-apoptotic signals. *J Biol Chem.* **273**, 7141-7147.

Wilson, K. P., Black, J.-A. F., Thomson, J. A., Kim, E. E., Griffith, J. P., Navia, M. A., Murcko, M. A., Chambers, S. P., Aldape, R. A., Raybuck, S. A., and Livingston, D. J. (1994). Structure and mechanism of interleukin-1β converting enzyme. *Nature* **370**, 270-275.

Wolf, D., Witte, V., Laffert, B., Blume, K., Stromer, E., Trapp, S., d'Aloja, P., Schurmann, A., and Baur, A. S. (2001). HIV-1 Nef associated PAK and PI3-Kinases stimulate Akt-independent Bad-phosphorylation to induce anti-apoptotic signals. *Nat. Med.* **7**, 1217-1224.

Woo, M., Hakem, R., Soengas, M. S., Duncan, G. S., Shahinian, A., Kagi, D., Hakem, A., McCurrach, M., Khoo, W., Kaufman, S. A., Senaldi, G., Howard, T., Lowe, S. W., and Mak, T. W. (1998). Essential contribution of caspase 3 /CPP32 to apoptosis and its associated nuclear changes. *Genes Dev* **12**, 806-819.

Wright, A. J., and Hunter, C. P. (2003). Mutations in a β-tubulin disrupt spindle orientation and microtubule dynamics in the early *Caenorhabditis elegans* embryo. *Mol. Biol. Cell* **14**, 4512-4525.

Wu, Y. C., and Horvitz, H. R. (1998). *C. elegans* phagocytosis and cell-migration protein CED-5 is similar to human DOCK180. *Nature* **392**, 501-504.

Wu, Y. C., and Horvitz, H. R. (1998b). The *C. elegans* cell corpse engulfment gene *ced-7* encodes a protein similar to ABC transporters. *Cell* **93**, 951-960.

Wu, Y. C., Stanfield, G. M., and Horvitz, H. R. (2000). NUC-1, a *C. elegans* DNase II homolog, functions in an intermediate step of DNA degradation during apoptosis. *Genes Dev.* **14**, 536-548.

Wu, Y. C., Tsai, M. C., Cheng, L. C., Chou, C. J., and Weng, N. Y. (2001). *C. elegans* CED-12 acts in the conserved CrkII/DOCK180/Rac pathway to control cell migration and cell corpse engulfment. *Dev Cell.* **1**, 491-502.

Xing, H., Zhang, S., Weinheimer, C., Kovacs, A., and Muslin, A. J. (2000). 14-3-3 proteins block apoptosis and differentially regulates MAPK cascades. *EMBO J.* **19**, 349-358.

Xu, K., Tavernarakis, N., and Driscoll, M. (2001). Necrotic cell death in *C. elegans* requires the function of calreticulin and regulators of Ca^{2+} release from the endoplasmic reticulum. *Neuron* **31**, 957-971.

Xue, D. and Horvitz, H. R. (1995). Inhibition of the *Caenorhabditis elegans* cell death protease CED-3 by a CED-3 cleavage site in baculovirus p35 protein. *Nature* **377**, 248-251.

Xue, D., Shaham, S., and Horvitz, H. R. (1996). The *Caenorhabditis elegans* cell-death protein CED-3 is a cysteine protease with substrate specificities similar to those of the human CPP32 protease. *Genes Dev.* **10**,1073-1083.

Xue, D. and Horvitz, H. R. (1997). *Caenorhabditis elegans* CED-9 protein is a bifunctional cell-death inhibitor. *Nature* **390**, 305-308.

Yan, N., Gu, L., Kokel, D., Chai, J., Li, W., Han, A., Chen, L., Xue, D., and Shi, Y. (2004). Structural, biochemical, and functional analyses of CED-9 recognition by the proapoptotic proteins EGL-1 and CED-4. *Mol Cell.* **15**, 999-1006.

Yan , N., Chai, J., Lee, E. S., Gu, L., Liu, Q., He, J., Wu, J. W., Kokel, D., Li, H., Hao, Q., Xue, D., and Shi, Y. (2005). Structure of the CED-4-CED-9 complex provides insights into programmed cell death in Caenorhabditis elegans. *Nature* **437**, 831-837.

Yang, J., Liu, X., Bhalla, K., Kim, C. N., Ibrado, A. M., Cai, J., Peng, T.-I., Jones, DP, and Wang X. (1997). Prevention of Apoptosis by Bcl-2: Release of cytochrome from mitochondria blocked. *Science* **275**, 1129-1131.

Yoshida K., Yamaguchi, T., Natsume, T., Kufe, D., and Miki, Y. (2005). JNK phosphorylation of 14-3-3 proteins regulates nuclear targeting of c-Abl in the apoptotic response to DNA damage. *Nat. Cell Biol.* **7**, 278-285.

Yu, X., Acehan, D., Menetret, J-F., Booth, C. R., Ludtke, S. J., Riedl, S. J., Shi, Y., Wang, X., and Akey, C. W. (2005). A structure of the human apoptosome at 12.8A resolution provides insights into this cell death platform. *Structure* **13**, 1725-1735.

Yuan, J., and Horvitz, H. R. (1990). The Caenorhabditis elegans genes ced-3 and ced-4 act cell autonomously to cause programmed cell death. *Dev. Biol.* **138**, 33-41.

Yuan, J., and Horvitz, H. R. (1992). The *Caenorhabditis elegans* cell death gene *ced-4* encodes a novel protein and is expressed during the period of extensive programmed cell death. *Development* **116**, 309-320.

Yuan, J., Shaham, S., Ledoux, S., Ellis, H. M., and Horvitz, H. R. (1993). The *C. elegans* cell death gene *ced-3* encodes a protein similar to mammalian interleukin-1β-converting enzyme. *Cell* **75**, 641-652.

Yuan, J., and Yankner, B. A. (2000). Apoptosis in the nervous system. *Nature* **407**, 802-809.

Zauli, G., Gibellini, D., Secchiero, P., Dutartre, H., Olive, D., Capitani, S., and Collette, Y. (1999). Human immunodeficiency virus type 1 Nef protein sensitizes CD4(+) T ;ymphoid cells to apoptosis via functional upregulation of the CD95/CD95 ligand pathway. *Blood* **93**, 1000-1010.

Zinkel, S. S., Hurov, K. E., Ong, C., Abtahi, F. M., Gross, A., and Korsmeyer, S. (2005). A role for proapoptotic BID in the DNA damage response. *Cell* **122**, 579-591.

Zinkel, S. S., Ong, C. C., Ferguson, D. O., Iwasaki, H., Akashi, K., Bronson, R. T., Kutok, J. L., Alt, F. W., and Korsmeyer, S. (2003). Proapoptotic BID is required for myeloid homeostasis and tumour suppression. *Cell* **122**, 579-591.

Zha, J., Harada, H., Yang, E., Jockel, J., and Korsmeyer, S. J. (1996). Serine phosphorylation of death agonist BAD in response to survival factor results in binding to 14-3-3 not Bcl-xl. *Cell* **87**, 619-628.

Zhang, L., Chen, J., and Fu, H. (1999). Suppression of apoptosis signal-regulating kinase 1-induced cell death by 14-3-3 proteins. *Proc. Natl. Acad. Sci. USA* **96**, 8511-8515.

Zheng, T. S., Hunot, S., Kuida, K., and Flavell, R. (1999). Caspase knockouts: matters of life and death. *Cell Death Differ.* **6**, 1043-1053.

Zhou, L., Song, Z., Tittel, J., and Steller, H.(1999). HAC-1, a Drosophila homolog of APAF-1 and CED-4 functions in developmental and radiation-induced apoptosis. *Mol. Cell.* **4**, 745-755.

Zhou, Z., Caron, E., Hartwieg, E., Hall, A., and Horvitz, H. R. (2001). The *C. elegans* PH domain protein CED-12 regulates cytoskeletal reorganisation via a Rho/Rac GTPase signalling pathway. *Dev. Cell* **1**, 477-489.

Zou, H., Li, Y., Liu, X., and Wang, X. (1999). An Apaf-1 cytochrome c multimeric complex is a functional apoptosome that activates procaspase-9. *J Biol. Chem.* **274**, 11549-11556.

Zou, H., Henzel, W. J., Liu, X., Lutschg, A., and Wang, X. (1997). Apaf-1, a human protein homologous to *C. elegans* CED-4, participates in cytochrome *c*-dependent activation of caspase-3. *Cell* **90**, 405-413.